Universidade do Minho
Escola de Engenharia

Hélder Manuel da Silva e Sousa

METHODOLOGY FOR SAFETY EVALUATION OF EXISTING TIMBER ELEMENTS

October, 2013

METHODOLOGY FOR SAFETY EVALUATION OF EXISTING TIMBER ELEMENTS
Hélder Manuel da Silva e Sousa
UMinho| 2013

FCT Fundação para a Ciência e Tecnologia
MINISTÉRIO DA EDUCAÇÃO E CIÊNCIA Portugal

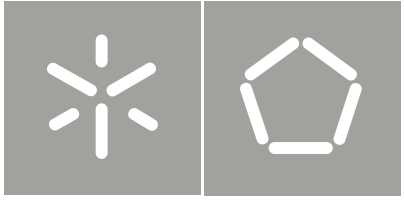

Universidade do Minho
Escola de Engenharia

Hélder Manuel da Silva e Sousa

METHODOLOGY FOR SAFETY EVALUATION OF EXISTING TIMBER ELEMENTS

Philosophy Doctorate Thesis
Civil Engineering

Work conducted under supervision of:
Professor Doctor Jorge Manuel Gonçalves Branco
Professor Doctor Paulo José Brandão Barbosa Lourenço

October, 2013

DECLARATION

Name:	Hélder Manuel da Silva e Sousa
E-mail:	hssousa@civil.uminho.pt
Title of the thesis:	Methodology for safety evaluation of existing timber elements
Supervisors:	Jorge Manuel Gonçalves Branco Paulo José Brandão Barbosa Lourenço
Year of conclusion:	2013
Field ok knowledge:	Philosophy Doctorate in Civil Engineering

University of Minho, ___ / ___ /_____

Signature:

To Carmen, for the light of her eyes
that always guided me.

This page intentionally left blank

Two roads diverged in a wood, and I
I took the one less travelled by,
And that has made all the difference.

Robert Frost (The Road Not Taken, 1916)

This page intentionally left blank

Acknowledgments

I would like to express my great appreciation to all that contributed to the completion of this PhD thesis.

My sincere gratitude to my supervisors, Prof. Paulo B. Lourenço and Prof. Jorge M. Branco for providing me with inspiring and motivating working conditions. Their guidance and knowledge were essential on each step of this work. I would like also to acknowledge their availability and willingness to discuss each and every single idea and their enthusiastic help in filtering the best ones.

My gratitude goes also to the to all the staff of the Civil Engineering Department of University of Minho for the positive and productive atmosphere, to the Structural Lab from University of Minho and its staff who offered me their assistance, experience and advices.

I am particularly grateful for the assistance of Prof. Luís C. Neves, who always provided me with creative discussions in a constructive atmosphere.

I wish also to acknowledge to Dr. Jochen Köhler for making possible my presence in a short scientific mission on the scope of research activity COST E55: Modelling the performance of timber structures. Within that research activity, my gratitude goes also to Prof. John D. Sørensen and Prof. Poul H. Kirkegaard for hosting me at Aalborg University, Denmark, where their guidance and stimulating discussions where an important contribute to the present work.

The financial support of the Portuguese Science Foundation (Fundação para a Ciência e a Tecnologia, FCT), through PhD Grant SFRH/BD/62326/2009, is gratefully acknowledged. I also acknowledge the support of Augusto de Oliveira Ferreira e Companhia Lda. for providing me with the specimens for the experimental campaign and to the invaluable discussions about the conservation and rehabilitation of existing buildings.

To all the PhD students colleagues in the Civil Engineering Department of University of Minho, I would like to thank for the hours spent together discussing each

other works, even within so different fields of research. Their different perspectives allowed me to see outside the box and were a fruitful contribution to the present work.

I also thank all my friends that supported me during these years.

My gratefulness to my grandparents and godparents that taught me the knowledge of times, even in my younger age.

To my brother, who was a strong source of encouragement and optimism I give my gratitude.

My gratitude to my devoted father and mother who have always been present and that, through their work, commitment and affection, taught me a strong sense of responsibility and confidence, providing me with the tools to overcome life difficulties. Thank you for making me the man I am today.

Finally, I dedicate this thesis to my girlfriend Carmen who accompanied me on this long journey, without any hesitation and always giving me the strength, happiness, encouragement and source of inspiration that I needed, through the wisdom of her advices, the brightness of her eyes, the tenderness of her smile and... her unconditional love.

Abstract

The past decades have seen a renewed interest in timber research related topics. As instance, timber engineering is not only confined to the design of new construction with innovative wood based products, but also an increasing awareness for the preservation of existing timber structures is visible in nowadays society. Therefore, arises the need for a better understanding of timber performance as a construction material aiming at a better safety assessment of existing timber structures and possible necessary actions to maintain their integrity.

It is important to provide methods and tools to assess the safety level of existing timber structures by describing and evaluating each of its components. However, timber is a rather complex material and its mechanical properties present large variation within and between elements of the same structure. In that scope, this work was proposed regarding the assessment of existing timber elements with the purpose of establishing a methodology for structural safety evaluation. To that aim, initially a multi-scale experimental campaign was made regarding 20 timber chestnut (*Castanea sativa* Mill.) beams taken from an old building's floor. After, the database resulting from that experimental campaign allowed for the correlation between mechanical properties of timber between and within elements and in different size scales.

In a second phase, the results of non-destructive tests and local mechanical sampling are used to predict and infer about reference key properties of timber. The results of visual grading and local bending tests were used to predict the global stiffness of a structural size element. Random sampling was also taken into account in the prediction models. Moreover, the use of Bayesian methods was considered to update the mechanical properties of timber based on non-destructive tests and different levels of belief. Posterior distributions for bending stiffness and strength were also obtained, through use of Bayesian Probabilistic Networks with different combinations of prior information. The proposed networks consider information from different size scales and results from different types of tests. Example cases were considered to illustrate the different methods and to demonstrate their applicability and value in the context of safety evaluation.

The main outcomes of the present work are related to the prediction and inference of reference properties of timber, using a hierarchical model that combines information from visual grading and non-destructive testing with local mechanic testing information, attending to possible onsite conditions and available data.

The work presented in this thesis was carried out at the Civil Engineering Department of University of Minho, Portugal.

This page intentionally left blank

Resumo

As últimas décadas presenciaram um interesse renovado da investigação em diversas áreas da construção em madeira. Por exemplo, em engenharia, a investigação não é restrita à construção nova recorrendo aos mais recentes derivados de madeira, como também se verifica na sociedade atual uma crescente consciencialização para a preservação de estruturas existentes em madeira. Assim, surge a necessidade de uma melhor compreensão do desempenho da madeira como material de construção, visando uma melhor avaliação de segurança das estruturas existentes para uma adequada previsão das consequentes ações de manutenção necessárias à sua integridade estrutural.

Dessa forma, é de extrema importância disponibilizar métodos e ferramentas que permitam aferir o nível de segurança de estruturas existentes em madeira através da avaliação de cada componente. No entanto, a madeira é um material complexo, cujas propriedades apresentam grande variabilidade tanto entre elementos como ao nível do próprio elemento. Nesse âmbito, este trabalho foi proposto para definir uma metodologia de avaliação de segurança para estruturas existentes de madeira. Inicialmente, apresenta-se uma campanha experimental com base em 20 vigas de piso em castanho (*Castanea sativa* Mill.) retiradas de um edifício antigo em remodelação. Posteriormente, a base de dados obtida nessa campanha experimental permitiu a realização de correlações entre diversas propriedades mecânicas da madeira entre elementos e em diferentes escalas dimensionais.

Numa fase seguinte, os resultados de ensaios não destrutivos e de testes a pequenas amostras são utilizados na previsão e inferência de propriedades de referência da madeira. Os resultados de classificação visual e de ensaios de flexão localizados são utilizados na previsão do módulo de elasticidade de um elemento estrutural. Os modelos de previsão consideram também a amostragem aleatória de dados. Para além disso, foram considerados métodos Bayesianos na atualização das propriedades mecânicas, através de informação de ensaios não destrutivos com diferentes níveis de confiança. A utilização de redes probabilísticas Bayesianas permitiu também a obtenção de distribuições posteriores para a resistência e rigidez à flexão considerando diferentes combinações de informação. As redes propostas consideram informação proveniente de diferentes escalas dimensionais e de resultados de ensaios. Os diferentes métodos são apresentados através de exemplos por forma a evidenciar a sua potencialidade de uso no contexto da verificação de segurança.

Os principais resultados deste trabalho são a previsão e inferência de propriedades de referência de madeira, utilizando para esse efeito um modelo hierárquico que combina classificação visual e ensaios não-destrutivos com informação de ensaios mecânicos, atendendo a possíveis dados disponíveis e condições no local da estrutura.

O presente trabalho foi realizado no Departamento de Engenharia Civil da Universidade do Minho, Portugal.

This page intentionally left blank

Contents

Nomenclature

Latin upper case letters:

A - area
A_d - ratio of minimal knot diameters
ANOVA - analysis of variance
CC - consequence classes
CDF - cumulative density function
COV - coefficient of variation
CWS - clear wood section
D - maximum knot diameter
DT - destructive test
E - expected value
$E_{0,mean}$ - mean value MOE parallel to grain
$E_{0,05}$ - characteristic value MOE parallel to grain
$E_{90,mean}$ - mean value MOE perpendicular to grain
$E_{c,0}$ - modulus of elasticity in compression parallel to grain
E_{din} - dynamic modulus of elasticity
E_m - modulus of elasticity
$E_{m,g}$ - global bending MOE
$E_{m,l}$ - local bending MOE
$E_{t,0}$ - modulus of elasticity in tension parallel to grain
F_{est} - estimated load
F_{max} - maximum load
FORM - first order reliability methods
G - permanent load
G_k - characteristic value for permanent load
GTM - global test methods
G_v - shear modulus
H - stochastic variable with h ( )
I - inertia moment
K_V - coefficient of volumetric shrinkage
K - species proportionality constant
LTM - local test methods
M1,2 - models
MC - moisture content
M_i - safety margin
MLE - maximum likelihood estimates
MM - method of moments
MOE - modulus of elasticity
NC - non-classifiable
NDT - non-destructive test
PDF - probability density function
PMC - probabilistic model code
Q - variable load
$Q_{1,2...}$ - quartiles
Q_k - characteristic value for variable load
R - resistance function
RC - reliability classes
RD - relative difference
RM - drilling resistance measure
RP - drilling reducing parameter
S - load effect function
SDT - semi-destructive test
V - volume
VI - visual inspection
W_d - ratio of minimal knot diameters
W - section modulus
W_Δ - deflection
WK - weak section
X - stochastic variable
X_d - design value of material property
X_k - characteristic value of material property

Latin lower case letters:

a - distance between a loading position and the nearest support
a_W - scale factor

b - width
b_W - location factor
$c_{1,2...}$ - constants
cor - correlation
d - minimal knot diameter
d_w - wave path length
$f_{c,0}$ - compressive strength parallel to grain
$f_{c,0,k}$ - characteristic compressive strength parallel to grain
$f_{c,90,k}$ - characteristic compressive strength perpendicular to grain
f_m - bending strength
$f_{m,0}$ - bending moment capacity
$f_{m,k}$ - characteristic bending strength
$f_N(\ )$ - likelihood function
$f_Q'(\ )$ - prior density function
$f_Q''(\ )$ - posterior density function
$f_{t,0}$ - tension strength parallel to grain
$f_{t,0,k}$ - characteristic tension strength parallel to grain
$f_{t,90,k}$ - characteristic tension strength perpendicular to grain
$f_{v,k}$ - characteristic shear strength
$f_X(\ )$ - density function
g - limit state equation
$g_i(\ )$ - failure function
h - height
$h(\ )$ - event function
k - dispersion constant
k_1 - partial safety modification factor
k_a - aging modification factor
$k_{climate}$ - parameter of climate conditions
k_{con} - conservation modification factor
k_{def} - stiffness modification factor
k_h - size factor
k_{mod} - strength modification factor
k_s - shape factor
k_{size} - size factor for DT
k_{wood} - parameter of timber durability class
l - length
l_1 - gauge length
m - sample mean
m' - prior function hypothetical sample average
m'' - posterior function hypothetical sample average
$m_{1,2...}$ - mass
$m_{I,II...}$ - test measurements
n - number of tests
n' - prior function hypothetical number of observations for m'
n'' - posterior function hypothetical number of observations for m'
p_f - probability of failure
p_f^P - probability of failure of a parallel system
p_f^S - probability of failure of a series system
q - vector of distribution parameters
r - penetration rate
r^2 - coefficient of determination
r_k - characteristic resistance
s - sample standard deviation
s' - prior function hypothetical sample value
s'' - posterior function hypothetical sample value
$s_{G,k}$ - characteristic permanent load effect
$s_i(\ )$ - stress component
s_{pi} - allowable stress
$s_{Q,k}$ - characteristic variable load effect
s_{ui} - ultimate stress
s_w - ratio of wane
t - time
$t_{\nu''}$ - central t-distribution value
t_k - sum of minimal knot diameters
t_{lag} - time between construction and the point that noticeable decay commences
v' - prior function hypothetical number of degree of freedom for s'
v'' - posterior function hypothetical number of degree of freedom for s'
v_p - propagation velocity
$\hat{x}$ - sample of realizations
z_d - design value

Greek upper case letters:

ΔF - load increment

Δw - deformation increment

Φ - standard normal distribution function

ϑ - bending test constant

ψ_2 - factor for quasi-permanent value of a variable action

ψ_g - generic structure point

Greek lower case letters:

α - factor for modelling the fraction of variable and permanent load

α_{class} - reduction factor for VI classes

α_i - regression parameter

β - reliability index

χ - normal distributed variable

δ_L - allowable deflection limit

γ_G - partial safety factor for permanent loads

γ_M - partial safety factor for material properties

γ_R - partial safety factor for resistance

γ_Q - partial safety factor for variable loads

ε - lack-of-fit

ϕ_r - safety factor

λ - failure rate

λ_{rel} - slenderness ratio

μ - mean value

μ_{depth} - average of pin penetration tests

μ_{DT} - average of destructive tests

μ_{Edin} - average of ultrasound tests

μ_{RM} - average of resistance drilling tests

σ - standard deviation

$\sigma_{1,2...}$ - stresses

ρ - density

τ - perimetral loss of cross section

υ - unknown logarithm of mean strength

ϖ - normal distributed variable

List of Figures

List of Tables

This page intentionally left blank

Chapter 1

Introduction

ABSTRACT: Presently, a manifold of research topics are found on the context of wood based products and timber engineering. Timber has been used as a construction material for several centuries by different civilizations, with numerous examples of structures which are still standing. In these cases, it is of utmost importance to provide methods and tools to assess the safety level of existing timber structures by describing and evaluating each of its components. However, timber is a rather complex material and its mechanical properties present large variation within and between elements of the same structure.

In that scope, this work is proposed regarding the assessment of existing timber elements with the purpose of establishing a methodology for structural safety evaluation. This introductory chapter further explains this research interest and its scope, by providing an insight to the aim and objectives of the present work. The specific area of research and limitations of the work are also delineated attending to the objectives. Moreover, for better understanding of the interaction between chapters, an outline and overview of the work is described and schematically presented.

1.1 Research in timber structures

The use of timber as a construction material goes back to when the Human species first started to employ tools and even farther. Timber structures have evolved through time as the Human race necessity grew and also the expertise and knowledge about the material and the interaction between elements in different structural types increased. One may only speculate how the first timber constructions were erected but, as many of mankind accomplishments, they might have been fruit of a trial and error procedure that was eventually improved and refined. Then, the expertise and knowledge was passed from generation to generation, making possible new techniques and bolder solutions.

Nowadays, research topics on timber structures are immense, spreading to a broad variety of themes ranging from the microscopic characterization of wood's constituents to the safety analysis of large complex structures. New building techniques and innovative wood based materials are now available, allowing for the construction of timber structures which until now were unfeasible.

Despite all achievements and developments seen in the past decades regarding new timber constructions, existing timber structures are still an important object of research, specially taking into account the valuable historical contribution that some pose in the social and cultural tapestry of ancient and present civilizations. Notwithstanding all available historical documents and knowledge that was transmitted throughout generations of wood crafters, carpenters, engineers and architects, many aspects, such as some prerequisites for material selection, building techniques and design methods were lost and thus the complete understanding of these structures is still to be reached. Furthermore, considering a safety assessment, aging and often degradation of timber members that compose these structures must also be considered, resulting in much more complex process than for new constructions. This unequivocally opens a door for multiple research topics in the context of existing timber structures.

Timber constructions have an important significance in the cultural, architectural and historical heritage in Europe, from which Portugal cannot be excluded. Among the numerous cases of Portuguese architectural heritage, timber has been used for several purposes in many different construction types. It often appears as partial constructive element (particularly in roof structures, floors and walls) and occasionally as integral constructive element. The use of timber, in its various forms, differs from North to South concerning the type of building, the constructive methodologies and mainly the wood species available on the region.

1.2 Scope of work

Despite all the advantages of timber as a construction material, its full mechanical characterization is rather complex, since it is an anisotropic material and therefore its properties are dependent of grain direction. As mentioned by Dinwoodie (1989), variability

in wood is one of its characteristic deficiencies as a material. Differences in structure and hence performance occur not only between different species of timber but also between trees of the same species growing in different environments, or between different parts of a single tree. For instance, the material properties of a timber member vary both in different parts of the same cross section, as well as along the element itself. Moreover, its properties also vary not only in space, but also in time, as aging or degradation phenomena may take place. However, granted that, concerning a given purpose or function and required durability, the proper wood species is selected and correct construction techniques are applied, it provides a good mechanical behaviour and durability associated to an efficient relation between resistance and density.

The large material variability of timber inevitably resulted that design of timber structures has always to a large degree been based on experience and subjective engineering judgment, having, more than often, led to conservative solutions. One of the consequences of that premise, is that safety evaluation of timber structures, either assessment of existing structures or at the design of new ones, is much more complex than for other material evidencing less variability. Moreover, in several countries, prejudices persist against timber structures, based on the assumptions that they have a brittle failure behaviour, are vulnerable to fire, and dependent on unreliable workmanship and unknown quality, which often are not supported by scientific evidence. Many other myths arise regarding the performance of timber structures as mentioned in Machado *et al*. (2003b), which can only be diminished by the use of certified specifications and standards based on empirical proof. To that extent, the role of research on timber structures has been to develop efficient procedures to assess and predict the mechanical properties of timber members, either onsite or based on the strength grading of materials prior to construction.

At the present state of knowledge, due to several research projects, rational design rules, based on a detailed material description validated by comparison with a significant number of empirical results are made available to a timber construction designer. However, safety assessment of existing structures and characterization of traditional wooden building techniques remain a true challenge.

When dealing with existing timber structures, the structural safety assessment and evaluation of each component, either the member themselves or the connections, and the system reliability must be determined according to the present conditions of the structure. On the other hand, maintenance plans, or when necessary repair or strengthening actions, must be considered attending to the lifecycle evaluation of the structure based on its predicted durability and vulnerability to exterior actions.

As it may be concluded by this reality of various research topics in timber structures, either at a component or at a system level, the demand for an assessment of existing timber structures comprises several fields of knowledge, each one providing its own piece of information aiming at a better and more complete answer. To address the different influences from these sources of information it is of utmost interest to experimentally study the behaviour of large-scale timber specimens, but even more to predict its behaviour from

small specimens. This premise arises from the condition that often it is not possible to experimentally evaluate full scale structures or members due to onsite conditions, social or cultural restrictions or even economic impediments. Therefore, inspection and evaluation of the onsite structural properties, often by use of visual grading and non-destructive testing, represent an important step to the assessment of existing timber structures and perform a significant role in their analysis, diagnosis and conservation. To that aim, the conception and implementation of methodologies for safety assessment of existing timber structures are needed, in particular through the analysis of small scale specimens aided by the information of visual grading and non-destructive testing.

1.3 Objectives and limitations

The objective of this work is to provide an insight of different methods for the assessment of the mechanical properties of members in existing timber structures. These methods are to be conceived based on different sources of information and different size scales, and therefore, a hierarchical modelling for inference on the reference properties is adopted.

The proposed models have to consider the introduction of new information and its consequent updating. By this procedure it is intended to have a more reliable and informed tool for the decision making process, regarding possible interventions or maintenance in timber members.

The study is limited to the inference and assessment of the mechanical properties at the member scale. As the mechanical properties are to be assessed along each timber members as individual components, the mechanical characterization and modelling of timber joints was outside the scope of this work.

The assessment of existing timber members also comprises the evaluation of deterioration (damage or decay) which in the present work will be assessed by reduction of the members' geometry, in order to obtain a residual cross section. Decay is considered by the models found in literature, since it is an usually slow phenomena, and thus development of these models requires monitoring data from a considerable long time, which was not compatible with the timeline of this work.

For the development of this work, chestnut (*Castanea sativa* Mill.) old timber beams were considered, as it is a commonly used species for construction purposes in North of Portugal, in the past. The experimental campaign was limited to 20 elements with more than 100 years of age in the construction site. The limited number regards the low availability of members with this age for destructive mechanical testing.

1.4 Chestnut timber as a structural material

Chestnut wood is one of the most common species found in Portuguese historical timber structures. Its natural durability has long been appreciated and thus its use was favoured for structures with social and cultural importance, however it is also found in floors and roofs of dwellings, at lintels, windows and doors, and even was the wood of choice for traditional altarpieces of the 18th century (Faria, 2002). Regarding the experimental campaign and case studies presented in the following chapters of this work, where structural members of chestnut timber are analysed, a brief characterization of this wood species is given hereafter.

Chestnut is the designation used for any species of the genus *Castanea,* deciduous trees of the family *Fagaceae*. The usual species found in Portugal is *Castanea sativa* Mill. (the Latin word *sativa* means cultivated), which is native to Mediterranean region of Europe and Asia Minor and widely cultivated throughout temperate regions. Detailed information about the origin and cultivation of Chestnut in Europe is found in Conedera and Krebs (2007). This deciduous tree produces an edible seed, the chestnut, which was one of the basis of alimentation to many ancient cultures prior to the introduction of potatoes or to cultures with scarce access to wheat flour. Trees may reach heights of 20 to 35 m and the appearance of the bark resembles a net-shaped pattern with fissures running spirally in both directions up the trunk (Figure 1.1). The leaves measuring from 10 to 30 cm long and 4 to 10 cm wide present a simple, ovate or lanceolate shape with serrated perimeter.

a) b)

Figure 1.1: Chestnut tree: a) tree; b) detail of a cross section[1].

Chestnut timber is considered of medium availability in Portugal having in the last decades about 32000 ha of pure chestnut forest (Fioravanti and Galotta, 1998). Often its density ranges from 540 to 650 kg/m^3 and having an average hardness between 2.1 and 2.5 (Sánchez *et al.*, 2004). It also presents moderate shrinking and it is difficult to dry.

[1] source: b) *http://commons.wikimedia.org*, institution: Museum of Toulouse (retrieved August, 2013).

Accounting its natural durability, it presents a good performance regarding fungi attack and termites, being more sensitive to wood boring beetles. Chestnut is porous, with low impregnable heartwood and medium impregnable sapwood. Its durability decreases when exposed to changing environments. The European standards EN 350-1 (CEN, 1994a) and EN 350-2 (CEN, 1994b) classifies it as durable and suitable for all applications with and without contact with soil, except of particular cases of very extreme conditions. Due to its high content of acids (tannic acid), tends to speed up metal corrosion, which is more evidenced in the presence of high humidity. Due to this, blue discolorations may be found when in contact with iron based materials.

The Italian standard UNI 11119 (UNI, 2004) considers three classes regarding visual grading of timber elements in onsite inspections and diagnosis and provides, for different species of timber such as chestnut, indicative values for characteristic strength stresses for compression and tension, both parallel and perpendicular to the grain, shear parallel to the grain and static bending. Also mean values for modulus of elasticity (MOE) in bending are provided.

Sánchez *et al.* (2004) mentions that for clear wood samples, chestnut reaches a bending strength between 63 to 79 N/mm^2 with a bending MOE between 8200 to 12600 N/mm^2. The same authors also indicate values between 40 to 52 N/mm^2 for compression strength parallel to grain and of 7.8 N/mm^2 for compression strength perpendicular to the grain, meanwhile indicating values between 7.8 and 9.3 N/mm^2 for shear strength and 5.5 to 5.9 J/cm^2 for dynamic bending. Mechanical characterization of small clear chestnut wood specimens may also be found in Lourenço *et al.* (2007) and Feio *et al*. (2007) regarding correlations with non-destructive test results.

Whereas, evaluation of structural size chestnut elements was considered in Branco *et al.* (2011) and Faggiano *et al.* (2011). Sánchez *et al.* (2004) also provides indicative values for structural chestnut timber, such as mean bending MOE of 10400 N/mm^2.

1.5 Outline and thesis overview

In Chapter 1, the scope and objectives of this work are presented. Description of the methods and aim of each task within the main framework is provided.

In Chapter 2, a review of relevant topics is given, aiming at providing the necessary information to understand and support each step of the following chapters. Initially a brief review of evaluation schemes and testing for existing timber members is provided with clarification of methods for timber grading. Following, different procedures for safety assessment evaluations are described regarding its analysis approach, either deterministic or probabilistic. In this chapter, the hierarchical modelling of timber elements is also mentioned with reference to the distinction of clear wood segments and segments with defects at a structural size scale.

In Chapter 3, a multi-scale experimental campaign is described regarding the assessment of chestnut timber beams retrieved from a building in North of Portugal. Each test scale is described in a specific phase and the results obtained through different types of tests are evidenced. For that aim, a combination of either or both non-destructive, semi-destructive and mechanical testing is considered in each phase. Special attention is given to the analysis of bending stiffness and strength, as reference properties, in different test phases. Further on, testing on clear wood specimens is also considered for assessment of parallel to the grain mechanical properties. Visual inspection and bending tests in elastic range are used as comparative parameter within different scales. The outcome of this chapter is a database for the assessment of mechanical properties of chestnut timber members,

Following in Chapter 4, the results obtained in the experimental campaign previously described are analysed. Variability within and between elements is statistically assessed, and complemented by an analysis of outlier values. Correlations between the same mechanical property in different size scales are proposed. Moreover, correlations between different properties are considered within and between size scales.

In Chapter 5, the global modulus of elasticity in bending is assessed and predicted by means of visual grading and mechanical testing of small size elements. Several models assuming different combinations of local data in the prediction of bending stiffness are proposed and analysed regarding their correlation with the experimental data. Random sampling of local data is considered attending to the visual grading in a lower scale level.

In Chapter 6, the application of data updating by Bayesian methods is exemplified in single elements and in an example of a truss. The prior information is obtained through a database of mechanical properties of clear wood specimens with non-destructive testing results.

In Chapter 7, Bayesian Probabilistic Networks are used for infer of bending stiffness and strength of timber members in different size scales, accounting the results of visual grading and bending tests in Chapters 3 and 4. According to the target mechanical property to be inferred and the level of prior information, different arrangements of the networks are considered.

Finally, Chapter 8 presents the summary and final conclusions of this work, also accounting to found limitations. A brief consideration of future works is made.

A global overview is given in Figure 1.2, accounting the interaction of the different chapters. In essence, Chapter 2 presents the review of tools and basics for the following chapters, whereas Chapter 3 and 4 provides the necessary database of results and correlations between mechanical properties of existing timber members. Chapters 5 to 7, incorporate the information of different sources, applying it to the prediction and updating of models for the reference properties of timber. Finally, Chapter 8 sums up the main findings of the previous chapters.

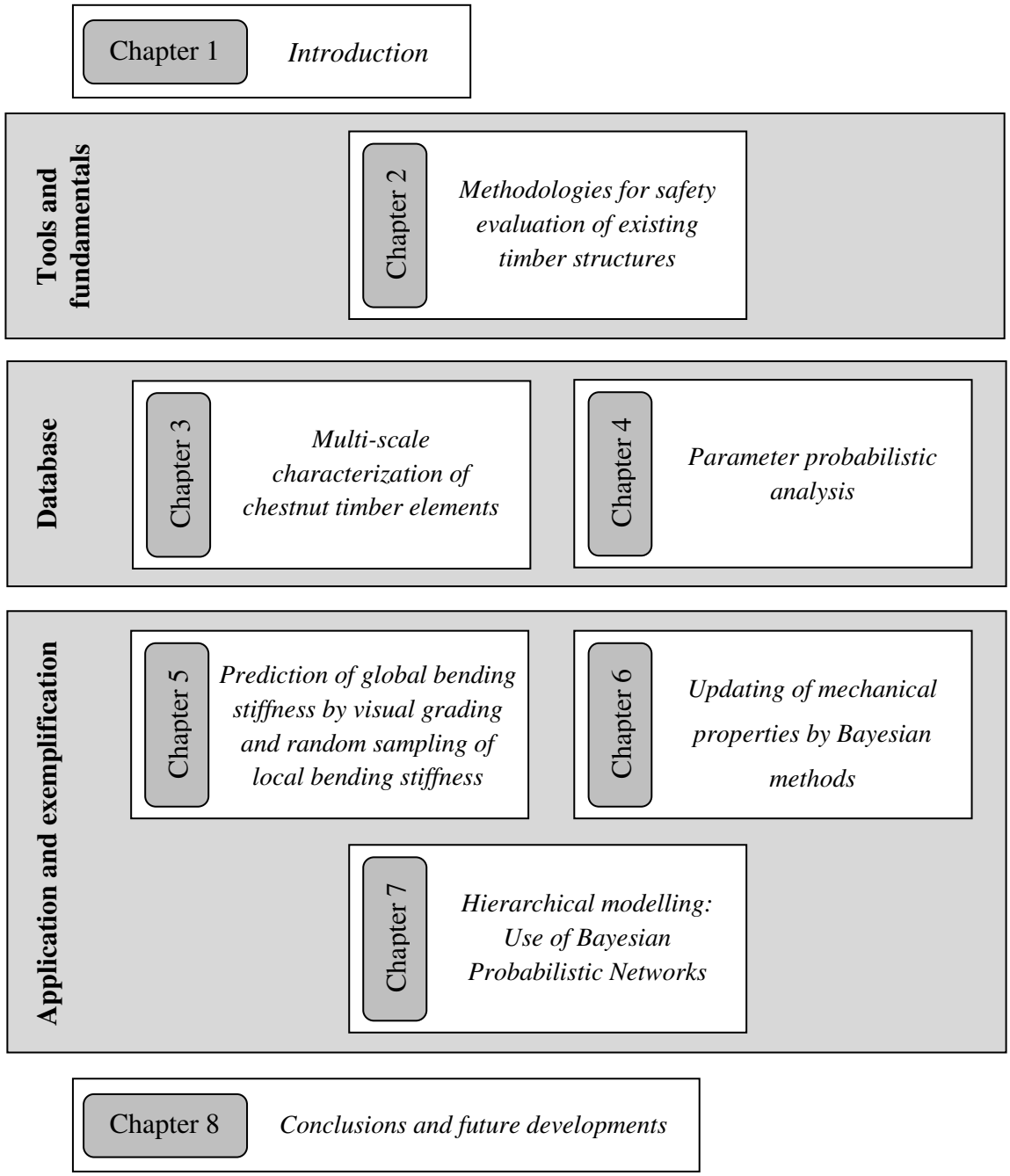

Figure 1.2: Schematic overview of the thesis' chapters.

Chapter 2

Methodologies for safety evaluation of existing timber structures

ABSTRACT: A better understanding of timber performance as a construction material and of its durability allows for a better safety assessment of existing timber structures and the possible necessary actions to maintain its integrity. However, modelling the characteristics of existing structures may sometimes lead to costly procedures, and therefore careful planning of works is imperative. Nonetheless, many times the costs of an adequate inspection and monitoring plan are far less inferior to those compared to time inadequate maintenance, repairing interventions or, in extreme situations, to the consequences of a structural collapse.

On the following chapter, a brief description of different common tests made to timber elements and respective grading rules is provided. Moreover, the differences between distinct design and assessment methodologies is highlighted, with special relevance to enumeration of examples of hierarchical modelling in timber structures. The use of updating methods, within probabilistic approaches and regarding information gathered from different sources, is also mentioned.

2.1 Testing of timber mechanical properties

Timber, as with all construction materials, is chosen for a specific purpose regarding its suitability, which can range from its aesthetic and availability to its physical properties, but most importantly, to its predicted performance, both mechanical and durability. However, it differs from other materials, as it is a natural material evidencing large variability in its physical and mechanical properties, and it is necessary to perform an adequate material characterization in order to reliably predict its performance. This is often achieved by testing it by different means and procedures, which are chosen regarding the scope and objective to which the material is intended.

Several different testing methods were made available during the last decades, as to answer different questions regarding the characterization of timber. Depending on its nature, application and damage that they produce to the inspected elements, these tests are defined into different categories. The most important division is that which defines the amount of damage made to the material while performing the test, resulting into three categories (Kasal and Anthony, 2004). When a test does not produce damage it is denominated as non-destructive testing (NDT), or semi-destructive (SDT) when only minor damage is made. On the other side, destructive testing (DT) has taken place when the material is damaged in such way that cannot be recovered. Although NDT has the advantage of maintaining the full integrity of the element, it does not provide a high level of information and a large amount of measurements are necessary to provide a preliminary material characterization (see Figure 2.1). In this case, only DT allows for a complete and reliable material characterization, however it destroys the sample in analysis and thus incompatible in the assessment of historic structures.

In DT methods, a member can be extracted from a structural system and its properties are analysed via full-scale or reduced scale (small clear wood specimens) experiments. Although it produces a precise inference about the mechanical properties of that particular member, it may not be reliable for inference of other members due to the high variability found between members even within the same structure (Kasal, 2010). In SDT methods, small specimens are extracted from the structural member, such that its dimensions are smaller than wood's natural defects or significantly smaller than the member itself, ensuring that the strength of the member is not affected. In this case, regarding the variability within member, the number of measurements will greatly affect the reliability of the prediction of the desired parameter. Often a large number of samples is required in order to obtain a stable sample coefficient of variation (COV). As in DT, the advantage of SDT is that the mechanical property in study is measured directly and not by basis of correlation, whereas NDT relies on the relationship (most commonly the correlation) between the measured parameter and a mechanical (either strength or stiffness) parameter.

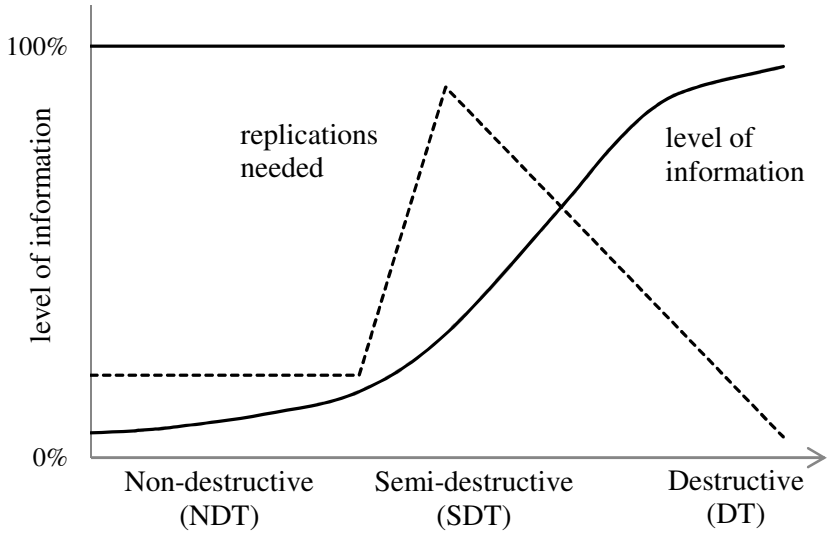

Figure 2.1: Relationship between evaluation technique and expected level of information (adapted from Kasal, 2010).

Some examples of different tests divided by its damage level are provided in Table 2.1. While the division between DT and other tests is well defined, the distinction between SDT and NDT is less clear, as some authors have different opinions regarding the damage level made by techniques that do not require specimen extraction and only perform low surface damage (usually punctual damage).

Table 2.1: Testing methods for evaluation of timber.

Method type	Example of the method
Destructive	Testing of full-size members
Semi-destructive	Micro-tension tests Core drilling Small specimen extraction Screw withholding tests Hardness tests Resistance drilling Penetration tests Moisture measurements
Non-destructive	Videoscopy Microscopy Acoustic methods Ultrasonic methods Stress waves Radiography IR thermography Ground penetrating radar Species identification Visual inspection

Another important division between timber testing methods, is the type of parameter obtained regarding the measurement extent, which can be either local or global (Baldassino *et al.*, 1996). In local test methods (LTM) the properties of small areas are known and inferences about the properties of the full member must be considered by correlation or empirical knowledge. SDT is an example of LTM, as they only provide information regarding the extracted specimens or of a punctual measurement (*e.g.*: resistance drilling, pin penetration tests). On the other hand, global test methods (GTM) measure parameters over relatively large areas or even properties of an entire section or member. Both NDT and DT commonly result in global parameter estimation.

Although, in an overall sense, all of these tests and procedures intend to give a better understanding of the timber member's material characterization, they often individually provide only insight of a specific parameter or property. For instance, many NDT require information provided by SDT in order to correlate with the mechanical properties of timber (*e.g.*: ultrasonic methods depend on the knowledge of density and moisture contents, obtained by SDT, for a reliable estimation of timber's stiffness). Therefore, the timber assessment should comprise a thorough testing procedure, combining different tests and regarding a variety of parameters (*e.g.*: dimensional stability, mechanical strength, durability, water content), so it can be correctly graded accounting to accepted or imposed criteria, such as professional guidelines or national regulation.

In what concerns existing structures, several methods have been established to evaluate timber onsite, and the choice of a specific method depends on the particular information that is required. Further information about individual test methods are summarized in the RILEM TC 215 state-of-the-art report (Kasal and Tannert, 2010). In this document the evaluation of historic timber can be summarized in the following steps: *i*) visual inspection; *ii*) specie identification; *iii*) moisture measurement; and, *iv*) evaluation of specific properties or parameters.

Here, special highlight will be provided to the NDT, SDT and DT which were used during the experimental campaign presented in Chapter 3[2].

2.1.1 Non and semi-destructive testing

Ross and Pellerin (1994) refer to non-destructive evaluation as the science of identifying physical and mechanical properties of a piece of material without altering its end-use capabilities. However, a more refined definition is needed, as some SDT also allow for the timber member to fulfil its end-use purpose but in exchange of minor damage to the surface of the element.

Historically, the wood community has developed and used NDT almost exclusively for sorting or grading structural elements in a production line. As instance, it has long been a common procedure to couple visual sorting criteria with NDT inferring to stiffness of a

[2] Chapter 3: Multi-scale characterization of chestnut timber elements.

piece of lumber, in order to establish different grades in a machine stress rating, as reported by Galligan *et al.* (1977). However, there are NDT techniques that have proven useful and efficient for an initial material characterization for onsite timber members. In fact, the fundamental principle of NDT use for timber structural assessment has long been established. This hypothesis stands that the energy storage and dissipation properties of wood materials, which can be measured by means of NDT, are governed by the same mechanisms that determine the static behaviour of such material (Jayne, 1955). As a result, correlations between these properties and static elastic and strength may be obtainable through statistical regression analysis.

NDT in timber greatly varies from those made to other materials, namely homogeneous and isotropic materials, such as metals, plastics and ceramics. In other construction materials, NDT's main function is to detect manufacturing defects, as the presence of discontinuities, voids, or inclusions. Whereas, in timber, defects are naturally present and may easily be induced by environmental degradation agents, thus in this case, NDT have also to account how natural and environmental defects or pathologies affect the mechanical properties of the structural member. Nowadays, the use of NDT in existing timber structures is expanding due to an increasing amount of resources being devoted to repair and rehabilitation of existing timber structures rather than to new construction, and thus a more consistent onsite assessment is demanded.

Visual inspection

Visual inspection is a global testing method used to identify the overall condition of the structure and wood members, and it is considered the most important step in the assessment process (Kasal, 2010). Several authors even mention that visual inspection is required to determine the original timber characteristics and the damage history during its service life (Ceccotti and Uzielli, 1989; Uzielli, 1992; Tampone, 1996a; Tampone, 1996b; Ross *et al*., 1998; Tampone *et al*., 2002). Although it may be preceded by preliminary desk survey, when doing, for example the historical survey of heritage structures, visual inspection is the first step to a full diagnostic of an existing structure and often a crucial factor that determines the plan of interventions (Cruz, *et al.* 2013) (see Figure 2.2).

During a visual inspection, the natural defects and deterioration are detected, characterized and inventoried. Natural defects, include features such as knots, slope of grain, deformation, wane and seasoning checks, while deterioration includes damage from insect infestation or fungal decay (biologic attack) (see Figure 2.3). Besides the presence of defects in elements, it is crucial to survey the moisture content and / or water infiltrations as those may contribute to the presence of biological activity. Regarding timber structures, special attention must be drawn to the connections between elements and to its level of preservation. The safety conditions of a timber structure are highly dependent on the performance of the connections, however few standards address the visual inspection of connections with due concern.

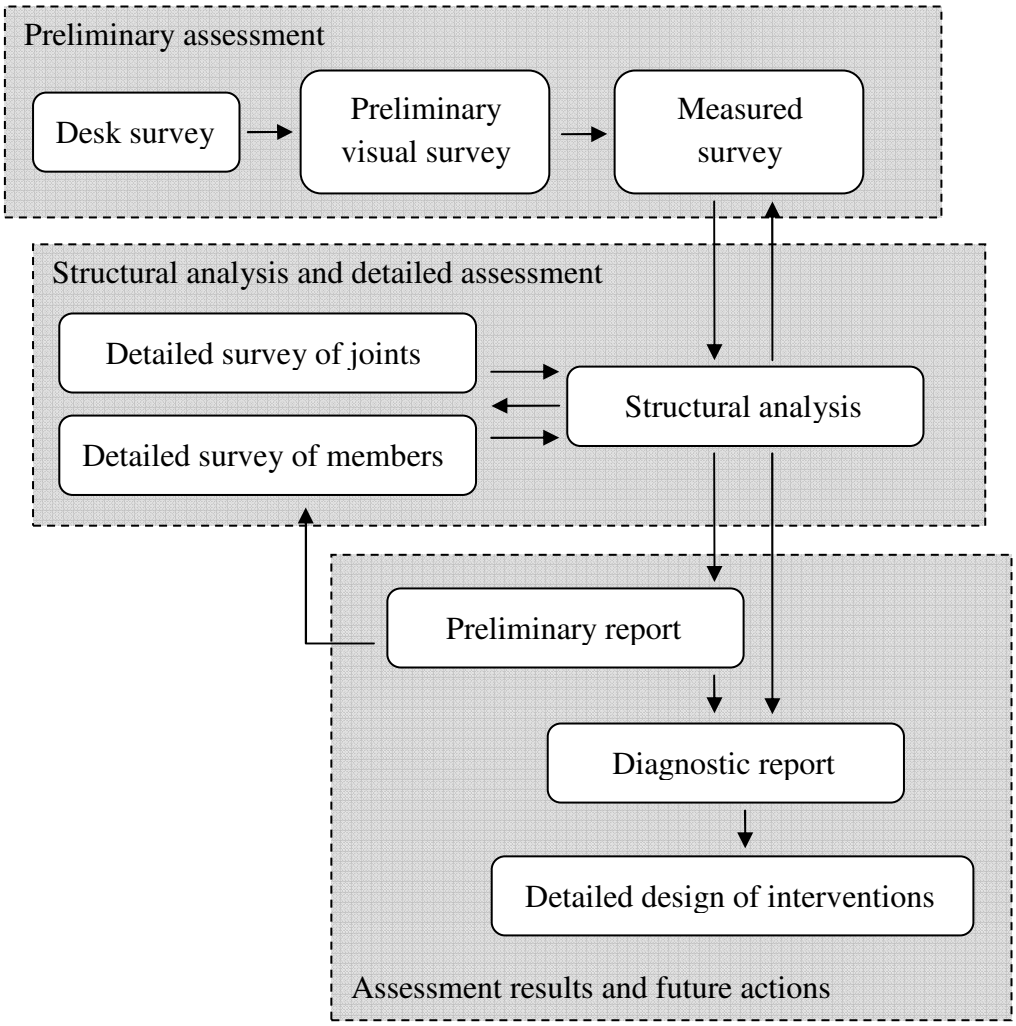

Figure 2.2: Steps required for the assessment and planning of interventions in historic timber structures (adapted from Cruz *et al*., 2013).

After the visual inspection, a visual grading is made based in the size, number and location of defects related to the timber member's size and structural use. This grading is often attributed with respect to a critical segment[3] of the timber member and accounting to its residual cross section (section without the portion decayed by biotic agents).

On the past decades, several national grading rules were introduced in Europe, but widely differing with respect to grading criteria, number of grades and grade limits. These differences are mainly derived from the need to evaluate diverse species or group of species (such as softwoods and hardwoods), geographic origin, different dimensional characteristics, quality of material as well as historic value and common craftsmanship. To overcome these differences, general guidelines were suggested in the European standard EN 518 (CEN, 1997) and the subsequent national standards were developed in order to establish strength classes for local timbers, whereas, assignment of species and visual

[3] critical segment may be defined as a region of the timber element with more than 150 mm length (measured parallel to the direction of the biggest member dimension), that due to high level of defects, location, conservation state or loading condition is considered as relevant to the purpose of the inspection.

grades from national standards to strength classes is provided by EN 1912 (CEN, 2012). Comparison between different visual strength grading standards from different countries has been widely researched (*e.g.* Almazán *et al.*, 2008; Muñoz *et al.* 2011). However, besides defining visual strength classes, an onsite inspection must also identify significant areas that, due to local damage, defectiveness or higher stress concentration, might pose as critical segments for the structural system.

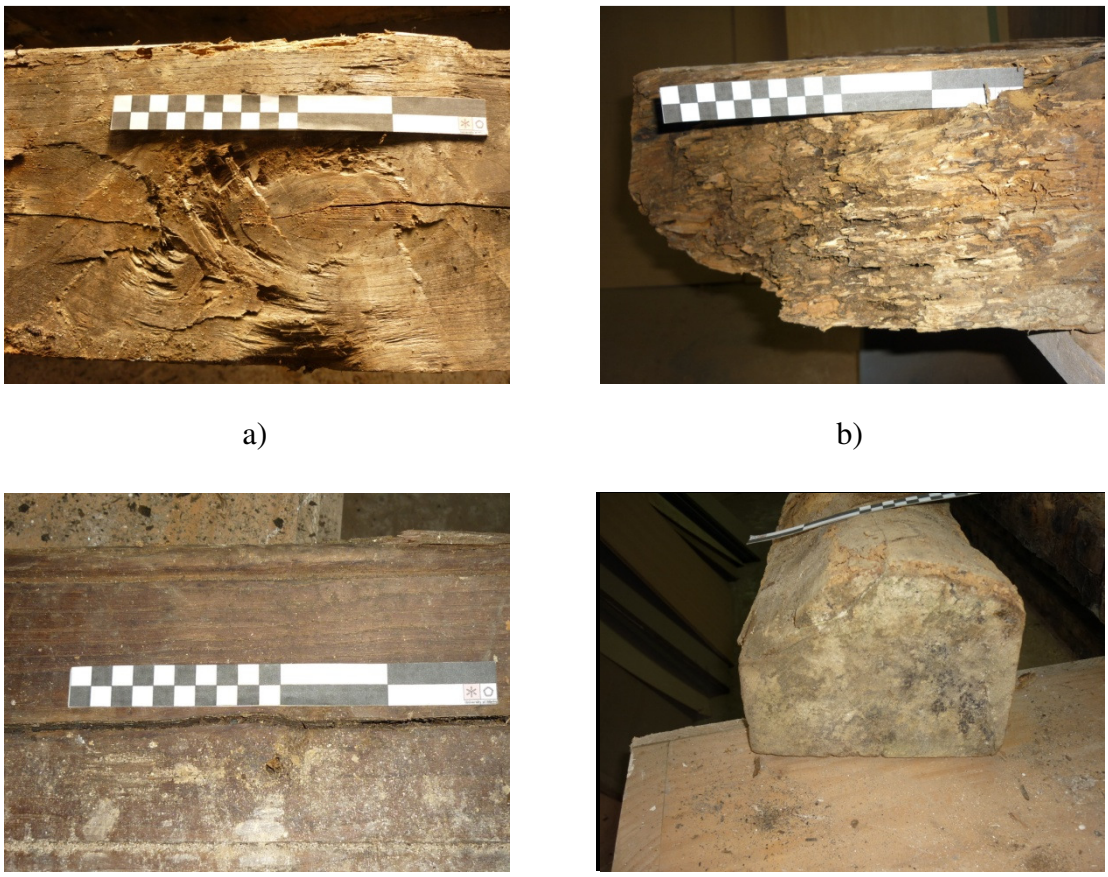

a) b)

c) d)

Figure 2.3: Example of common visually assessable timber defects and pathologies: a) knots; b) biological decay; c) fissures; d) wane.

The need to relate the presence of defects to the stress distribution in a member has, for instance, been pointed by the Italian standard UNI 11119 (UNI, 2004). According to that standard, an individual member may be given an unique strength class once the critical areas are identified. However, as mentioned by Branco *et al.* (2010), if the visual grading is based on the evaluation of local defects but the result is the assignment of the entire timber element to a specific strength class, this will lead to the loss of the evaluation of local defectiveness.

The standard UNI 11119 (UNI, 2004) establishes objectives, procedures and requirements for the diagnosis of the state of conservation and estimates the mechanical properties (resistance and stiffness) for structural wood elements present in cultural heritage buildings. Its methodological approach consists in the execution of a visual inspection and application of NDT. For visual strength grading of a single member, this

norm considers three classes (I, II and III) regarding onsite diagnosis for a given timber specie. The timber member is from a given class if it fulfils all the imposed requirements (Table 2.2), otherwise is graded as non-classifiable (NC). The complete inspection also requires a perfect and safe accessibility to the timber elements, a correct lighting and the cleaning of timber. Moreover, UNI 11119 (UNI, 2004) indicates values for the mechanical properties of different species of timber regarding its visual grade classes (see Table 2.3 for the case of chestnut timber).

Table 2.2: Grading rules for structural timber members in an onsite diagnosis as considered in UNI 11119 (UNI, 2004).

Parameter for classification		Class for onsite diagnosis		
		I	II	III
Wane[1)]		$s_w \leq 1/8$	$s_w \leq 1/5$	$s_w \leq 1/3$
Various defects; Cracks due to frost and Ring shakes		absent	absent	admissible in limited occurrence
Single knots[2)]		$A_d \leq 1/5$ $d \leq 50$ mm	$A_d \leq 1/3$ $d \leq 70$ mm	$A_d \leq 1/2$
Groups of knots[3)]		$W_d \leq 2/5$	$W_d \leq 2/3$	$W_d \leq 3/4$
Inclination of fibers (slope %)	in radial section	$\leq 1/14$ (≈7%)	$\leq 1/8$ (≈12%)	$\leq 1/5$ (20%)
	in tangential section	$\leq 1/10$ (10%)	$\leq 1/5$ (20%)	$\leq 1/3$ (≈33%)
Shrinkage radial cracks		admissible if not passing through the whole section		

[1)] s_w is the ratio of the wane oblique dimension and the height of the cross section;
[2)] A_d is the ratio of the minimal diameter d of the biggest knot, to the width of the element face;
[3)] knot clusters are evaluated through the ratio W_d of the sum of the minimal diameters of all knots, in a 150 mm range (or until the fibers are not realigned), to the width of the element face.

Table 2.3: Mechanical properties regarding the application of UNI 11119 (UNI, 2004), for 12% moisture content.

Class for on site diagnosis		Mechanical properties[1)] (N/mm^2)					
		compression		static bending	tension // to grain[2)]	shear // to grain	MOE in bending
		// to grain	⊥ to grain				
Chestnut (*Castanea sativa* Mill.)	I	11	2.0	12	11	0.8	10000
	II	9	2.0	10	9	0.7	9000
	III	7	2.0	8	6	0.6	8000

[1)] Applicable for the method of admissable stresses.
[2)] tension ⊥ to grain is conventionally assumed to be equal to zero.

Single knots are measured considering the ratio A_d of the minimal diameter d of the knot to the width of the element face, while knot clusters are evaluated through the ratio W_d of the sum of the minimal diameters t_k of all knots, in a 150 mm range (or until the fibers have not realigned to their normal direction), to the width of the element face. Wane

is measured considering the ratio s_w of the oblique dimension and the height of the cross section. General slope of grain is usually detected by means of a scribe, or when present, by measuring shrinkage splits on the longitudinal faces. Presence of biological attack is also identified and reported, and a residual cross section was defined accounting to the loss of material due to decay.

The Italian norm UNI 11035-2 (UNI, 2003b) identifies the most common wood species used in the Italian construction. For each case, it indicates the rules to use for a strength grading based in visual inspection regarding the prescriptions given in norm UNI 11035-1 (UNI, 2003a). Each element is classified regarding different requirements assessable by visual inspection and attributed a class. In case of hardwoods only a class *S* is considered (Table 2.4). If the elements fulfils all the imposed requirements it may be classified with that class and indicative values for strength and stiffness are given (see Table 2.5), otherwise the element is considered non-classifiable.

Table 2.4: Grading rules for visual inspection of hardwoods by application of UNI 11035-2 (UNI, 2003b).

Parameter for classification	Single class
	S
Wane	$s_w \leq 1/4$ and at each side of the section, for at least 2/3, should not have wane
Single knots	$A_d \leq 1/2$; $d \leq 70$ mm; $D \leq 150$ mm
Groups of knots	$W_d \leq 2/5$; $t_k \leq 70$ mm
Ring amplitude	no limitation
Density	$\rho > \rho_{min}$ (ρ_{min} = 395 kg/m^3 for *Castanea Sativa* Mill.)
Inclination of fibers	$\leq 1/6$
Fissure: - shrinkage - ring shake - lightning, ice, damage	 admissible in limited occurrence admissible in limited occurrence non admissible
Decay by white or brown fungi	non admissible
Tension wood	no limitation
Insect attack	admissible in limited occurrence
Ivy plant	non admissible
Deformation: - bow - crook - twist - cup	 10 mm every 2 m in length 8 mm every 2 m in length 1 mm every 25 mm in width no restriction

Table 2.5: Mechanical properties in the application of the UNI 11035-1 (UNI, 2003a), for different species hardwoods.

Broadleaves timber species and class regarding visual inspection / Mechanical properties (N/mm^2) and Density (kg/m^3)		Chestnut	Decidious Oak	Poplar and Alder	other Broadleaves
		Class			
		S	S	S	S
Bending strength (5-percentil)	$f_{m,k}$	28	42	26	27
Tension // to grain (5-percentil)	$f_{t,0,k}$	17	25	16	16
Tension ⊥ to grain (5-percentil)	$f_{t,90,k}$	0.5	0.8	0.4	0.5
Compression // to grain (5-percentil)	$f_{c,0,k}$	22	27	22	22
Compression ⊥ to grain (5-percentil)	$f_{c,90,k}$	3.8	5.7	3.2	3.9
Shear (5-percentil)	$f_{v,k}$	2.0	4.0	2.7	2.0
MOE // to grain (mean)	$E_{0,\,mean}$	11000	12000	8000	11500
MOE // to grain (5-percentil)	$E_{0,05}$	8000	10100	6700	8400
MOE ⊥ to grain (mean)	$E_{90,\,mean}$	730	800	530	770
Shear modulus (mean)	G_{mean}	950	750	500	720
Density (5-percentil)	ρ_k	465	760	420	515
Density (mean)	ρ_{mean}	550	825	460	560

Despite its invaluable importance, visual inspection is subjective and may even be inaccurate as evidenced in Huber *et al.* (1985), when inspectors achieved only 68% of the expected result in recognizing, locating and identifying defects in grading red oak lumber. Also Lychen (2006) refers that the quality yield for the automatic system was found to be between 52% and 75%, while manual grader only reached between 31% and 61%, comparing to the optimal grade defined by decision of several manual graders. Human visual inspection rarely achieves better than 70% performance in grading lumber (Silvén *et al.*, 2003). While Grönlund (1995) found that when grading boards into four grades, only 60% were assigned the same grade by two different expert inspectors. Regarding the subjectivity and effectiveness of visual inspection made by inspectors with different levels of expertise, statistical analysis was performed by Sousa *et al.* (2013), where it was found that the combination of information by different inspectors may improve the overall efficiency of the visual grading. Also, in the same study it was found that inspectors with more experience will tend to have lower variation of results within a visual grade and better differentiate between them.

Overall, the result of visual strength grading is the attribution of indicative values or allowable stress levels for indirect prediction of key properties which due to its correlation

to other properties, allow for the mechanical characterization of the material. For a more reliable prediction, complementary diagnostic methods based on NDT and SDT are necessary.

Pin penetration tests

Pin penetration tests, or also called pin driving tests, consist of releasing a steel pin of a fixed diameter into the material by a dynamic force (Figure 2.4). This dynamic force results from the release of a spring that transforms the elastic potential energy into impact energy, and in principle the measurements are free of operator bias (Cown 1978; Hansen 2000). The penetration of a metallic needle can be measured and the depth is inversely proportional to the density of the wood as found by Görlacher (1987). In the same study, correlation coefficients varying from 0.74 and 0.92 were found depending on number of measurements and species. Also the empirical relationships are affected by moisture content (Ronca and Gubana, 1998), and therefore it is convenient to adjust the test measurements to a common wood moisture content, such as 12%. Depth of pin penetration is also used as a measure to detect and define different degrees of degradation (Hoffmeyer, 1978; Zombori, 2001; Sousa *et al*., in press_a).

a)

b)

Figure 2.4: Pin penetration tests: a) example of a device; b) illustration of use.

Pin penetration tests are widely used for evaluating pole decay, or standing trees as well as sawn lumber density. Since it provides a fast and cheap response, and induces minor damage to the timber member, it results in an overall higher gain in the selection or culling of seedling seed orchards comparing to standard density measurements that require sample removal (Greaves *et al*., 1996).

Several researches have considered the measurements of pin penetration tests for prediction, through linear correlation, of timber's mechanical properties (Piazza and Turrini, 1983; Lourenço *et* al., 2007; Feio *et* al., 2007; Wu *et al*., 2010).

In Wu *et al*., (2010), the effectiveness of pin penetration tests for evaluating wood basic density and modulus of elasticity (MOE) was considered for eucalyptus clones in

standing trees. Moderate negative correlations were found with coefficient of correlation from -0.43 to -0.76 for density and of -0.59 to -0.66 for MOE, with better correlations when removing the bark layer. In the same study, the coefficient of variation for depth penetration ranged from 9.2% to 11.8% for measurements over the bark, whereas when removing the bark it ranged from 13.4% to 14.5%, evidencing the possible influence of bark thickness and branch cluster frequency. Similar coefficients of variation were also found in the study of other hardwoods by Wei (1997) ranging from 12.3% to 13.6%, and by Yin (2008).

In the study of small clear specimens of chestnut wood, Lourenço *et al.* (2007) found a correlation of depth penetration with density with coefficient of determination (r^2) of 0.78, and evidenced that the results were independent of the orientation of the annual growth rings and the wood age. However, it must be noted that penetration of the pin only comprised up to three annual rings and thus considerations to practical applications must be taken with caution. Ronca and Gubana (1998) found that the variability in measurements obtained in either radial direction or with less than 30º to the grain orientation, is less than 10%. The same authors also mention that with moisture content above 30%, differences between radial and tangential penetration decrease approximately 5 to 6%, whereas for low moisture contents the difference may increase up to 20%.

Lourenço *et al.* (2007) also concluded that a correlation of penetration depth with either MOE or strength in compression perpendicular to the grain, was inexistent. A better correlation with density was found by Feio *et al.* (2007) with a value of $r^2 = 0.91$, which also found moderate to low correlations with MOE and strength in compression parallel to the grain with r^2 of 0.43 and 0.37, respectively.

Despite its advantages, the prediction of density taken from pin penetration tests must be assessed carefully as the striker pin only penetrates a small part of the superficial layer of the element, thus it does not permit to assess the core of the element. On the other hand, a higher or smaller penetration may also be derived, as previously mentioned, from other factors rather than from density only, such factors may be the level of decay (timber quality) and moisture content. Nevertheless, this test allows to define superficial weak spots and also to give qualitative information about different cross sections if an adequate mesh of inspected values is guaranteed.

Drilling resistance tests

Resistance drilling is based on the micro-drilling of wood at constant cutting speed by a standard drill, either per cutting edge of a drill bit or per revolution, and measuring the required energy in the procedure. It is usually adopted to obtain density profiles and allows characterizing the full size of the specimen cross section (Rinn *et al.*, 1996). Depending on the relative energy change (either increase or decrease), this method allows to infer on internal defects of the member, such as inner voids, cracks, inclusions or decay. The method is relatively sensitive to changes in wood composition and is able to differentiate

between individual growth rings (Wang *et al*., 2003; Frattari and Pignatelli, 2005). In structural timber, which is mostly dry, small-diameter drilling points may tend to follow the curvature of the growth rings, resulting in measurement errors. This can be mitigated by increasing the stiffness of the drill bit by use of larger needle diameters (Kasal, 2010).

The mean levels of the drilling profiles were found to closely correlate with gross density of dry wood, with r^2 higher than 0.8 by Rinn *et al*. (1996). However, similar procedure indicated weaker correlations with values ranging from 0.21 to 0.69 (Isik and Li, 2004). Combining drilling resistance measurements and decay classes, Kahl *et al.* (2009) was able to increase the correlation with density and found a $r^2 = 0.73$.

An example of a drilling resistance profile is presented in Figure 2.5, where the horizontal axis of the profile measures the length of the drilling path and the vertical axis provides the power consumption of the device as a measure of drilling resistance. Here is clearly visible that resistance drilling measurements provides one-dimensional mapping. However, the combination of drilling measurements in different directions of the same cross section allows for a two-dimensional representation of the internal section (Calderoni *et al.*, 2010; Faggiano *et al*., 2011).

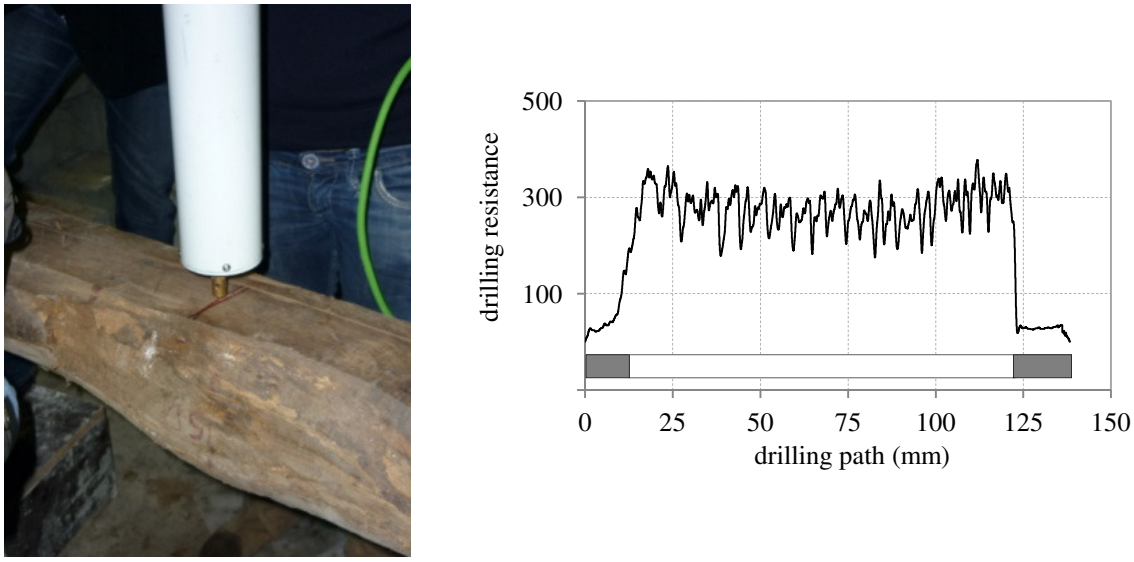

a) b)

Figure 2.5: Drilling resistance tests: a) illustration of use; b) output example in form of a typical drilling profile.

As considered by Feio (2005), the result of a drilling resistance test can be taken by the resistance measure (*RM*) given by the integral of the area beneath the resistance profile with respect to the length of drilling path, *h* (eq. 2.1).

$$RM = \frac{\int_0^h Area}{h} \tag{2.1}$$

With respect to *RM*, Feio (2005) showed a $r^2 = 0.81$ with for density of chestnut clear wood specimens. The same author, also presented r^2 correlating *RM* with MOE in compression of 0.61 for new timber and 0.67 for different fiber alignments, whereas in longitudinal compressive strength the r^2 with *RM* were 0.59 and 0.41 for new and old timber, respectively.

In Frankl *et* al. (2006), the *RM* was further refined with consideration of the diameter of the drill, *d*, resulting in the reducing parameter, *RP* (eq. 2.2), which allows for the comparison between results of equipments with different drill diameters.

$$RP = \frac{\int_0^h Area}{h \cdot d} \tag{2.2}$$

The major drawback in the use of these tests is that they are influenced by many factors, such as sharpness of drilling bit, direction of drill path in wood, angle of drilling tool against rings (Lear, 2005) and wood moisture content (Machado and Cruz, 1997). In Ukrainetz and O'Neill (2010), the sensitivity of drilling resistance tests were evaluated by seven experimental factors, where it was concluded that drill bit flexion (a measure of operator steadiness), moisture content of wood, and air temperature significantly affected the results, whereas influence of knots was minimized at a vertical distance of 3 cm and battery type, sharpness of the drill bit (at least up to 350 uses), and battery charge (at least up to 310 uses with a 12 V motorcycle battery) had no significant effect. Also, its local character in the evaluation of the member is a limitation (Bonamini, 1995; Emerson *et al*., 1998). Moreover, its onsite usefulness might be low for elements with larger thickness due to the increase of lateral friction of the needle and possible deviation of the drilling path, and full onsite access to both parallel sides of an existing element may not be possible.

Nowadays, the resistance drilling method is one of the most used methods for the assessment of existing timber structures, and several test campaigns were carried out using this technique, both in controlled laboratory conditions (Lourenço *et* al., 2007; Feio *et al*., 2007; HouJiang *et al.*, 2010), from members taken from the construction site (Branco *et al.*, 2010; Faggiano *et al*., 2011) and as well in onsite members (Medeiros, *et al*., 2010; Imposa *et al.*, 2012, Palanti *et al*., 2013).

Ultrasonic testing

Ultrasound method for testing timber is based on the physical principle that any wave causes the oscillation of the particles of the medium in which it propagates. This results in the oscillatory movement of the particles around its equilibrium position with decreasing amplitude due to the loss of wave energy. In the analysis of mechanical properties of wood the most favourable frequency range lies between 20 kHz and 500 kHz, mainly due to the high attenuation at higher frequencies timber (ASTM, 1989; Tanasoiu *et al*., 2002).

During the propagation in a given material, the ultrasonic wave may be reflected, absorbed or attenuated. However, a feature which remains unchanged is its frequency, whereas the intensity decreases with the distance to the transducer. In a material such as wood, defects are regarded as obstacles to propagation of ultrasonic waves and as such, in theory, the greater the number and significance of these defects the greater the loss of intensity. As such, the analysis and detection of discontinuities by ultrasonic testing has the choice of frequency as a primary condition. The wavelength, which is inversely proportional to the wave frequency, plays an important role in this choice, since in general, defects smaller than half the wavelength of the signal may not be detected. Thus, higher frequencies (smaller wavelengths) have a greater capacity for detecting smaller defects, however also have a higher attenuation. When the objective is to detect large discontinuities, a lower frequency should be adopted, especially if it is also required greater penetration of the ultrasonic wave (Kasal and Tannert, 2010). Also grain direction influences the wave propagation process such that, according to McDonald (1978), in hardwoods the propagation velocity can be three times higher in the parallel direction than in the perpendicular direction to the grain, thus allowing to assess and check for defects that led to deviations on the grain.

Depending on the relative position between the transmitting and receiving transducers and the element, different types of measurements are possible. In an overall sense, an indirect measurement is considered when the transducers are placed in contact with the same surface of the element, while a direct measurement is obtained when the transducers are placed in direct line but in opposite surfaces of the element (Figure 2.6). With regard to these different types of measurements, Machado *et al*. (2009) found a relative difference between measurements of approximately 10%, using 150 kHz frequency transducers, and also refers that a 40 cm distance between transducers for the indirect method results in lower relative difference.

Figure 2.6: Ultrasonic measurements: a) illustration of use; b) indirect measurement; c) direct measurement.

The last few decades have witnessed extensive research aimed at finding a hypothetical correlation between the propagation of elastic waves in a timber member and its mechanical properties. One of the most common indicators calculated from the

ultrasonic measurements is the dynamic modulus of elasticity, E_{din}, which for prismatic, homogeneous and isotropic elements, and for those with a section width smaller than the stress wavelength, is determined through the relation:

$$E_{din} = v_p^2 \cdot \rho \tag{2.3}$$

where, E_{din} is the dynamic modulus of elasticity (N/mm^2), v_p is the propagation velocity of the longitudinal stress waves (m/s) and ρ is the density of the specimen (kg/m^3).

For practical purposes, the relation between the dynamic modulus of elasticity and the static value is particularly relevant ($E_{din} \geq 0{,}9 \cdot E_{sta}$) and explained by the viscous-elastic behaviour of wood (Bonamini *et al.*, 2001). Generally a linear relation is adequate (U.S. Forest Products Laboratory, 1999; Bonamini *et al.*, 2001):

$$E_{sta} = K \cdot E_{din} = c_1 \cdot E_{din} + c_2 \tag{2.4}$$

where K is a proportionality constant dependent of the timber species, while c_1 and c_2 are constants depending on the material in analysis.

The use of ultrasonic method for estimating the mechanical properties of existing timber elements is found in many studies concerning conifers. Regarding the static modulus of elasticity, in Sandoz (1985), measurements by ultrasonic technique resulted in a coefficient of correlation higher than 0.80, while by measuring the E_{din}, r^2 above 0.75 were also found (Oliveira *et* al., 2003; Divós and Tanaka, 2005; Machado and Palma, 2011). In Machado *et al.* (2003a), the measurement analysis of wave propagation velocity resulted in r^2 of 0.48 and 0.69 with the compressive strength parallel to the grain for indirect and direct measurements, respectively.

In the case of hardwoods, Lourenço *et al.* (2007) showed that E_{din} was strongly correlated with some mechanical properties of chestnut clear wood specimens, presenting coefficients of determination above 0.71 and 0.74 respectively, for obtaining the strength and MOE in compression perpendicular to the grain. However, for similar sampling conditions but for the parallel to the grain direction, Feio *et al.* (2007) presented r^2 above 0.39 and 0.60, for compression strength and MOE, respectively, and r^2 above 0.27 and 0.58 for tension strength and MOE, respectively.

Besides being used in clear wood samples, ultrasonic measurements are also applied to identify different stages of decay propagation (Lee and Bae, 2004; Sousa *et al.*, in press_a).

Although it is an easy to use technique, its application onsite presents several difficulties often combined with large variation on results within a same member. The wave propagation velocity is influenced by several parameters, such as wave frequency (Bucur and Feeney, 1992; Bucur and Böhnke, 1994), pressure applied by the user (Biernacki and Beall, 1993; Emerson *et al.*, 1999), contact between transducers and the

element, as well as coupling material (Machado, 2000; Beall, 2002), among others. The natural variability of wood and presence of defects should be added to the uncertainty and variability of the measurements.

Small size specimens

The use of NDT are often complemented with information taken from SDT based on the evaluation of small size specimens. These small dimension specimens are extracted from the timber element and allow to bridge the gap between indirect NDT information with the direct fully destructive methods of strength and stiffness assessment. To that purpose, specimens are chosen from clear wood segments with sufficient distance from natural defects in order to avoid their influence.

Common forms of extracting these specimens are made by core drilling or in form of mesospecimens. Core drilling is a semi-destructive method where cores of small diameter of about 5 mm are extracted from members (Kasal and Tannert, 2010), whereas mesospecimens can be obtained by cutting a small volume of wood with diagonal cuttings parallel to the grain (Brites *et al.* 2012). The specimens taken from either method, allows to test wood's mechanical properties and its variation (Table 2.6), instead of only predicting. However, they must be followed by a combination of other methods in order to evaluate the full-scale timber element (Tannert *et al.*, 2013).

Table 2.6: Variability of properties of small clear wood specimens (Burley *et al.*, 2004).

Property	Coefficient of variation (%)
Bending strength	7-20
Modulus of elasticity in bending	9-23
Impact bending	25
Compression parallel to grain	8-29
Compression perpendicular to grain	28
Side hardness	20
Shear parallel to grain, shearing strength	14-22
Tension parallel to grain	25
Toughness	34

Small diameter cores are generally extracted from members and tested in compression, but a variety of properties can be established including density, moisture content, MOE and other strength properties (Kasal and Tannert, 2010). For instance, MOE and compression strength along the grain of clear wood, were obtained through these technique by Rug and Seemann (1991) and Kasal (2003).

In Kasal *et al.* (2003), the results obtained with core sampling and through testing of samples regarding the American Society of Test Materials (ASTM) D 143-94e1 specifications (ASTM, 2000a), were compared in compression and tension testing. A

strong relationship was obtained between the different procedures for compression strength and MOE with r^2 of 0.89 and 0.76, respectively. Correlation within the core compressive strength and tension strength obtained by ASTM specimens was lower, providing only a r^2 of 0.67. Kasal and Tannert (2010) refer that these differences may be related to the amount of early and latewood present in the ASTM sample, as the cross section may not be sufficiently large to remove the bias of early and late wood effect.

It is also noted that loading methods and failure modes are significantly different. Bending is often the predominant loading mode for structural timber members, however it is not easy to estimate bending strength or stiffness onsite. Correlations with bending strength are known to be stronger with tension strength rather than to compression strength. However, correlation between compression and tension strength of cores are often low, thus it is useful to obtain information about tension strength by use of mesospecimens.

In Kasal and Anthony (2004) it was mentioned that the experimental and equipment design is such that the cross sectional area of the tension micro-specimens are comparable to the cross sectional area of the standard ASTM tension specimens for small clear wood, and therefore no correlation was needed for comparison to the standard tests. However, in Brites *et al.* (2012), the regression curves obtained for MOE, when comparing mesospecimens obtained through a new extraction technique and standard clear wood specimens, showed a r^2 of 0.53 and 0.67 for maritime pine and chestnut, respectively. For the same study and regarding tension strength, lower r^2 of 0.25 and 0.45 were found for maritime pine and chestnut, respectively. With these results it was concluded that the piece geometry and/or grip conditions of specimens have an important influence on the results.

The disadvantages of these techniques, compared to NDTs, are that measurements are often costly in terms of manpower and money because they involve extraction and processing of specimens. Another important factor is that extraction of specimens are restricted to only a few samples to avoid over damaging the timber element. When considering these techniques, random sampling of the member location for extraction of specimens should be taken into account in order to obtain an accurate representation of the member strength (ASTM, 2000b; Kasal and Tannert, 2004).

2.1.2 Destructive testing

The direct assessment of mechanical properties of a structural size timber element can only be obtained through destructive testing, which for the assessment of existing timber structures is, more than often, not a valid option. However, in specific cases, it may be required that a precise mechanical characterization is obtained. In that case, selected members of the structure may be taken and mechanically characterized, even if the results have to take into account for a significant variation within different members of the same structure.

In the scope of this work, destructive tests were made regarding the calibration of models and also in order to obtain a database for property correlation. The specifications of the European norm EN 408 (CEN, 2010a) were considered. This norm specifies laboratory methods for determination of physical and mechanical properties of timber in structural sizes. Although this norm is not intended for grading or quality control, it provides a standardized framework to obtain basic material properties that may be complemented with grade determining features, given for instance by visual inspection, for strength class grading.

For bending, this norm suggests the determination of a local modulus of elasticity, $E_{m,l}$, and of a global modulus of elasticity, $E_{m,g}$. The $E_{m,l}$ is measured in a central distance, while the $E_{m,g}$ is measured along the full span of the beam between supports. Bending strength is obtained attending the maximum load applied in a 4-point bending test. Discussion about 4-point bending tests is given in Brancheriau *et al.* (2002) while a comparison between $E_{m,l}$ and $E_{m,g}$ is addressed in Boström (1999) and Solli (2000).

Test piece geometry and procedures to obtain stiffness and strength parameters for compression and tension parallel to the grain are also proposed in EN 408 (CEN, 2010a) for structural size cross sections, whereas ASTM D143-94e1 (ASTM, 2000a) is considered for small clear wood specimens.

Comparison and correlation of destructive testing with NDT has long been subject of study (Barlett and Lwin, 1984), and still nowadays several efforts are employed for estimating the mechanical properties of timber by a combination of NDT and destructive testing (Branco *et al.*, 2011; Calderoni *et al.*, 2011; Faggiano *et al.*, 2011; Ramundo *et al.*, 2011, Sousa *et al.*, 2012).

2.1.3 Structural grading

Structural grading is the process by which timber is divided into groups (grades) that, in theory, possess similar structural properties. Structural grading may be performed using different techniques, such as: visual stress-grading, machine stress-grading or machine proof-grading.

Initially, grading rules were implemented as a method to select and sort lumber within the sawmill production. Only after, these rules were applied for the evaluation of timber members in existing structures. Several efforts have been made in different countries to develop standards and guidelines that would allow for a consistent procedure for grading timber onsite. To achieve a significant level or reliability, these methods must ensure consistency and allow for repeatability of results, however, they are still not able to satisfactorily meet the full variety of different structural situations and local specifications. Usually these rules are, therefore, based on either industrial procedures or national standards.

Visual grading is the traditional process, through which a trained inspector/grader examines each piece of timber and attributes a classification regarding visually assessable parameters. Visual inspection is undertaken with consideration to the species of wood and to visual grading standards, which define rules as to characterize different types, size and position of physical characteristics that are allowed into each structural grade. Natural defects, such as knots, grain misalignment, decay, among other potential strength reducing characteristics, are often considered as limiting parameters according to their extent and number. In this basis, the highest grades allow fewer and smaller characteristics that may decrease the mechanical performance of the timber element. For example, in chestnut timber, knots are the most relevant characteristic regarding strength downgrading (Bonamini *et al.*, 1998; Vega *et al.*, 2012). A grading protocol for lumber and timber on historical structures was proposed in Anthony *et al*. (2009), which also accounted for visually assessable parameters.

In Portugal, there is a lack of guidelines and standards regarding the visual stress-grading of timber elements onsite. In the case of grading elements in a sawmill before being used in construction, visual stress-grading is established for *Pinus pinaster* by NP 4305 (IPQ, 1995). In that standard, two structural grades are proposed corresponding in terms of mechanical properties attributes to classes C18 and C35 of EN 338 (CEN, 2009). However, for hardwoods still low information is available. In Spain, *Eucalyptus spp*. is the only hardwood structurally characterized (Golfín *et al.*, 2007) and included in the Spanish visual grading standard UNE 56546 (AENOR, 2011) and in the European system of strength classes from visual grading by species EN 1912 (CEN, 2012). Spanish chestnut has not yet been included in this standard, however Vega *et al.* (2013) proposed a visual grading criteria for this specie. Chestnut timber from Italy has recently been included in the National Grading Standard UNI 11035-2 (UNI, 2003b) and incorporated in European standard EN 1912 (CEN, 2012), being allocated to strength class D24 (Brunetti *et al.*, 2009).

Machine stress-grading is based on the results of bending tests made to each piece of timber (generally about its minor axis), performed by a machine automatic process. The machine measures the stiffness of the piece and uses an inputted correlation between stiffness and strength to assign a stress grade. The obtained value of stiffness may also be used to infer other structural properties, including tension, compression and shear strength. Machine stress-grading results in the sorting of timber on the basis of measured structural properties and thus is often perceived as more objective and efficient than visual grading methods. Modern grading machines are computer controlled and allow for the allocation of a grade to the whole timber piece based on the lower stiffness found along the length of the element. Overall, this technique allows for a better distinction and separation between different grades, with lower overlap of stiffness between adjacent grades. Also, it was concluded by Stapel and Kuilen (2013) that, when grading into more than two strength classes, machine stress-grading requires lower material safety factors than visual stress-grading, as the latter presents higher coefficients of variation of the graded materials. However, machine stress-grading is influenced by the correlation used for strength

prediction which can sometimes be low, and consequently a larger overlap between the strength properties between grades may be achieved. After machine stress-grading, qualified graders inspect the elements visually and can downgrade the piece of timber if necessary.

Although not as common as the visual grading and machine stress-grading, proof-grading is also performed by several mills to certificate the quality of their products. Proof-grading initiates with a preliminary sort of timber into different groups, regarding an accepted grading method. After, each sorted group is tested by application of a predetermined bending load, known as the proof load. Each target stress grade has its specific proof test. Loading is applied until reaching its proof stress value.

The main differences with machine-stress grading concern the loaded axis, the method to define weak sections and the speed of operation. Proof-grading often considers loading of the major axis (on edge), while machine stress-grading considers the minor axis (on flat). Proof-grading also considers higher values of loading and finds weak sections by its failure, whereas machine stress-grading considers lower values of loading and finds weak sections by the presence of segments with lower stiffness. Due to these differences, proof-loading is a slower process than machine stress-grading.

2.2 Semi-deterministic and safety factor methods

Full deterministic procedures do not take into account the variability of either demand (load and exterior effects) or resistance (material stiffness, strength, geometry and structural configuration), and the uncertainty related to both parameters are provided by a single global safety factor. Although this procedure was firmly established on the past, nowadays it is considered obsolete for the evaluation of structural safety (Neves and Cruz, 2001). Current methods and procedures for assessment and evaluation of structural safety are based on semi-deterministic approaches, such as the "safety factor" and the "partial safety factor" procedures. Within these procedures, safety is expressed as a deterministic measure since it results from the consideration of fixed (deterministic) values for both demand and resistance, usually considering the mean or characteristic values of those parameters. To that scope, values for resistance and demand are taken conservatively, such that, demand estimation is considered as sufficiently high and, the resistance estimation, as sufficiently low, to ensure an adequate safety level.

A common method to define structural safety is by means of the safety factor, which is usually associated with elastic stress analysis requiring that (Köhler, 2007):

$$s_{\mathrm{i}}\left(\psi_{\mathrm{g}}\right) \leq s_{\mathrm{pi}} \tag{2.5}$$

where s_{i} (ψ_{g}) is the i^{m} applied stress component calculated at the generic point ψ_{g} in the structure, and s_{pi} is the allowable stress for the i^{th} stress component. The allowable stresses

s_{pi} are commonly derived from the reduction of the material strength as the ultimate moment, tension or compression stresses, s_{ui}, by the consideration of a safety factor ϕ_r:

$$s_{pi} = s_{ui}/\phi_r \tag{2.6}$$

This safety factor may be selected taking into account results from empirical observations, prior experience, economic and social consequences. In this case, failure of a structure is considered when the calculated i^{th} elastic stress s_i (ψ_g) component is equal to the local permissible stress component s_{pi}.

Another, common method to define structural safety is the load and resistance factors, which is actually a derivation from the allowable stress format. In this method, the limit state function can be expressed at the level of stress resultants as (Köhler, 2007):

$$\frac{z_d \cdot r_k}{\gamma_R} = \gamma_G \cdot s_{G,k} + \gamma_Q \cdot s_{Q,k} + \ldots \tag{2.7}$$

where r_k is a characteristic member resistance, γ_R is the partial factor on r_k and $s_{G,k}$, $s_{Q,k}$ are the characteristic permanent and variable load effects, respectively, with associated partial factors γ_G and γ_Q, and z_d is the design value. Characteristic values are commonly defined in design codes, corresponding to fractile values of the underlying distribution of the associated parameter.

In Europe, the Eurocode 5 describes several procedures based on the concept of limit states (both ultimate and serviceability) and partial safety factors, for the design of new timber constructions. In this case, the properties of timber are selected in correspondence to a selected stress-grading technique and, then, the design values are derived from the mechanical properties of each specific grade or class. The uncertainty on the material properties is considered by use of characteristic values for the mechanical properties, taken as the 5^{th} percentile of its probability distribution, and by the application of a safety factor for the material property, γ_M. This safety factor also takes into account the model uncertainties, dimensional variations and the possibility of an unfavourable deviation from the characteristic value.

In Eurocode 5, the design value for wood strength also takes into account the effect of moisture content and load duration by use of different partial safety factors, as:

$$X_d = \frac{k_1}{\gamma_M} \cdot X_k \cdot k_h \tag{2.8}$$

where X_d is the design value of a material property, k_1 is the partial safety modification factor taking into account the effect of load duration and moisture content, that can be either $k_1 = k_{mod}$ for strength or $k_1 = 1/(1 + k_{def})$ for stiffness properties, γ_R is the material

partial safety factor, X_k is the characteristic or mean value of timber strength or stiffness, respectively, and k_h is a size factor.

Although its simplicity of use, the procedure of Eurocode 5 may not be recommend to existing timber structures evaluation as it may be over-conservative, regarding traditional construction techniques. As mentioned by Machado *et al.* (2011), in the case of onsite timber elements, a factor considering the conservation level of the structures, k_{con}, regarding degradation by fungi or insects with implication in the reduction of the material properties, and a factor considering aging, k_a, regarding the physical and mechanical deterioration of the timber materials due to time in service, should also be considered, as:

$$X_d = \frac{k_1}{\gamma_M} \cdot X_k \cdot k_h \cdot k_{con} \cdot k_a \tag{2.9}$$

where k_{con} is the partial safety factor for reduction of wood properties due to conservation level, and k_a is the partial safety factor for reduction of wood properties due to time in service.

Aiming at the definition of the mechanical properties of existing timber structures, Machado *et al.* (2011) also evidences the procedure outlined in Figure 2.7, which combines the evaluation of the mechanical properties by stress-grading with the use of modification factors in a comparable procedure to the Eurocode 5.

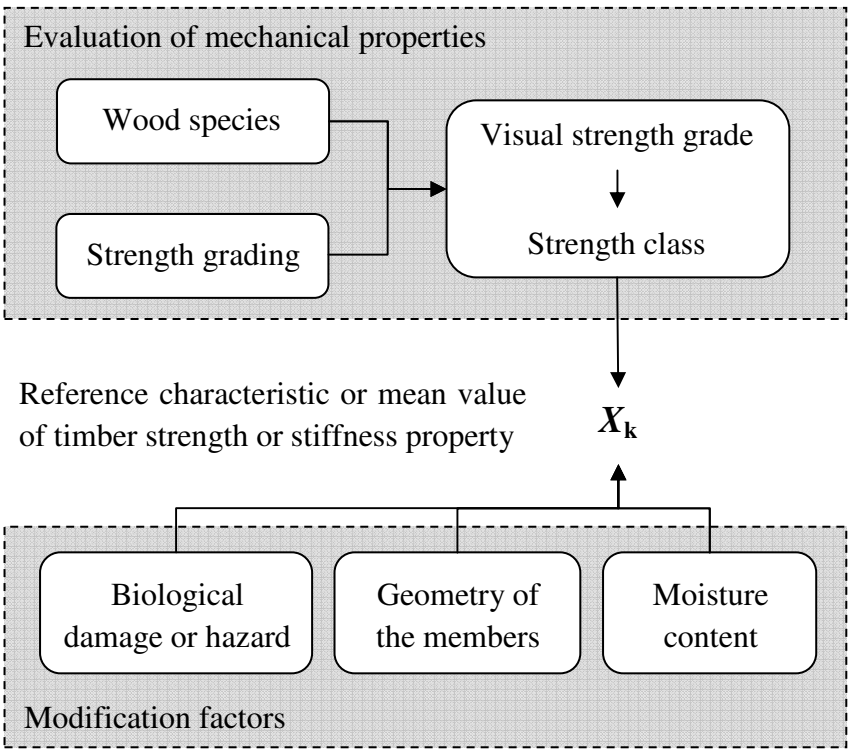

Figure 2.7: Current factors used to define the mechanical performance of timber elements onsite (adapted from Machado *et al.*, 2011).

2.3 Reliability assessment

In the past decades, an increasingly interest in reliability for civil engineering structural concepts is visible, mainly to higher computational performances and lower time costs that are now available. Also the possibility of implementing a certain degree of randomness and uncertainty to structural problems, when considering a stochastic analysis, is also an advantage. Generally, the probabilistic design method may be considered more rational and consistent than the partial factor design and, as mentioned by Vrouwenvelder (1997), there is a tendency to use probabilistic methods not only as a background for codes, but also directly in the assessment of special or important existing structures, as well as under design.

The concept of structural reliability may be defined by the evaluation of the probability of a determined limit state function being violated. The basic reliability problem may essentially be assumed, in probabilistic terms, to be how a certain structure will perform its functions, on a specific period of time and according to defined conditions (Schneider, 1997). Thus, it is possible to define a probability of failure, p_f, as the complementary probability to the definition of reliability, consequently obtaining a quantifiable parameter for the evaluation of a structure's safety.

In a structural reliability problem, the random variables that define and characterize the behaviour of the structure are called basic variables (*e.g.* cross section dimensions, density, strength values, applied loads). When choosing the necessary basic variables in order to define a given problem, one must try to find independent variables, although that is not always possible. Modelling of these variables is possible through probability distributions depending on the available information about them, and also their statistical parameters have to be chosen carefully. After obtaining a structural model, this must be confronted with existent information so it can be improved or revised. In the eventuality of insufficient information to describe the probabilistic function or to corroborate the proposed model, one might use a representative expected value, so-called estimate point or, of most likelihood.

The failure of a structural element is considered when the value of its resistance R is exceeded by the value of the load effect S resultant of a determined loading Q, on that specific element. Therefore, p_f may be assumed as the probability that the structural resistance R, modelled by a random variable with a known probability function $f_R(r)$, being inferior or equal to the load effects S, equally modelled by a random variable with a known probability function $f_R(s)$. According to this definition, the probability of failure may be expressed by one of the following ways (Melchers, 1999), which also shows that the limit state function can be formulated in different mathematical ways:

$$p_f = P(R \leq S) \tag{2.10a}$$

$$P(R - S \leq 0) \tag{2.10b}$$

$$P(R / S \leq 1) \tag{2.10c}$$

$$P(\ln(R) - \ln(S) \leq 1) \tag{2.10d}$$

$$P[g(R,S) \leq 0] \tag{2.10e}$$

where $g(\ )$ defines the limit state function which probability of violation is identical to the probability of failure. The safety margin M is consequently stated by:

$$M = R - S \tag{2.11}$$

When both R and S are given by normal random variables, with means μ_R and μ_S and variances σ_R^2 and σ_S^2, respectively, the probability of failure according to Cornell (1969) may be stated as:

$$p_f = \Phi\left[\frac{-(\mu_R - \mu_S)}{(\sigma_S^2 + \sigma_R^2)^{1/2}}\right] = \Phi(-\beta) = 1 - \Phi(\beta) \tag{2.12}$$

where $\beta = \mu_M/\sigma_M$ is defined as reliability index and $\Phi(\ )$ represents the standard normal distribution function. In this case, it is visible that p_f increases when either one of the variances increase or when the difference between means of R and S decreases.

The basic concept of structural reliability accounting the random variables R and S with respective distributions $f_R(x)$ e $f_S(x)$, is presented in Figure 2.8, as well as the distribution that characterizes the safety margin M, where the failure region $M \leq 0$ is presented in shadowed.

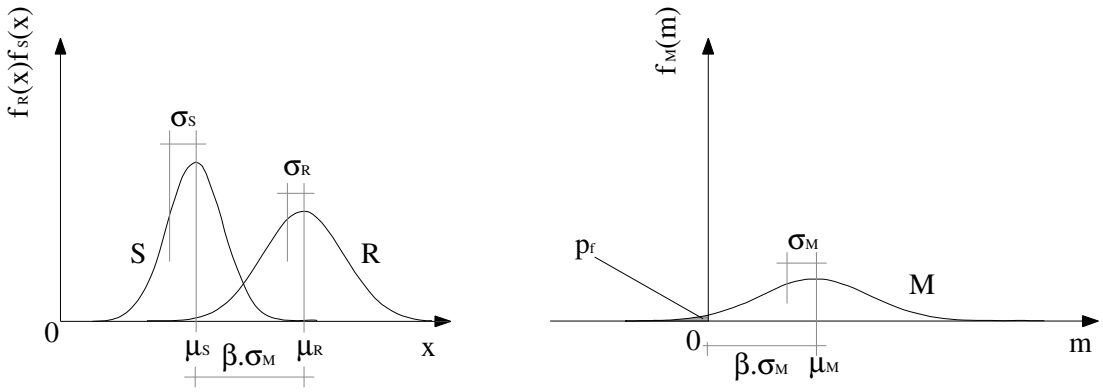

Figure 2.8: Structural reliability basic problem and safety margin distribution (adapted from Schneider, 1997).

Through the graphical representation of the reliability index β, its definition can be inferred as the number of times the standard deviation may be included between the mean of M and the origin. The relation between β and p_f, according to Equation 2.12, is shown for different values in Table 2.7.

Table 2.7: Relation between β and p_f according to Equation 2.12.

Probability of failure: p_f	10^{-1}	10^{-2}	10^{-3}	10^{-4}	10^{-5}	10^{-6}	10^{-7}
Reliability index: β	1.28	2.32	3.09	3.72	4.27	4.75	5.20

When the stochastic variables are non-normally distributed or the failure function is not too non-linear, the probability of failure may be stated as:

$$p_f = P(g(X) \leq 0) \cong \Phi(-\beta) \tag{2.13}$$

where $\Phi(\ )$ is the standard normal distribution function.

The stochastic reliability methods due to their probabilistic nature, when applied to structural engineering problems, allow considering a large amount of information about the basic variables involved in the safety assessment of an existing structure. In structural reliability applications, often is necessary to consider the characteristic values of demand and resistance, and thus in the large majority of cases the solution is found in the probability distribution extremes. This type of problems is usually denominated as tail sensitivity problem. Accounting this premise, it is verified that p_f is extremely sensitive to the probabilistic parameters chosen for the probability distribution, and thus the importance of correctly define and calibrate the probabilistic model according to the existing data.

Regarding the assessment of timber components, Köhler *et al*. (2007) considered an ultimate limit state equation for a cross section subjected to stress in one particular direction, as:

$$g = z_d \cdot R \cdot X_M - \sum_i S_i \tag{2.14}$$

where z_d is a design variable, *e.g.* cross section area, R is the resistance, *e.g.* tension strength and bending moment capacity, ΣS_i is the sum of all possible load effects, *e.g.* axial stresses, X_M is the model uncertainty.

Also, serviceability limit state equation (Köhler *et al*., 2007), such as when a deflection exceeds an allowable deflection limit, can be expressed as:

$$g(t) = \delta_L - W_\Delta\left(\sum S_i, E_{0,mean}, t\right) \cdot X_M = 0 \tag{2.15}$$

where δ_L is the allowable deflection limit, $W_\Delta\left(\sum S_i, E_{0,mean}, t\right)$ is the deflection in time t, dependant on load effects $\sum S_i$ and modulus of elasticity $E_{0,mean}$.

In order to design both for ultimate and serviceability limit states, diverse target reliability indices are established for various structural situations by considering different consequence classes, reference periods of time and relative cost of safety measures. The European standard EN 1990 (CEN, 2002), also known as Eurocode 0, refers three

reliability classes RC1, RC2 and RC3 associated with three consequence classes CC1, CC2 and CC3. The definition of the three reliability classes is given in Table 2.8, and the correspondent minimum target values for the reliability index β regarding ultimate limit states are stated in Table 2.9. RC is normally related directly to CC.

Table 2.8: Definition of consequence classes (adapted from CEN, 2002).

Consequence classes	Description	Examples of buildings and civil engineering works
CC1	Low consequence for loss of human life, and economic, social or environmental consequences small or negligible	Agricultural buildings where people do not normally enter, greenhouses
CC2	Medium consequence for loss of human life, economic, social or environmental consequences considerable	Residential and office buildings where consequences of failure are medium
CC3	High consequence for loss of human life, or economic, social or environmental consequences very great	Grandstands, public buildings where consequences of failure are high

Table 2.9: Recommended minimum values for reliability index β for ultimate limit states (adapted from CEN, 2002).

Reliability Class	Minimum values for β	
	1 year reference period	50 year reference period
RC1	4.2	3.3
RC2	4.7	3.8
RC3	5.2	4.3

2.3.1 The Probabilistic Model Code

When performing a full probabilistic analysis, often insufficient data is available to make objective estimates and, consequently, subjectivity is increased in the procedure. To that purpose, there is a need for codes which allow and provide a sufficient guidance in terms of probabilistic models. Therefore, these codes should (Vrouwenvelder, 1997):

- provide a complete and consistent set of models and methods allowing for a probability based decision and design;
- be written in a code-type manner, such that unique solutions for each problem are anticipated, and where physical or statistical evidence is not sufficient to provide unique solutions, rules should be specified on the basis of agreement;
- be an operational guideline intended for use in the context of probability based expertise.

In this scope, the Joint Committee for Structural Safety, JCSS, proposed the elaboration of a probabilistic based code after several preliminary studies (JCSS, 2000). In the past decade, the JCSS issued a document regarding the probabilistic model code (PMC) for timber structures, where stochastic resistance models for timber as a construction material are specified (JCSS, 2006). The stochastic models that characterize the mechanical properties of timber are described in that document, where from the knowledge of some specific properties, considered explicitly, one may obtain the others implicitly. Therefore, a full and precise application of this code requires the capability to predict these properties. The explicitly considered properties are defined as reference properties or also so-called key properties. These properties are generally chosen in accordance with visual stress-grading (Machado *et al*., 2011) or from tests carried with similar material (Toratti *et al*., 2007). In the case of the PMC, these properties are the bending strength f_m, bending modulus of elasticity E_m, and density ρ_m. The other resistance properties of timber can be defined based in the key properties through empirical expressions.

The models and values present in the PMC (JCSS, 2006) are intended as generic models in the case no further detailed information is available. If further information is obtainable, the information in the code may be considered as the prior information in a Bayesian updating process.

2.3.2 Hierarchical Modelling

Research on multi-scale hierarchical modelling has evidenced increased interest in the field of mechanics in the recent decades, and also in the field of wood products and timber engineering. One of the main motivations for hierarchical modelling is to understand how properties, composition and structure at lower scale levels may influence and be used to predict the material properties on a macroscopic and structural engineering scale (Burgert, 2006; Salmén and Burgert, 2009; Hofstetter and Gamstedt, 2009).

Hierarchical levels

Wood is a natural material that by itself has its own hierarchical structure, comprising its cellular components (Lakes, 1993). In this case, the hierarchical order of wood (as a solid material structure) is defined as the number of levels of scale with recognized structure.

Hierarchical modelling requires the distinction and differentiation between different scales, such that a homogenization step may be taken to each of those scales in order to define similar properties within a given scale (Hofstetter and Gamstedt, 2009). In a microscopic level, multi-scale modelling can be considered by linking ultra-structural composite models, laminate cell wall models, cellular mechanics and layered models for the early wood and latewood structure. Although simpler for softwoods, the strong influence of ray cells makes the hierarchical modelling more difficult for hardwoods (Badel and Perré, 2007). In an analogous way, the presence of defects such as knots makes

the analysis on the structural macroscale even more difficult, often requiring the need for detailed finite element models that account for inhomogeneities (Foley, 2001). In these cases, special attention should address the problem of separating distinct levels (or segments) with different length scales, when influenced by structural defects.

In Köhler (2007), the hierarchical levels of timber were defined regarding the structural member as the main unit of analysis. In that case, three levels were defined: micro (material), meso (local) and macro (global). The description of each one is given, from higher to lower size scale, as follows and also represented in Figure 2.9:

- macro level: refers to timber of different origins and graded in different grading schemes into specific grade classes. Each single timber grade may evidence differently distributed material properties and the variability of the distribution parameters represent a global parameter variable. Parameter variations may also be due to statistical uncertainties;
- meso level: refers to the variations between timber test specimens or components of one specific sub-population. Parameter variation may be reduced by information from mechanical tests, where the scale of the test specimens is in the same order as the size of a structural member;
- micro level: includes the representation of the inhomogeneities and irregularities in the timber material itself. The natural variability of timber, such as random distribution of knots and grain deviation, is included in this level often by distinguishing clear wood segments and weak sections.

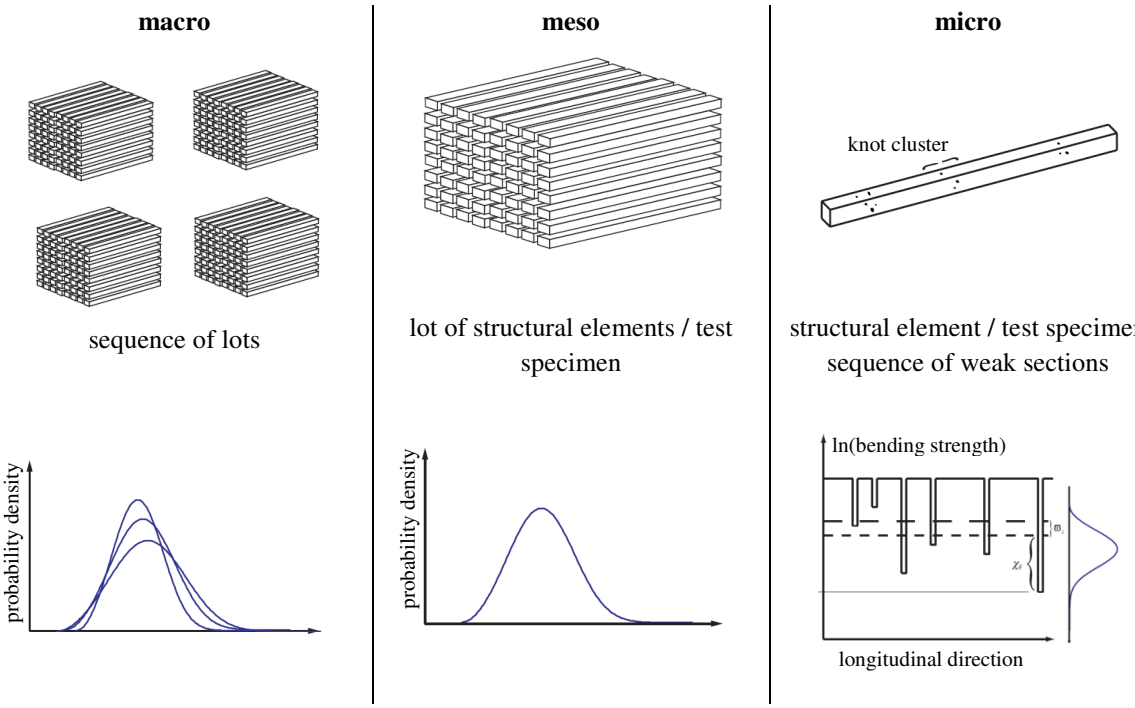

Figure 2.9: Different scales of modelling for timber material properties (adapted from Köhler, 2007).

Spatial variability

At the micro level described by Köhler (2007), several attempts have been made to hierarchically model the stiffness and strength of timber members, by considering the presence of weak sections separated by segments of clear wood (Riberholt and Madsen, 1979; Isaksson, 1999; Fink and Köhler, 2011; Machado and Palma, 2011).

In Riberholt and Madsen (1979), it is mentioned that low bending strength and stiffness are prone to coincide with the presence of knots or group of knots. Therefore, it was assumed that failure would inevitably occur in such one of those individual weak sections. According to that premise, an idealized model is proposed assuming the discrete distribution of knots and group of knots as the discrete distribution of weak sections that are separated by strong segments of clear wood (Figure 2.10).

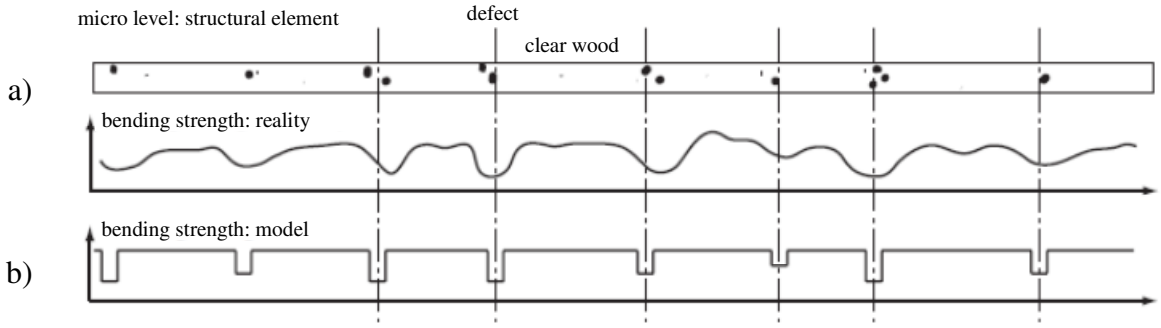

Figure 2.10: Bending strength of a timber beam: a) implied reality; b) proposed model (adapted from Riberholt and Madsen, 1979 and Köhler, 2007).

In this model, the strength of weak sections is equicorrelated, meaning that the correlation between the strength of weak sections is independent on their distance over the length of the structural element. Also, the failure of the element is considered equal to the failure of one of the individual weak sections, therefore evidencing a series system behaviour (Ditlevsen and Källsner, 1998). The strength of the weak sections is modelled by a random variable considering the measurements of indirect indicators (such as bending stiffness) or by existing strength tests according to EN 408 (CEN, 2010). Meanwhile, the location of the weak sections is determined by a Poisson process attending to direct measurements of the distances between knots.

The mentioned model was later applied for the variation of bending strength properties by Czmoch (1991), regarding the length and load configuration effects on beams. However, it was concluded that the available experimental information was unable to verify the parameters of the proposed model. This problem was further addressed by Isaksson (1999), where a model was proposed for evaluation of bending strength within and between members. As mentioned previously, timber properties present spatial variability, thus the value of strength in one point of an element may not be the equal when compared with another point of the same element. Following in a model proposed by Isaksson (1999), the bending strength $f_{m,ij,}$ at a particular point j in the component i of a structure/batch has a lognormal distribution and is given as:

$$f_{m,ij} = \exp\left(\nu + \varpi_i + \chi_{ij}\right) \tag{2.16}$$

where ν is the unknown logarithm of the mean strength of all sections in all components (see Figure 2.11a), ϖ_i is normal distributed with mean value equal to zero and standard deviation σ_ϖ and represents the difference between the logarithm of the mean strength of the sections within a component i and ν, χ_{ij} is normal distributed with mean value equal to zero and standard deviation σ_χ and represents the difference between the strength weak section j in the beam i and the value $\nu + \varpi_i$, χ_{ij}. The parameters ϖ_i and χ_{ij} are statistically independent. In the case of this model the strength of the strong sections is equal to the strength of the strongest weak section in the timber member, whereas in the PMC (JCSS, 2006) the bending strength of a cross section, $f_{m,0}$, may be related with the bending strength of a test specimen $f_{m,t}$, as:

$$f_{m,0} = f_{m,t}^{\vartheta} \tag{2.17}$$

where ϑ is a constant depending on the applied bending test standard and the type of timber and can be obtained by simulation (Köhler, 2007). The bending moment capacity, $f_{m,0}$, is assumed to be constant within one section, but not necessarily between sections (Figure 2.11b).

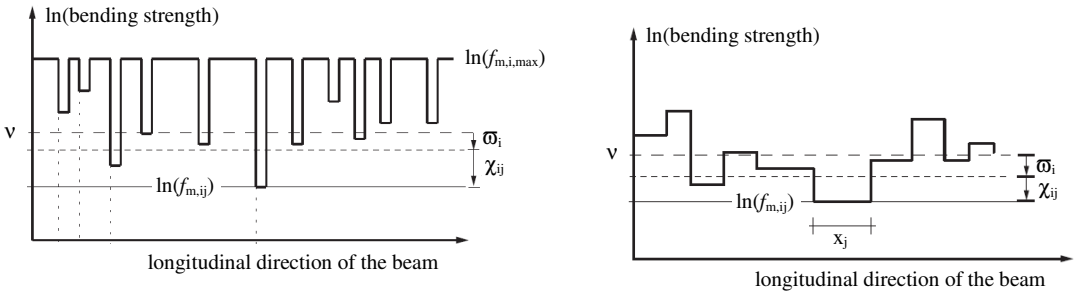

a) b)

Figure 2.11: Section model for the longitudinal variation of bending strength, with strength of the strong sections equal to: a) the strength of the strongest weak section; b) the strength of bending specimen (adapted from Isaksson, 1999 and JCSS, 2006).

With concern to Nordic spruce, the following conclusions were made by Isaksson (1999):

- the variation of the logarithm of the bending capacity $\ln(f_{m,0})$ was related by 40% to the variable ϖ and by 60% to the variable χ. The expected length of a section was 480 mm;
- the different values for ϑ were due to the different definitions of bending strength of test specimen;
- for bending modulus of elasticity and for density no within component variation was assumed.

In Fink and Köhler (2011), a hierarchical model was built for the multi-scale variability of stiffness that included an explicit representation of the stiffness variability between timber boards (meso scale) and the stiffness variability within boards (micro scale). All parameters of the hierarchical stiffness model were estimated based on a sample of 30 randomly selected timber boards within the strength class L25 of Norway spruce grown in southern Germany.

In this study, the definition of knot sections length was initially modelled by a shifted log-normal distribution, however, due to model simplification, a weak section unit length of 150 mm, with an associated gamma distribution, was used instead. The hierarchical model was composed of three components: a model for stiffness of weak sections (*WK*); a model for clear wood sections (*CWS*); and the correlation between them (*cor*), described as follows:

$$\mathrm{MOE}_{ij}\begin{cases}\exp\left(\mu_{WS}+\tau_{i,WS}+\varepsilon_{ij,WS}\right) & , \quad \text{for } j=\{1,3,5,\ldots,n\} \\ \exp\left(\mu_{CWS}+\tau_{i,CWS}+\varepsilon_{ij,CWS}\right) & , \quad \text{for } j=\{2,4,6,\ldots,n-1\} \\ cor\left(\tau_{i,WS},\tau_{i,CWS}\right)=0.787 & \end{cases} \tag{2.18}$$

where MOE_{ij} is the MOE of either the weak section (*WS*) or of the clear wood section (*CWS*) of the section *j* in a board *i* (with a lognormal distributed random variable), μ is the logarithm mean of all *WS* or *CSW* within a sample of boards (deterministic value), τ_i is the difference between logarithm mean of all sections (either *WS* or *CSW*) within one board *i* and μ (modelled as a normal distributed random variable with mean zero and standard deviation σ_i), ε_{ij} is the difference between sections *j* (either *WS* or *CSW*) in a board *i* and the logarithm mean of all sections (either *WS* or *CSW*) within one board *i* (modelled as a normal distributed random variable with mean zero and standard deviation σ_j). These parameters may be estimated using the maximum likelihood method.

In Machado and Palma (2011), also a hierarchical model for inferring the reference properties of timber was proposed by considering the distinction between clear and knot wood zones. This work, however, presented a framework for timber members in service and thus differentiated from the previously mentioned. The model procedure is based in three main steps: *i*) visual identification of clear and knot wood zones; *ii*) non-destructive prediction of the properties of clear wood zones; *iii*) prediction of the reference materials using clear wood properties and applying a knot factor for predicting the strength reduction effect of knots on those clear wood properties.

The application of this procedure to maritime pine timber beams evidenced a good relationship between experimental and predicted global modulus of elasticity (r^2 between 0.76 and 0.55). Nevertheless, for bending strength weaker results were obtained, evidencing the need for improvement in the method for determining the strength reduction effect of weak zones.

Size effect

Accounting the same scale level, also the dimensions of a specific timber element affect the strength, since there is higher probability of having a weaker section for an element with higher length or also, in general, with any increase of cross section dimensions. When the strength parameter is described by a Weibull distribution, the probability of failure may be stated as:

$$p_{\mathrm{f}} = 1 - e^{-\left(\frac{a_{\mathrm{W}} - b_{\mathrm{W}}}{a_{\mathrm{W}}}\right)^{1/k_s}} \tag{2.19}$$

where a_{W} is the scale factor, b_{W} the location factor and k_{s} shape factor.

Generally it can be shown that the following relationship will apply between two volumes V if the location factor is set to zero:

$$\frac{\sigma_2}{\sigma_1} = \left(\frac{V_1}{V_2}\right)^{k_s} \tag{2.20}$$

where σ_1 and σ_2 are the stresses causing failures for volumes V_1 and V_2, respectively.

In Eurocode 5 (CEN, 2004), a factor k_{h} is applied, when heights in bending or widths in tension of solid timber are less than 150 mm, to increase the strength characteristic values of $f_{\mathrm{m,k}}$ and $f_{\mathrm{t,0,k}}$, respectively. This value is given as:

$$k_{\mathrm{h}} = \min\begin{cases}\left(\frac{150}{h}\right)^{0.2} \\ 1.3\end{cases} \tag{2.21}$$

where h is the depth for bending members or width for tension members, in mm.

Also in standard EN 1194 (CEN, 1999) size factors, k_{size}, are considered for destructive tests. Those factors are due to the probability of defects in a given element. In bending, if the element dimensions are inferior to the reference dimensions of width b and height h (b = 150 mm; h = 600 mm) then the test results must be multiplied by:

$$k_{\mathrm{size}} = \left(\frac{b}{150}\right)^{0.05} \cdot \left(\frac{h}{600}\right)^{0.1} \tag{2.22}$$

In tension, if the element dimensions are inferior to the reference dimensions of height h and length l (h = 150 mm; l = 2000 mm) then the test results must be multiplied by:

$$k_{\mathrm{size}} = \left(\frac{h}{150}\right)^{0.1} \cdot \left(\frac{l}{2000}\right)^{0.1} \tag{2.23}$$

2.3.3 Data updating methods

When assessing existing structures a manifold of information may be gathered from several distinct sources, which may be available or can be made available at a given cost. Qualitative together with quantitative information may allow defining the general condition of an existing structure, such as:

- the structure's level of deterioration (if the structure has survived till present days);
- the structure's level of damage;
- material and physical characteristics;
- geometrical surveying;
- load bearing capacity by load tests or similar;
- static and dynamic response (natural frequencies, modal shapes, damping coefficient, etc.).

A description about the steps to be taken in an onsite assessment of historic timber structures is further discussed in Cruz *et al.* (2013).

In the assessment of existing structures, this new information can be taken into account and combined with *prior* probabilistic models and then resulting in so-called *posterior* probabilistic models. However, not all structures are suitable for every type of inspection technique. Historical structures, due to their social and cultural value are not prone to invasive or non-reversible inspection techniques. For those structures, the following phases should be accomplished in order to obtain a full inspection and diagnosis, and consequently to gather data for model updating (Ramos, 2010): historic survey; visual inspections; foundations inspection; NDT; SDT; load tests; monitoring; structural analysis; report with the conclusions and recommendations for the intervention / maintenance.

Regarding design assisted by results taken from testing, Annex D of Eurocode 0 (CEN, 2002) provides different procedures to statistically determine a single property, in terms of design and characteristic value, and also provides information to statistically determine resistance models with use of additional *prior* information.

The next subtopics are related to implementation techniques required to update data into stochastic models for reliability assessment.

Bayesian methods

In the Bayesian probability methods, probabilities are considered as the best possible expression of the degree of belief in the occurrence of a certain event. The Bayesian probabilistic approach does not consider that probabilities are direct and unbiased predictors of occurrence frequencies that can be observed in practice. The only consideration is that, if the analysis is carried out carefully, the probabilities will be correct if averaged over a large number of decision situations (Vrouwenvelder, 2002). To fulfil that consideration it is necessary that the subjective and purely intuitive part is neither

systematically over conservative nor over confident. Therefore, calibration to common practice on the average and to empirical data may be considered as an adequate path to that aim.

Throughout their lifetime, structures change due to many aspects from natural causes (such as material deterioration, environment exposure and long term effects of loads in structures), to human decisions (such as modification of the structure or change of use) or even by accidental actions, only to point a few. Thus, the assessment of existing structures should be regarded as a successive process of model updating and consequent evaluation regarding new information. The Bayesian probabilistic assessment for structures is illustrated schematically in Figure 2.12.

The JCSS PMC (JCSS, 2000) concludes that, compared to the frequentistic interpretation, the Bayesian interpretation is the only one that makes sense in the end, as it overcomes the difficulties of updating distributions when more statistical data is available. The Bayesian interpretation overcomes these difficulties and provides the most logical and useful framework for consistent decision making when uncertainties are present (Vrouwenvelder, 2002).

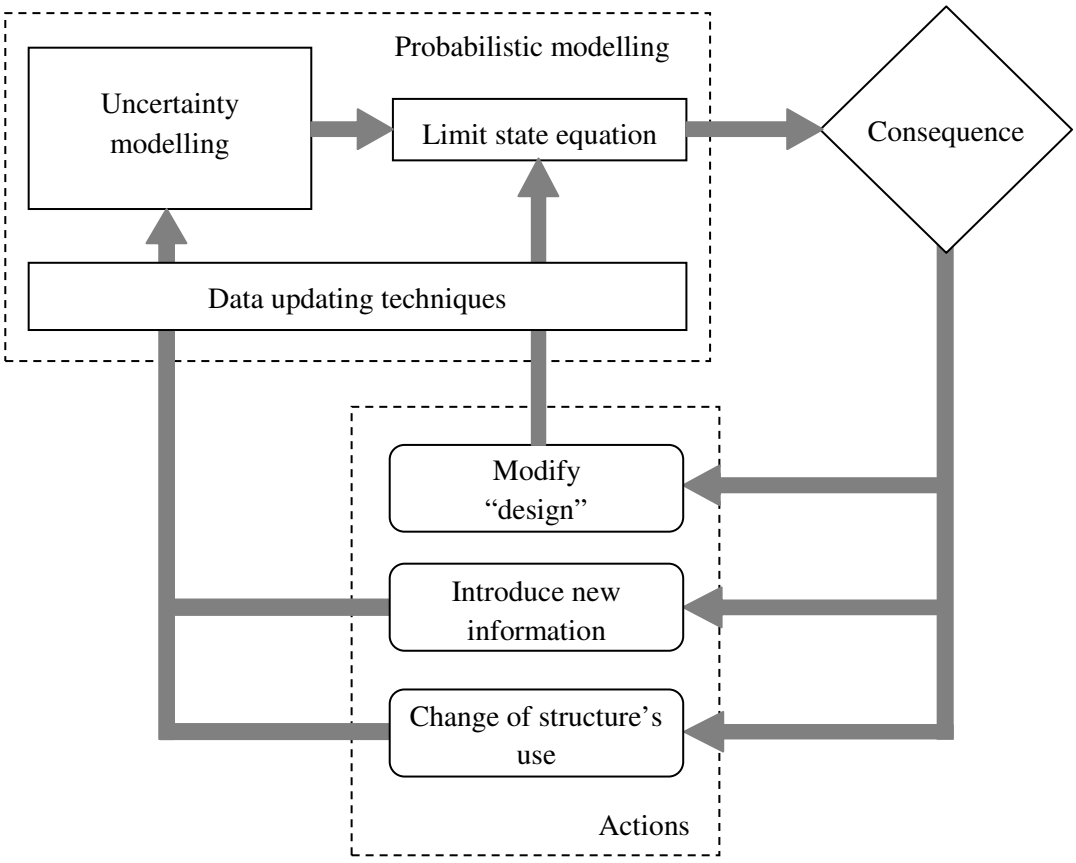

Figure 2.12: Bayesian probabilistic assessment for structures (adapted from Diamantidis, 2001).

When the source of new information is given by observation of events described by one or more stochastic variables, the observed events are modelled by an event function h introduced as:

$$H = h(X) \tag{2.24}$$

where the event function h corresponds to the limit state function. The actual observations are considered as realizations (samples) of stochastic variable H. These observations are then modelled by comparison with a certain limit by inequality events, such as $H \leq 0$, or by equality events, such as $H = 0$.

When inequality events are used, the updated probability of failure, p_f^U, is estimated by:

$$p_f^U = P(g(X) \leq 0 \mid h(X) \leq 0) = \frac{P(g(X) \leq 0 \cap h(X) \leq 0)}{P(h(X) \leq 0)} \tag{2.25}$$

where $M = g(X)$ is the safety margin related to the limit state function $g(X)$ and $X = (X_1,...,X_n)$ are stochastic variables.

When equality events are used, the updated probability of failure, p_f^U, is estimated by:

$$\begin{aligned} p_f^U = P(g(X) \leq 0 \mid h(X) = 0) &= \frac{P(g(X) \leq 0 \cap h(X) = 0)}{P(h(X) = 0)} \\ &= \frac{\frac{\partial}{\partial z} P(g(X) \leq 0 \cap h(X) \leq z)\big|_{z=0}}{\frac{\partial}{\partial z} Ph(X) \leq z\big|_{z=0}} \end{aligned} \tag{2.26}$$

For reliability evaluation of both inequality and equality events it is possible to implement either simulation or first order reliability methods (FORM).

Bayesian methods allow quantifying an approximation about the statistical uncertainty related to the estimated parameters, regarding both the physical uncertainty of the considered variable as well as the statistical uncertainty related to the model parameters. Therefore, they offer a suitable method for parameter estimation and model updating. However, for making this possible, it is necessary to take into account the measurement and the model uncertainties in the probabilistic model formulation. Since Bayesian methods grant the opportunity to incorporate different considerations about the uncertainty of models in the upgraded stochastic model, the comparison between different reassessment engineers' results may be regarded as a problem, such that a consensus about a comparison basis has not yet been established.

Prior, posterior and predictive distributions

When samples or measurements of a stochastic variable X are provided, the probabilistic model may be updated and, thus, also the probability of failure. Considering a stochastic variable X with density function f_X (x), and if q denotes a vector of parameters defining the distribution for X, the density function of the stochastic variable X can be derived as:

$$f_{\mathrm{X}}(x,q) \tag{2.27}$$

In the case that X is normally distributed then q may enclose the mean and the standard deviation of X. When the parameters q are uncertain then f_X (x,q) can be considered as a conditional density function: f_X $(x|Q)$ and q denotes a measurement of Q. The initial density function for the parameters Q is denoted f_Q' (q) and is termed the *prior* density function.

Taking into account the source of new information, it is assumed that n observations or measurements of the stochastic variable X are available making up a sample $\hat{x} = (\hat{x}_1, \hat{x}_2, ..., \hat{x}_n)$. Each measurement is assumed to be independent. The updated density function $f_Q''(q|\hat{x})$ of the uncertain parameters Q given the realizations is denoted the *posterior* density function and is given by:

$$f_{\mathrm{Q}}^{''}(q \mid \hat{x}) = \frac{f_{\mathrm{N}}(\hat{x} \mid q) \cdot f_{\mathrm{Q}}^{'}(q)}{\int f_{\mathrm{N}}(\hat{x} \mid q) \cdot f_{\mathrm{Q}}^{'}(q) dq} \tag{2.28}$$

where $f_{\mathrm{N}}(\hat{x} \mid q) = \prod_{i=1}^{\mathrm{N}} f_{\mathrm{X}}(\hat{x}_i \mid q)$ is the probability density at the given observations assuming that the distribution parameters are q. The integration in Equation 2.28 is over all possible values of q. Then the updated density function of the stochastic variable X given the realization $\hat{x}$ is denoted the *predictive* density function and is defined by:

$$f_{\mathrm{X}}(x \mid \hat{x}) = \int f_{\mathrm{X}}(x \mid q) \cdot f_{\mathrm{Q}}^{''}(q \mid \hat{x}) dq \tag{2.29}$$

Given the distribution function for the stochastic variable X, the *prior* distribution is often chosen such that the *posterior* distribution will be of the same type as the *prior* distribution.

According to the type of existing and new information, different types of distributions may be attributed to characterize these data. Depending of the sensitivity and experience of the reassessment engineer responsible for the reliability analysis, different assumptions may be taken. On one hand, the information must be considered in such way that it is described appropriately and accurately. On the other hand, data must also be considered properly so the costs of computation and processing are equivalent to the importance of the analysis. Therefore, *prior* and *posterior* distributions are many times chosen accordingly to the data available and to the importance of the analysis. Normal or also called Gaussian distributions are often used for that purpose, and so an example will be considered further on (Annex A).

In Annex D of Eurocode 0 (CEN, 2002), information is provided for several procedures mainly related to design assisted by testing. In this topic, focus will be given for the general principles for statistical evaluations regarding the determination of single properties and resistance models. In Eurocode 0 (CEN, 2002), normal distributions are often used, however, in general this may lead to conservative results. The choice of other distributions, such as lognormal or Weibull, will eventually give more suitable results if their use may be justified on basis of previous experimental experience. Regarding the generalized use of normal distributions, an example for a resistance model is given in Annex A.

2.3.4 Bayesian Probabilistic Networks

A Bayesian Probabilistic Network (BPN) is a probabilistic modelling method which allows a consistent and robust reasoning within a complex system with uncertain knowledge. BPNs are used to represent knowledge upon a system based on Bayesian regression analysis describing the causal interrelationships and the logical arrangement of the network variables. In that scope, they provide a causal and graphical mapping representation of the system properties and features, as they explicitly define the dependency among variables, see *e.g.* Pearl (1988), Jensen and Nielsen (2007) for general introduction and Aguilera *et al*. (2011) and Weber *et al.* (2012) for advantages and disadvantages of this method compared to other techniques.

The common representation of a BPN consists in a directed acyclic graph (DAG), composed by a set of nodes, representing each system variable, connected by a set of directed edges, linking the variables as regards to their dependency or cause-effect relationship. The causal relationship structure of a BPN is often described by family relations that, as mentioned by Bayraktarli *et al.* (2005), differentiates child node variables with ingoing edges (effects), from parent node variables with outgoing edges (causes). A (parent) node without any ingoing edges, thus without any parent node converging to it, is often called a root node. The direction-dependent criterion of connectivity, called *d-separation*, evidences the induced dependency relationship among variables and according to different arrangements are defined as converging, diverging or serial (or cascade) (Pearl, 1988). Experts often promptly assert the causal relationships among variables in a domain, using those premises to construct the BPN without pre-ordering the variables in different levels. In almost all cases, by doing so results in a BPN whose conditional-independence implications are accurate (Heckerman and Breese, 1996). Each variable node represents a random variable, which is either defined as a continuous random variable or as a finite set of mutually exclusive discrete states (intervals). In a BPN it is possible to coexist different nodes with either continuous or discrete variables, in so called hybrid BPNs (*e.g.* Lauritzen, 1992; Moral *et al.*, 2001; Neil *et al.*, 2008; Langseth *et al.*, 2009).

The main objective of a BPN is to calculate the distribution probabilities regarding a certain target variable, by carrying out the variables' joint distribution factorization based

on the conditional interrelationships within a generic algorithm developed for that purpose. In this light, the DAG is the qualitative part of a BPN, whereas the conditional probability functions serve as the quantitative part. Therefore, the algorithms themselves are indifferent to the scope for which the BPN is employed, and thus have been employed in several different real-world problems including diagnosis, forecasting, automated vision, sensor fusion, manufacturing control, and information retrieval (Heckerman *et al.*, 1995). A review of application of BPNs in environmental modelling is found in Aguilera *et al.* (2011), while a review in BPNs applications on dependability, risk analysis and maintenance is provided by Weber *et al.* (2012). The applicability and framework for construction of BPNs in the field of reliability analysis has been addressed in *e.g.* Langseth and Portinale (2007) and Marquez *et al.* (2010).

Dynamic BPNs have also been implemented as to incorporate a time dimension, mainly by adding a direct mechanism for representing temporal dependencies among the variables, see *e.g.* Allen (1981) and Ghahramani (1998). Dynamic BPNs have also been extended to the modelling of deterioration as reported in Straub (2009), while aspects of optimization inspection and maintenance decision regarding deterioration have also been addressed by BPN analysis in *e.g.* Friis-Hansen (2000), Attoh-Okine and Bowers (2006) and Montes-Iturrizaga (2009).

In the case discrete states are used, each random variable is defined by conditional probability tables, with the exception of nodes without parents which, in that case, are defined by their marginal probabilities. Taking as example a converging BPN with two parent nodes (A and B) with corresponding marginal probabilities $P(A_i)$ and $P(B_i)$ for each given state i (i = 1, 2, 3,... n with n = number of states), the conditional probability of the child node (C) given states of A and B is calculated as:

$$P(C|A,B) \tag{2.30}$$

The joint probability of all nodes is then calculated by the multiplication of the conditional probabilities of the individual nodes, as:

$$P(C,A,B) = P(C|A,B)\cdot P(A)\cdot P(B) \tag{2.31}$$

The marginal probabilities of the child node C are obtained by the sum of the individual joint probabilities in every state, as:

$$P(C) = \sum_{A}\sum_{B} P(C,A,B) \tag{2.32}$$

One of the main advantages of BPNs is that information may be easily implemented to the network allowing for an update of the target variable. By instance, if information about the state of a parent node is known with certainty, then is referred that an evidence, e, is given in that state. Back to the example of the converging BPN, considering that information is given to the state of parent node A by evidence e_A as it belongs to state 1 (i = 1), therefore $A = A_1$ and the probability $P(A_1) = 1$, the probability distribution of the remaining variables of the network can be updated following Bayes theorem, as:

$$P(C,B|A_1)=\frac{P(A_1|C,B)\cdot P(C,B)}{P(A_1)} \tag{2.33}$$

By application of Equation 2.33 the posterior joint probabilities are obtained regarding the prior given evidence. The previous equations can also be extended to converging BPNs with more than two parent nodes, or even to diverging or serial BPNs, being most often found that complex engineered systems are composed by the combination of smaller BPNs with these different arrangements. The arrangement of the nodes and smaller BPNs in different levels allows for a hierarchical modelling of the system at study. To that aim, Bayesian hierarchical models are employed such as the causal relationships between nodes of different levels are first established globally based on scientific knowledge without specifying the probabilistic characteristics of the variables or assuming weak prior distributions (Nishijima *et al.*, 2009). The parameters of the variables may after be estimated or updated using observed data. BPNs have been used to address hierarchical modelling in several works, such as Neil *et al.* (2008), Gyftodimos and Flach (2002) and Gyftodimos and Flach (2004), while multilevel system reliability is studied in Wilson and Huzurbazar (2007). In timber engineering, hierarchical modelling by use of BPNs has been considered in Deublein *et al.* (2011), to describe the influence of different origins or dimensions of sawn structural timber on the relevant timber material properties conditional on indicator values assessed by machine stress-grading.

Chapter 3

Multi-scale characterization of chestnut timber elements

ABSTRACT: The purpose of this chapter is to compile a database on the mechanical properties of chestnut timber elements with respect to different testing procedures and size scales. Special attention is given to the visually assessable parameters and its influence in the bending MOE variation within members (meso scale) and within a same member (micro scale). Characterization of the mechanical properties in stress parallel to the grain are also provided regarding small clear wood specimens, in order to evaluate its relationship to the reference properties.

For these purposes, a multi-phase experimental campaign, conducted to twenty old chestnut beams (*Castanea sativa* Mill.), and its results are presented and analysed.

3.1 Sample and general adopted procedures

The more than a century old chestnut (*Castanea sativa* Mill.) timber beams were taken from a building in the city of Braga, Northern Portugal, where they served as simply supported structural floor beams, in both endings, by granite masonry walls (Figure 3.1). The floor itself consisted in a traditional solution with wooden planks nailed to the top surface of the beams by iron nails. These beams were selected since they presented a state of conservation commonly found for existing timber structures.

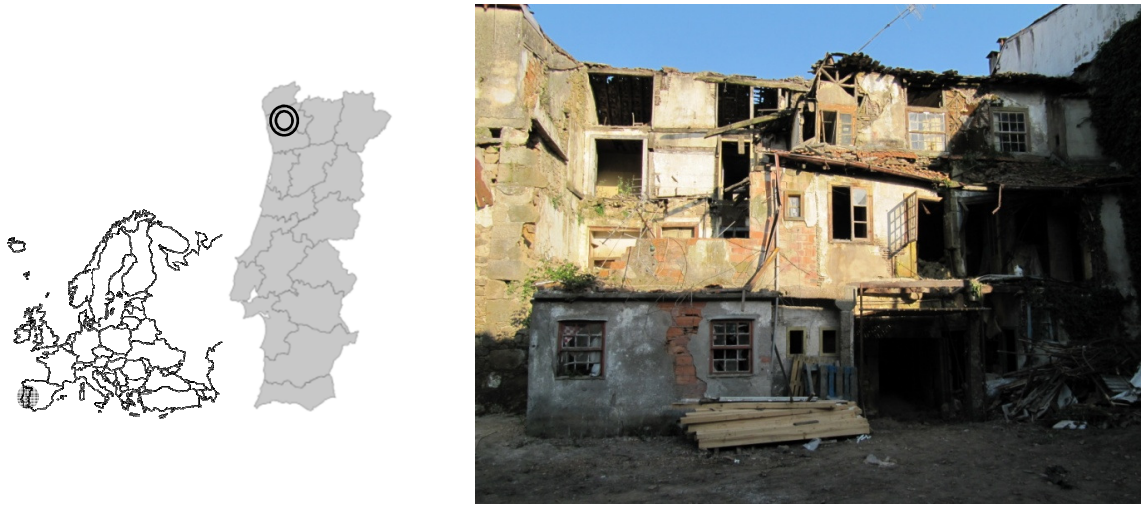

a) b)

Figure 3.1: Original location of the timber beams: a) geographic location in Europe and Portugal; b) construction site.

Attending to oral statements, the wood beams were initially placed in the building in the beginning of the first decade of the XIX century and did not undergo any major rehabilitation or retrofitting action. After being removed from the construction site, the beams were then taken to a material deposit where they were marked (with a capital letter A to T) and visually inspected. As the timber beams were removed from the building, it was possible to assess all the faces of the beams, which often is not possible for an onsite evaluation.

Following the initial visual inspection, the exterior degradation (signs of decay by biological attack) was removed and afterwards mechanical characterization was made regarding different size scales of the elements. From one to the next experimental phase, the timber elements were sawn into smaller sizes in order to isolate the influence of defects and better define their relationship to a more precise distribution of stiffness and strength along the length and height of the timber element.

Firstly, the timber members were cut to 7×15×300 cm^3 sawn beams. The beams were marked on seven segments (1 to 7) of 40 cm and the defects found in each segment were accounted. Then 4-point bending tests, according to EN 408 (CEN, 2010a), were made to each beam (4 beams until failure (beams H, L, P and T) and 16 only in elastic range). The timber beams were submitted to ultrasound testing by indirect method on each 40 cm

interval on bottom and lateral faces before and after the bending tests. After the bending tests, the beams that were not taken to failure were sawn into 3 boards with 7×4×300 cm^3, obtaining a total of 48 boards. Each board was then visually inspected and assessed by ultrasound, penetration impact test and drilling resistance test on each 40 cm segment. To each segment of each board a 4-point bending test in elastic range was made in order to assess the variation of the modulus of elasticity along the element's length, thus obtaining a total of 336 tests, from which 51 segments were also tested until failure.

After the completion of the bending tests in the sawn boards, clear wood samples were removed from each set of three boards in order to perform compression parallel to grain, tension parallel to grain and density tests. For each full beam, 3 compression, 6 tension and 3 density samples were removed. Ultrasound pulse velocity test was made for each compression and tension sample before the respective destructive test. Destructive tests were made with displacement control until reaching failure, obtaining modulus of elasticity and ultimate strength. Density, ρ, and moisture content, MC, were also assessed. The order of testing and sample origin is shown in Figure 3.2.

Phase	Test sequence	Outcome
1	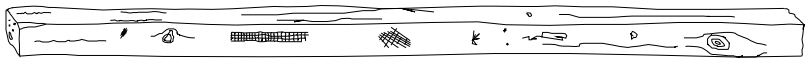	visual grading NDT
2	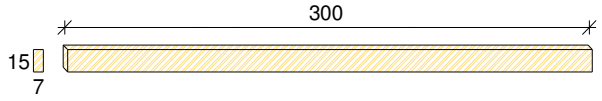	visual grading NDT $E_{m,l}$, $E_{m,g}$, f_m
3	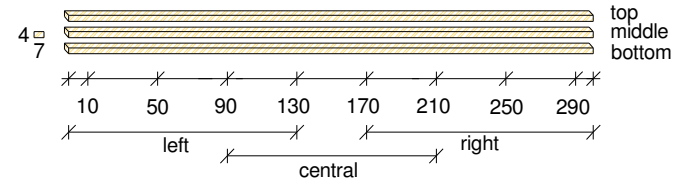	visual grading NDT $E_{m,l}$, $E_{m,g}$, f_m
4	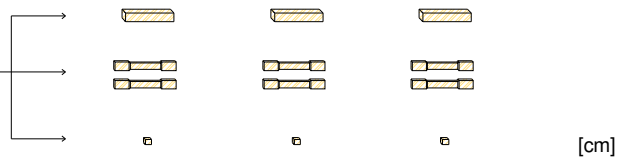	$E_{c,0}$, $f_{c,0}$ $E_{t,0}$, $f_{t,0}$ NDT ρ , MC

Phase description:
1 - visual inspection and NDT on full size old timber beams
2 - visual inspection, NDT and bending tests on full size sawn beams (7×15 cm^2)
3 - visual inspection, NDT and bending tests on sawn boards (7×4 cm^2)
4 - small wood specimens in parallel to grain tests, and density and moisture content determination

Figure 3.2: Testing phases and results obtained for each scale.

3.1.1 Non and semi-destructive testing

Visual inspection

The timber elements, in the different test phases, were visually inspected and graded, accordingly to the Italian norms UNI 11119 (UNI, 2004) and UNI 11035-2:2003 (UNI, 2003b), on each 40 cm segment. All defects present on each face were identified, measured and mapped. However, in Phase 1, since timber elements were placed in the structure already with the wane that resulted from the initial sawing process and the alignment of fibers was not disrupted, a visual strength grading was considered without the limitation of wane. This procedure was only considered adequate since the only the residual cross section without wane was accounted and, also because wane, for this case, was not influencing the effective connection between elements and joints.

Attending to the mentioned norms, the methodology presented in Figure 3.3 was used for the visual inspection carried to the twenty old chestnut beams. The proposed methodology consists in two separate parts. The first concerns the information that should be considered previously to the visual inspection and also the necessary actions to be taken to assure a safe and adequate inspection. The second part refers to the visual inspection itself that includes the identification and mapping of the principal and more relevant features, the corresponding classification and consequent attribution of indicative values for strength and stiffness properties.

In this case, the timber elements were taken from the place of use to a storage place and thus it was possible to examine all faces and ends.

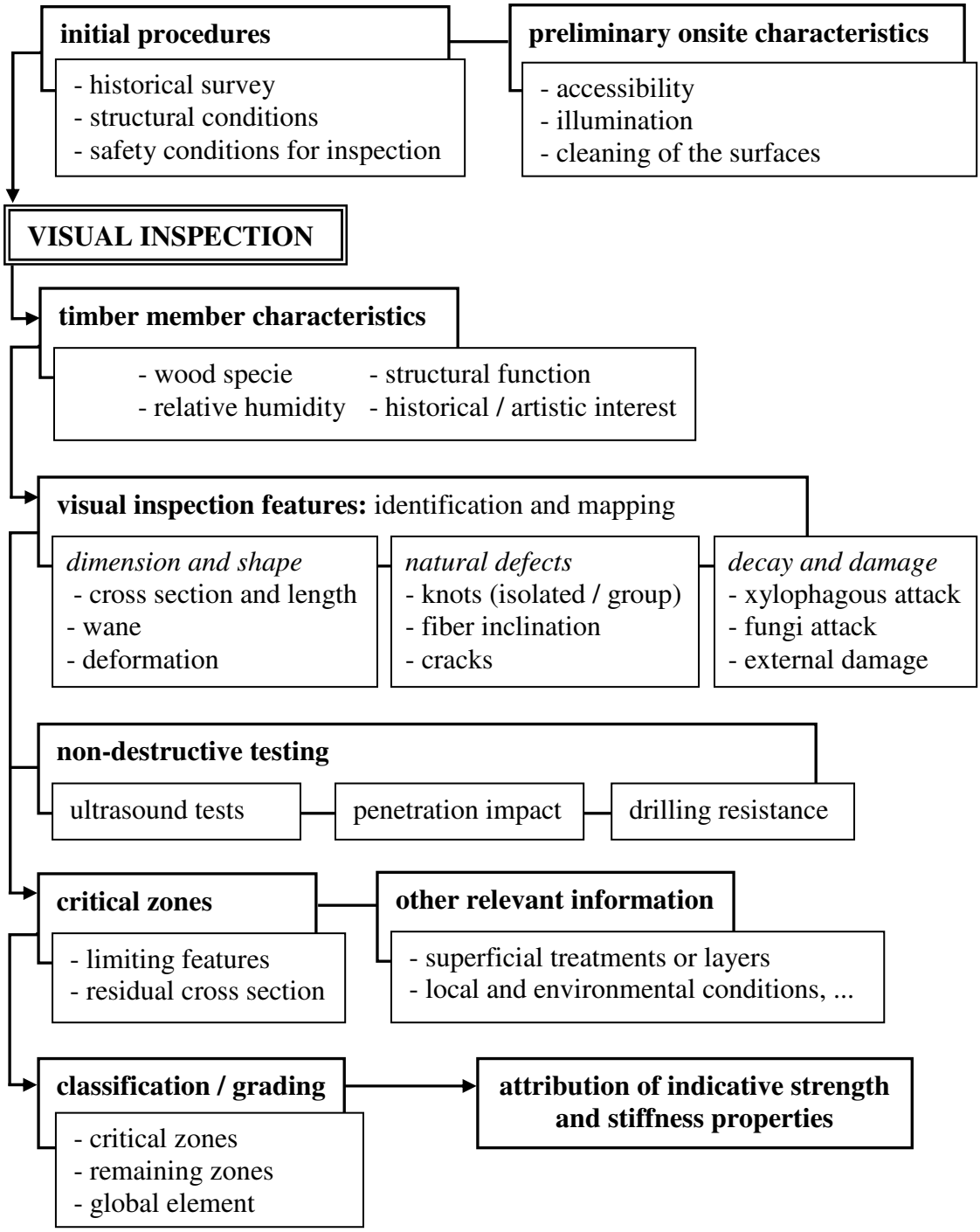

Figure 3.3: Flowchart of the visual inspection methodology applied in the experimental campaign.

Penetration impact tests

For the penetration impact test a Pilodyn 6J device was used, with a 2.5 mm diameter metallic needle. The original beams (Phase 1) and the sawn boards (Phase 3) were tested in two consecutives faces of each beam and five measurements were made in each 40 cm segment in different levels of the cross section (Figure 3.4). From the five measurements

the maximum and minimum values were disregarded and an average value was taken from the remaining three. The testing mesh and the exclusion of the extreme values pretend to minimize the influence of local defects in the measurements.

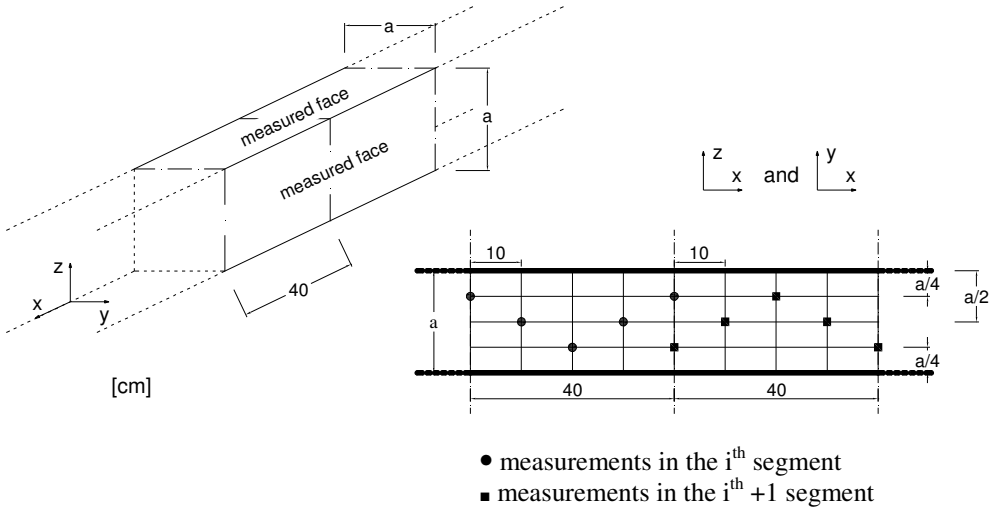

Figure 3.4: Testing mesh of pin penetration measurements for two consecutive segments.

Drilling resistance tests

In order to assess the severity of decay in critical sections, drilling resistance tests were made in the sections that exhibited a higher degree of deterioration (Phase 1). The tests were performed in the end parts of the beams since they were the segments that presented poorer visual condition and a higher amount of cross section was lost. Measurements were also made to clear wood samples in the sawn board scale (Phase 3). A Resistograph3450 equipment was used, which has a drill needle with 3 mm diameter on the extremity and 1.5 mm diameter along the length of the needle.

The profiles obtained by the drilling resistance equipment were analysed, accounting to each initial measurement (needle entry) and last measurement (needle exiting) in the timber elements, as to minimize the effect of possible lateral friction. Measurements deviating from the expected straight path more than 5% of the path length were not considered, and the measurement was repeated. These actions were feasible since access to both analysed surfaces was possible.

Ultrasound tests

The timber sawn beams and boards (Phases 2 and 3) were subjected to ultrasound testing by indirect method on each 40 cm interval on bottom and lateral faces (seven segments) (Figure 3.5) before and after the bending tests. Although direct or semi-direct arrangements permit a better signal transmission between transducers, the indirect method was used since it is particularly useful to determine the quality of the surface layer and to cases where it is only possible to assess one surface, which is common for this kind of elements

in existing timber structures. The bottom face was also chosen for the location of measurements, since it will be the section of the beam subjected to tension in the 4-point bending tests.

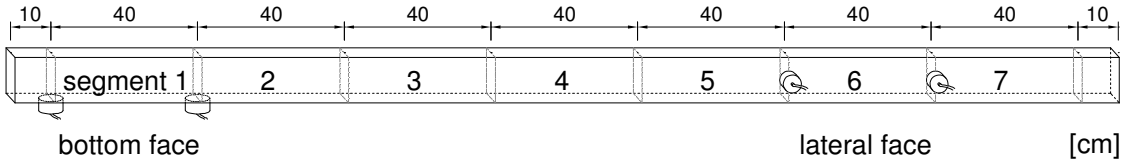

Figure 3.5: Location of ultrasound tests for indirect measurements.

In Phase 4, both direct and indirect measurements were made to compression parallel to grain test specimens, whereas only indirect measurements were made to the tension parallel to grain test specimens due to its geometry (small cross section dimensions).

The tests were made with a Pundit Lab equipment with 0.1 μs precision and 54 kHz frequency transmission transducers. A coupling agent was used to provide a better acoustic transmission between the transducers and the element's surface. Two solutions for coupling agents were considered. The first consisted in the use of a mineral gel on both the transducer and the element's surface, while the second consisted in a thin layer of soft oil-based modelling clay. The measurements given by the ultrasound equipment for the second solution were identical (± 0.2 μs), providing that only a uniform thin layer was used, covering the surface between the transducer and the element. For rougher surfaces the oil-based clay provided an adequate coupling condition with use of less material, because the mineral gel was partially absorbed by the timber element when used, requiring a new quantity of mineral gel for each additional measurement. Constant pressure between measurements was provided using stiff rubber bands constraining the transducer against the element's surface.

For each segment, two measurements were taken and averaged, if the two first measurements differed more than 5%, then an additional third measurement would be taken and the average would be done with the three measurements.

The results of the ultrasound testing consisted in the determination of the propagation time t (s), taken by the sonic wave to go from the emitting to the receiver transducer. Considering the distance between the centre of each transducer (wave path length) d_w (m), it was possible to calculate the propagation velocity v_p (m/s), as:

$$v_p = \frac{d_w}{t} \tag{3.1}$$

3.1.2 Mechanical tests

Bending tests in Phases 2 and 3 were made according to EN 408 (CEN, 2010a). The test specimen length, l, and the distance between the supports and the loading positions, a, are

proportional to the depth of the cross section, h. The MOE, both local, $E_{m,l}$, and global, $E_{m,g}$, values were calculated according to Equations 3.2 and 3.3, respectively, as:

$$E_{m,l} = \frac{a \cdot l_1^2 \cdot (F_2 - F_1)}{16 \cdot I \cdot (w_2 - w_1)} = \frac{a \cdot l_1^2 \cdot \Delta F}{16 \cdot I \cdot \Delta w} \tag{3.2}$$

$$E_{m,g} = \frac{3 \cdot a \cdot l^2 - 4 \cdot a^3}{2 \cdot b \cdot h \cdot \left(2 \cdot \frac{\Delta w}{\Delta F} - \frac{6 \cdot a}{5 \cdot G_v \cdot b \cdot h} \right)} \tag{3.3}$$

where b is the width of the cross section (mm), h is the height of the cross section (mm), ΔF is an increment of load (N), Δw is the increment of deformation (mm) corresponding to ΔF, a is the distance between a loading position and the nearest support (mm), l is the span between supports (mm), l_1 is the gauge length (mm) for the determination of $E_{m,l}$, I is the inertia moment (mm^4) and G_v is the shear modulus (N/mm^2). If unknown G may be taken as infinite (CEN, 2010a).

The bending strength, f_m, of an element taken to failure was calculated according to Equation 3.4, where F_{max} is the maximum applied load before failure and W is the section modulus (mm^3):

$$f_m = \frac{a \cdot F_{max}}{2 \cdot W} \tag{3.4}$$

In Phase 3, although the indications of EN 408 (CEN, 2010a), the height was chosen to be the smaller cross section dimension (h = 4 cm) in order to establish a consistent measurement of the stiffness parameters, expressed by the bending MOE, with size variation. Aiming to analyse the bending MOE variation along the elements length, $E_{m,l}$ and $E_{m,g}$, were measured in the segments corresponding to those evaluated by visual inspection. Seven consecutive bending tests were made to each board, with supports placed in different locations. The tests were equally spaced and the assumed gauge lengths for the determination of MOE were centred with the visual inspection segments. In the case of the extremity segments, the centre of the bending tests could not coincide with the centre of the segments considered in the visual grading, as adequate support conditions would not be assured due to necessary length between support points. To provide adequate support conditions (at least h/2 after supports), the centre of the bending tests made to the extremity segments was moved 2 cm to the centre of the board with reference to the centre of the segments considered for the visual grading (Figure 3.6).

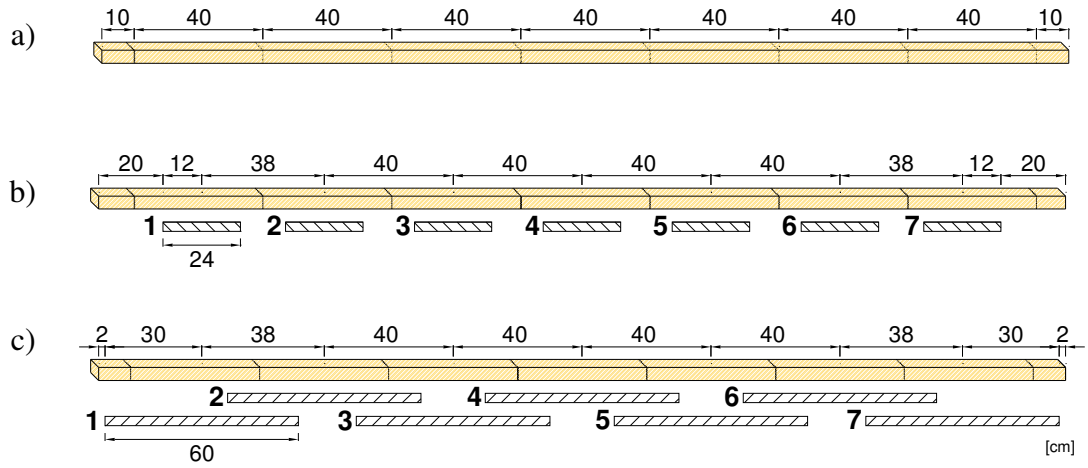

Figure 3.6: Location for the sequential bending tests: a) visual inspection segments; b) gauge length for $E_{m,l}$ (in shade); c) gauge length for $E_{m,g}$ (in shade).

In Phase 4, in order to correlate the values of the previous tests with compression parallel to the grain, after conducting the bending tests to each segment of each board, prismatic samples were taken from each left (board length from 10 cm to 130 cm: segments 1 to 3), middle (board length from 90 cm to 210 cm: segments 3 to 5) and right (board length from 170 cm to 290 cm: segments 5 to 7) fractions of the beams (see Figure 3.2). Samples were also taken from the beams that were submitted to bending test until failure, thus obtaining a total of 60 test samples. These samples were chosen along the segments length where no macro defects were visible, thus assessing clear wood specimens. The test procedure for the destructive testing and sample dimensions were obtained with consideration to EN 408 (CEN, 2010a). The length of the test sample was considered to be six times the smaller cross sectional dimension and the end surfaces were prepared such that they were plane, parallel to one another and perpendicular to the longitudinal axis of the sample. Since the boards were sawn to 4 cm height elements, the compression specimens were considered to have a square cross section of 4×4 cm^2, and length 24 cm (Figure 3.7).

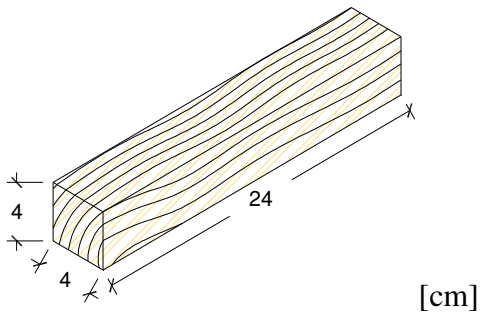

Figure 3.7: Test sample for compression parallel to the grain.

With respect to the tension parallel to the grain tests, after conducting the bending tests to each segment of each board, two samples were taken from each left (board length from 10 cm to 130 cm: segments 1 to 3), middle (board length from 90 cm to 210 cm: segments 3 to 5) and right (board length from 170 cm to 290 cm: segments 5 to 7) fractions

of the beams (see Figure 3.2). Each pair of samples are taken within the same length of the boards only varying its position regarding the height of the board, (Figure 3.8). The samples nearest to the top surface of the board are considered as the first sample group (A), whereas the samples nearest to the bottom of the board are considered as the second sample group (B).

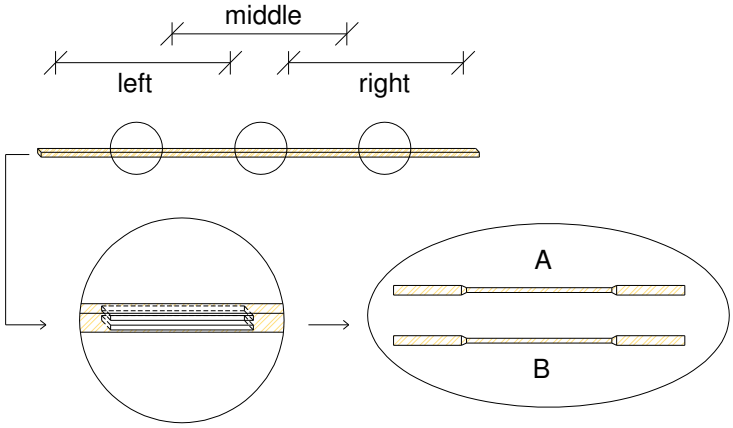

Figure 3.8: Location of tension parallel to grain sample extraction.

One sample per segment was also taken from the beams that were submitted to bending test until failure, thus obtaining a total of 108 test samples. The test procedure for the destructive testing and sample dimensions were obtained with consideration to EN 408 (CEN, 2010a) and the Brazilian norm NBR 7190/97 (ABNT, 1997). Modifications were made to the samples in the gripping area in order to consider the existent grips and load machine in laboratory. The tension specimens had a middle cross section of 0.5×3 cm^2 and gripping section of 1×4 cm^2, this geometry had a double purpose, on one hand to have a sufficient gripping area in order to avoid eventual compression or sliding of the grips, on the other hand a decrease of cross section area in the middle section was made to induce a pure tensile failure in that region (uninfluenced by the gripping area) (Figure 3.9).

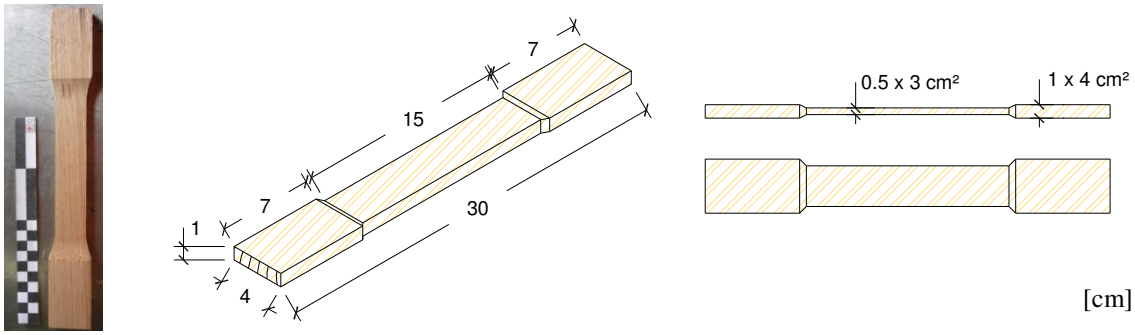

Figure 3.9: Test sample for tension parallel to the grain.

Modulus of elasticity in compression, $E_{c,0,}$ and tension, $E_{t,0}$, were calculated from the load deformation curves with use of linear regression with correlation coefficient of at least 0.99, as:

$$E_{X,0} = \frac{l_1 \cdot (F_2 - F_1)}{A \cdot (w_2 - w_1)} \tag{3.5}$$

where $(F_2 - F_1)$ is an increment of load (N) on the straight line portion of the load deformation curve, $(w_2 - w_1)$ is the increment of deformation (mm) corresponding to $(F_2 - F_1)$, A is the cross sectional area of the central cross section (mm^2) and l_1 is the gauge length (mm) for the determination of $E_{X,0}$ (either compression $E_{c,0,}$ or tension $E_{t,0}$) (N/mm^2).

In compression, the deformation was measured over a central gauge length of four times the smallest cross section dimension of the sample, using one pair of LVDT's placed on opposite faces to eliminate the effect of possible distortion. In tension specimens, deformation was measured over a central gauge length of ten times the smallest cross section dimension, using a clip gauge extensometer. Compression and tension parallel to the grain strength, respectively $f_{c,0}$ and $f_{t,0}$, were calculated as:

$$f_{X,0} = \frac{F_{max}}{A} \tag{3.6}$$

where F_{max} (N) is the maximum applied load until failure and the A (mm^2) is the cross sectional area near the section in failure.

Before being tested, all samples were conditioned in a climatic chamber capable of keeping a temperature of 20 ± 2ºC and a humidity of 65 ± 5%, until constant mass was obtained. Constant mass is considered to be attained when the results of two successive weighting, carried out at an interval of six hours, do not differ by more than 0.1% of the mass of the test piece. Weightings were made to ten specimens chosen randomly, using a weighting scale with a precision of 0.01 g in intervals of six hours until the conditioned state was achieved.

3.2 Phase 1 results

This experimental phase allows, by use of NDT and SDT, the definition of the mechanical properties found for structural size elements accounting for a common state of conservation in existing old timber structures.

3.2.1 Non and semi-destructive testing

Visual inspection

The first step of the visual inspection comprised the geometrical characterization of each element. For that purpose, the beginning and end of each segment was measured using a three side ruler (precision of mm). By using this tool, it was possible to obtain a reasonable

definition of the geometry of each cross section including wane with only two measurement positions (Figure 3.10).

The length of the elements varied between 4 m and 6 m with a mean value of 5.32 m (COV = 11.8%). The average values for the nominal cross section dimensions were 18.0 cm (COV = 3.1%) for height and 13.0 cm (COV = 6.0%) for width. Even if the variation in the nominal cross section dimensions within each element was low, significant wane was found. This wane was mainly consequence of the initial sawing process rather than from deterioration (elements still presented sharp edges) and did not pose problems to the existing connections to other structural elements.

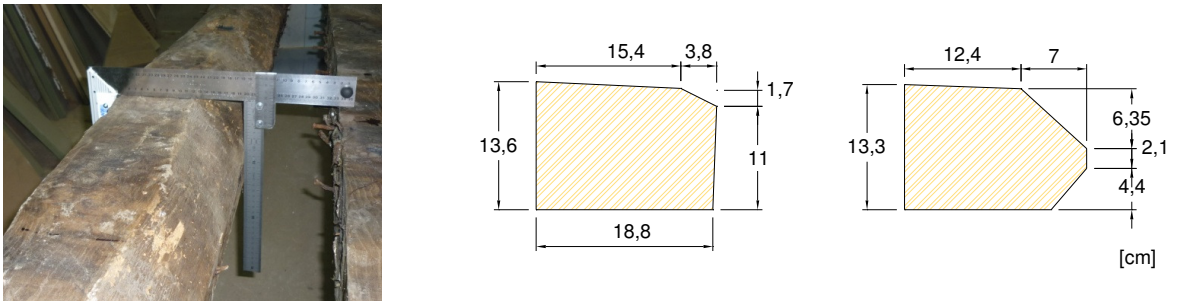

Figure 3.10: Measurement of the cross section dimensions: example of two consecutive sections.

In each 40 cm segment, the significant parameters for visual strength grading were reported. Along the length of a timber element, it is well noticeable the variation in both quantity and size of defects, anomalies and decay (Figure 3.11) and therefore even if a section presents damage that may limit its structural behaviour, others may still present a satisfactory condition.

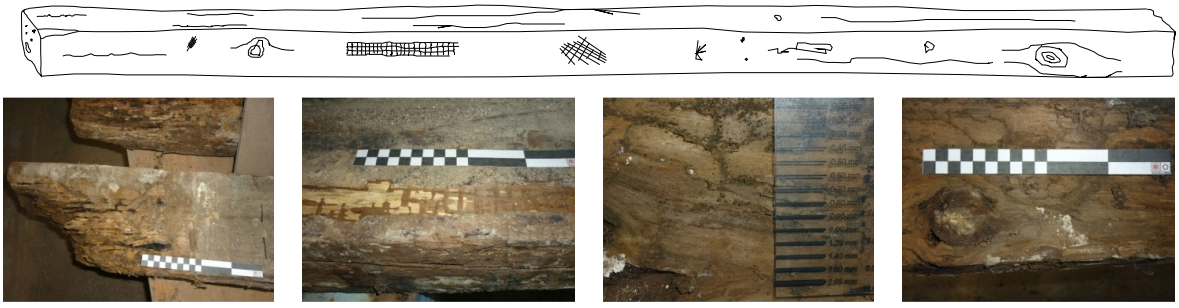

a) b) c) d)

Figure 3.11: Examples of defects and anomalies found in the wood elements: a) deterioration of internal fibers by xylophagous; b) decay by fungi; c) superficial attack of xylophagous; d) knots and fiber misalignment.

Visual grading was considered for the residual cross section, thus not considering the decayed external layers and also assuming a rectangular section without wane. By this process it is intended to obtain the mechanical properties related to the material itself and its defects rather than to the state of conservation. Another purpose of this classification

without the parameters of external damage is to obtain reference values for comparison with the small samples that will be taken in the following steps of the experimental campaign. In order to have a qualitative comparison along the timber beams length but also between different beams, the percentage of segments that is included in a given visual class is accounted for each beam (see Figure 3.12).

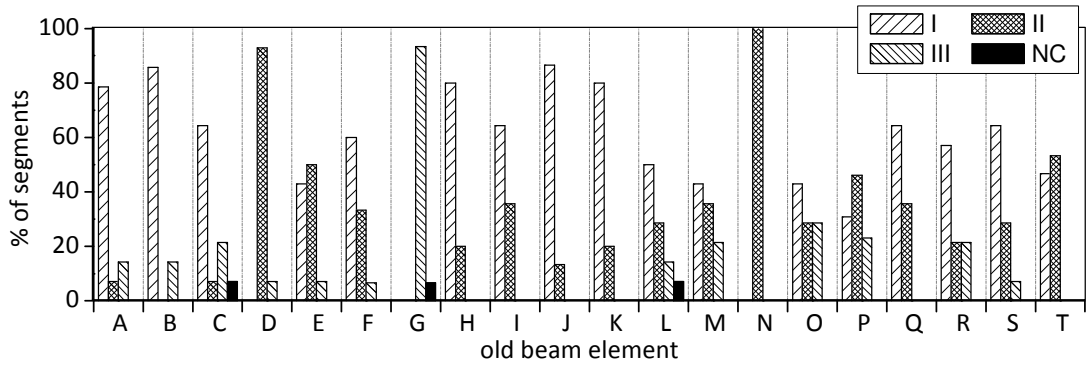

Figure 3.12: Percentage distribution of segments of old beams included in each visual grading class regarding UNI 11119 (UNI, 2004).

In this case, only beams C, G and L have segments with grade NC, resulting from the presence of significant knots. With exception of beam G, a minimum percentage of 70% for the sum of classes I and II is found for each beam.

Penetration impact tests

The results of the impact tests evidenced a mean value of 11.3 mm penetration depth, moreover presenting that measurements made within the same segment had lower variation compared to the measurements made within member and between members. In almost all beams the coefficient of variation is higher when analysing the values along the total beam (mean COV = 17.6%) than when analysing the measurements within a segment (mean COV = 13.1%). This is due to the local nature of the test and its dependency to the decay level. Since decay is not evenly spread through the length of the beam the variation increases when assuming the global values rather than the local measurements.

By complementing a traditional visual inspection with NDT results permitted, in this case, to verify that the decay found in some parts of the timber beams was essentially superficial, since the difference between visible decayed and non-decayed segments had an average increase of approximately 1.1 mm in the penetration depth.

Drilling resistance tests

The drilling resistance tests were performed in the ending parts of the beams (segments that presented higher extent of visible decay) in a section that still presented a defined cross section, obtaining values of resistance measure, RM_{decay}. A mean value of 245 bit

with COV of 22.6% was found, while neither significant voids nor lower resistant sections in the inner regions of the cross section were found in the drilling resistance profiles. Drilling resistance tests were useful to estimate the depth of the decayed layer, even if it should be noted that the measurements are made regarding only the drilling path of the device needle, and therefore only evaluate the material locally.

3.3 Phase 2 results

This experimental phase allows for the definition of the mechanical properties found for structural size elements without the influence of external decay and damage, thus providing a better definition of the material properties influenced mainly only by knots (or clusters of knots) and the alignment of fibers.

3.3.1 Non-destructive testing

Visual inspection

The beams were marked on 7 segments of 40 cm (leaving 10 cm from each extremity) on which the defects were found and accounted (Figure 3.13). Since the exterior signs of decay were removed during the sawing process, and only superficial cracks were present, exclusively knots (isolated and cluster) and alignment of fibers were considered as limiting parameters for the visual inspection.

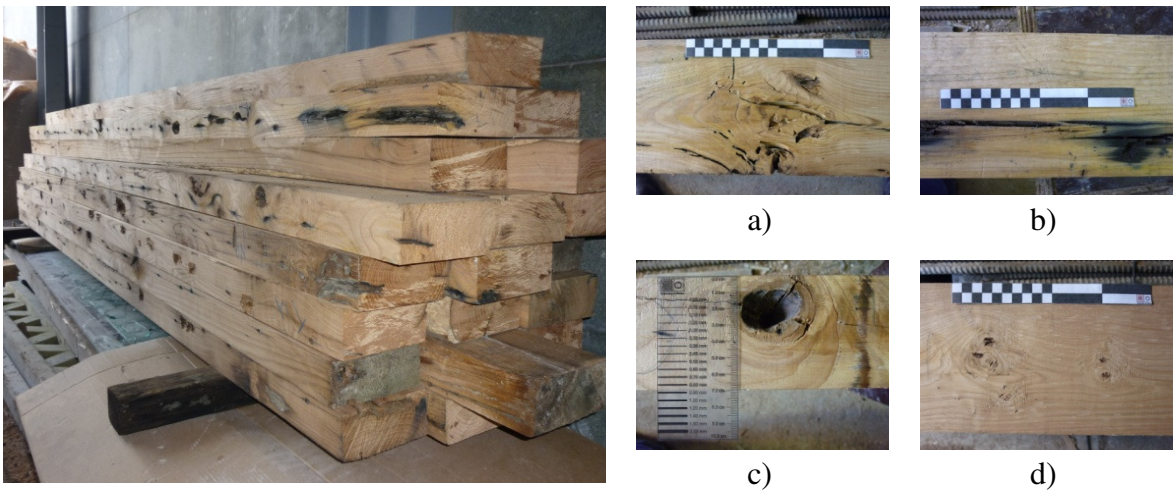

Figure 3.13: Sawn beams and example of inspected defects: a) knots and insect tunnels; b) cracks and oxidation stains (iron nails); c) decayed knot; d) knot cluster.

The percentage of segments included in each class of the visual inspection classification was also reported (see Figure 3.14). With respect to a global structural grading, the visual class of each sawn beam is given by the classification of the critical zones. The selection of critical zones attended to a static analysis regarding the configuration of the 4-point bending tests. Therefore, the segments which will be submitted

to maximum bending stress (mid span) and the segments submitted to higher shear stress (segments near supports) were considered as critical zones if significant defects were found in their extent.

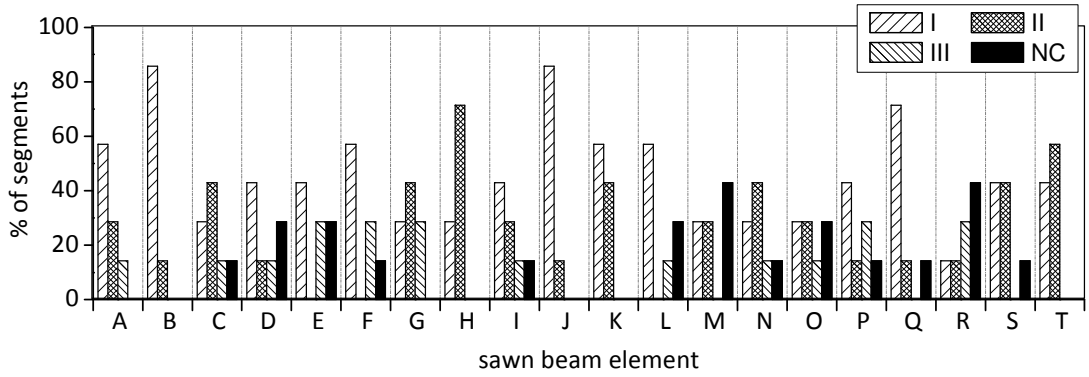

Figure 3.14: Percentage distribution of segments of sawn beams included in each visual grading class regarding UNI 11119 (UNI, 2004).

Similar qualitative grading of segments per class are observed between each old and sawn beam (comparison with Figure 3.12), especially regarding the extreme classes (class I and NC). Accounting the different percentages of segments attributed to a given class for each beam between phases, it is noticed that in 60% of the cases, a difference lower than 15% is found between Phase 1 (Figure 3.12) and Phase 2 (Figure 3.14). On the other hand, 19% of the cases have a difference higher than 30%. The mean difference between the same class in different phases is for class I of 19% and for class NC of 15%. In an overall analysis, in 95% of cases, Phase 2 presents higher or equal percentages of class NC than Phase 1 (the exception is beam G), indicating that a larger percentage of lower classes is observed in sawn beams due to the increase of the ratio *d/h* (diameter of knots / cross section height) when reducing the cross section area of the elements. On the opposite side, Phase 2 presents higher percentages of class I, in 30% of the cases, corresponding to the situations where the defects that limited the visual grading in the previous phase were only superficial and were removed during the sawing process (beams D, G, L, N, P and Q). In these cases, from Phase 1 to 2, a shift of percentage value from classes II and III to class I is noted.

Ultrasound testing

Ultrasound tests were performed to bottom and lateral faces of the sawn beams and the results were considered in terms of propagation velocity, v_p. The mean value of the v_p for all beams in the bottom face is 4846.5 m/s and 4821.6 m/s in the lateral face with coefficient of variation of 8.6% and 6.6%, respectively. The average of the coefficients of variation for the measurements in each beam is 6.3% and 4.9%, respectively for bottom and lateral faces. The decrease of the coefficient of variation between the measurements of all beams and the measurements within a same beam, represent an increase of variation when assessing different timber elements, even from the same structure and timber specie.

For comparison between results regarding the same parameter or segment, but tested with more than a measurement or by different types of measurements, a relative difference, *RD*, was considered according to:

$$RD(\%) = \left| \frac{m_{II} - m_{I}}{m_{II}} \right| \cdot 100 \tag{3.7}$$

where m_I corresponds to the first type of measurement and m_{II} to the second type of measurement with respect to the same parameter or segment.

The average relative difference between beams regarding these measurements are less than 10% for all cases except in beams S and T. Those beams presented a segment where the difference between bottom and lateral faces measurements were 28% and 25%, respectively for beam S and T. In these two cases, by visual inspection, it was found that the ultrasounds indirect measurements resulted in much lower propagation velocities for the faces where a higher superficial concentration of knots was detectable. An analysis to the measurements made by each segment presented that the relative difference is inferior to 25% in 97.1% of the cases, inferior to 10% in 78.6% of the cases and inferior to 5% in 40% of the cases. The distribution of values of relative difference between bottom and lateral are presented in Figure 3.15a.

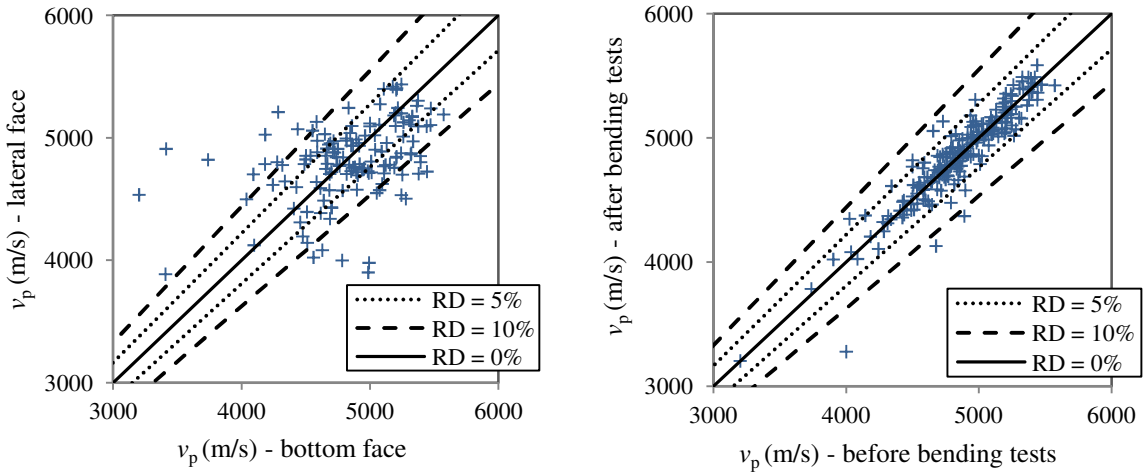

a) b)

Figure 3.15: Distribution of propagation velocity values with respect to relative difference between measurements: a) in bottom and lateral faces; b) before and after bending tests.

After the 4-point bending tests, new ultrasound measurements were made in the same locations as done previously, in order to observe if any significant change occurred. This procedure was implemented with intention of confirming that the timber beams were only subjected to loads in the elastic regime and no significant change was made to the macro-structure of the timber element. The ultrasound measurement would work as an instrument to determine non visible damage or early signs of damage. For this analysis, 16 beams were considered since 4 beams were taken to failure in the 4-point bending tests.

For those 16 beams, the mean value of the relative difference between measurements was 1.9%. Also, the relative difference was lower than 10% for 98.7% of the measurements and lower than 5% for 94.2% of the measurements. The distribution of values of relative difference between measurements before and after the bending tests are presented in Figure 3.15b.

3.3.2 Mechanical tests

Bending tests

The totality of the sawn beams were submitted to bending tests in elastic regime in order to obtain $E_{m,l}$ and $E_{m,g}$. Four beams (corresponding to 20% of the total sample) were also selected to be tested until failure (beams H, L, P and T). The tests were carried out in the laboratory facilities of the Civil Engineering Department of the University of Minho using a Sentur II hydraulic unit with a 500 kN load cell. The used loading equipment was capable of measuring the load to a required accuracy of 0.1% of the applied load. Linear variable differential transformers (LVDT's) with range ± 12.5 mm were used for displacement measurement. The reaction structure consisted in a frame composed by metallic I beams bolted to a 80 cm thick concrete floor slab.

The tests were made under displacement control with a displacement rate such that the maximum applied load for the determination of the bending strength was to be reached within the interval of 300 ± 120 s. For that purpose, also an estimated load, F_{est}, corresponding to the maximum load was calculated. For the determination of the load/displacement diagrams in elastic regime, a four cycle test was conducted. In each test, four cycles were considered with loading phase of 300 s each, reaching 50% of the estimated maximum load, F_{est}, and a respective unloading phase. The first stage was only considered for calibration and adjustment of the test and was disregarded in the results. For the calculation of the elastic moduli a displacement rate of 0.04 mm/s was considered for the four first cycles. An extra fifth cycle with a single loading stage was considered for the beams that were taken to failure (Figure 3.16), with a displacement rate of 0.08 mm/s.

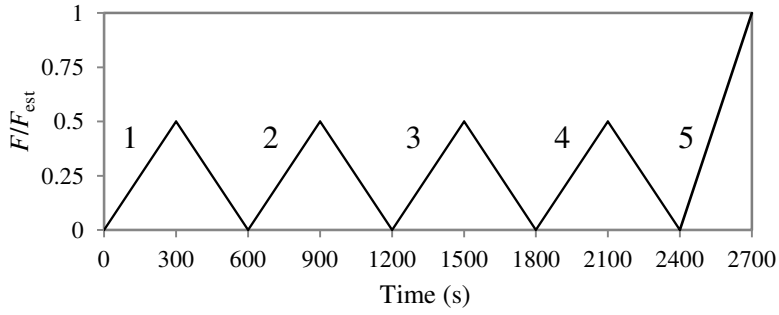

Figure 3.16: Loading procedure for the calculation of $E_{m,l}$ and $E_{m,g}$ (cycle 2 to 4) and f_m (cycle 5).

The results of the bending tests for stiffness parameters are compiled in Figure 3.17, where a mean value of 10840 N/mm^2 was found for $E_{m,l}$ and 10940 N/mm^2 for $E_{m,g}$ with

COVs of about 25%. This variation is higher than the COV of 13% for MOE suggested in the Probabilistic Model Code (JCSS, 2006) for softwoods. A strong relation is found between $E_{m,l}$ and $E_{m,g}$ (coefficient of determination, $r^2 = 0.82$) which maintains strong for the correlation with tendency line intercepting the origin with a 45º angle ($r^2 = 0.76$). More than 50% of the values of both MOE are distributed within the range [9;13] kN/mm^2. Histograms and cumulative frequencies are also plotted (Figures 3.17c, 3.17d).

	mean (N/mm^2)	COV (%)
$E_{m,l}$	10840	25.3
$E_{m,g}$	10940	22.0

a)

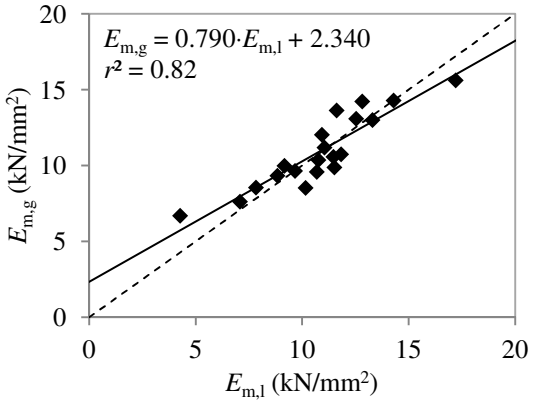

b)

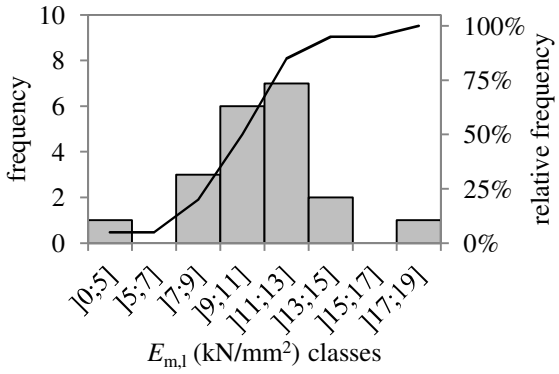

c)

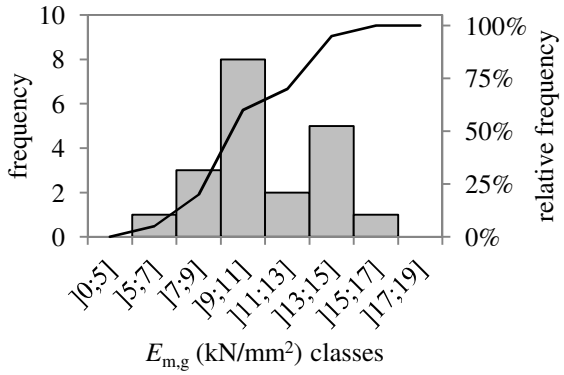

d)

Figure 3.17: Sawn beams bending tests in elastic regime: a) test set-up and results; b) correlation between MOE; c) histogram and cumulative frequencies for $E_{m,l}$; d) histogram and cumulative frequencies for $E_{m,g}$.

The old beams with at least 20% in lower classes (III and NC) in the visual inspection (Phase 1, Figure 3.12), resulted in sawn beams with $E_{m,g}$ values lower than the mean, while old beams with higher percentage of class I and II (higher than 80%) originated sawn beams with higher values of $E_{m,g}$. However, in the cases of beams D, E and F, although with only 7% of lower visual classes, the value of $E_{m,g}$ was lower than the mean. In these cases, the critical sections were located in the central third of the span and were more influencing for the results, in accordance with the consideration of a critical section for determination of the global characteristics. The exceptions to these premises were beams H and T, which although not evidencing any lower class percentage in visual grading, also evidenced lower $E_{m,g}$ values than the mean. The mean value of $E_{m,l}$ is similar to the value given for class I in UNI 11119 (10000 N/mm^2) (UNI, 2004). This indicates

that clear wood elements for these particular beams would have much higher values than those indicated in the norm for class I.

The bending strength results for the four beams taken to failure (H, L, P and T) are shown in Figure 3.18. The strength values are consistent with the visual inspection even if present similar results in beams H, P and T (COV = 10.5%). Visual inspection proved to be correct in assessing qualitatively the four beams. On one hand, beam T presented higher f_m than the remaining three beams, consistent with the previous visual inspection where beam T was attributed higher percentages of visual class I and II. On the other hand, the beam with lower f_m (beam L) had the higher percentage of NC sections in the same visual inspection. The beam failure initiated in all cases with respect to a segment with higher percentage of defects.

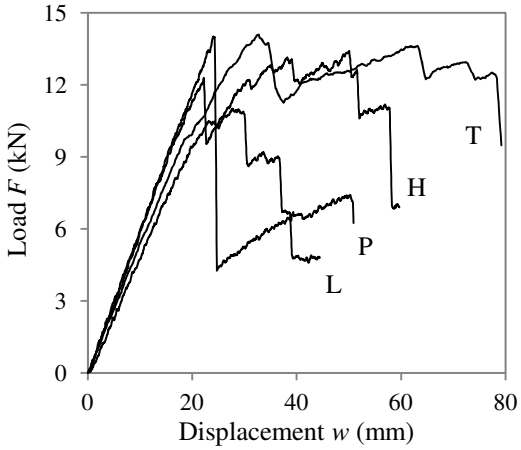

a)

f_m H = 23.66 N/mm^2 f_m P = 24.58 N/mm^2

f_m L = 19.53 N/mm^2 f_m T = 24.69 N/mm^2

b)

Figure 3.18: Bending tests until failure of beams H, L, P and T: a) load / displacement diagrams; b) failed beams and results.

The failure mechanism began with the formation of thin longitudinal cracks in the lower layers of wood subjected to tension (Figure 3.19). The reduction of loading capacity occurred with the increased opening of cracks in the lower half of the cross section (under the neutral axis) and compression of the upper half. With increase of deformation and loss of strength contribution by the lower fibers of the cross section, new cracks initiated in the upper quarter of the cross section mainly due to the new location of the neutral axis (upper in the cross section). The formation of longitudinal cracks is mainly found in the middle span within the length between loading points.

Since all failure mechanisms were related to sections within the span between the applied loads, strong correlations were found with respect to f_m and MOE, specially for $E_{m,l}$ (r^2 = 0.87 and 0.78, respectively for $E_{m,l}$ and $E_{m,g}$). However these correlations must be considered with care due to the small number of f_m measurements.

a) b)

Figure 3.19: Development of the failure mechanism in sawn beams subjected to bending tests: a) initiation near a knot cluster; b) formation of large longitudinal cracks at the lower half height of the cross section (tensioned side).

3.4 Phase 3 results

In order to analyse the spatial variability of the mechanical properties within a timber element, the sawn beams were cut longitudinally dividing each beam into three sawn boards and then numbered *X*1 to *X*3 from top to bottom (Figure 3.20), *X* corresponding to the identification of the original sawn beam. The longitudinal cuts were made dividing the height of the beam, thus making possible to isolate, in that direction, some defects by board. The cuts were made maintaining the upper and lower faces of the element. The dimensions of the sawn boards were 7×4×300 cm^3, since part of the height is lost due to the cutting process (thickness of the saw blade).

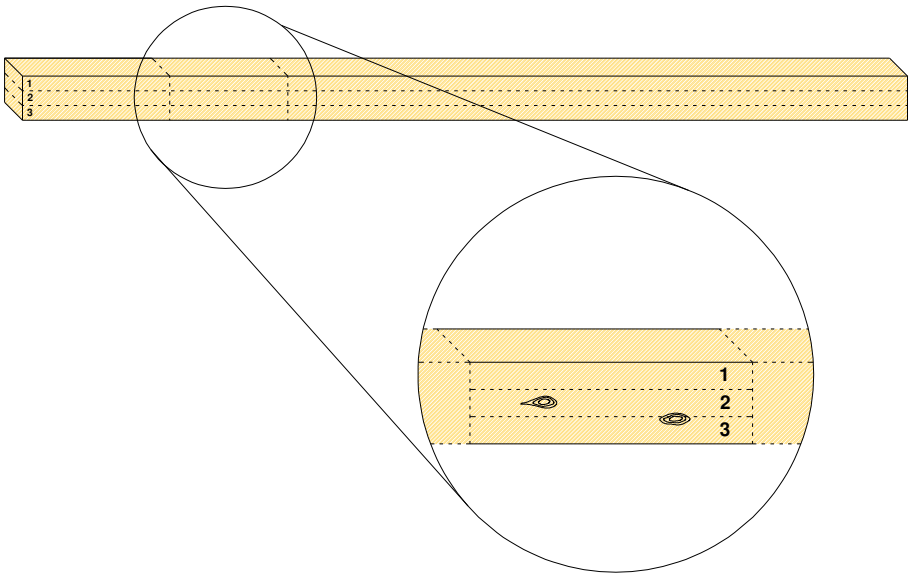

Figure 3.20: Sawn boards location within an original sawn beam with representation of defect division by boards.

From the initial old beams, only 80% were cut to boards since 20% of the beams (four beams: H, L, P and T) were already tested in destructive bending tests. This experimental phase allows for the definition of the mechanical properties by isolating the influence of defects in height and also assessing the variation of properties along the length of a timber element.

3.4.1 Non-destructive testing

Visual inspection

The boards were marked on 7 segments of 40 cm (leaving 10 cm from each extremity) on which the defects were found and accounted. Since the influence of defects was intended to be eliminated in the height dimension, visual inspection was considered for the top and bottom faces excluding the inspection of minor superficial defects found only at the lateral faces. For this experimental phase, the percentage of segments included in each class of the visual inspection classification was also reported (Figure 3.21).

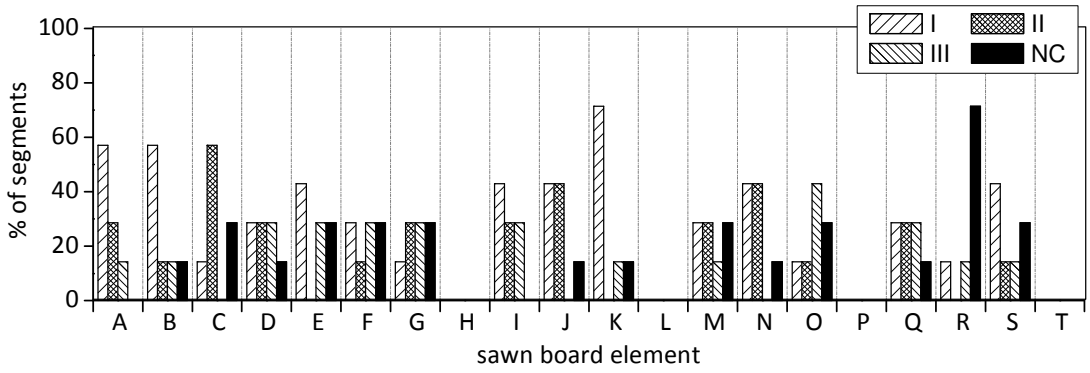

Figure 3.21: Percentage distribution of segments of sawn boards included in each visual grading class regarding UNI 11119 (UNI, 2004) (beams H, L, P and T were tested until failure in Phase 2).

Similar percentages per class are observed between each sawn beam and sawn board. However, a larger percentage of lower classes is observed in some boards due to the increase of the ratio *d/h* (diameter of knots / cross section height) when reducing the height of the elements.

Ultrasound testing

The timber sawn boards were subjected to ultrasound testing by indirect method on each 40 cm interval (seven segments per board) on the bottom face. The mean value of the propagation velocity for all beams is 4860 m/s with coefficient of variation of 8.4%. The average of the coefficients of variation for the measurements in each beam is 6.9% and for each board is 6.3%. The decrease of the coefficient of variation between the measurements of all beams and the measurements within a same beam and a same board, represent an increase of variation when assessing a higher scale element.

The velocity of propagation measurements taken to each segment of each set of boards is consistent with the performed visual inspection. When important macro defects, such as knot clusters or significant misalignment of fibers, were visually assessed a lower propagation velocity was found. The partition of each beam in three boards also resulted in a better definition and location of the influence of defects. Such is exemplified in Figure 3.22, where for a set of boards of a given beam (beam J) a considerable decrease in the propagation velocity in segment 4 for the bottom board is visible, being consistent with a significant knot found by visual inspection for that location.

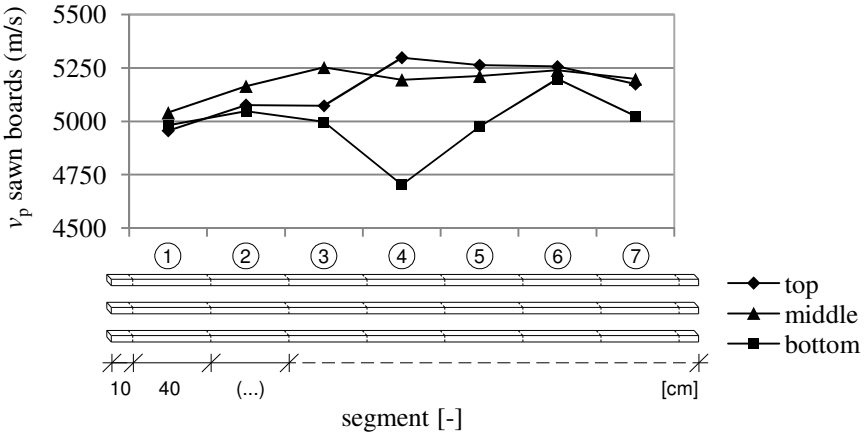

Figure 3.22: Propagation velocity, v_p, for indirect measurements along the length of the bottom face of each board and segment of beam J.

The measurements also revealed that the propagation velocity varies both in height and length of each beam, being the variation higher when a larger concentration of knots was found. The mean coefficient of variation for the measurements made to the same segment of each set of boards (*e.g.* measurements in A1, A2 and A3 for segments 1), thus the variation in height, is equal to 5.2%, whereas the mean coefficient of variation for the measurements made to all segments of a given board (*e.g.* measurements in A1 for segments 1 to 7), thus the variation in length, is slightly higher being equal to 6.3%.

In order to assess the influence of different sample sizes in the analysis of the propagation velocity, these results are compared to the equivalent measurements obtained for the sawn beams. For that purpose, the values regarding board 3 (bottom board) of each set of boards are compared to the values of the ultrasound tests done to the bottom face of the sawn beams, since the measurement location is the same. The measurement values of the sawn beams are also compared to the mean value between the same segments of each set of boards (*e.g.* mean value of the measurements in A1, A2 and A3 for segments 1). For comparison basis, the relative difference, *RD*, was calculated (Equation 3.7). From that analysis, two segments, on which large defects (knots and fiber detachment) were present in the totality of a cross section height, presented a very high *RD* (higher than 20%), and thus considered as outliers and non-representative of this analysis. Disregarding those two segments, a mean *RD* equal to 2.4% was found when considering the measurements in the bottom boards, whereas for the mean values per segment of all boards the *RD* increased to

4.6%. When analysing the structural element globally, the mean of all ultrasound measurements done to the same beam, either sawn beam or group of sawn boards, were compared and a mean *RD* equal to 2.8% was found.

Penetration impact tests

The results of the impact tests, for each board for bottom face measurements and lateral faces measurements, indicate a mean penetration depth of 8.2 mm and 8.5 mm, respectively. In almost all boards and for both faces, the coefficient of variation is higher when analysing the values along the total board (mean COV = 10.7%) than when analysing the measurements within a segment (mean COV = 6.7%). This is an expectable result since the variation of timber mechanical properties increases with the consideration of a larger measurement length and thus increasing the possibility of including defects or wood with different growth characteristics. Comparing to the penetration impact tests made in Phase 1, it is noticed the decrease in variation for lower scales from 13.1% (beams) to 6.7% (segments in boards).

The coefficient of determination was calculated for the measurements between lateral and bottom faces for each equivalent segment, obtaining a r^2 of 0.56 (Figure 3.23).

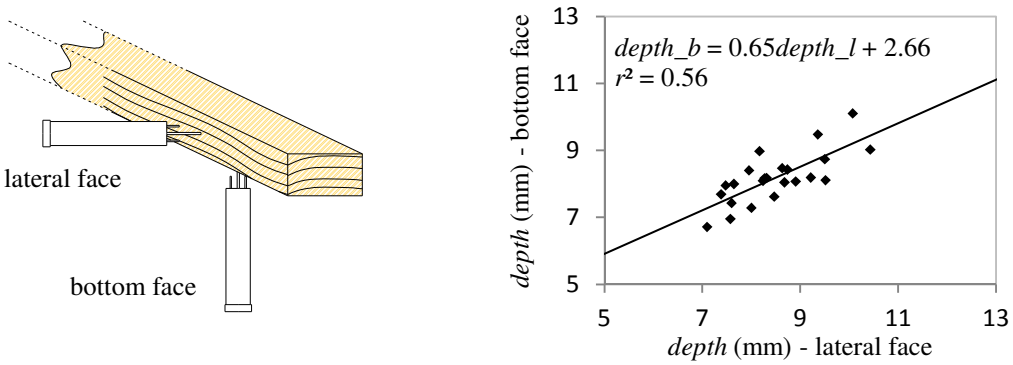

Figure 3.23: Correlation of measurements of penetration impact tests between bottom and lateral faces.

Drilling resistance tests

The drilling resistance tests were performed perpendicularly to the top and bottom faces, thus with a drilling path of 4 cm. A mean value of 304 bit with COV of 10.4% was found. Comparing these results with the ones obtained in Phase 1, an increase of 19.4% is found but, more significantly, the COV obtained is less than half of the provided earlier. The differences are mainly due to the decayed sections that were previously found in Phase 1 which later were removed.

3.4.2 Mechanical tests

Bending tests

The totality of the sawn boards was submitted to bending tests in elastic regime in seven segments each, in order to obtain $E_{m,l}$ and $E_{m,g}$ (336 segments). Selected segments, with

different visual grades, were also tested until failure (51 segments, corresponding to 15% of the total sample).

The tests were carried out in the laboratory facilities of the Civil Engineering Department of the University of Minho using a Sentur II hydraulic unit with a 25 kN load cell. The used loading equipment was capable of measuring the load to a required accuracy of 0.1% of the applied load. Linear variable differential transformers (LVDT's) with range ± 12.5 mm were used for displacement measurement. The same reaction frame structure used in the sawn beam bending tests was considered for these tests. The tests were made with displacement control with rate such that the maximum applied load for the determination of the bending strength was reached within the interval of 300 ± 120 s. The first stage was only considered for calibration and adjustment of the test and was disregarded in the results. For the calculation of the MOE, a displacement rate of 0.014 mm/s was considered for the loading phases, while for the bending strength calculation a 0.03 mm/s displacement rate was considered in the last cycle (Figure 3.24a). The gauge length was considered to be 15*h* (60 cm) and 6*h* (24 cm), respectively for $E_{m,g}$ and $E_{m,l}$ determination. The span between supports for each segment was considered to be 15*h* (60 cm) (Figure 3.24b).

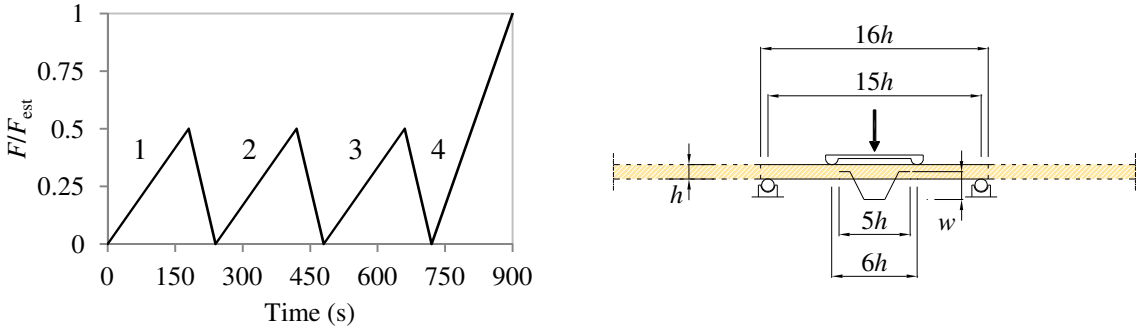

a) b)

Figure 3.24: Bending tests procedure and setup: a) loading procedure for the calculation of $E_{m,l}$ and $E_{m,g}$ (cycle 2 and 3) and f_m (cycle 4); b) test layout.

The results of the bending tests in sawn boards for stiffness parameters are compiled in Figure 3.25, where a mean value of 12190 N/mm^2 was found for $E_{m,l}$ and 11660 N/mm^2 for $E_{m,g}$ with COVs of about 25%. The values given by segments for a given beam were averaged and a strong correlation is found between $E_{m,l}$ and $E_{m,g}$ ($r^2 = 0.89$). More than 50% of the values of both MOEs are distributed within the range [10;16] kN/mm^2, as shown by histograms and cumulative frequencies in Figure 3.25c and Figure 3.25d. The results revealed that bending MOE varied in different proportions in height and length, with higher variation when a larger concentration of knots was found in a board. The mean COV for the same segment of a set of boards (*e.g.* measurements along the height in A1, A2 and A3 for segments 1) is equal to 20.1% and 15.7%, respectively for $E_{m,l}$ and $E_{m,g}$, whereas the mean COV for all segments of a given board (*e.g.* measurements along the length of A1, for segments 1 to 7) is slightly higher being equal to 25.8% and 17.9%, respectively, for $E_{m,l}$ and $E_{m,g}$.

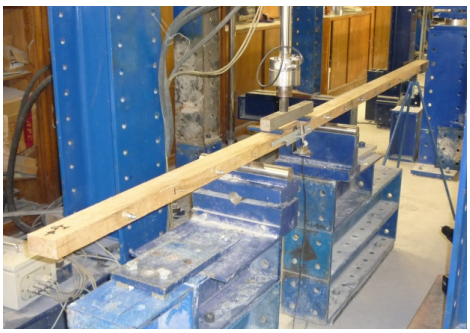

	mean (N/mm^2)	COV (%)
$E_{m,l}$	12910	30.4
$E_{m,g}$	11660	22.8

a)

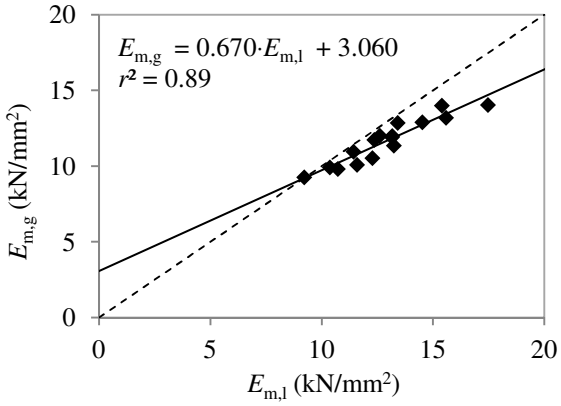

b)

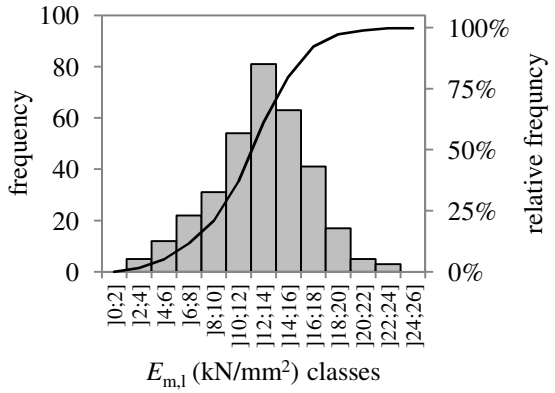

c)

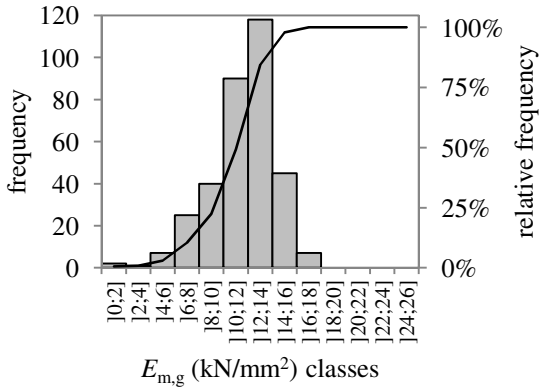

d)

Figure 3.25: Sawn boards bending tests in elastic regime: a) test set-up and results; b) correlation between MOE; c) histogram and cumulative frequencies for $E_{m,l}$; d) histogram and cumulative frequencies for $E_{m,g}$.

The stiffness parameters of each segment of each set of boards, are consistent with the performed visual inspection and ultrasound tests. When significant macro defects, such as knot clusters or significant misalignment of fibers, were visually assessed, a lower stiffness was found. The partition of each beam in three boards also resulted in a better definition and location of the influence of defects. Such is exemplified in Figure 3.26 where for a set of boards of a given beam (beam J, also exemplified in 3.22), a considerable decrease in $E_{m,l}$ and $E_{m,g}$ in segment 4 for the bottom board is visible, being consistent with a significant knot found in visual inspection and lower value of propagation velocity also found for that location.

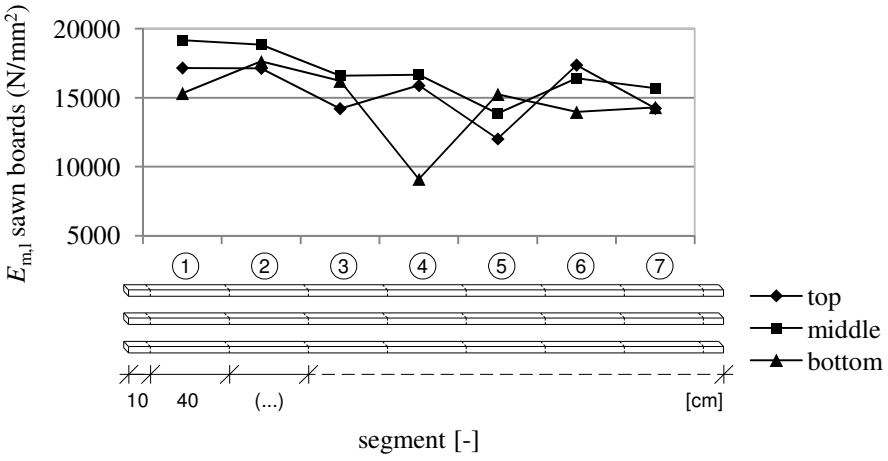

a)

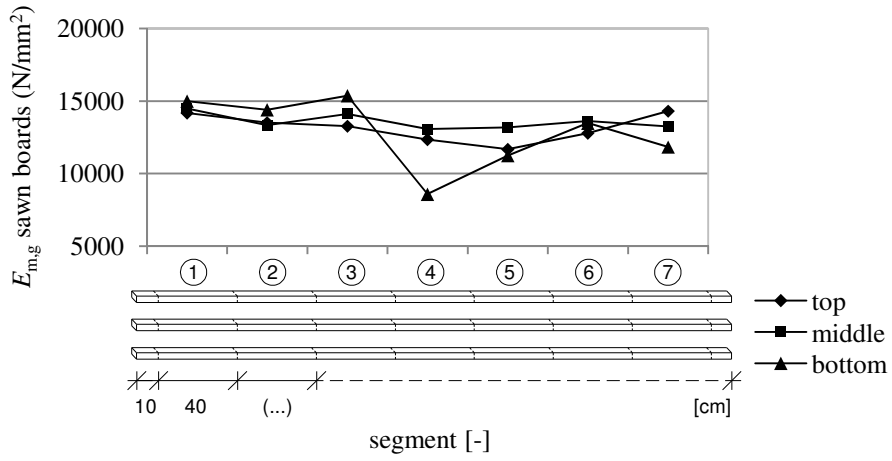

b)

Figure 3.26: Modulus of elasticity along the length of each board and segment of beam J: a) local, $E_{m,l}$; b) global, $E_{m,g}$.

Aiming to assess the correlation between results obtained in Phase 3, an analysis of variance (ANOVA) was made regarding the parameters $E_{m,l}$ and $E_{m,g}$ with respect to the visual grading. In this case, ANOVA was used to test whether visual strength grading contributes significantly, or not, to the variation in bending MOE. In this case, for $E_{m,l}$ and $E_{m,g}$, a single-factor ANOVA and a confidence level of 95% revealed a significant variance in bending MOE between the different considered visual strength classes ($F > F_{crit}$ and *p-value* < 0.05). Therefore, it is demonstrated that the partition of the results of bending MOE with consideration to the visual strength classes allows obtaining samples with significant statistic variation values between them, evidencing different clusters of measurements. Accounting this premise, visual inspection grading may be used as an indicator to distinguish segments with different bending MOE results within a same timber member.

The mean value of all bending test measurements is higher than the equivalent values obtained for the sawn beams. The biggest difference is observed between $E_{m,l}$, where also a larger COV is obtained for the sawn boards. This is an expectable result since the gauge

length for the determination of $E_{m,g}$ for the sawn beams included all the gauge length of the $E_{m,g}$ for the sawn boards, whereas the gauge length for the $E_{m,l}$ of the sawn beams only considers segments 3, 4 and 5 of the sawn boards. Considering the mean value for that segments a $E_{m,l}$ of 12720 MPa is obtained which is closer to the value of the $E_{m,l}$ for the sawn beams. Nevertheless, even comparing the equivalent segments in terms of gauge length measurement the values of stiffness for the sawn boards are 18% and 7% higher, respectively $E_{m,l}$ and $E_{m,g}$, compared to the sawn beams. This increase of stiffness may also be explained due to the decrease of the influence of defects in the global behaviour when the beam was divided into boards, resulting also in a higher COV due to the higher difference obtained between segments with and without defects.

When analysing the structural element globally, the means of all bending test measurements done to the same beam, either sawn beam or group of sawn boards, were compared and a mean *RD* equal to 15.7% was found for $E_{m,l}$. For the same analysis, a mean *RD* equal to 10.8% was found for $E_{m,g}$. Considering only segments 3 to 5 for determination of the mean $E_{m,l}$ of a set of boards, a mean *RD* equal to 14.4% was found.

The results of the bending tests in sawn boards for strength parameters are compiled in Figure 3.27, where a mean value of 42.94 N/mm^2 was found for f_m with COV of 45%. Since the segments were not chosen randomly, as they were selected according to their visual grading, a more uniform distribution between strength classes is obtained and, therefore, also a larger COV. In order to properly assess the values of f_m, also the mean values and COV are given regarding each visual grade in Figure 3.27a, where it is noticed the expected decrease of strength and increase of variability from higher to lower grades.

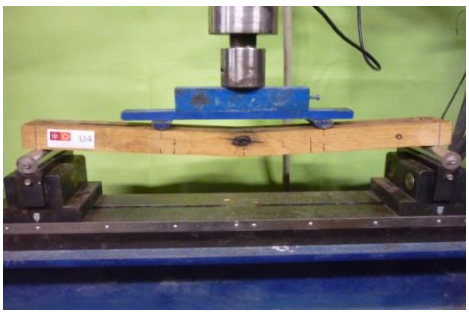

f_m sample	mean (N/mm^2)	COV (%)
all	42.94	44.9
class I	57.30	22.7
class II	38.70	26.3
class III	33.06	45.4
class NC	16.26	35.8

a)

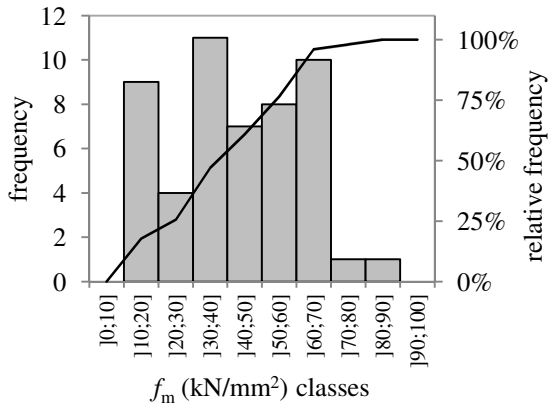

b)

Figure 3.27: Sawn boards bending tests in failure: a) test set-up and results; b) histogram and cumulative frequencies for f_m.

The values of COV for classes I and II are similar to the values proposed in the PMC (JCSS, 2006), whereas when defects start to be visibly noticeable (classes III and NC) the

variation strongly increases. The relationship between local and global stiffness with strength in bending are presented in Figure 3.28a and 3.28b, respectively. It is noticed a higher coefficient of determination for $E_{m,g}$ compared to $E_{m,l}$ ($r^2 = 0.69 > 0.38$), evidencing the importance of globally assess the element and attend to all present defects. Also it should be noted that the correlation with $E_{m,g}$ is stronger as some of the failures were initiated near the loading points, which were out of the gauge length for measuring $E_{m,l}$.

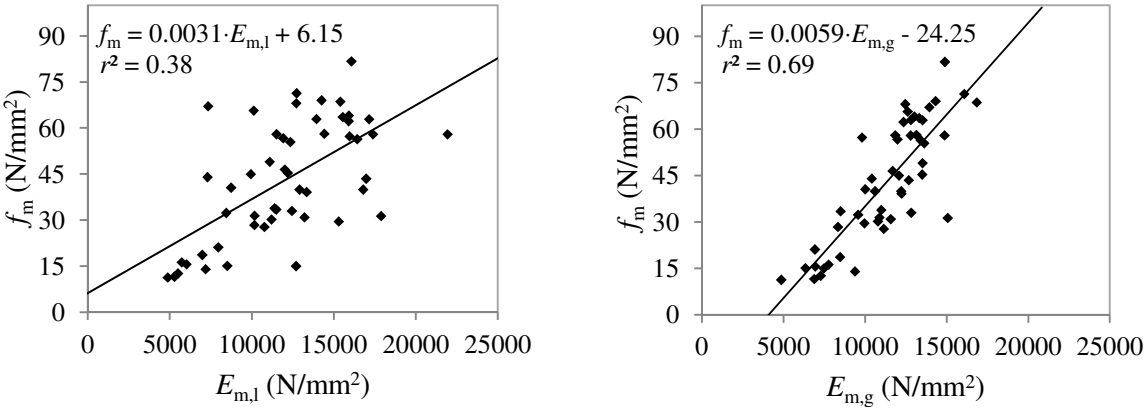

a) b)

Figure 3.28: Correlation of f_m of boards with MOE: a) $E_{m,l}$; b) $E_{m,g}$.

3.5 Phase 4 results

3.5.1 Compression parallel to grain tests

Ultrasound testing

The specimens were subjected to ultrasound testing by both direct and indirect methods (Figure 3.29). The same measurement methodology and equipment used previously for the sawn beams and boards was considered also for the measurements in the compression parallel to the grain specimens.

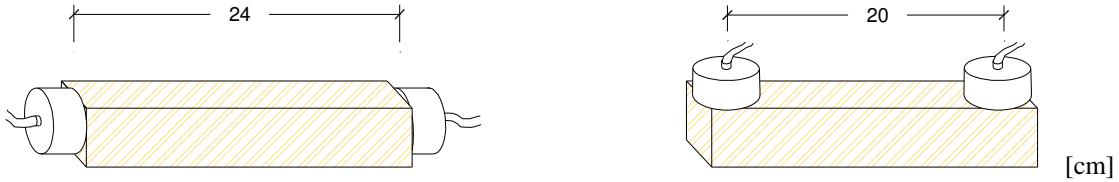

a) b)

Figure 3.29: Test sample for compression parallel to the grain in ultrasound testing: a) direct and; b) indirect methods.

The mean value of the propagation velocity was 4890 m/s for the indirect method and 5220 m/s for the direct method with COV of 9.7% and 3.7%, respectively. The average of the COV for the measurements in each beam is 7.9% and 2.6%, respectively for indirect and direct methods. The decrease of the coefficient of variation between the measurements of all beams and the measurements within a same beam, represent an

increase of variation when assessing different timber elements, even from the same structure and timber specie, as already evidenced in the ultrasound measurements made to the structural size beams and sawn boards.

The average *RD* between indirect and direct measurements is 7.6% with 28.3% of the elements with a relative difference higher than 10%. The distribution of values of relative difference between indirect and direct measurements is presented in Figure 3.30a. The coefficient of determination between indirect and direct measurements ($r^2 = 0.05$) indicates a non existing correlation between these two different measurements for this case (Figure 3.30b).

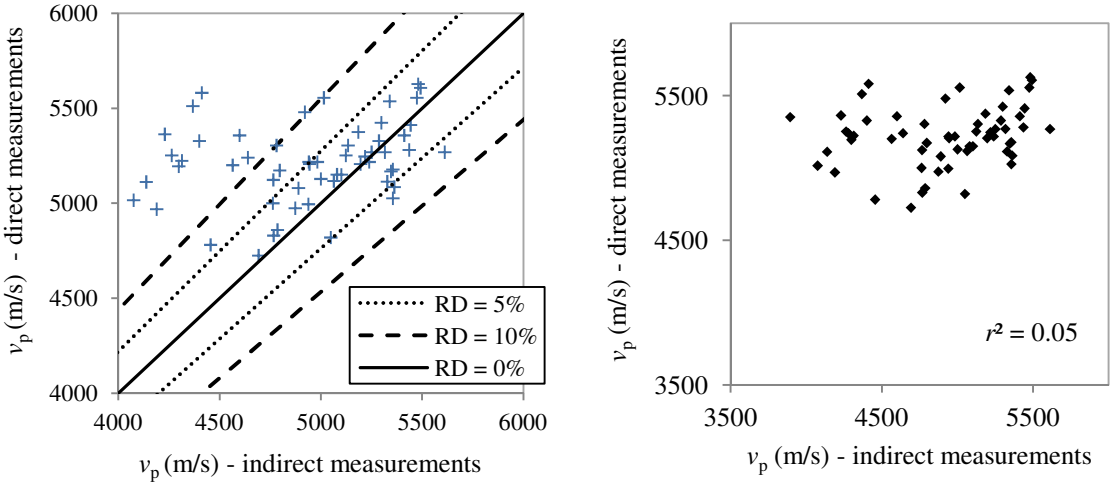

Figure 3.30: Velocity of propagation for indirect and direct measurements in compression parallel to the grain specimens: a) relative difference; b) relationship.

Destructive test

The pretended results from the tests are the compression parallel to the grain strength, $f_{c,0}$, and the elastic modulus of elasticity in compression, $E_{c,0}$, which are parameters commonly found in strength grading tables for timber structural elements. Deformation was measured over a central gauge length of four times the smallest cross section dimension of the sample (160 mm), using one pair of LVDTs (range ± 12.5 mm) placed on opposite faces to eliminate the effect of possible distortion (Figure 3.31).

The compression parallel to grain tests were carried out in the laboratory facilities of the Civil Engineering Department of the University of Minho using a Sentur II hydraulic unit with a 25 kN load cell. The used loading equipment was capable of measuring the load to a required accuracy of 0.1% of the applied load. The tests were made with displacement control and the displacement rate was calculated following the same assumptions taken to the bending tests, however regarding the estimated compression strength. Three preliminary tests were made to the specimens chosen randomly with the purpose of determining the displacement rate. According to those tests a single cycle test was

conducted with a constant displacement increment phase, and a displacement rate of 0.009 mm/s was found adequate.

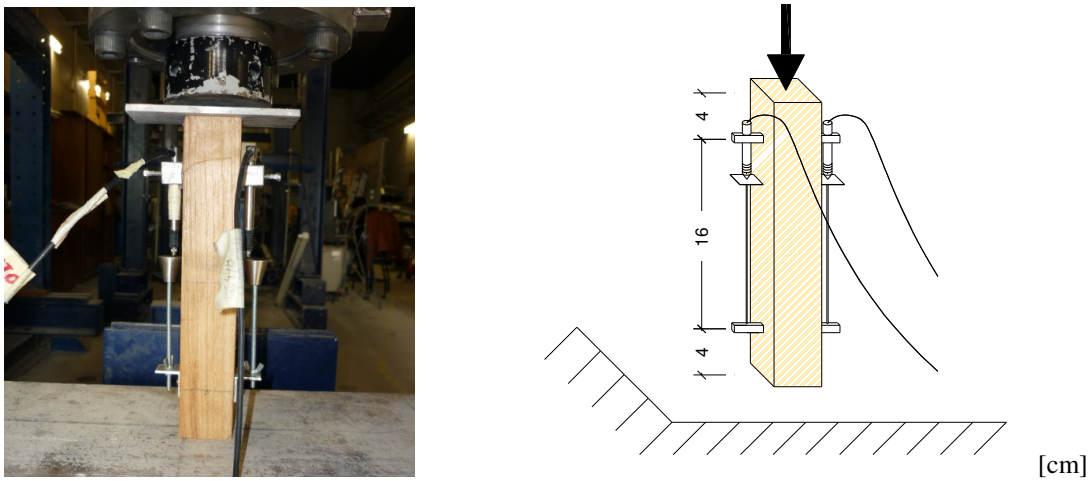

Figure 3.31: Test sample for compression parallel to the grain: photograph and schematic of test set-up.

The compression parallel to the grain tests were characterized regarding different types of failure modes, such as the following modes: crushing, wedge splitting, shearing, splitting, crushing and splitting, and brooming or end rolling (Bodig and Jayne, 1993) (Figure 3.32).

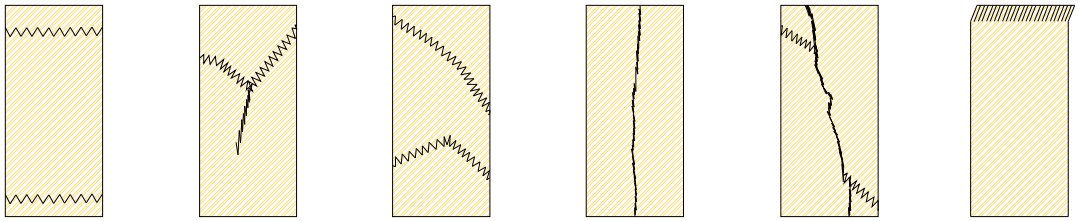

Figure 3.32: Types of compression failure modes: a) crushing; b) wedge splitting; c) shearing; d) splitting; e) crushing and splitting; f) brooming.

Attending to those failure modes an ANOVA was made. Regarding a single-factor ANOVA and a confidence level of 95% a non-significant variance in $E_{c,0}$ or $f_{c,0}$ ($F < F_{crit}$ and $p\text{-}value > 5 \times 10^{-2}$) was found, thus evidencing that for this experimental analysis the different failures modes did not pose as a significant parameter of differentiation for the mechanical properties variation. Therefore, the result values are mentioned regarding the entire sample without failure mode discrimination. An example of the load/displacement curves for samples with different failure modes is presented in Figure 3.33. Samples have been considered with similar peak loads in order to compare the post failure behaviour. The main difference after the peak load is observed regarding the failures conditioned by splitting where a more fragile behaviour is present, whereas for crushing or brooming a ductile behaviour is observed post peak. In the crushing and splitting failure mode a slight

constant decrease of the load capacity is visible, whereas for shearing failure a more marked decrease is found.

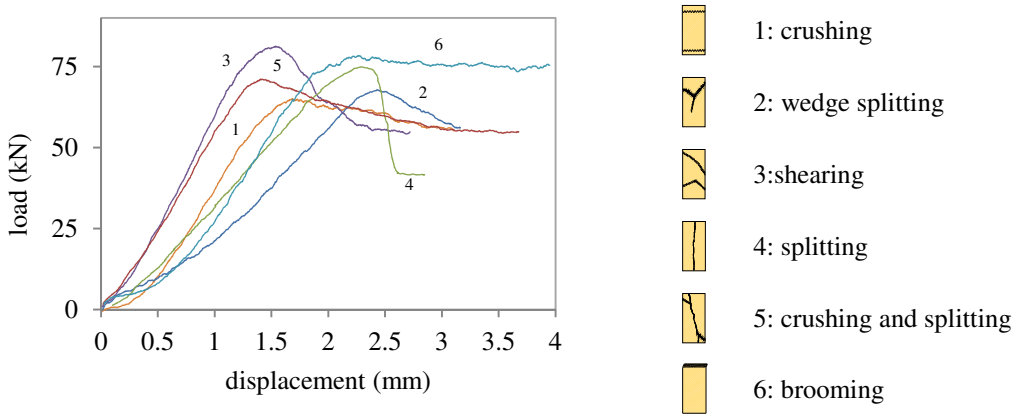

Figure 3.33: Load/displacement curves for different compression failure modes.

For the global sample, a mean value of 12620 N/mm^2 was found for $E_{c,0}$ with COV of 15.7%, whereas for $f_{c,0}$ a mean value of 42.99 N/mm^2 was found with a COV of 17.2%. The average of the COV for the measurements in each beam is 11.6% and 15.2%, respectively for $E_{c,0}$ and $f_{c,0}$. The decrease of the COV between the measurements of all beams and the measurements within a same beam was also present in the ultrasound tests.

The linear correlation between $f_{c,0}$ with the propagation velocity in ultrasound tests with its respective coefficient of determination are presented in Figure 3.34, where it is visible that no significant correlation was found. Detail about correlation with stiffness will be provided in a following chapter[4].

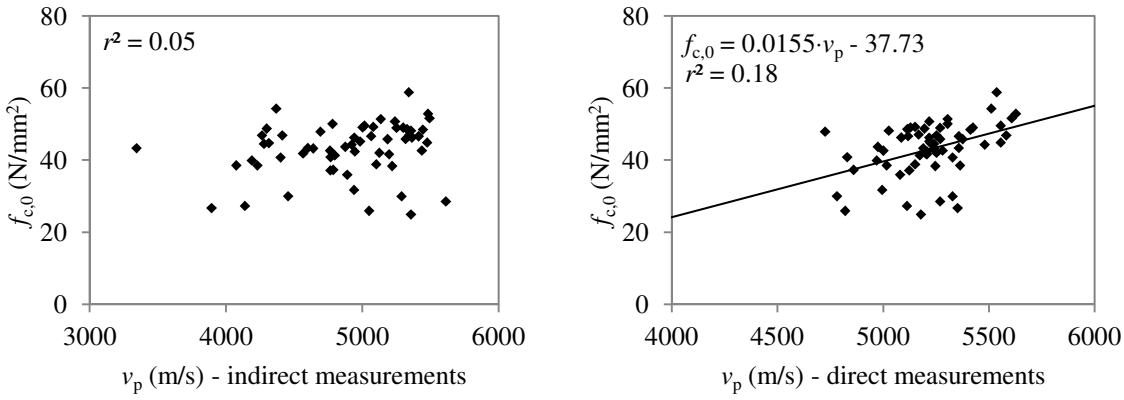

a) b)

Figure 3.34: Correlation between compression parallel to grain mechanical properties and propagation velocity: a) $f_{c,0}$ and v_p indirect measurements; b) $f_{c,0}$ and v_p direct measurements.

[4] Chapter 4: Probabilistic parameter analysis

3.5.2 Tension parallel to grain tests

Ultrasound testing

The specimens were subjected to ultrasound testing by indirect method (Figure 3.35). The same measurement methodology and equipment used previously for the compression parallel to grain measurements was used here.

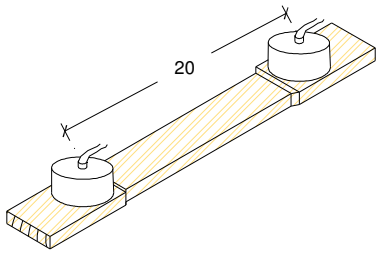

Figure 3.35: Indirect ultrasound of tension parallel to grain test samples.

The mean value of the propagation velocity was 4200 m/s for the first samples and 4210 m/s for the second samples with coefficients of variation of 3.7% and 3.8%, respectively. Considering the total sample (the sum of the two samples) a mean propagation velocity of 4190 m/s with COV = 3.5% was found. The average of the COV for the measurements in each beam (considering all samples derived from the same beam) was COV = 2.9%. The decrease of the COV between the measurements of all beams and the measurements within a same beam, represent an increase of variation when assessing different timber elements, even from the same structure and timber specie, as already evidenced in the previous test phases.

The average *RD* between measurements on sample A and B is 3.4% with 27.0% of the elements with a relative difference higher than 5%. The distribution of values of relative difference between measurements on sample A and B is presented in Figure 3.36a. The coefficient of determination between measurements on sample A and B ($r^2 = 0.11$) indicates a non existing correlation between these two different measurements (Figure 3.36b). A non existing correlation was expectable since the measured parameter is the same for both sample groups (being visible in the graph by the concentration of the values around the mean value). Only a correlation could be possible between the values of a pair of samples taken from the same segment of beam, thus *RD*, in this case, is a better indicator of the similarity or disparity of values between samples.

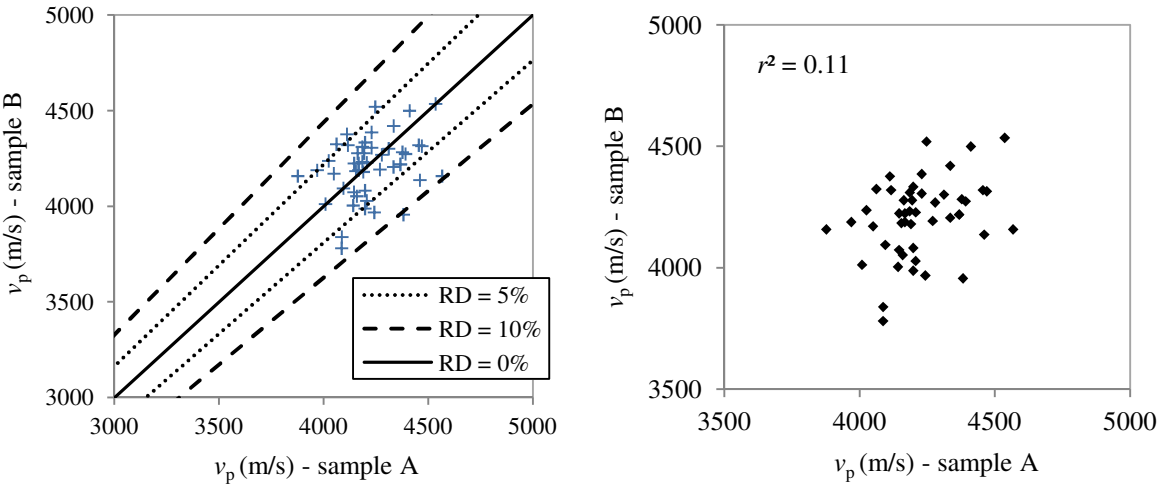

Figure 3.36: Velocity of propagation for sample A and B in tension parallel to the grain specimens: a) relative difference; b) relationship.

Destructive test

The pretended results from the tests are the tension parallel to the grain strength, $f_{t,0}$, and the elastic modulus of elasticity in tension, $E_{t,0}$, which are parameters commonly found in strength grading tables for timber structural elements. Deformation was measured over a central gauge length of 50 mm (one third of the middle section length), using one clip-on extensometer (measuring length 50 mm) with the contact points placed in the middle longitudinal axis (Figure 3.37).

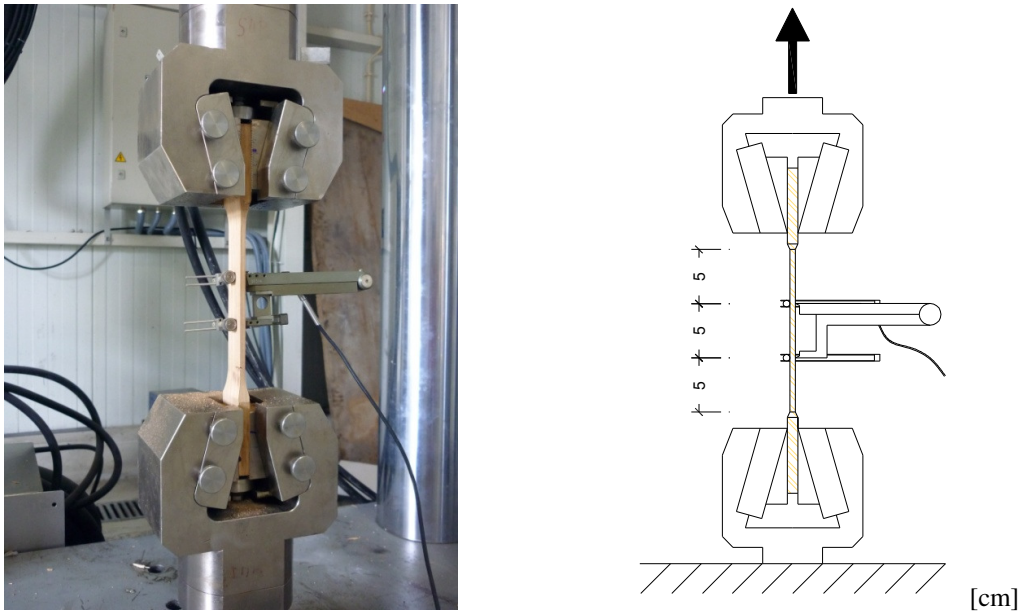

Figure 3.37: Test sample for tension parallel to the grain: photograph and schematic of test and set up.

The tension parallel to grain tests were carried out in the laboratory facilities of the Civil Engineering Department of the University of Minho using a MICROTEST (SCM4000) hydraulic unit with a 200 kN load cell. The used loading equipment was capable of measuring the load to a required accuracy of 0.1% of the applied load. The tests were made with displacement control and the displacement rate was calculated following the same premises as previously mentioned for the destructive tests for bending and compression strength determination. Three preliminary tests were made to the specimens chosen randomly with the purpose of determining the displacement rate. According to those tests a single cycle test was conducted with a constant displacement increment phase, and a displacement rate of 0.02 mm/s was found adequate (when significant slope of grain was found the displacement rate was decreased to a minimum of 0.014 mm/s).

The mean value of $E_{t,0}$ was 12690 N/mm^2 for the first samples and 12900 N/mm^2 for the second samples with coefficients of variation of 12.9% and 13.0%, respectively. Considering the total sample (the sum of the two samples) a mean $E_{t,0}$ of 12670 N/mm^2 with COV = 12.5% was found. The average of the COV for the measurements in each beam (considering all samples derived from the same beam) was 9.7%.

The mean value of $f_{t,0}$ was 72.52 N/mm^2 for the first samples and 74.63 N/mm^2 for the second samples with coefficients of variation of 27.1% and 26.5%, respectively. Considering the total sample (the sum of the two samples) a mean $f_{t,0}$ of 71.78 N/mm^2 with COV = 27.1% was found. The average of the COV for the measurements in each beam (considering all samples derived from the same beam) is 25.1%. The decrease found for the COV in the $E_{t,0}$ and $f_{t,0}$ results between the measurements of all beams and the measurements within a same beam was also present in the ultrasound tests. After assessing the variation within the full sample, the tension parallel to the grain tests were characterized regarding different types of failure modes, such as the following modes: splintering tension, combined tension and shear, shear and brittle tension (Bodig and Jayne, 1993), considering also failure due to defects and failure in the gripping area (Figure 3.38).

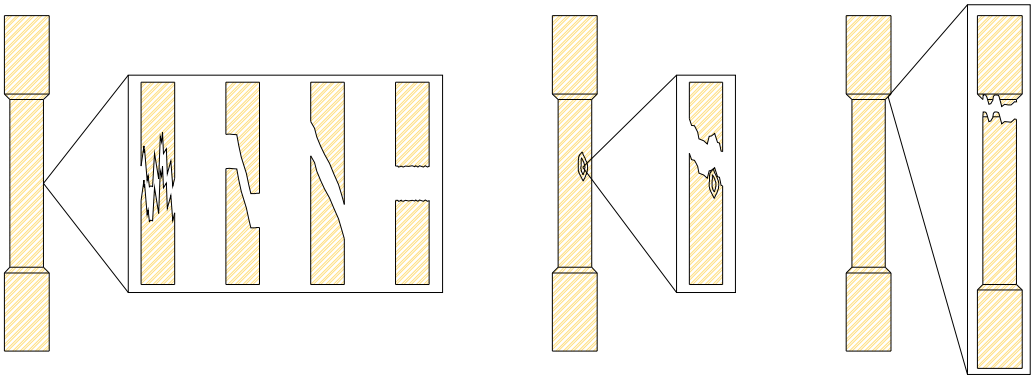

a) b) c) d) e) f)

Figure 3.38: Types of failure modes in tension parallel to grain: a) splintering tension; b) combined tension and shear; c) shear; d) brittle tension; e) defect influence; f) gripping influence.

Attending to those failure modes an ANOVA was made. Regarding a single-factor ANOVA and a confidence level of 95% a significant variance in both $E_{t,0}$ and $f_{t,0}$ ($F < F_{crit}$ and $p\text{-}value > 5 \times 10^{-2}$) was found, thus evidencing that for this experimental analysis the different failures modes pose as a significant parameter of differentiation for the mechanical properties variation. Therefore, the result values are mentioned regarding the entire sample without failure mode discrimination and also regarding the different failure modes in Table 3.1 (specimens are considered as individual samples without consideration of the mean value between A and B locations in the board's height, since different failure modes were observed even between those pairs of samples).

Table 3.1: Results of $E_{t,0}$ and $f_{t,0}$ from tension parallel to the grain tests attending to different failure modes.

Failure mode*	$E_{t,0}$ (N/mm^2)				$f_{t,0}$ (N/mm^2)			
	min	max	mean	COV (%)	min	max	mean	COV (%)
splinter	9539	16245	13608	10.64	44.88	113.89	79.99	21.99
shear	9386	14250	11539	13.85	46.01	83.36	61.54	22.53
tension	9868	14558	12165	10.60	28.56	103.69	72.40	31.11
defect	9038	15682	12867	21.03	13.96	67.22	47.62	46.03
gripping	10224	14290	12437	10.22	50.02	106.17	73.57	19.71
all	9038	16245	12783	12.88	13.96	113.89	73.23	26.69

* combined tension and shear was not found in any of the test specimens

The results present that a larger COV is found, in both stiffness and strength, when the failure mode was influenced by the presence of defects (mainly small diameter knots that were only detected during the preparation of specimens). The variation of values is smaller for the $E_{t,0}$ since it is a parameter calculated in the elastic range where the influence of defects is less significant. The mean value of $f_{t,0}$ when considering the influence of defects is significantly smaller than the other failure modes, evidencing the importance of defects in tension parallel to grain behaviour. On the other hand, for mean $E_{t,0}$ the difference between failure modes is less significant, although splintering in tension presents higher values of elasticity.

The envelope load/displacement curves regarding each separate failure mode is given in Figure 3.39. The lower horizontal line corresponds to the minimum applied load after peak found for each case, whereas the higher peak corresponds to the maximum applied load. A longer horizontal length of the envelope curve corresponds to a more significant post peak behaviour of the specimen before complete failure. This is found for tension related failures (splintering and brittle), whereas shear and defect influenced failures present less significant post peak behaviour. The amplitude between upper and lower limit curves with respect to the origin, corresponds to the possible range for elastic moduli. In this case, it was found that higher values of amplitude were in correspondence with higher

values of COV for $E_{t,0}$ and lower values of amplitude were in correspondence with lower values of COV for $E_{t,0}$. The envelope load/displacement curve for all considered types of failure is presented in Figure 3.39f, where the contribution of each failure mode is presented in dashed line.

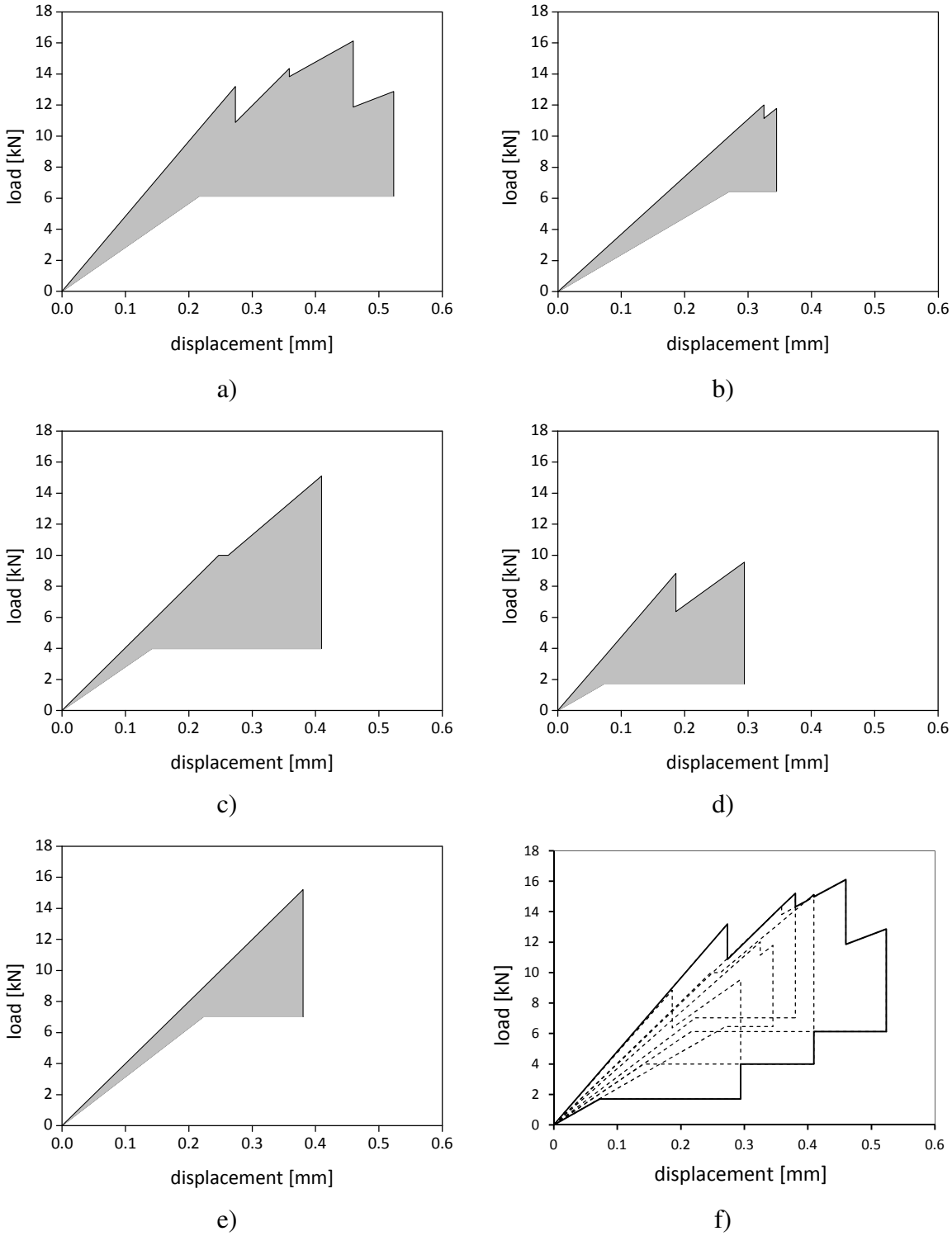

Figure 3.39: Envelope load/displacement curves for tension parallel to grain tests for different failure modes: a) splintering tension; b) shear; c) brittle tension; d) defect influence; e) gripping influence; f) all failures.

The linear correlations between the tension parallel to grain strength with stiffness (Figure 3.40) and propagation velocity (Figure 3.41) were calculated assuming the different failure modes. Detail about correlation with stiffness and NDT parameters will be provided in a following chapter[5].

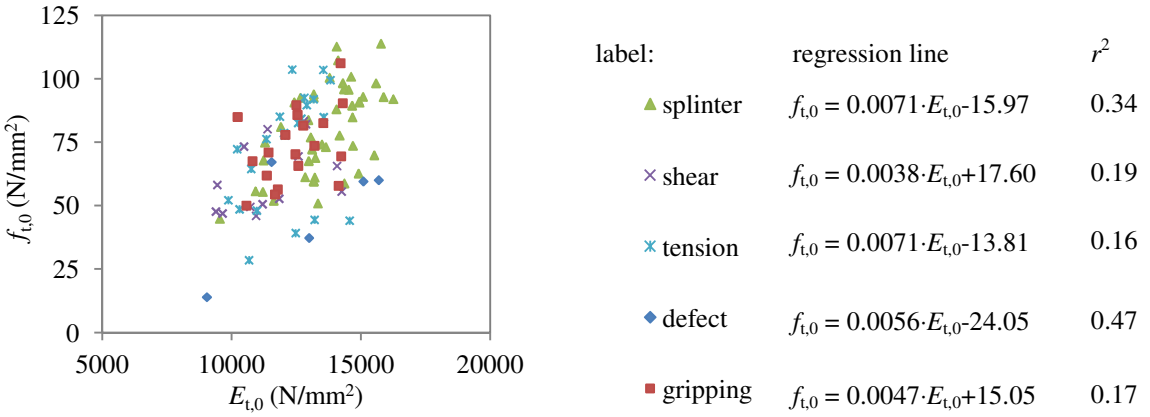

Figure 3.40: Correlation between $E_{t,0}$ and $f_{t,0}$ with consideration of different failure modes.

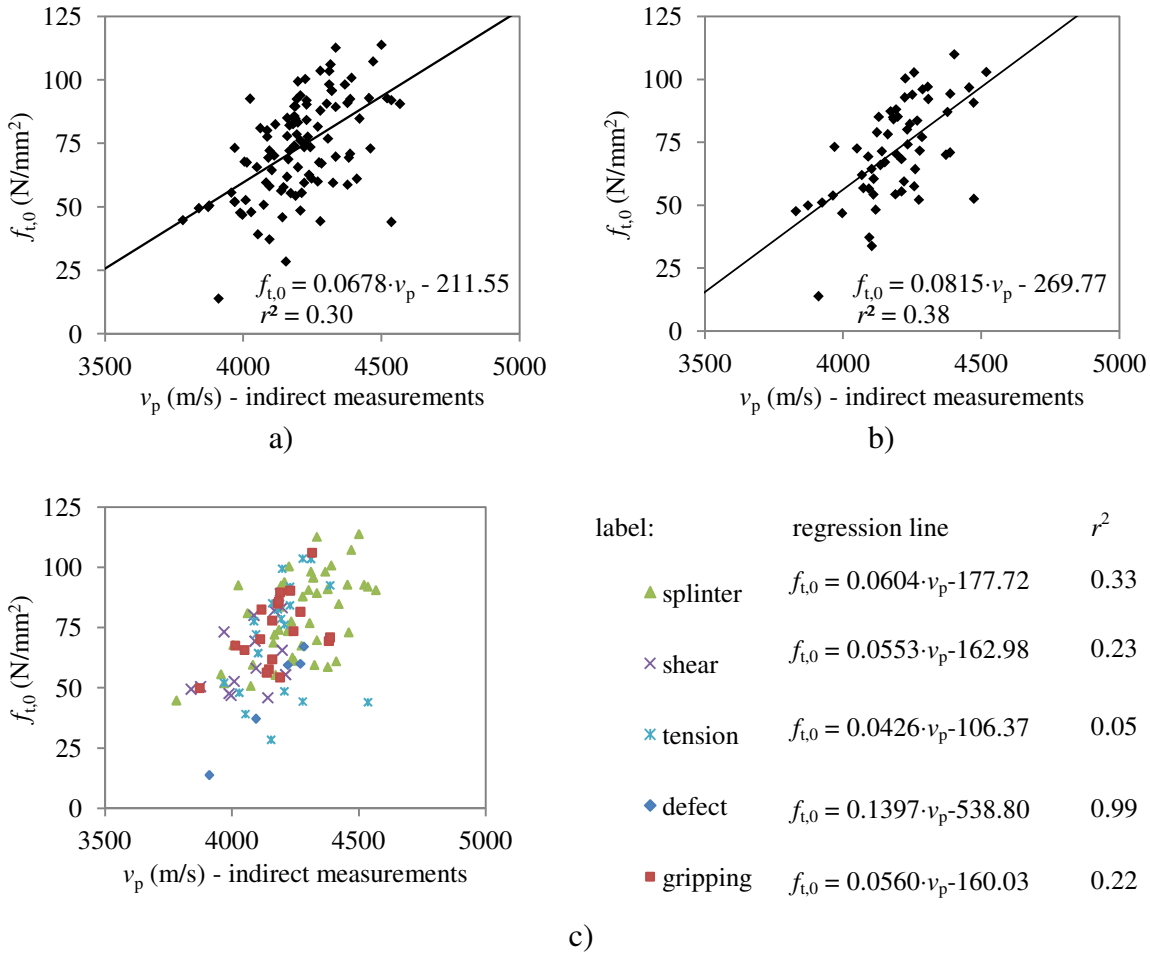

Figure 3.41: Correlation between v_p and $f_{t,0}$: a) all samples; b) mean of samples A and B; c) all samples with consideration of different failure modes.

[5] Chapter 4: Parameter probabilistic analysis

When considering the mean value of the two measurements by location, the coefficient of determination is slightly improved regarding the consideration of all samples. The consideration of different failure modes led to a better r^2 in the cases of splinter and defect influenced failures, but led to lower r^2 for the remaining failures modes. Overall, low correlations were found with exception of moderate correlations between the propagation velocity and $E_{t,0}$. Also a strong correlation was found between propagation velocity and $f_{t,0}$ of samples with defect influenced failure, however this correlation must be considered with caution due to the rather low number of samples for that failure mode.

3.5.3 Density and moisture content tests

In this test campaign, density and moisture content values were obtained using three small clear wood samples of 2 × 2 × 2.5 cm^3 (Figure 3.42), taken from each beam (one per each left, middle and right segments). After stabilized, in climatic chamber under conditions of 20 ± 2ºC and a relative humidity of 65 ± 5%, the samples were measured, weighed and corrected to a 12% MC density, ρ_{12}, then placed inside an oven (103 ± 2ºC) for determination of the dry-oven density, ρ_0, and moisture content, MC. The procedure and test methodology applied were in consistence with norms ISO 3130 (ISO, 1975a), ISO 3131 (ISO, 1975b) and UNI 13183-1 (UNI, 2003c).

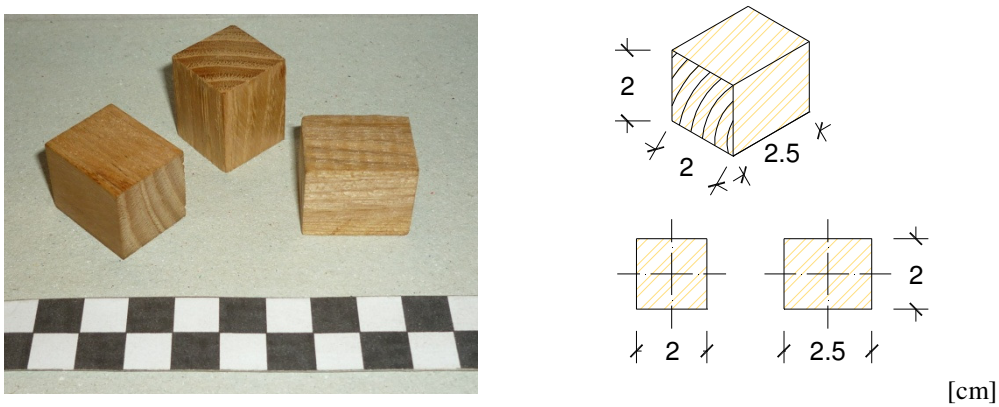

Figure 3.42: Test samples for density and moisture content determination.

The samples were considered stabilized (with constant mass) in a climatic chamber when the results of two successive weightings, carried out at an interval of six hours, did not differ by more than 0.5% of the mass of the test piece (ISO, 1975b). Weightings were made to five specimens chosen randomly, using a weighting scale with a precision of 0.01 g in intervals of six hours until the conditioned state was achieved. After reaching a stabilized condition the samples dimensions were measured with use of an electronic calliper (precision of 0.01 mm). Measurements were made in the symmetry axes of all faces. The density corresponding to this particular MC was then calculated, since it corresponds to the same conditions of the compression and tension parallel to grain test samples before testing. Density in a specific moisture content equal to W, ρ_W, is calculated as:

$$\rho_W = \frac{m_W}{a_W \cdot b_W \cdot l_W} = \frac{m_W}{V_W} \tag{3.8}$$

where m_W is the mass (kg or g) of the test piece at MC = W and a_W, b_W, l_W are the dimensions (m or cm) of the test piece at MC = W and thus V_W is the volume (m^3 or cm^3) of the test piece at MC = W. The above calculated density is then adjusted to a 12% MC by the formula given in Equation 3.9 valid for MC from 7 to 17%,

$$\rho_{12} = \rho_W \left(1 - \frac{(1-K)\cdot(W-12)}{100}\right) \tag{3.9}$$

where K_V is the coefficient of volumetric shrinkage for a change in MC of 1%. The value of K_V can be considered as 0.85×10^{-3} ρ_W when density is expressed in kg/m^3 and 0.85 ρ_W when density is expressed in g/cm^3.

The test pieces were then placed inside an oven in order to obtain ρ_0 and MC. The mass of the test pieces were considered stabilized when the results of two successive weightings, carried out at an interval of two hours, did not differ by more than 0.1% of the mass of the test piece (UNI, 2003c). When the stabilized state was achieved, the test pieces were taken to a desiccator with a silica based absorbent for drying air. After being cooled the test pieces dimensions and weight were measured (sufficiently rapid to avoid an increase of MC of more than 0.1%) and the ρ_0 was calculated through Equation 3.10, while MC was calculated, as percentage by mass, through Equation 3.11, as:

$$\rho_0 = \frac{m_0}{a_0 \cdot b_0 \cdot l_0} = \frac{m_0}{V_0} \tag{3.10}$$

where m_0 is the mass (kg or g) of the test piece at absolute dry condition and a_0, b_0, l_0 are the dimensions (m or cm) of the test piece at absolute dry condition and thus V_0 is the volume (m^3 or cm^3) of the test piece at absolute dry condition,

$$\mathrm{MC} = \frac{m_1 - m_2}{m_2} \cdot 100 \tag{3.11}$$

where m_1 is the mass (g) of the test piece before drying and m_2 is the mass (g) of the test piece after drying.

The density and moisture content measurements resulted in a mean value of density of 533.66 kg/m^3 for dry-oven conditions (MC = 0%) and 571.71 kg/m^3 for 12% MC with COV of 8.0% and 7.9%, respectively. The average of the COV for the measurements in each beam is 5.6% and 5.4%, respectively for 0% and 12% MC. Attending to the moisture content measurements, the mean value of MC was 12.21% with COV of 8.1%, while the average of the COV for the measurements in each beam was 3.8%.

3.6 Final remarks

The mechanical properties of a timber element may be assessed by several approaches, however only by a holistic methodology is possible to have a correct definition of its real performance and behaviour when subjected to different load scenarios. In this scenario, the presented experimental campaign evidenced the results obtained regarding different techniques (NDT, SDT and mechanical characterization) in a multi-scale size analysis.

Visual inspection and other NDT and SDT, are used as a connection between different size scales, and the mechanical properties of timber in bending, compression and tension were assessed. Visual inspection evidenced different percentages of segments included in a visual grade for the separate testing phases (Figure 3.43). In Phase 1, at the old beams scale, the average of segments in each visual grading class is 52.0% for I, 32.1% for II, 14.8% for III and 1.1% for NC. In Phase 2, at the sawn beams level, visual grading indicates an increase of the average percentage of segments for NC and a decrease for class I. A decrease in the average COV of the percentage of a given visual class between different members is also found. The average of segments in each visual grading class is 45.7% for I, 27.1% for II, 12.1% for III and 15.0% for NC. In Phase 3, when dealing with sawn boards, the average of segments in a visual grading class is 35.7% for I, 23.2% for II, 18.8% for III and 22.3% for NC. It was noticed that visual grading often leads to a large percentage of rejection of the analysed samples, depending on the considered restricting parameters.

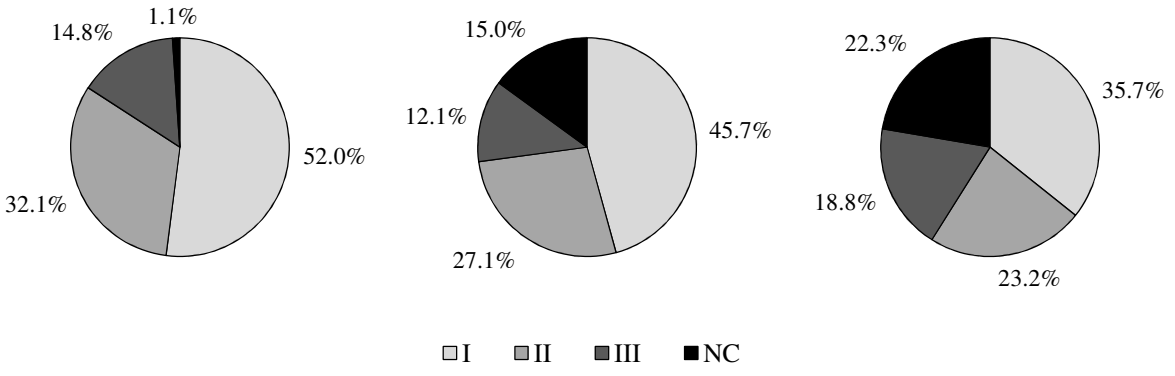

Figure 3.43: Percentage distribution of segments included in each visual grading class according to UNI 11119 (UNI, 2004) for the entire sample: a) old beams; b) sawn beams; c) sawn boards.

Visual inspection was accurate for predicting qualitatively the performance of the sawn beams, since the elements with larger percentage of lower grade timber exhibit lower values of bending MOE, despite the fact that it proved to be conservative for elements with higher grade class percentages. The old beams with at least 20% in lower classes in the visual inspection, resulted in the sawn beams with $E_{m,g}$ values lower than the mean, while old beams with more than 80% of percentage in higher visual classes originated sawn

beams with higher values of $E_{m,g}$. Also, in the lower size scale, when assessing the variability between visual grading in sawn boards, it was noticed a significant difference in the values of bending strength, such that a reduction factor of 32%, 42% and 72% are found for downgrading from class I, respectively to class II, III and NC.

In terms of bending stiffness, the mean values of sawn boards results were 18% and 7% higher than the equivalent values obtained for sawn beams, respectively for $E_{m,l}$ and $E_{m,g}$. As mentioned by Kasal and Anthony (2004), the timber member mechanical properties will always be lower than those of small clear specimens because of the inevitable presence of defects in structural size pieces. When the specimen size increases also the stressed volume increases and for brittle materials or systems organized in series, a higher probability exists that a weak link occurs in the volume (Weibull, 1939).

This increase is, thus, explained by the decrease in influence of defects in the global behaviour when the beam was divided into boards, resulting also in a higher COV due to the higher difference obtained between segments with and without defects. By isolating the effect of knots, timber mechanical properties will improve, as for example in the case of glulam beams which have better performance comparing to solid members of the same quality (Baltrušaitis, 1999).

Regarding clear wood specimens, compression and tension parallel to the grain tests were made. For the global sample, a mean value of 12620 N/mm^2 was found for $E_{c,0}$ with COV of 15.7%, whereas for $f_{c,0}$ a mean value of 42.99 N/mm^2 was found with a COV of 17.2%. No significant variation was found when considering different failure modes in compression. Also for the global sample, a mean value of 12670 N/mm^2 was found for $E_{t,0}$ with COV of 12.5%, whereas for $f_{t,0}$ a mean value of 71.78 N/mm^2 was found with a COV of 27.1%. In this case, significant variation was found when considering different failure modes in tension. The values of compression and tension stiffness were found to be very similar both in mean value and COV, however a significant higher tensile strength was found but also with higher COV.

Density and moisture content were also determined. After stabilized (in climatic chamber under conditions of 20°C and 59.6% RH), a mean value of density equal to 519 kg/m^3 was obtained with COV of 7.9% for all the sample and 5.5% within beams, whereas a mean value of 12.2% was determined for moisture content with COV of 8.1% for all the sample and 3.8% within beams.

This page intentionally left blank

Chapter 4

Parameter probabilistic analysis

ABSTRACT: Wood is an anisotropic material and its mechanical properties vary not only between different species, but also within the same species and even within the same element. The variation of wood's mechanical properties is inherent to the natural microscopic structure and arrangement of its fibers. Due to this aspect, timber must be assessed not only regarding the surrounding environmental conditions but also considering the direction of solicitation. Although the complex mechanisms through which timber behaves in different solicitations, it is often assumed that the mechanical properties of timber may be defined by so-called reference properties, which through its knowledge, will allow to define the other properties by empirical correlations.

The following chapter presents a framework for assessment of variation of experimentally tested timber mechanical properties (both by NDT, SDT and mechanical testing) in order to establish correlations that may permit to assess an existing timber element by measurement of a reference property. For that purpose, the coefficients of variation in each type of test are analysed regarding different scales assumed by the phases of the experimental campaign and by the size of the sample. An analysis regarding the dispersion and outliers is also provided. Moreover, the results of the previous described experimental campaign are used as a database for the definition of the correlation between measured mechanical properties regarding its variability.

Finally, fitting of the data to probability distributions will be discussed, taking into account the use of Maximum Likelihood Estimates and Goodness-of-fit significance tests.

4.1 Variation of results

4.1.1 Introduction

Non-destructive testing provides the means to rapidly inspect and detect potential weak zones in timber, however these methods often produce unreliable results in the prediction of material properties. As stated in Kasal and Anthony (2004), these methods can give reasonable comparative measurements, but present weak correlations with material strength and with mechanical properties assessed by destructive testing. This correlation is often weak, due to natural variability of wood properties, both between and within samples. However, even if destructive methods are the most reliable source of information about the strength properties of a given element, they require the extraction and destruction of the tested sample, which is often unacceptable, especially in historic structures. The same authors, also state that the gap between indirect non-destructive and direct fully destructive methods of strength measurement may be overpassed by use of semi-destructive methods, however these methods present an increased variability in the test observations due to use of small size specimens. So, in order to obtain representative data, a careful spatial distribution of samples and statistical experiment planning and evaluation are of utmost importance. Nevertheless, these methods only present information about the material properties that must be first correlated with macroscopic parameters, such as size and location of natural defects, in order to calculate the strength and stiffness of full scale timber members.

One must note that the range of coefficients of variation (COV) for a given property may be quite significant, and that the mechanical properties of wood vary significantly within a species. Variability in wood is also dependent of the scale of analysis, such that, the variability of properties within a member is fairly lower than the variability between members, and is usually greater across the timber thickness when compared with the variability along the timber (Brown *et al.*, 1952). In Machado and Cruz (2005), the mechanical properties of Maritime Pine timber were observed to evidence a decrease trend along the stem (from bottom to top), where juvenile wood seemed to be a key factor of differentiation. Variation within-stem was found to be significant, such that a clear increase on bending strength (55%), modulus of elasticity parallel to grain (99%), compression strength parallel to grain (44%) and tension strength perpendicular to grain (27%) for distance to pith from 10% to 90% of the trunk radius was observed. For Norway spruce of both fast and slow-grown stands, Kliger *et al.* (1998) found an increase of bending strength (47%) and of modulus of elasticity in bending (30%) in mature wood compared to wood near the pith. Also for Norway spruce, Ormasson *et al.* (1998) mentions a positive correlation between distance to pith and modulus of elasticity parallel to grain, as the region near the bark presents up to four times the stiffness near the pith.

4.1.2 Variation within phases and scales

The properties of wood located between defects (clear wood) are expected to correspond to both higher strength and modulus of elasticity (MOE) and to present less variability

compared to sections of timber influenced by defects. Therefore, it is not prudent to consider the results of mechanical tests that only assess small wood samples without defects, since the presence of defects may largely influence the structural behaviour of the element. The measurement of both weak segments and clear wood sections, leads to the definition of the boundary for a possible range of values that a given segment may take within an element and its contribution to the global safety analysis. Nevertheless, even within this range, the mechanical properties may vary significantly.

Variability of mechanical properties is an important aspect in structural safety analysis, since a higher variability will inevitably lead to higher uncertainty on the global assessment. In order to minimize the effects of variability, large amounts of data are often required which may be inconsistent with an analysis of an existing structure where a large campaign test is usually both costly and time consuming. Therefore, it is normally assumed that the measurement of a given selected sample of segments might be representative of the global element.

In this topic, COV has been used to measure the dispersion and variability of the results from each experimental phase and scale. To each phase, the results were differentiated according to its origin by use of different size scales. These scales are, respectively from bigger to smaller size, referent to the measurements made to all beams (S1), to each beam (S2) and to each board (S3), see Figure 4.1. In Phase 4, the full set of small clear samples from a given beam is assumed to be equivalent to the scale of a beam (S2).

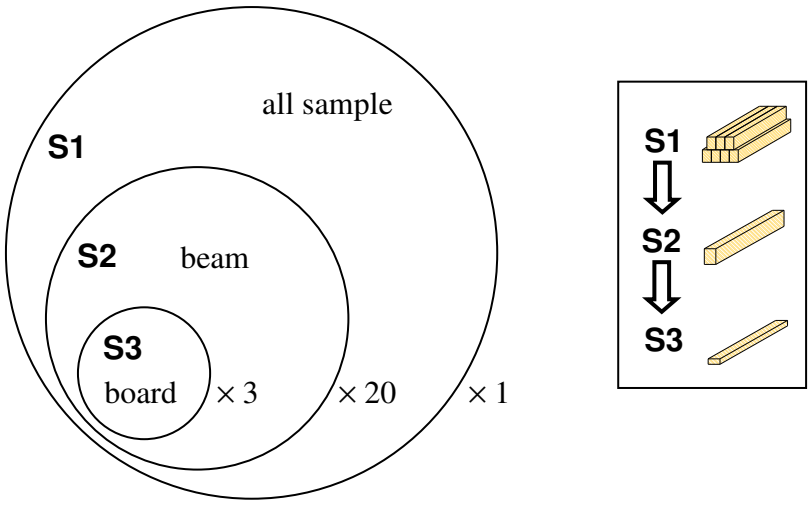

Figure 4.1: Definition of scales for sample differentiation with respect to origin and size.

Experimental campaign phases

With respect to experimental campaign Phases 1 to 3, Table 4.1 shows the COV for different tests and scales. From its analysis it is noticeable that the value of COV tends to decrease when a smaller scale is considered (decrease of COV from S1 to S3). This is mainly due to the higher influence of outliers when found in a larger scale, as the sample

size was smaller in the larger scales. The higher values of dispersion were found when evaluating the MOE resulting from the 4-point bending tests, evidencing that the range of values obtained in such tests was significantly higher than the obtained for the remaining ones. Amongst the NDT, the smaller dispersion was found for the ultrasound tests (ultrasound pulse velocity, UPV), whereas the penetration depth evidenced the higher values.

Table 4.1: Coefficients of variation (%) for the different tests made in Phases 1 to 3.

scale \ measure		penetration depth[1)]		resistance measure[1)]		UPV[1), 2)]		MOE		ultimate strength
		bottom	lateral	bottom	lateral	bottom	lateral	$E_{m,l}$	$E_{m,g}$	
Phase 1	all sample	23.4	22.5	22.6	---	---	---	---	---	---
	per beam	15.0	12.9	---	---	---	---	---	---	---
Phase 2	all sample	---	---	10.4	---	8.6	6.6	25.3	22.0	10.5
	per beam	---	---	---	---	6.3	4.9	---	---	---
Phase 3	all sample	14.3	14.7	10.2	10.2	8.4	---	30.4	22.8	44.9[3)]
	per beam	11.7	13.0	8.7	8.2	6.9	---	26.5	19.7	---
	per board	10.5	10.8	7.6	6.5	6.3	---	25.8	17.9	---

[1)] test performed perpendicularly to the face
[2)] propagation velocity in indirect measurement
[3)] high value due to a selected sample accounting different visual grades

Table 4.2 shows the COV for different tests and scales concerning experimental Phase 4, where, as seen in the previous phases, the value of COV tends to decrease when a smaller scale is considered. The dispersion of NDT results (in this case, the ultrasound tests) is also smaller than the dispersion found in the mechanical tests. Although similar, the COV of MOE in compression parallel to grain ($E_{c,0}$) was found to be higher than the COV of MOE in tension parallel to grain ($E_{t,0}$). The COV of strength found in tension parallel to the grain ($f_{t,0}$) was found to be much higher than the COV of strength found in compression parallel to the grain ($f_{c,0}$), justified by the higher sensibility that wood has to defects in tension rather than in compression and also due to the ductile behaviour in compression failure compared to a much more fragile failure characteristic for tension.

Table 4.2: Coefficients of variation (%) for the different tests made in Phase 4.

scale	measure		UPV[1)] direct	UPV[1)] indirect	MOE	ultimate strength	density 12% MC	density 0% MC	MC
Phase 4	compression \\ grain	all sample	3.9	9.7	15.7	17.2	---	---	---
		per beam	2.6	7.9	11.6	15.2	---	---	---
	tension \\ grain	all sample	---	3.5	12.5	27.1	---	---	---
		per beam	---	2.6	8.0	24.7	---	---	---
	density	all sample	---	---	---	---	7.9	8.0	---
		per beam	---	---	---	---	5.4	5.6	---
	moisture content	all sample	---	---	---	---	---	---	8.1
		per beam	---	---	---	---	---	---	3.8

[1)] propagation velocity

Visual inspection

In order to assess the variability between visual inspection made within each phase of the experimental campaign, and thus to different scales of the element, the difference (in absolute value) between percentages of segments found in a given strength class was calculated. The mean value of the differences and the respective COV are given in Table 4.3, where it is noticeable that the differences between two consecutives phases (from Phase 1 to 2, or from Phase 2 to 3) is smaller than the differences between the two non consecutive phases (from Phase 1 to Phase 3). Although, the differences between phases are relatively small regarding the subjectivity inherent to a visual inspection, the COV are considerably high. For classes I and II the variation is higher in the differences between Phases 2 and 3, whereas for classes III and NC, the variation is higher in the differences between Phases 1 and 2.

Table 4.3: Difference (in absolute value) between percentages of segments found in a given strength class.

Scale phases[1)]	Visual strength class (UNI 11119 (UNI,2004))							
	I		II		III		NC	
	mean	COV	mean	COV	mean	COV	mean	COV
1 to 2	18.99	81.89	26.51	80.35	11.04	134.69	14.64	94.47
2 to 3	14.28	103.19	12.51	101.19	11.62	80.63	11.61	80.57
1 to 3	27.12	51.27	26.61	70.04	16.14	102.19	21.48	75.83

[1)] Phases: 1 - old timber beams; 2 - sawn beams; 3 - sawn boards

Ultrasound testing

In Figure 4.2, the dispersion of the COV regarding different scales is presented for both measurement in sawn beams and boards. For different scales the average values of COV are connected by a continuous line. Lower COV are found when assessing the lateral face of the sawn beams, whereas a higher dispersion of values is found when considering the measurements made to the sawn boards. Comparing the bottom face measurements in the experimental Phases 2 and 3, it is visible that the COV for the full sample (all beams and all boards) is similar and that the COV for the beam (real or equivalent) scale is also similar.

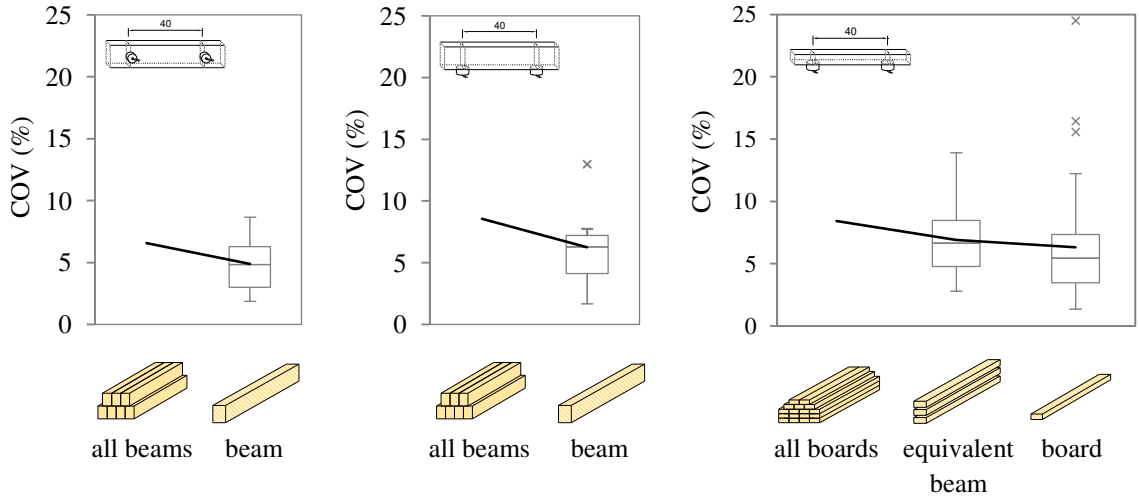

Figure 4.2: Dispersion of the COV of propagation velocity in different element scales, measurements in: a) lateral face of sawn beams; b) bottom face of sawn beams; c) bottom face of sawn boards.

Bending tests

The values of $E_{m,g}$ and $E_{m,l}$, were divided according to the visual inspection made to each segment and the results, in terms of mean and COV, are presented in Table 4.4. A decrease in the mean value and an increase of the COV is visible for lower visual inspection classes. For classes I and II, the COV is lower than for the other classes and similar between them. The COV is larger for lower classes (III and NC) since the presence of defects increases the variability of the results.

Table 4.4: $E_{m,l}$ and $E_{m,g}$ according to differentiation between visual inspection classes.

Parameter		Visual inspection classes			
		I	II	III	NC
$E_{m,l}$	mean (N/mm^2)	14026	12603	10718	8805
	COV (%)	25.4	25.7	34.9	41.0
$E_{m,g}$	mean (N/mm^2)	12580	11246	10032	8395
	COV (%)	17.6	18.8	24.7	32.3

4.2 Dispersion of values and outliers

In the previous topics, it was found that the variation and dispersion of results are largely influenced by the presence of values that appear to deviate markedly from the sample. These values are often denominated as outliers, defined in ISO 16269-4 (ISO, 2010) as a member of a small subset of observations that appears to be inconsistent with the remainder of a given sample. Outliers can indicate a measurement error or that the sample has a heavy-tailed distribution. In the first case, one may suggest to discard the outliers or to use robust statistics, while in the second case the presence of outliers may indicate that the adjacent distribution has a high kurtosis (probability distribution evidencing a sharper peak and longer, fatter tails, while low kurtosis distribution has a more rounded peak and shorter, thinner tails). For the case of high kurtosis distributions, an outlying observation is merely an extreme manifestation of the random variability inherent in the data and the value should be retained and processed in the same manner as the other observations in the sample (ASTM E178, 2008).

Model-based methods which are often used for outlier detection take as premise that the data may be represented by a normal distribution, and by that assumption they identify observations that are likely outliers based on mean and standard deviation. A commonly used method is the Grubbs' test for outliers, where in a two-sided hypothesis test (either having or not having outliers in the sample), the test statistic is given by the largest absolute deviation from the sample mean in units of the sample standard deviation. The hypothesis of no outliers in a Grubb's test is then rejected regarding a given significance level.

Graphical methods, without any premise about the statistical distribution, are also used to evidence the dispersion of the sample and the possible presence of outliers. Within these methods, box plots are one of the most common. A box plot is a graphical method to describe the dispersion of a numerical data sample through the representation of five parameters: the smallest observation (sample minimum), the lower quartile (Q_1), the median (middle quartile, Q_2), the upper quartile (Q_3) and the largest observation (sample maximum). The body of a box plot is composed by a rectangular shape box delimited by the lower and upper quartiles. The box is then connected to the maximum and minimum values by straight lines usually known as whiskers. In a box plot, outliers are identified based on the interquartile range, such that an outlier may be defined as any observation that is outside the range (respectively for lower and upper outliers):

$$[Q_1 - k \cdot (Q_3 - Q_1) \quad , \quad Q_3 + k \cdot (Q_3 - Q_1)] \tag{4.1}$$

where k is a constant, that for usual analysis takes the value of 1.5 or 3.

Box plots are non-parametric since they display differences between populations without any inference or assumption of the underlying statistical distribution. The interval between the different sections of the box permits to evaluate the degree of dispersion and skewness in the data, and to identify outliers.

Skewness is a measure of the asymmetry of a probability distribution of a certain random variable, being either negative or positive, respectively depending whether data points are skewed to the left or to the right of the data average. A null skewness indicates that the data is relatively evenly distributed on both sides of the mean. In a box plot, the median line (Q_2) can also suggest skewness in the distribution if it is noticeably shifted away from the centre. The location of the box within the whiskers can provide insight on the normality of the sample's distribution, such that if the box is shifted significantly towards the minimum value it presents positive skewness, whereas if shifted towards the other direction (maximum value) it may be indicative of a negative skewness. Box plots may also bring insight to the kurtosis of the distribution, such that a very thin box in relation to the whiskers may evidence a higher concentration of values within the interquartile range, as found in distributions with high kurtosis. A larger box compared to the whiskers may be associated to a low kurtosis distribution. Nevertheless, assumptions about the shape parameters of the underlying sample distribution, either skewness or kurtosis, must be taken with caution when only assessing a box plot, since it may lead to erroneous conclusions.

In this study, a dispersion analysis using box plots was made to the different test result samples in the four experimental phases. For outlier range definition a k = 1.5 was chosen.

4.2.1 Phase 1

The penetration depth was analysed in terms of dispersion by box plot and the results evidenced that no outlier was found (Figure 4.3). However, a rather significant dispersion is found regarding that the distance between maximum value and third quartiles is higher than the interquartile difference (Q_3 - Q_1). Attending to the location of the box plot, a small positive skewness is found.

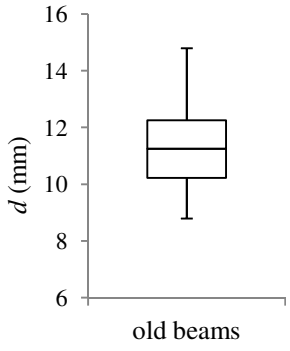

Figure 4.3: Box plot for penetration impact depth in old beams.

4.2.2 Phase 2

With respect to the experimental tests made to the sawn beams, the propagation velocity, the MOE in bending (both local and global) and the bending strength were analysed. When

considering the propagation velocity results (Figure 4.4a), it was found that both tests made to lateral and bottom faces evidenced a significant number of lower outliers, denoting extreme values in the left tail of the underlying distribution (specially to the lateral face measurements). Comparing lateral and bottom measurements, a higher dispersion between quartiles Q_1 and Q_3, and longer whiskers, are found in the bottom measurements. However, both present similar median. No significant indication about the shape of the distributions is noticeable.

A comparative analysis between $E_{m,l}$ and $E_{m,g}$ (Figure 4.4b) indicates a higher dispersion for the sample of the latter, although two outliers (one lower and one upper) were found when analysing the values of the $E_{m,l}$ sample. The median value of $E_{m,l}$ is higher and its position is more centred with the quartiles Q_1 and Q_3 when compared to the $E_{m,g}$ median value which is closer to the inferior quartile Q_1, indicative of a possible positive skewness. In both cases, the dispersion is quite high taking into account the range between the maximum and minimum values without outliers. The box plot for the bending strength (Figure 4.4c) must be considered with care, since the sample number is insufficient to construct a reliable dispersion statistic.

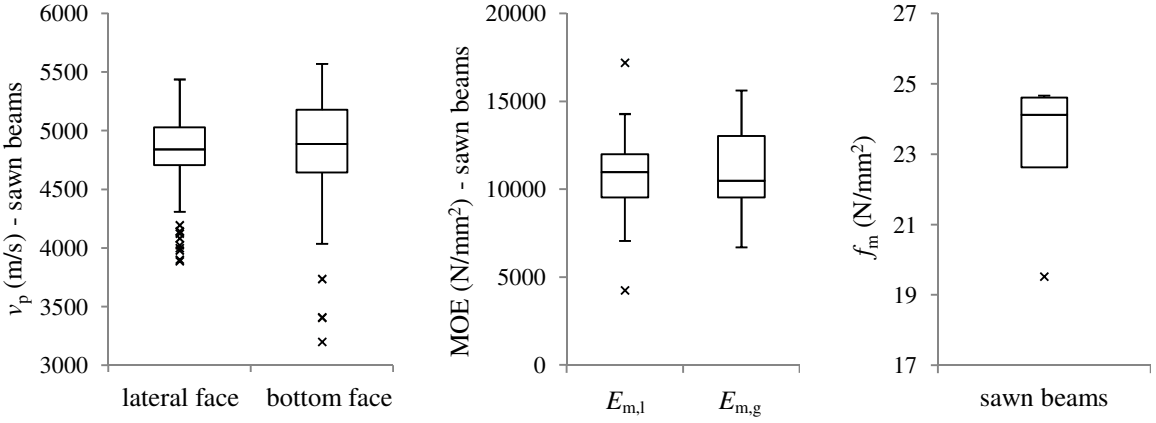

a) b) c)

Figure 4.4: Box plot for tests made on sawn beams: a) propagation velocity in ultrasound testing by the indirect method; b) MOE in bending tests; c) bending strength.

4.2.3 Phase 3

With respect to the experimental tests made to the sawn boards, the propagation velocity, the MOE in bending (both local and global), penetration depth and drilling resistance were analysed. When considering the propagation velocity results (Figure 4.5a), it was found that the tests made to bottom face of the boards by indirect method, presented a large number of lower outliers. This evidences extreme values in the left tail of the underlying distribution, which has also similarly occurred in the previous phase for the analogous measurements. In this case, by comparison to the distance from quartile Q_1 to the lower outliers, a rather thin box is found, however, a small difference is found if comparing the size of the box with the length of the whiskers without outliers. The median is centred with quartiles Q_1 and Q_3.

The dispersion analysis of MOE in bending (Figure 4.5b) evidences a higher dispersion for the $E_{m,l}$ rather than the $E_{m,g}$, which did not occur in the previous phase, however, the median of $E_{m,l}$ is still higher than the median of $E_{m,g}$. In both cases, a significant number of observations are considered lower outliers, and also upper outliers are found for $E_{m,l}$. The significant dispersion found in $E_{m,l}$ is consequent of the existence of a large number of extreme observations and a rather thin difference between quartiles Q_1 and Q_3, thus evidencing a possible underlying distribution with high kurtosis.

Regarding the penetration depth and drilling resistance, a larger dispersion of values was found for the samples of tests made to the lateral faces, although in both cases, a larger number of outliers were found in the bottom face measurements (Figure 4.5c, d). Within the same test, penetration depth median was similar in both bottom and lateral measurements, whereas in the case of the drilling resistance, a quantitative increase of quartiles Q_1, Q_2 and Q_3 was found for the lateral measurements.

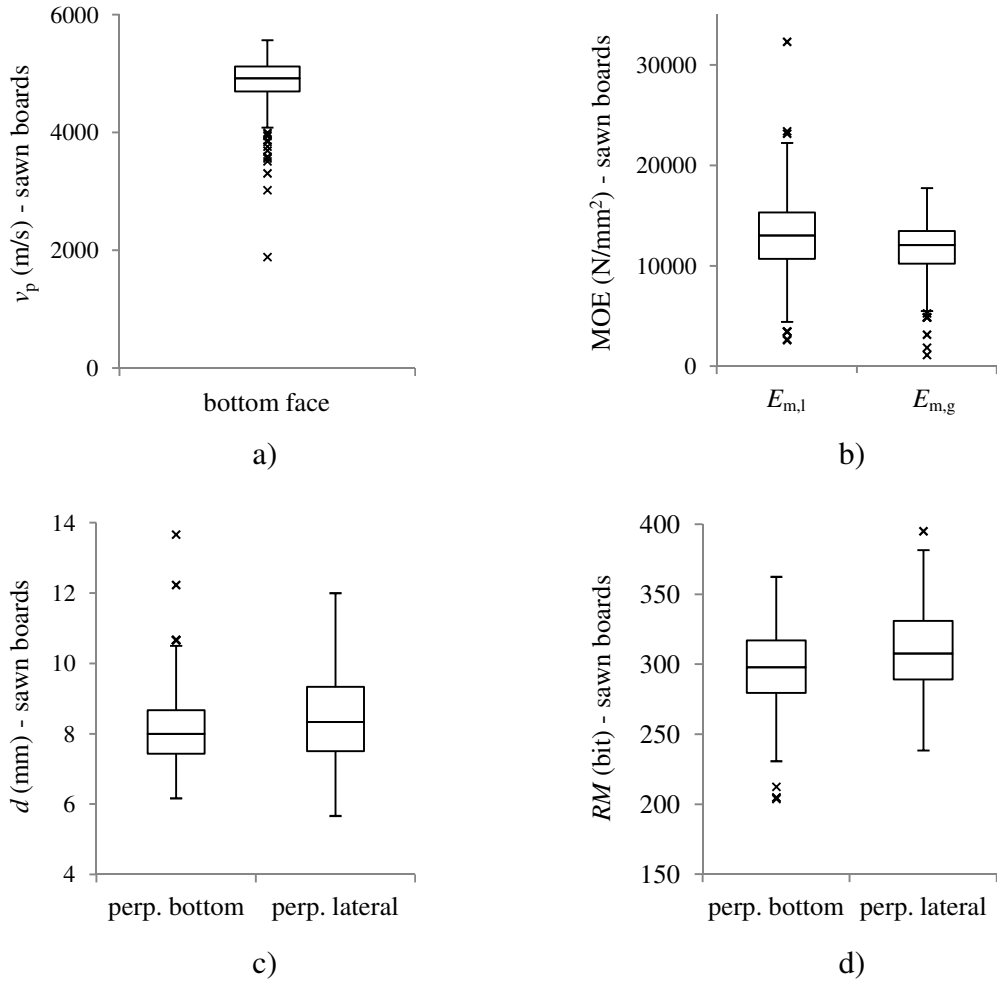

Figure 4.5: Box plot for tests made on sawn boards: a) propagation velocity in ultrasound testing by the indirect method; b) MOE in bending tests; c) penetration impact depth; d) drilling resistance by resistance measure.

4.2.4 Phase 4

Phase 4 comprised a set of tests made to small wood specimens, and thus it is expectable that dispersion due to the material variability is decreased, since the specimens are selected in order to minimize the presence of defects which are a cause of mechanical property higher variation.

In the compression parallel to the grain tests, the propagation velocity, the MOE and ultimate strength in compression parallel to grain, were analysed. When considering the propagation velocity results (Figure 4.6a), a larger dispersion in the indirect measurements, with an extreme lower outlier is found. For direct measurements the values are more concentrated, especially in the interquartile interval (between Q_1 and Q_3). In both cases the median is centred within the box and both evidence lower outliers. The quartile Q_3 and the maximum value are similar in both measurements.

A moderate dispersion in the $E_{c,0}$ sample (Figure 4.6b) is found, however it presents lower outliers and the box is closer to the minimum value, which may be indicative of a positive skewness. On the other hand, the $f_{c,0}$ sample (Figure 4.6c) presents a higher dispersion, also evidencing lower outliers. Its median is centred in the interquartile interval and the box is centred within the extent of the whiskers.

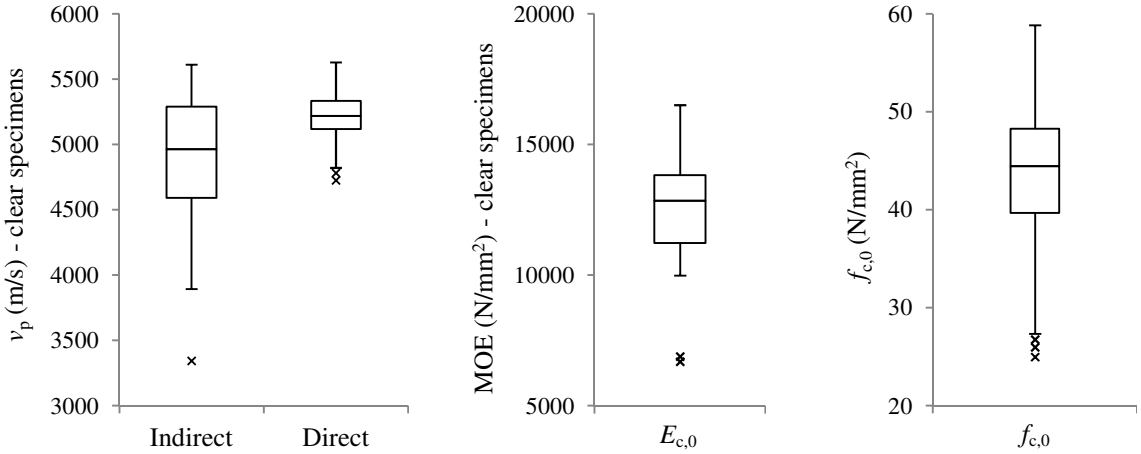

Figure 4.6: Box plot for tests made on compression parallel to grain specimens: a) propagation velocity in ultrasound testing; b) MOE in compression parallel to grain tests; c) compression parallel to grain strength.

In the tension parallel to the grain tests, the propagation velocity, the MOE and ultimate strength in tension parallel to grain were analysed. In neither tests an outlier was found although large dispersions were detected. When considering the propagation velocity results (Figure 4.7a), a relative thin box is found centred within the maximum and minimum values, which may be indicative of a significant dispersion in the tails of the underlying distribution with a possible high kurtosis. Analogous situations are found with respect to $E_{t,0}$ and $f_{t,0}$ (Figure 4.7b, c), where also significant dispersions are found with relative thin boxes compared to the length of the whiskers, being the values of $f_{t,0}$ more

disperse in the lower tail. In the analysis of the box plot of $f_{t,0}$, the approximation of the box to the upper quartile Q_3 may be indicative of a slight negative skewness.

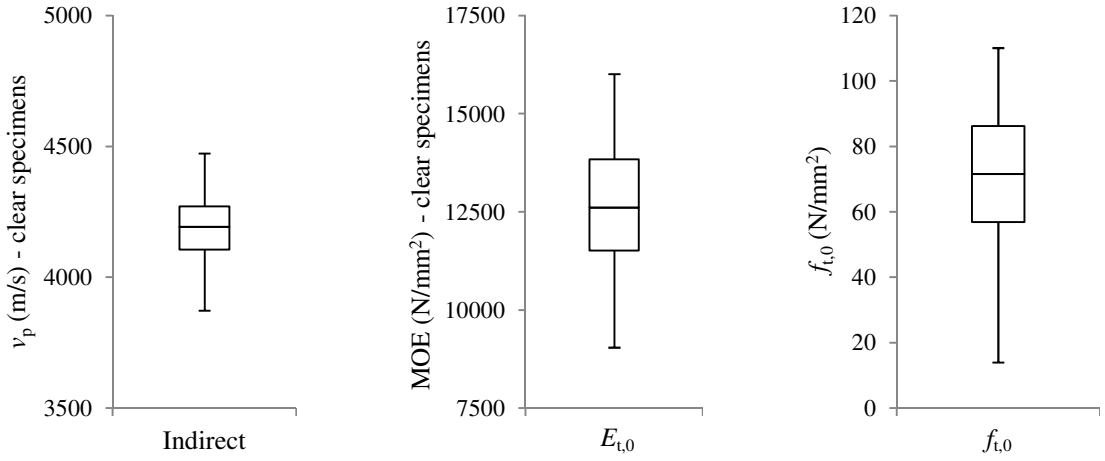

a) b) c)

Figure 4.7: Box plot for tests made on tension parallel to grain specimens: a) propagation velocity in ultrasound testing; b) MOE in tension parallel to grain tests; c) tension parallel to grain strength.

Comparing the box plots for compression and tension parallel to grain, it is found that the latter present a higher dispersion even though no outliers are present. Previously it was already found that the COV in the tension parallel to grain tests was higher than the equivalent values for compression parallel to grain tests. Therefore, in this case the dispersion analysis was in accordance with the COV analysis, which might not always necessarily happen since the COV is dependent of sample mean and thus is outlier sensitive, whereas the dispersion analysis given by a box plot is dependent only of the definition of the quartiles.

By analysing the propagation velocity measurements made to all samples in the different experimental phases, it is found that lower outliers are found in almost all cases which may be either indicative of a tendency of these measures to take left tailed distributions, or that a measurement error associated to these procedure is being systematically considered. Measurement errors are most commonly random, thus taking either negative or positive values, however in this case no upper outliers are found and so the probability of considering the lower outliers as consequence of measurement errors must be considered low.

With respect to the density and moisture content determination tests, high dispersions are found, although no outlier is found (Figure 4.8). The median is centred both within the box and between the extreme values, evidencing a possible symmetric distribution such as of a normal distribution. The box plots for ρ_0 and ρ_{12} are similar with only a shift of the values.

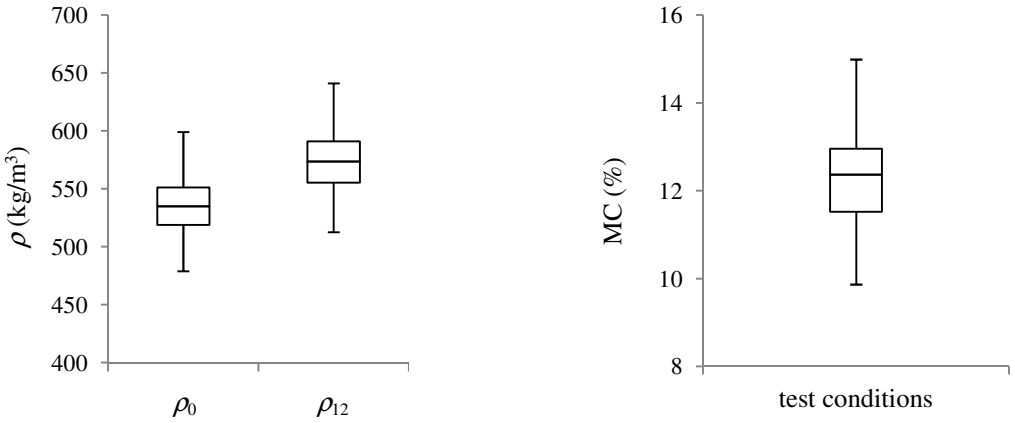

Figure 4.8: Box plot for tests made on small clear specimens: a) density; b) moisture content.

4.3 Correlations between test phases

The correlation between mechanical properties is often based in the explicit definition and use of so-called reference properties, which through its knowledge will allow to define implicitly the other properties by empirical correlations. The use of these reference properties is the cornerstone of the Probabilistic Model Code (JCSS, 2006) where bending strength, bending modulus of elasticity and timber density are considered for that purpose. Nevertheless, the material property in analysis may deviate in terms of type, of dimensions (scale) and of specific loading and climate conditions, but these behaviours are generally treated separately (Köhler, 2007).

Although density has a significant influence on wood mechanical properties (Dinwoodie, 1981) and on non-destructive analysis, it alone cannot explain the variability in other mechanical properties and should not be relied upon as the sole predictor (Kasal and Anthony, 2004). On the other hand, modulus of elasticity often present better correlations with other mechanical properties. Görlacher (1991) has concluded that reasonable correlations can be taken between modulus of elasticity and strength of both new and old timber, supported by the findings of Ehlbeck and Görlacher (1990) where no significant difference was found between compressive, bending and shear strengths of old and new timber. In the same perspective, Gloss (1986) mentions that the correlation coefficient between modulus of elasticity and strength (for bending, compression and tension) may range from 0.7 to 0.8.

In order to correlate the test results from the same segments of the timber elements, several scales have been considered. For instance, when comparing the values per beam, the results taken in a set of three boards were first averaged, whereas when considering the values per segment, the values of a beam would be given to all sections. Also when considering the small clear samples by location (left: 10-130 cm; centre 90-210 cm; right: 170-290 cm), the respective values given in the corresponding sections were

averaged to that location. In the case of measurements taken to a given region of the beam, such as in the case of $E_{m,l}$ in l_1, only that region was considered for the remaining measurements. A generic example for the determination of each scale regarding different measured data is given in Annex B. For this analysis, the scales represent:

- *sections*: measurements made in each 40 cm segments (when only a value is given by beam, the sections values are equal to the individual beam value);
- *left-centre-right (L-C-R)*: correspond to the regions from where the small clear samples were extracted, such that left is the region between [10;130] cm, centre is between [90;210] cm and right between [170;290] cm;
- *total/board*: the averaged value of the sections values per each board (1 to 3);
- l_1 *region*: measurements made in the l_1 region of the 4 point bending test in beams (l_1 *region* according to EN408 (CEN, 2010)) per each board, corresponding to the region [112.5;187.5] cm;
- *mean/section*: averaged value of the sections in the same position of each three boards of a given beam;
- *mean/L-C-R*: averaged value of the left, centre and right regions of each three boards of a given beam;
- *mean/total*: the averaged value of the sections values per each beam (A to T) or the individual value of a single test made to a beam;
- *mean/*l_1 *region*: measurements made in the l_1 region of the 4 point bending test in beams (l_1 *region* according to EN408 (CEN, 2010)) per each beam, corresponding to the region [112.5;187.5] cm.

In the following topics the most relevant correlations are presented regarding its adequate scale, different visual classes and samples without the outlier values found in previous topics.

In a first analysis, the correlation between $E_{m,l}$ and $E_{m,g}$ is assessed in different experimental phases (Figure 4.9), thus considering measurements taken by individual beam (Phase 2) and measurements taken to each segment of a board (Phase 3). A high correlation is found in the results of Phase 2, however a medium low correlation is found for Phase 3, due to higher variation of the values. By considering the average values of segments measurements by its respective beam, a high correlation value is now obtained. Therefore, in order to mitigate the variation of the results of E_m in a set of three boards, the results of the segments must be first averaged by beam. The visual inspection made to the sawn beams and boards evidenced sample coefficients of determination in the same order of those obtained when considering the full sample. However, these values are lower when the averaged value is assumed. The elimination of the outlier values did not produce significant increase on the sample coefficient of determination, and in some cases even led to a small decrease.

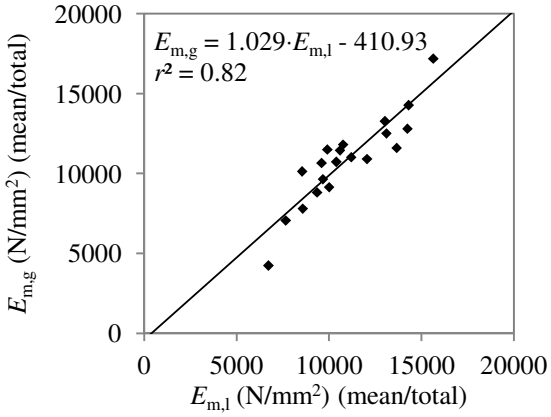

y = m·x + b	m	b	r^2
all	1.029	-410.93	0.82
class I	1.028	-434.75	0.82
class II	1.040	-653.03	0.82
class III	1.082	-900.48	0.85
class NC	1.088	-966.46	0.81
no outliers	0.792	2208.99	0.75

$E_{m,g}$ outlier probability = 0.000
$E_{m,l}$ outlier probability = 0.100

a)

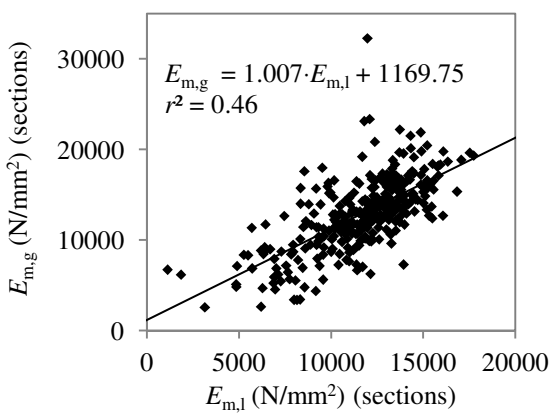

y = m·x + b	m	b	r^2
all	1.007	1169.75	0.46
class I	0.925	2250.95	0.35
class II	0.940	2142.80	0.42
class III	1.017	552.40	0.40
class NC	0.797	2310.20	0.33
no outliers	0.992	1266.57	0.47

$E_{m,g}$ outlier probability = 0.021
$E_{m,l}$ outlier probability = 0.024

b)

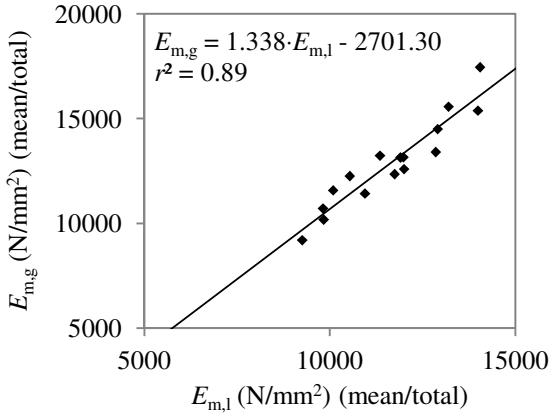

y = m·x + b	m	b	r^2
all	1.338	-2701.30	0.89
class I	1.040	709.09	0.69
class II	1.413	-3697.38	0.55
class III	0.883	1657.61	0.32
class NC	0.979	1172.92	0.69
no outliers	1.336	-2848.91	0.84

$E_{m,g}$ outlier probability = 0.021
$E_{m,l}$ outlier probability = 0.024

c)

Figure 4.9: Correlation between $E_{m,l}$ and $E_{m,g}$ in: a) Phase 2 with mean/total scale; b) Phase 3 with section scale; c) Phase 3 with mean/total scale.

In a second step, the coefficient of determination for $E_{m,l}$ and $E_{m,g}$ considering different phases is analysed. However, due to the multiple measurements in the sawn

boards, different size samples are obtained between phases. Thus, when considering the values per section it is evident that for the same value in Phase 2, an interval of values is obtained in Phase 3. Therefore, the correlations found in those cases are low and should not be considered.

In the case of $E_{m,l}$, the results are first considered to all the results of Phase 3 measurements (Figure 4.10). However, to obtain a more precise correlation between the same measured sections, in a second analysis, only the segments in the boards comprised in the region l_1 of the 4-point bending tests for the sawn beams were considered (Figure 4.11). A noticeable increase between scales is found when assessing equivalent regions ($r^2 = 0.68 > 0.54$).

In the case of $E_{m,g}$ (Figure 4.12), a moderate high correlation is found between experimental phases when considering the mean/total of values. The coefficient of determination is slightly higher between $E_{m,g}$ than between $E_{m,l}$ ($r^2 = 0.71 > 0.68$), mainly due to the larger variation found for $E_{m,l}$ in both Phases 2 and 3.

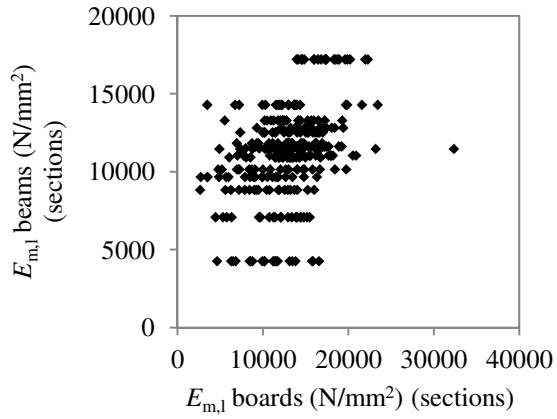

y = $m \cdot x$ + b	m	b	r^2
all	0.278	7575.86	0.15
class I	0.360	6481.11	0.16
class II	0.260	7408.31	0.09
class III	0.352	6861.08	0.16
class NC	0.165	8793.96	0.05
no outliers	0.143	9398.04	0.07

$E_{m,l}$ beams outlier probability = 0.100
$E_{m,l}$ boards outlier probability = 0.024

a)

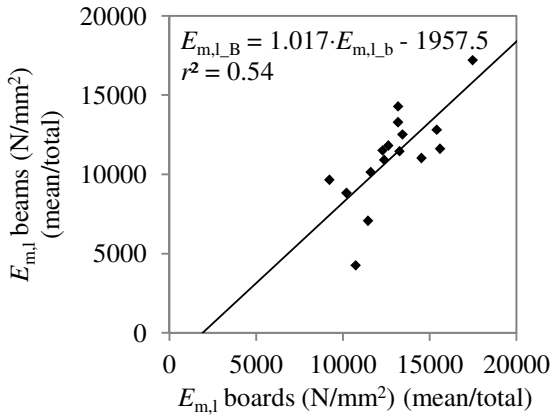

y = $m \cdot x$ + b	m	b	r^2
all	1.017	-1957.45	0.54
class I	1.148	-4454.33	0.52
class II	0.266	7862.43	0.05
class III	0.765	3039.22	0.38
class NC	0.465	5918.08	0.18
no outliers	0.691	2413.81	0.36

$E_{m,l}$ beams outlier probability = 0.100
$E_{m,l}$ boards outlier probability = 0.024

b)

Figure 4.10: Correlation of $E_{m,l}$ between Phases 2 and 3: a) between $E_{m,l}$ with section scale; b) between $E_{m,l}$ with mean/total scale.

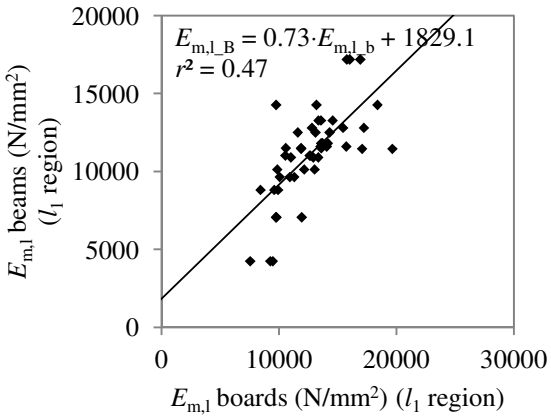

y = m·x + b	m	b	r^2
all	0.733	1829.06	0.47
class I	0.705	2006.18	0.38
class II	0.562	3974.60	0.28
class III	0.829	1769.31	0.44
class NC	0.053	8194.63	0.00
no outliers	0.657	2960.64	0.49

$E_{m,l}$ beams outlier probability = 0.100
$E_{m,l}$ boards outlier probability = 0.024

a)

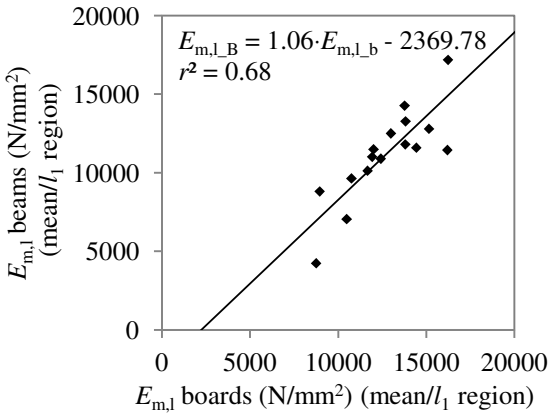

y = m·x + b	m	b	r^2
all	1.064	-2369.78	0.68
class I	1.362	-6985.05	0.79
class II	0.767	1696.57	0.37
class III	0.808	2051.36	0.47
class NC	0.706	1565.36	0.49
no outliers	0.906	-96.27	0.70

$E_{m,l}$ beams outlier probability = 0.100
$E_{m,l}$ boards outlier probability = 0.024

b)

Figure 4.11: Correlation of $E_{m,l}$ between Phases 2 and 3 in l_1 region: a) between $E_{m,l}$ with section scale; b) between $E_{m,l}$ with mean/total scale.

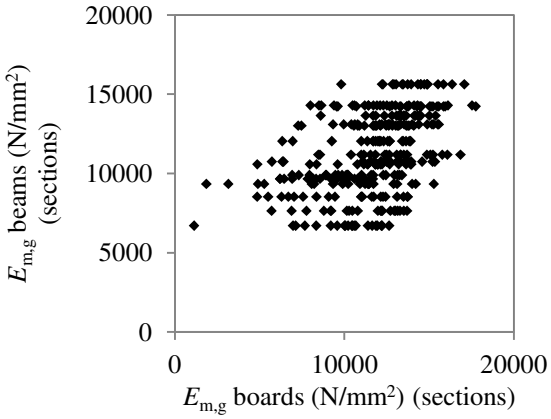

y = m·x + b	m	b	r^2
all	0.431	6246.52	0.21
class I	0.588	4213.18	0.23
class II	0.418	6234.08	0.14
class III	0.304	7487.91	0.07
class NC	0.160	8753.67	0.04
no outliers	0.467	5800.67	0.20

$E_{m,g}$ beams outlier probability = 0.000
$E_{m,g}$ boards outlier probability = 0.021

a)

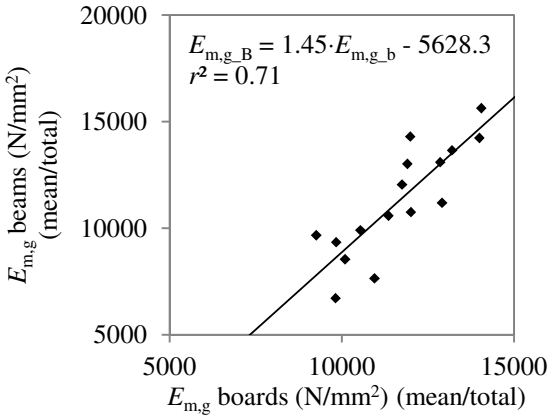

y = m·x + b	m	b	r^2
all	1.450	-5628.26	0.71
class I	1.296	-4801.46	0.54
class II	1.073	-1000.45	0.31
class III	0.611	4936.82	0.14
class NC	0.266	8282.28	0.06
no outliers	1.552	-7021.71	0.68

$E_{m,g}$ beams outlier probability = 0.000
$E_{m,g}$ boards outlier probability = 0.021

b)

Figure 4.12: Correlation of $E_{m,g}$ between Phases 2 and 3: a) between $E_{m,g}$ with section scale; b) between $E_{m,g}$ with mean/total scale.

In existing structures, it is impossible to assess the full element as described in Phase 3, and most often only NDT are allowed and made to specific parts of the element. In order to consider these constraints, also the correlations of E_m between Phase 2 and the results of the bottom board (board 3, equivalent to the face usually accessible onsite) are considered (Figure 4.13). The results evidence moderate high correlations (r^2 = 0.69; r^2 = 0.67) and the coefficient of determination did not decrease significantly with consideration to all measurements, thus the bottom boards may be considered representative of the global element in terms of E_m.

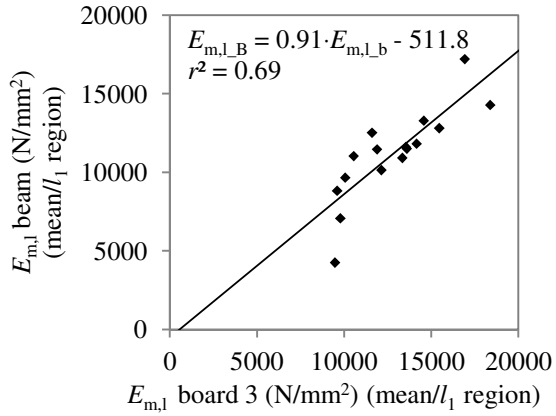

y = m·x + b	m	b	r^2
all	0.911	-511.77	0.69
class I	0.918	-733.53	0.76
class II	0.629	1801.67	0.12
class III	-0.091	11768.80	0.02
class NC	0.152	5907.23	0.02
no outliers	0.743	1880.46	0.69

$E_{m,l}$ beams outlier probability = 0.100
$E_{m,l}$ boards outlier probability = 0.024

a)

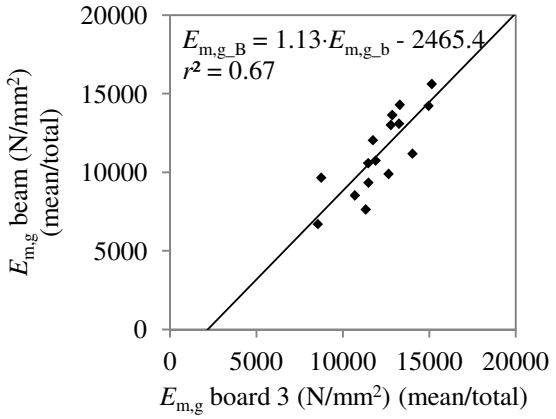

y = m·x + b	m	b	r^2
all	1.129	-2465.39	0.67
class I	1.049	-2340.15	0.51
class II	1.060	-1948.50	0.36
class III	0.805	1971.89	0.30
class NC	-0.101	10948.56	0.02
no outliers	1.192	-3334.00	0.64

$E_{m,g}$ beams outlier probability = 0.000
$E_{m,g}$ boards outlier probability = 0.021

b)

Figure 4.13: Correlation between bending tests in Phase 2 and 3 for the results only in the bottom board: a) between $E_{m,l}$; b) between $E_{m,g}$.

4.3.1 Modulus of elasticity with NDT

With respect to the ultrasound tests, the correlation with the stiffness material properties of the elements acquired from the mechanical tests was made regarding the propagation velocity. In a first analysis, the correlation between the measurements made to sawn beams and to sawn boards is assessed in order to attest the use of the ultrasounds in Phases 2 and 3. In order to do so, the measurements made to the bottom face of the sawn beams are compared to the measurements made to the bottom face of board 3 (bottom board) of each set of sawn boards, and also to the mean value per segment (scale mean/segment) in the boards (Figure 4.14). It is noticeable that the correlation between the results of the sawn beam measurements with the measurements only for the bottom boards, is higher than for the mean of the boards per segment (r^2 = 0.81 > 0.49). Although a higher correlation for the first case was evident and expectable (since the measurement locations are the same),

the significant decrease in the coefficient of determination for the second case indicates that indirect measurements of ultrasound revealed to be more indicated for the determination of local properties (or the properties of the superficial layers) rather than to the global element (interior of the element) for this case.

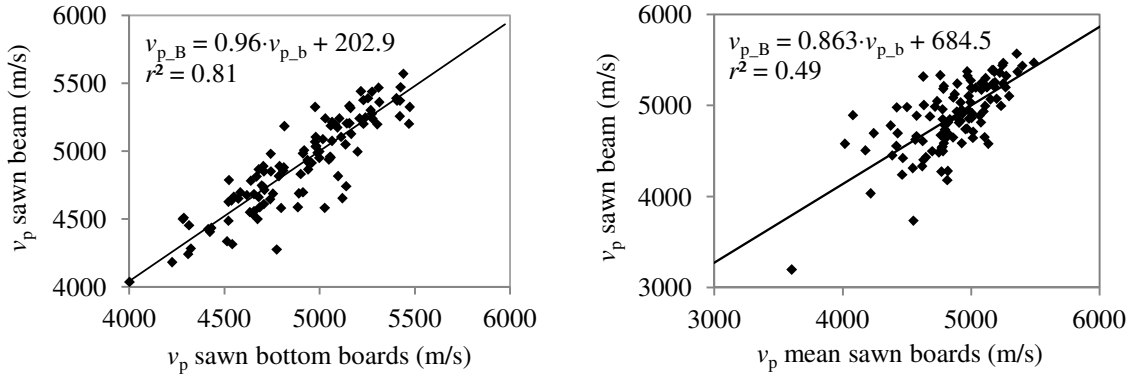

a) b)

Figure 4.14: Correlation between measurements of propagation velocity, v_p, for sawn beams and: a) bottom face of sawn boards; b) mean of the boards per segment.

When analysing the structural element globally, the mean of all ultrasound measurements done to the same element, either sawn beam or group of sawn boards, were compared and a coefficient of determination of 0.68 was obtained (Figure 4.15).

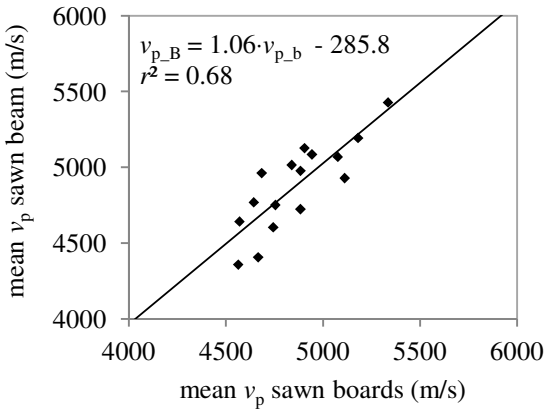

Figure 4.15: Correlation between mean of total measurements of propagation velocity, v_p, for each sawn beam and group of sawn boards.

Since the correlations between measurements in different experimental phases for equivalent segments were significant, it is possible to predict a measurement in a given scale by the measurement of the other with an acceptable residual.

After the analysis between results of ultrasound propagation velocity in different experimental phases, the results were compared to the stiffness results attained in the 4-point bending tests. In Phase 2, the ultrasound tests made within the l_1 region are averaged and compared to the $E_{m,l}$, while the average of all measurements is compared to

$E_{m,g}$ (see Figure 4.16). Medium correlations are found, and in both cases the consideration of the different visual classes, led to higher correlations with exception of class NC, where a very low (inexistent) correlation is obtained, due to the large variation in the sample.

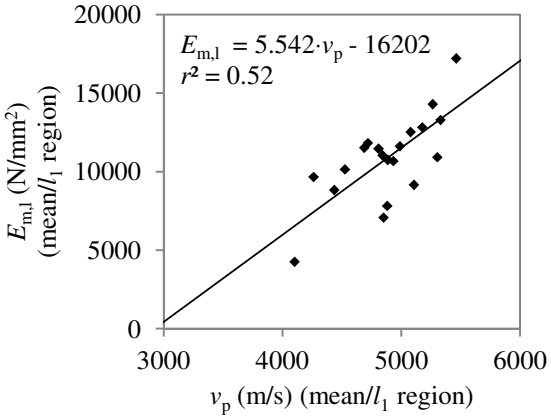

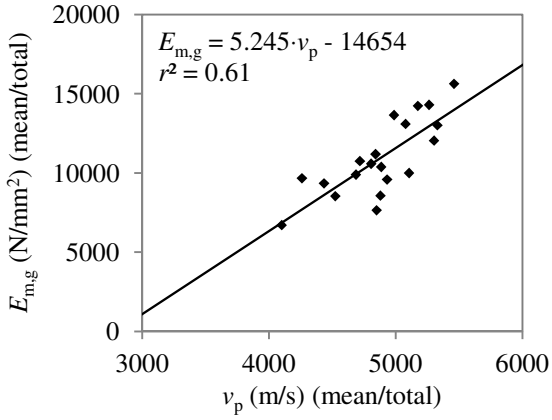

y = $m \cdot x$ + b	m	b	r^2
all	5.542	-16201.70	0.52
class I	5.873	-17407.05	0.64
class II	6.757	-22119.79	0.67
class III	6.027	-18405.14	0.63
class NC	-1.582	15668.64	0.03
no outliers	3.576	-6689.67	0.27

$E_{m,l}$ beams outlier probability = 0.100
v_p beams outlier probability = 0.029

a)

y = $m \cdot x$ + b	m	b	r^2
all	5.245	-14654.24	0.61
class I	5.527	-15610.52	0.73
class II	5.802	-17069.63	0.72
class III	5.382	-15057.28	0.71
class NC	-2.170	19015.96	0.05
no outliers	6.364	-20343.49	0.61

$E_{m,g}$ beams outlier probability = 0.000
v_p beams outlier probability = 0.029

b)

Figure 4.16: Correlation between propagation velocity and: a) $E_{m,l}$ in mean/l_1 region scale; b) $E_{m,g}$ in mean/total scale.

In the case of the correlation with $E_{m,l}$, two clusters of values are found with similar inclination of the respective linear tendency lines (Figure 4.17). Thus, if considering Equation 3.4 and density given by the mean value of all measurements, different ratios K are obtained. A group with 75% of the beams (G1) evidenced a mean K = 0.86, whereas a second group with 25% of the beams (G2: beams F, H, L, M and Q) evidenced a mean K = 0.56. Considering the two separate groups in the comparison between v_p and $E_{m,l}$, high correlations were found. Considering the same groups for the analysis with $E_{m,g}$, a high correlation was found for G1 but a medium low correlation was found for G2. Although from the same timber specie, the wood origin and its conditions of growth were not established, which may account to the found differences. Regarding these results, the correlations of E_m with ultrasound tests between different scales are also referred to each group separately.

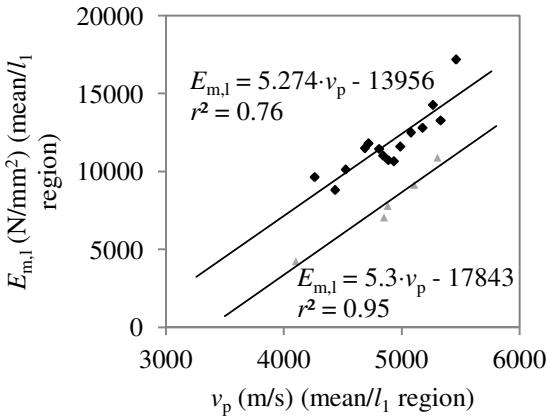

y = m·x + b	m	b	r^2
all	5.542	-16201.70	0.52
G1	5.274	-13956.37	0.76
G2	5.300	-17843.33	0.95

a)

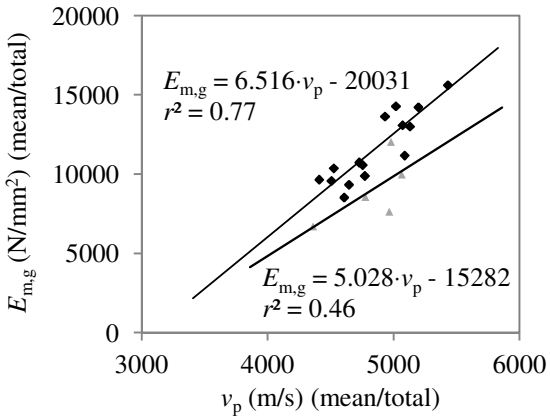

y = m·x + b	m	b	r^2
all	5.245	-14654.24	0.61
G1	6.516	-20030.68	0.77
G2	5.028	-15282.02	0.46

b)

Figure 4.17: Differentiation by groups and correlation of propagation velocity with: a) $E_{m,l}$ in mean/l_1 region scale; b) $E_{m,g}$ in mean/total scale.

The ultrasound measurements made in Phase 3 were also correlated to the sequential 4-point bending tests made to the sawn boards. In Figure 4.18 and 4.19, the ultrasound measurements in section and mean/total scales are considered for correlation with $E_{m,l}$ and $E_{m,g}$, respectively. Low correlations are found when considering the direct correlation between measurements in each segment (section scale) in both cases (r^2 = 0.29 and 0.47), whereas high correlations are found when assuming the average of the results by each beam (mean/total scale) (r^2 = 0.83 and 0.89), with better correlations when analysing $E_{m,g}$. Neither the consideration of different visual classes or groups G1 and G2 produced significantly higher correlations, nor even for lower classes (classes III and NC) considerable lower correlations are found.

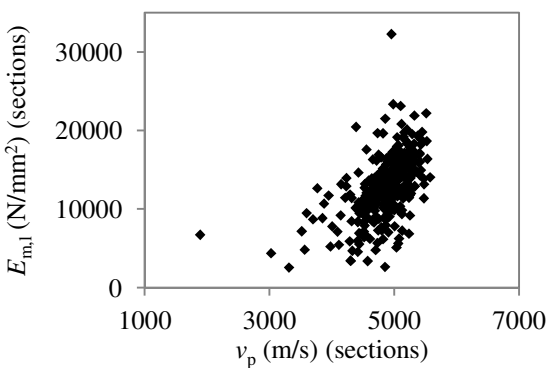

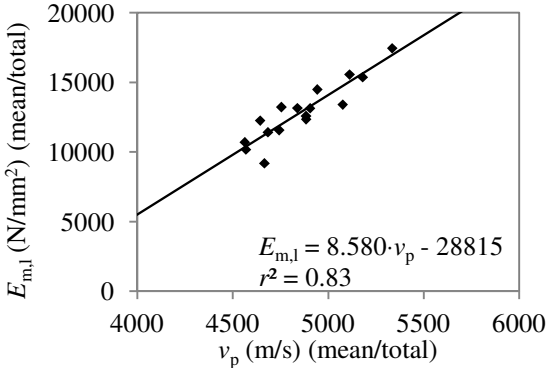

y = m·x + b	m	b	r^2
all	5.191	-12325.29	0.29
class I	5.310	-12480.67	0.28
class II	5.078	-11726.46	0.27
class III	2.328	105.42	0.06
class NC	2.312	-1139.98	0.08
no outliers	6.292	-17836.31	0.29
G1	5.689	-14622.51	0.29
G2	3.401	-4516.70	0.29

$E_{m,l}$ boards outlier probability = 0.024
v_p boards outlier probability = 0.039

a)

y = m·x + b	m	b	r^2
all	8.580	-28814.55	0.83
class I	7.501	-22858.77	0.84
class II	7.328	-23107.97	0.40
class III	3.469	-6240.98	0.10
class NC	5.971	-18373.37	0.24
no outliers	9.792	-35139.63	0.84
G1	8.718	-29453.01	0.82
G2	5.056	-12311.12	0.996

$E_{m,l}$ boards outlier probability = 0.024
v_p boards outlier probability = 0.039

b)

Figure 4.18: Correlation between measurements in sawn boards of propagation velocity and: a) $E_{m,l}$ in sections scale; b) $E_{m,l}$ in mean/total scale.

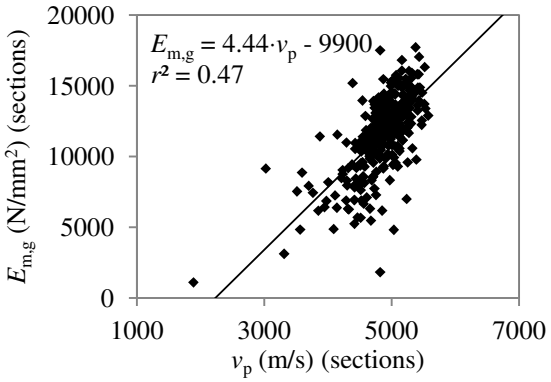

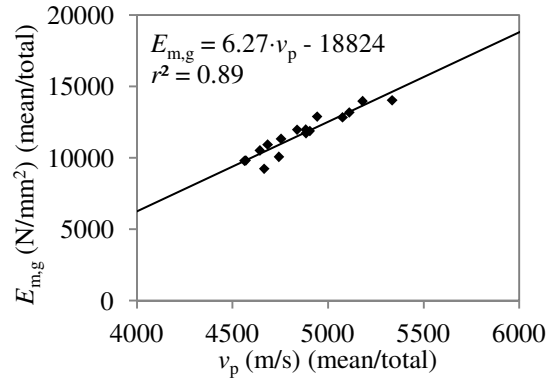

y = m·x + b	m	b	r^2
all	4.435	-9900.30	0.47
class I	3.377	-4147.28	0.28
class II	4.427	-10047.79	0.44
class III	4.219	-9432.58	0.47
class NC	2.960	-4594.36	0.26
no outliers	5.190	-13578.55	0.43
G1	4.677	-11051.10	0.44
G2	3.680	-6497.57	0.56

$E_{m,g}$ boards outlier probability = 0.021
v_p boards outlier probability = 0.039

a)

y = m·x + b	m	b	r^2
all	6.270	-18823.69	0.89
class I	5.135	-12558.61	0.62
class II	4.808	-11886.78	0.62
class III	2.220	-661.57	0.10
class NC	2.730	-3684.16	0.07
no outliers	6.599	-20585.80	0.82
G1	6.362	-19299.27	0.88
G2	5.802	-16495.99	0.94

$E_{m,g}$ boards outlier probability = 0.021
v_p boards outlier probability = 0.039

b)

Figure 4.19: Correlation between measurements in sawn boards of propagation velocity and: a) $E_{m,g}$ in sections scale; b) $E_{m,g}$ in mean/total scale.

In Phase 4, the correlations between ultrasound tests and MOE in parallel to grain direction were also assessed for both compression and tension. The correlations are considered with respect to the mean/L-C-R scale since the samples were taken with respect to the left, centre and right segments of each beam.

In compression parallel to grain, $E_{c,0}$ and the ultrasound in indirect tests presented a very low correlation (influenced by the short distance between transducers), whereas a medium low correlation is obtained with direct tests (Figure 4.20). Since a non-significant variation was found with respect to the different failure modes, the analysis was made considering all specimens.

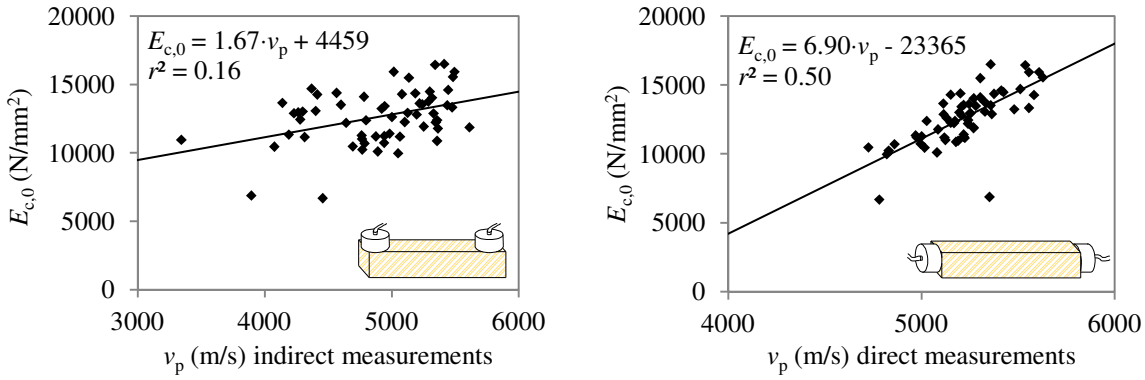

Figure 4.20: Correlation between compression parallel to grain mechanical properties and propagation velocity: a) v_p indirect measurements; b) v_p direct measurements.

In tension parallel to grain, medium correlations are obtained between $E_{t,0}$ and the ultrasound in indirect tests (Figure 4.21). A slightly better correlation is observed when assuming the average value of the measurements made to each two samples taken by segments.

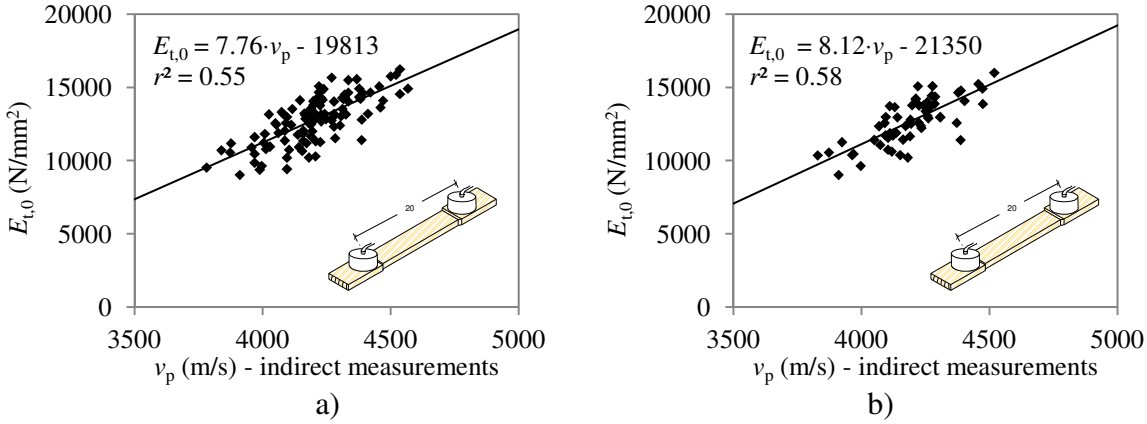

Figure 4.21: Correlation between v_p and $E_{t,0}$: a) all samples; b) mean of samples 1 and 2.

The analysis was also made considering the different failure modes (Figure 4.22), since a significant variation was found with respect to that parameter. With respect to the analysis of different failure modes, the coefficient of determination is similar with exception to the failures due to gripping influence.

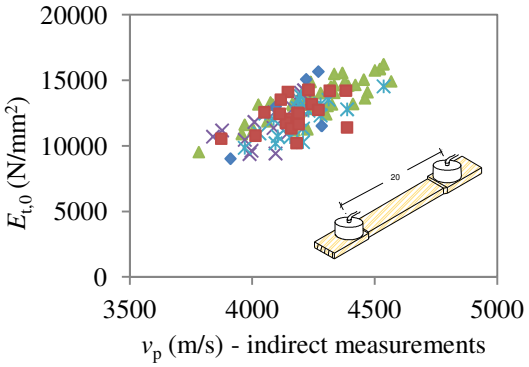

y = m·x + b	m	b	r^2
splinter	6.9263	-15926	0.64
shear	8.5765	-23293	0.41
tension	7.2553	-18255	0.48
defect	12.609	-39526	0.53
gripping	4.8987	-8013.9	0.22

Figure 4.22: Correlation between v_p and $E_{t,0}$ with consideration of different failure modes.

The propagation velocity was also correlated with MOE parallel to grain in compression, $E_{c,0}$, and tension, $E_{t,0}$, with respect to the averaged value within a single beam (mean/total scale). The results evidenced a lower correlation for $E_{c,0}$ but higher for $E_{t,0}$ when considering the mean/total scale (Figure 4.23).

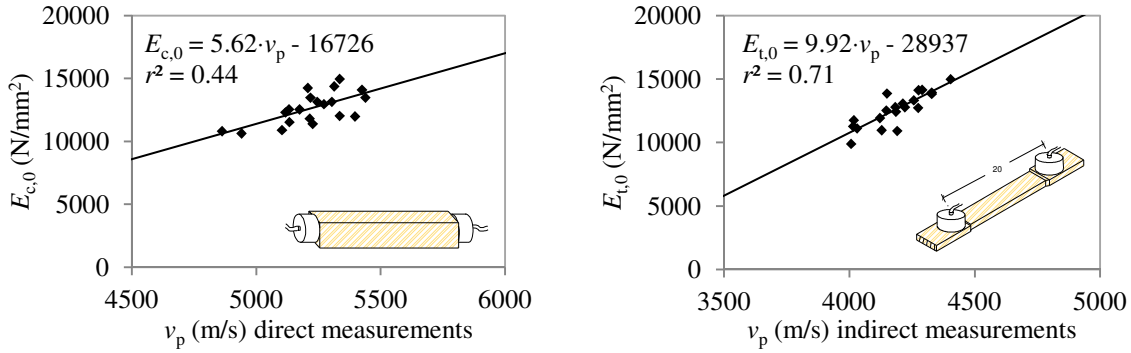

Figure 4.23: Correlation between parallel to grain stiffness and propagation velocity in mean/total scale: a) compression and v_p direct measurements; b) tension and v_p indirect measurements.

Pin penetration and drilling resistance tests made to the segments of sawn boards led to very low correlations (< 0.07). Although still low, correlations were found stronger when assuming the mean values per board and to the tests made perpendicularly to the lateral face (Table 4.5). In Ceraldi *et al.* (2001), although considering different kinds of wood in the same sample, the resistance measure presented a medium correlation with density ($r^2 = 0.66$) and no correlation with axial compressive strength. In this experimental campaign also no correlation was found between the resistance measurement and the compression parallel to grain stiffness or strength.

Table 4.5: Correlation between NDT, *depth* (mm), *RM* (bit), and E_m (N/mm²) in Phase 3.

Properties	*m*	*b*	r^2
$E_{m,l} = depth \cdot m + b$	-1571.9	25685.3	0.25
$E_{m,l} = RM \cdot m + b$	69.967	-7930.9	0.38
$E_{m,g} = depth \cdot m + b$	-1419.4	23095.8	0.30
$E_{m,g} = RM \cdot m + b$	60.337	-6415.8	0.41

4.3.2 Modulus of elasticity in bending and other MOE (compression and tension)

In this topic the stiffness regarding different solicitations to the grain is considered, with especial attention to bending. When an element is under bending, both compression and tension are present in the same section, and so E_m (Phases 2 and 3) correlations with $E_{c,0}$ and $E_{t,0}$ (Phase 4) will be addressed.

When considering the E_m of sawn beams, for both $E_{m,l}$ and $E_{m,g}$, the correlations with $E_{c,0}$ are very low (Figure 4.24). The differentiation by visual classes lead to similar coefficients of determination and the tendency lines present similar inclinations. The no inclusion of outliers produced better correlations within the parameters, which in any case present that $E_{c,0}$ is better correlated with $E_{m,g}$, although still with low correlations.

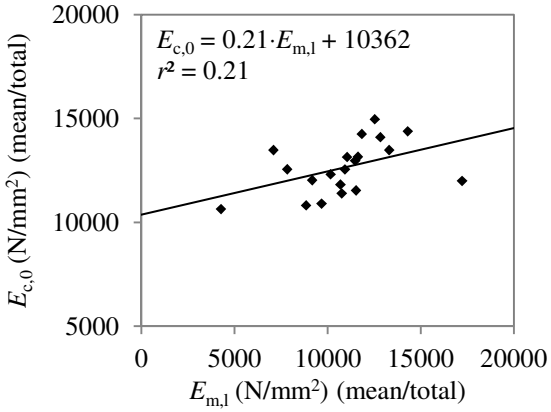

y = $m \cdot x$ + b	m	b	r^2
all	0.208	10362.14	0.21
class I	0.212	10420.79	0.22
class II	0.193	10747.23	0.20
class III	0.211	10414.42	0.22
class NC	0.167	10739.66	0.15
no outliers	0.345	9148.22	0.29

$E_{m,l}$ beams outlier probability = 0.100
$E_{c,0}$ outlier probability = 0.033

a)

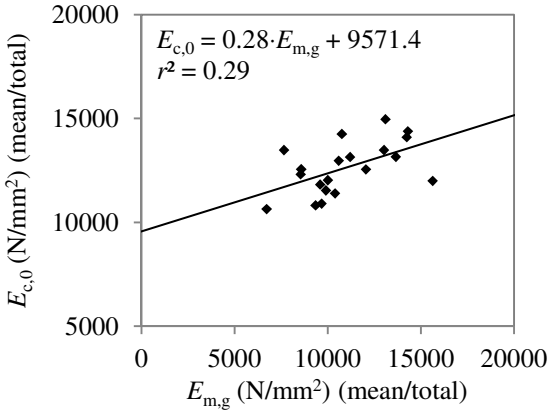

y = $m \cdot x$ + b	m	b	r^2
all	0.279	9571.43	0.29
class I	0.274	9704.80	0.28
class II	0.250	10050.55	0.26
class III	0.282	9636.55	0.28
class NC	0.217	10192.60	0.17
no outliers	0.375	8759.78	0.49

$E_{m,g}$ beams outlier probability = 0.000
$E_{c,0}$ outlier probability = 0.033

b)

Figure 4.24: Correlation between E_m in Phase 2 and $E_{c,0}$ for mean/total scale: a) $E_{m,l}$; b) $E_{m,g}$.

The stiffness measurements in Phase 3 are also correlated with $E_{c,0}$ in both mean/L-C-R (Figure 4.25) and mean/total (Figure 4.26) scales. In both scales, very low correlations are found with exception of the $E_{c,0}$ and $E_{m,g}$ in mean/total scale, with a low correlation ($r^2 = 0.43$). Moreover, when not considering outliers in $E_{c,0}$ and $E_{m,l}$ in mean/total scale, a low correlation was found ($r^2 = 0.47$). In the overall results $E_{c,0}$ is better correlated with $E_{m,g}$, although still with low correlations. Higher correlations were also noted in the higher classes, since the compression parallel to grain samples were taken from segments with the lower possible presence of defects.

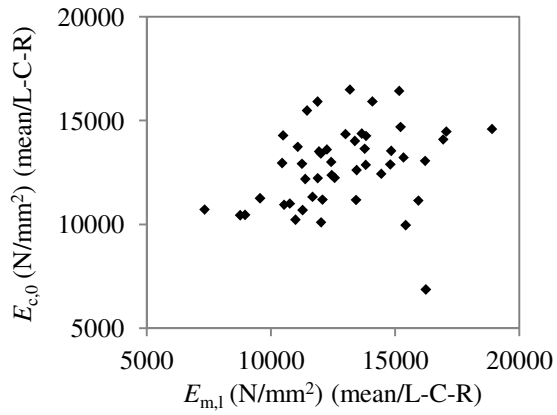

y = $m \cdot x$ + b	m	b	r^2
all	0.228	9854.41	0.08
class I	0.267	9165.39	0.08
class II	0.085	11718.68	0.01
class III	-0.152	14529.54	0.05
class NC	0.007	12435.04	0.00
no outliers	0.364	8246.34	0.19

$E_{m,l}$ boards outlier probability = 0.024
$E_{c,0}$ outlier probability = 0.033

a)

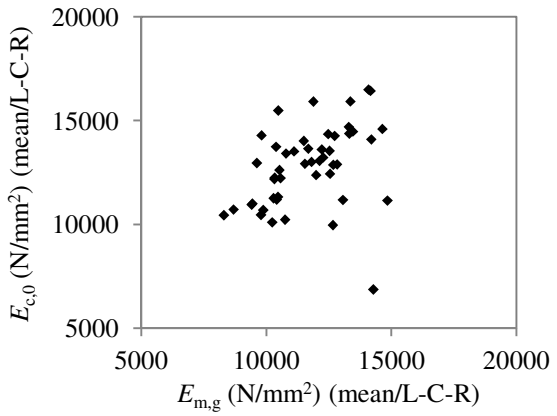

y = $m \cdot x$ + b	m	b	r^2
all	0.436	7710.15	0.14
class I	0.427	7485.22	0.11
class II	0.477	7321.42	0.15
class III	-0.232	15260.64	0.05
class NC	-0.060	13060.14	0.01
no outliers	0.596	5941.18	0.27

$E_{m,g}$ boards outlier probability = 0.021
$E_{c,0}$ outlier probability = 0.033

b)

Figure 4.25: Correlation between E_m in Phase 3 and $E_{c,0}$ for mean/L-C-R scale: a) $E_{m,l}$; b) $E_{m,g}$.

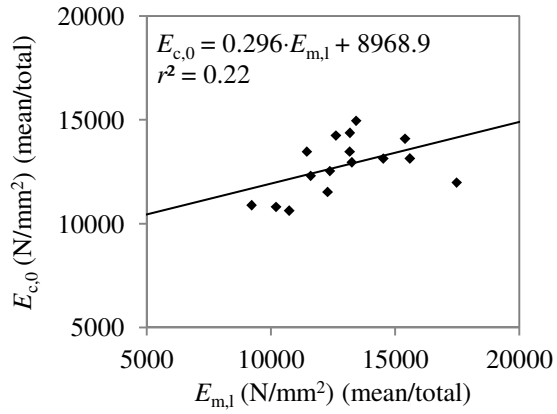

y = $m \cdot x$ + b	m	b	r^2
all	0.296	8968.87	0.22
class I	0.253	9353.84	0.12
class II	0.151	11000.47	0.09
class III	-0.052	13310.60	0.01
class NC	-0.111	13697.05	0.05
no outliers	0.477	6799.51	0.47

$E_{m,l}$ boards outlier probability = 0.024
$E_{c,0}$ outlier probability = 0.033

a)

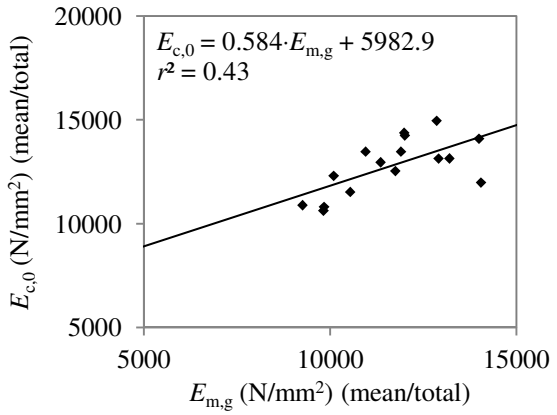

y = $m \cdot x$ + b	m	b	r^2
all	0.584	5982.89	0.43
class I	0.530	6219.61	0.34
class II	0.652	5355.60	0.48
class III	-0.132	14100.97	0.02
class NC	-0.153	13996.31	0.07
no outliers	0.345	9148.22	0.29

$E_{m,g}$ boards outlier probability = 0.021
$E_{c,0}$ outlier probability = 0.033

b)

Figure 4.26: Correlation between E_m in Phase 3 and $E_{c,0}$ for mean/total scale: a) $E_{m,l}$; b) $E_{m,g}$.

When considering the E_m of sawn beams, for both $E_{m,l}$ and $E_{m,g}$, the correlations with $E_{t,0}$ are low (Figure 4.27). The differentiation by visual classes lead to slightly higher coefficients of determination, especially for classes I and II. The overall correlations of E_m, in Phase 2, with $E_{t,0}$ are higher than the correlations with $E_{c,0}$, thus evidencing that the bending process of a timber element is more influenced by the tensioned region.

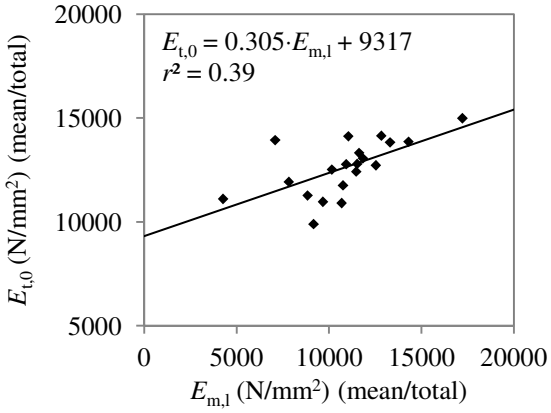

y = $m \cdot x$ + b	m	b	r^2
all	0.305	9317.02	0.39
class I	0.268	10007.70	0.46
class II	0.249	10383.35	0.51
class III	0.267	10002.67	0.45
class NC	0.252	10032.24	0.45
no outliers	0.314	9169.06	0.22

$E_{m,l}$ beams outlier probability = 0.100
$E_{t,0}$ outlier probability = 0.000

a)

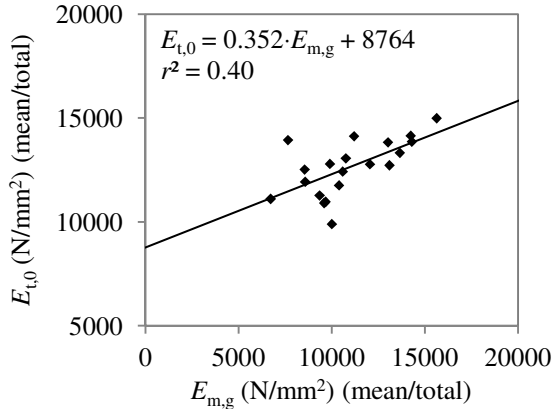

y = $m \cdot x$ + b	m	b	r^2
all	0.352	8764.31	0.40
class I	0.299	9620.74	0.44
class II	0.268	10116.19	0.45
class III	0.310	9531.32	0.44
class NC	0.284	9681.32	0.39
no outliers	0.352	8764.31	0.40

$E_{m,g}$ beams outlier probability = 0.000
$E_{t,0}$ outlier probability = 0.000

b)

Figure 4.27: Correlation between E_m in Phase 2 and $E_{t,0}$ for mean/total scale: a) $E_{m,l}$; b) $E_{m,g}$.

The stiffness measurements in Phase 3 are also correlated with $E_{t,0}$ in both mean/L-C-R (Figure 4.28) and mean/total (Figure 4.29) scales. In mean/L-C-R scale low correlations are found ($r^2 = 0.43$ and 0.33 for $E_{m,l}$ and $E_{m,g}$, respectively), however for mean/total scales moderate high correlations are obtained ($r^2 = 0.67$ for both $E_{m,l}$ and $E_{m,g}$). In the overall results, better correlations of E_m and $E_{t,0}$ are found for $E_{m,l}$ and for higher visual classes (classes I and II) where lower concentrations of defects exist. This is mainly due to the high influence of defects in tension behaviour, and also, it must be noted that the tension parallel to grain tests were made to clear wood samples, thus being more representative of classes I and II.

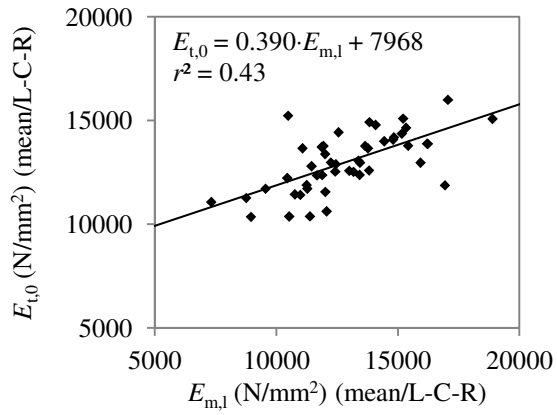

y = m·x + b	m	b	r^2
all	0.390	7967.79	0.43
class I	0.396	7618.13	0.32
class II	0.206	10441.70	0.19
class III	0.197	10954.79	0.18
class NC	0.087	11680.00	0.03
no outliers	0.420	7579.61	0.41

$E_{m,l}$ boards outlier probability = 0.024
$E_{t,0}$ outlier probability = 0.000

a)

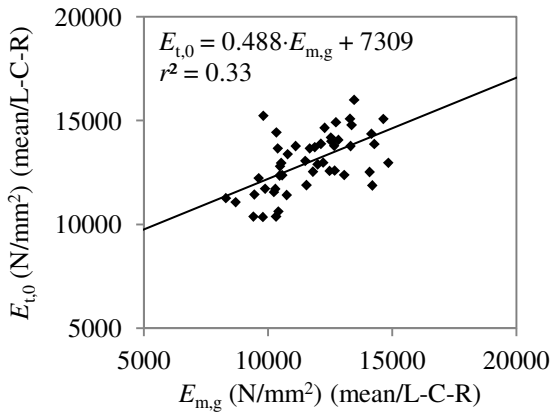

y = m·x + b	m	b	r^2
all	0.488	7309.03	0.33
class I	0.358	8543.05	0.15
class II	0.391	8558.18	0.24
class III	0.146	11611.82	0.04
class NC	0.034	12254.21	0.00
no outliers	0.484	7303.26	0.28

$E_{m,g}$ boards outlier probability = 0.021
$E_{t,0}$ outlier probability = 0.000

b)

Figure 4.28: Correlation between E_m in Phase 3 and $E_{t,0}$ for mean/L-C-R scale: a) $E_{m,l}$; b) $E_{m,g}$.

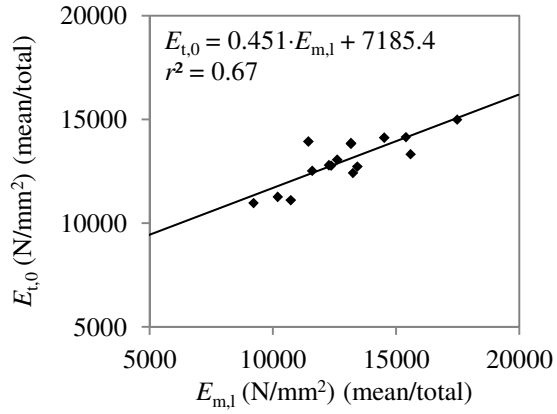

y = m·x + b	m	b	r^2
all	0.451	7185.36	0.67
class I	0.461	6725.74	0.53
class II	0.186	10820.03	0.21
class III	0.278	10034.08	0.32
class NC	0.084	11871.64	0.04
no outliers	0.474	6877.83	0.67

$E_{m,l}$ boards outlier probability = 0.024
$E_{t,0}$ outlier probability = 0.000

a)

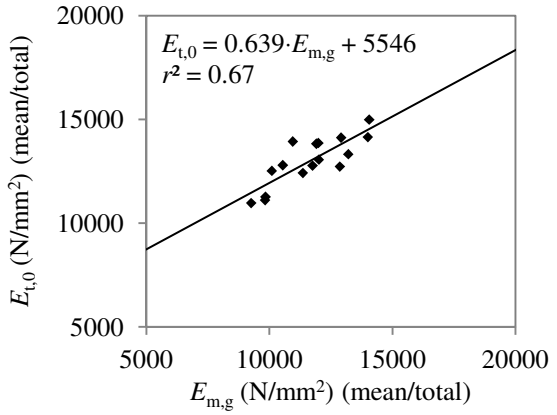

y = m·x + b	m	b	r^2
all	0.639	5545.99	0.67
class I	0.485	6982.46	0.37
class II	0.588	6369.97	0.58
class III	0.258	10365.88	0.11
class NC	0.025	12509.45	0.00
no outliers	0.314	9169.06	0.22

$E_{m,g}$ boards outlier probability = 0.021
$E_{t,0}$ outlier probability = 0.000

b)

Figure 4.29: Correlation between E_m in Phase 3 and $E_{t,0}$ for mean/total scale: a) $E_{m,l}$; b) $E_{m,g}$.

4.3.3 Modulus of elasticity with strength

In Phase 2, as previously mentioned, strong correlations were found with respect to f_m and MOE in bending, specially for $E_{m,l}$ ($r^2 = 0.87$ and 0.78, respectively $E_{m,l}$ and $E_{m,g}$). However, these correlations must be considered with care due to the small number of f_m measurements. In fact, in Phase 3, lower coefficients of determination were found with $E_{m,g}$ providing, nevertheless, a better correlation ($r^2 = 0.38$ and 0.69, considering $E_{m,l}$ and $E_{m,g}$, respectively).

Since segments for f_m determination were selected according to the visual grading, and therefore dependent of that grading, the correlation to MOE is also influenced. Considering that premise, the relation of MOE parallel to grain, E_0, with strength, f_0, was also investigated for the case of Phase 4, as the samples are restricted to clear wood samples. Moreover, strength and stiffness parallel to the grain are of interest especially when considering that many timber structures, such as timber roof trusses, are mainly designed to work under axial stresses in that direction. Correlations between E_0 and E_m have already been presented in a previous topic.

In the compression parallel to grain tests, low to very low correlations were found between $E_{c,0}$ and $f_{c,0}$ in both mean/L-C-R and mean/total scales ($r^2 = 0.38$ and 0.22), although it is noted a positive inclination of the tendency line (higher values of stiffness leads to higher values of strength) (Figure 4.30). A weak correlation is found between $E_{c,0}$ and $f_{c,0}$ ($r^2 = 0.38$). The correlation is mainly weakened by a sample group of elements that, although with similar values of $f_{c,0}$ (≈ 30 N/mm^2), they present a significant variation of $E_{c,0}$ within [10000;14000] N/mm^2. That group is mainly composed by samples that were conditioned in failure by splitting. By removing that sample an increase of the correlation is found, with $r^2 = 0.55$.

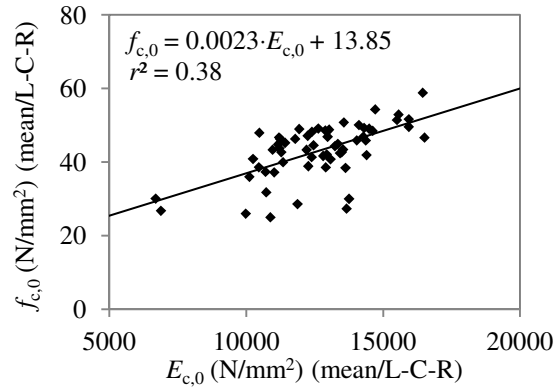

y = $m \cdot x$ + b	m	b	r^2
all	0.0023	13.85	0.38
no outliers	0.0018	20.77	0.23

$E_{c,0}$ outlier probability = 0.033
$f_{c,0}$ outlier probability = 0.050

a)

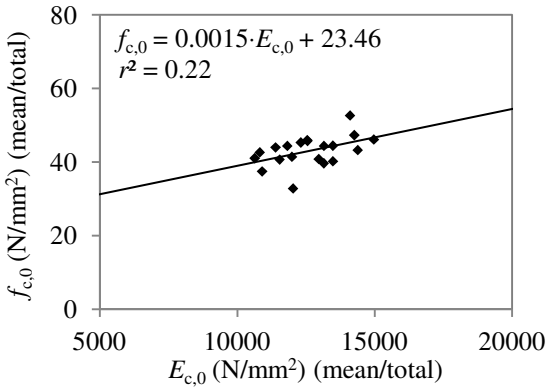

y = $m \cdot x$ + b	m	b	r^2
all	0.0015	23.46	0.22
no outliers	0.0017	21.43	0.36

$E_{c,0}$ outlier probability = 0.033
$f_{c,0}$ outlier probability = 0.050

b)

Figure 4.30: Correlation between $E_{c,0}$ and $f_{c,0}$ in Phase 4: a) mean/L-C-R scale; b) mean/total scale.

In the tension parallel to grain tests, low to medium correlations were found between $E_{t,0}$ and $f_{t,0}$ in mean/L-C-R and mean/total scales, respectively (r^2 = 0.30 and 0.54) (Figure 4.31). The results of tension in mean/total scale present the higher correlation in the parallel to grain tests. As seen for the compression parallel to the grain, also a positive inclination of the tendency line is noted in this case. Although the variation and dispersion of values is higher in the tension parallel to grain tests, rather than in the compression tests, no outliers were found, thus the sample for correlation without outliers is equal to the sample considering all the measurements.

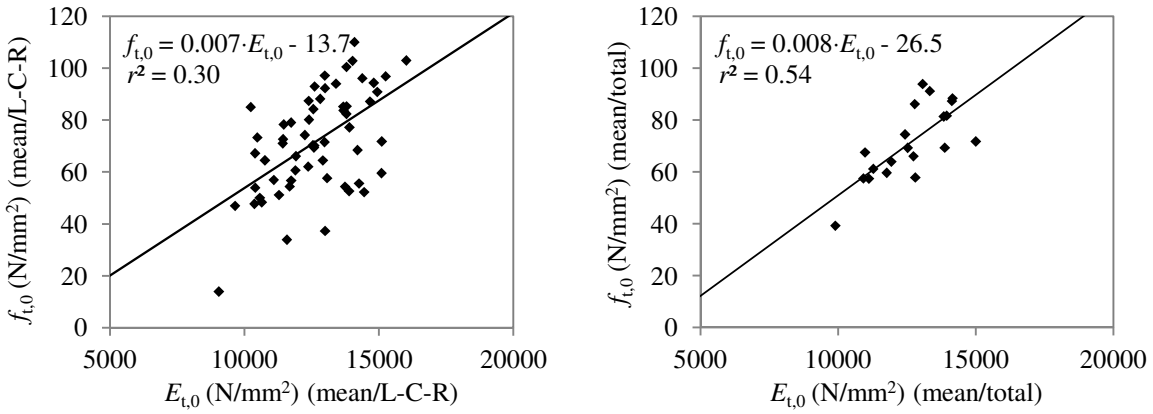

y = m·x + b	m	b	r^2
all	0.0067	-13.65	0.30
no outliers	0.0067	-13.65	0.30

$E_{t,0}$ outlier probability = 0.000
$f_{t,0}$ outlier probability = 0.000

a)

y = m·x + b	m	b	r^2
all	0.0077	-26.51	0.54
no outliers	0.0077	-26.51	0.54

$E_{t,0}$ outlier probability = 0.000
$f_{t,0}$ outlier probability = 0.000

b)

Figure 4.31: Correlation between $E_{t,0}$ and $f_{t,0}$ in Phase 4: a) mean/L-C-R scale; b) mean/total scale.

4.4 Probability distributions and parameter estimation

The layout of probabilistic models is often based on empirical data mostly combined with physical considerations, experience and good judgment. Constructing a probabilistic model in general requires the following steps (Köhler, 2007): *i*) assessment and statistical quantification (and qualification) of available data; *ii*) selection of a distribution function; *iii*) estimation of distribution parameters; *iv*) model verification; *v*) model updating.

The first step of the probabilistic model construction was considered previously in this chapter. Hereafter, attention will be given to the second and third steps.

4.4.1 Random variables and probability distributions

A sample value for a basic variable with a given (non-uniform) distribution is called a *random variable*. In statistics, the totality of possible observations or tests under the same

conditions is called a *population* and each individual test or each individual observation is an *element* of this population. This element can be investigated with respect to different *properties* which can be treated as a random quantity or a random variable. In engineering statistical investigations, often is only possible to consider a random subset of the elements of the population. This subset is called *random sample* and the number n of the elements contained in it is called the size of the sample.

In this work, the timber beams are a population. Each arbitrarily segment selected from a timber beam is an element of this population. Observations are necessarily limited to a number of segments tested in bending. The observed property is the modulus of elasticity of a given segment. The scale of all values is denoted by the random variable, which in this case is a quantity (modulus of elasticity in bending).

The selection of the design value of a random variable considering its uncertainty, is an important engineering task. In summary, the uncertainty in a random variable can be modelled by its underlying distribution, generally expressed in terms of PDF (probability density function) and CDF (cumulative density function) for continuous functions. To uniquely define the PDF, its parameters need to be estimated. Generally, the parameters are estimated using the information on mean, variance, and COV obtained from available data.

For information about different probability distributions, for common engineering problems, see Annex C.

4.4.2 Fitting the data to probability distributions

A classic procedure to assess if a given random variable may be well defined by a certain probability distribution is the use of probability papers. Having selected a probability distribution family, the probability paper is an extremely useful tool for the purpose of checking the plausibility of the selected family (Faber, 2012).

From probability papers, it is possible to assess the parameters of the inherent distribution with respect to the configuration of a given straight line (location and slope). However, a more efficient and accurate method is the Maximum Likelihood Method, which principle is based in finding the set of parameters of an assumed probability distribution function which most likely characterizes the underlying data sample.

The results of Phases 2 and 3, regarding bending MOE in sawn beams and boards, were fitted to different probability distributions using the Maximum Likelihood method. Description of the method and the resulting estimates are presented in Annex D.

Attending to the different visual classes, the results of MOE in boards were divided into four classes and each sample was fitted to the different probability distributions by probability papers. A qualitative analysis of the fitting is given in Table 4.6 and Table 4.7, respectively for $E_{m,l}$ and $E_{m,g}$.

Table 4.6: Qualitative analysis of the fitting to different probability distributions of $E_{m,l}$ of sawn boards regarding its visual class.

$E_{m,l}$ (sawn boards)	Distribution (*)			
Visual class	Normal	Lognormal	Gumbel	Weibull
I	+	+/-	-	+
II	-	+/-	+	+
III	+	+/-	-	+
NC	+/-	+	+/-	+

(*) qualitative description of fitting: + high; +/- moderate; - low.

Table 4.7: Qualitative analysis of the fitting to different probability distributions of $E_{m,g}$ of sawn boards regarding its visual class.

$E_{m,g}$ (sawn boards)	Distribution (*)			
Visual class	Normal	Lognormal	Gumbel	Weibull
I	-	+/-	+/-	+/-
II	+/-	+/-	+/-	+
III	+/-	+/-	+	+
NC	+/-	+	-	+

(*) qualitative description of fitting: + high; +/- moderate; - low.

For the MOE data, regarding sawn boards divided according to its visual class, the maximum likelihood estimates are given in Table 4.8. In all distributions, the estimated distribution mean decreased from higher visual classes to lower visual classes as also described by the statistical moments of the experimental data.

Table 4.8: Maximum likelihood estimates for $E_{m,l}$ and $E_{m,g}$ of sawn boards, divided by visual classes.

Property	Visual grading	Normal		Lognormal		Gumbel		Weibull	
		PAR1	PAR2	PAR1	PAR2	PAR1	PAR2	PAR1	PAR2
$E_{m,l}$	I	14026	3556	9.515	0.268	15890	4746	15371	3.955
	II	12603	3215	9.400	0.312	14122	2733	13791	4.664
	III	10718	3685	9.207	0.410	12568	3693	11961	3.199
	NC	8619	3438	8.974	0.437	10396	3611	9708	2.712
$E_{m,g}$	I	12580	2211	9.419	0.226	13605	1916	13443	6.794
	II	11246	2099	9.307	0.217	12219	1759	12069	6.556
	III	10032	2438	9.176	0.294	11182	2014	10949	4.953
	NC	8213	2469	8.948	0.422	9433	2316	9065	3.647

Normal (PAR1, PAR2) = (mean, standard deviation)
Lognormal (PAR1, PAR2) = (normal mean, normal standard deviation)
Gumbel (PAR1, PAR2) = (location parameter, scale parameter)
Weibull (PAR1, PAR2) = (scale parameter, shape parameter)

4.4.3 Goodness-of-fit significance tests

The knowledge of the nature of observed shapes of data may be combined with hypothesis tests, in such manner that one can discuss the hypothesis if a given data sample may be interpreted by a selected probability function. In the beginning of the 20th century, Karl Pearson established the principles to what is now one of the most popular significance hypothesis test for this purpose, the χ^2 goodness-of-fit test (Placket, 1983). Although the interpretation of Pearson's first test procedure may be less than straightforward at first, the basic principle is to test if certain data sample came from a population with a specific distribution. For that purpose the χ^2 test is defined by the null hypothesis (H_0) if the data is a random sample from the specified distribution and by the alternative (H_1) if the random sample does not follow the specified distribution.

The χ^2 goodness-of-fit tests were considered for the MOE of sawn boards with respect to different probabilistic functions with parameters obtained by both method of moments (MM), through the statistical estimation of the sample parameters, and maximum likelihood estimates (MLE). Description of the method and results are presented in Annex E.

For $E_{m,l}$ of sawn boards, a Normal distribution was found to be the best fit for the data. Although still not accepted for a 2.5% significance level, the Weibull distribution with respect to the maximum likelihood estimates produced a better fit than the Lognormal or Gumbel distributions. For $E_{m,g}$, the extreme distributions, both Gumbel and Weibull distributions, (with MLE distribution parameters) are accepted as good fits for the experimental data for a 2.5% significance level.

The χ^2 goodness-of-fit tests for the MOE of sawn boards in each separate visual class, with respect to different probabilistic functions with parameters obtained by method of moments and maximum likelihood estimates were also calculated and the results are presented in Annex E.

4.5 Final remarks

This chapter presents the analysis of variation and dispersion of mechanical properties of chestnut timber elements in different experimental phases and scales. The main objective is to provide an adequate framework for correlation between mechanical properties and further assessment of existing timber elements by information given by visual inspection, non-destructive testing and mechanical tests made to full size members and to small clear wood samples. Particular attention was given to the modulus of elasticity in bending since it is well known its correlation with other representative properties of timber.

For variation analysis, the coefficients of variation in each type of test were analysed regarding different scales assumed by the phases of the experimental campaign and by the size of the sample. An analysis regarding the dispersion and existence of outliers was

considered. Finally, the coefficients of determination between different mechanical properties and scales were established.

With respect to the different experimental phases, it was found that the coefficient of variation tends to decrease when smaller scales are considered. The measurements taken in bending tests for sawn boards also revealed that the stiffness properties vary both in height and length of each beam in different proportions. The mean coefficient of variation of measurements made to different levels in height of a beam was equal to 20.1% and 15.7%, respectively $E_{m,l}$ and $E_{m,g}$, whereas the mean COV of measurements made along the length was slightly higher being equal to 25.8% and 17.9%, respectively $E_{m,l}$ and $E_{m,g}$. Although similar, the coefficient of variation of MOE in compression parallel to grain was found to be higher than the MOE in tension parallel to grain. However, the opposite was verified for the compression parallel to grain strength that evidenced lower coefficient of variation than the tension parallel to grain strength.

Outliers were also defined for each sample considering the dispersion of extreme values. However it was found that, in this case, the elimination of outliers only produced a significant increase of correlation in a minor percentage of cases. Therefore, concluding that the extreme values were mainly due to heavy-tailed distributions of values rather than to measurement errors.

The mechanical properties of timber were correlated and high correlations were found between $E_{m,l}$ and $E_{m,g}$ assessed in different experimental phases, respectively of $r^2 = 0.82$ and 0.89 for sawn beams and boards. The correlation between experimental phases presented a $r^2 = 0.68$ and 0.71, respectively for $E_{m,l}$ and $E_{m,g}$, where also considering only the bottom board measurements moderate high correlations were found ($r^2 = 0.69$; $r^2 = 0.67$), thus the bottom boards may be considered representative of the global element in terms of E_m.

When analysing the structural element globally, the mean of all ultrasound propagation velocity measurements done to the same beam, either sawn beam or group of sawn boards, were compared and a $r^2 = 0.68$ was determined. After the analysis between results of ultrasound propagation velocity in different experimental phases, the results were compared to the stiffness results attained in the 4-point bending tests. In Phase 2, the ultrasound tests made within the l_1 region were averaged and compared to the $E_{m,l}$ while the average of all measurements was compared to $E_{m,g}$. Medium correlations were found ($r^2 = 0.52$ and 0.61), and in both cases the consideration of the different visual classes, led to higher correlations with exception of class NC where a very low (inexistent) correlation was obtained, due to the large variation in the sample. In Phase 3, high correlations were found when assuming the average of the results by each beam ($r^2 = 0.83$ and 0.89). The propagation velocity was also correlated with MOE parallel to grain in compression and tension with respect to the averaged value within a single beam. The results evidenced a low correlation for $E_{c,0}$, but moderate high for $E_{t,0}$ ($r^2 = 0.44$ and 0.71).

Pin penetration and drilling resistance tests made to the segments of sawn boards led to very low correlations (< 0.07). Although still low, correlations were found stronger

when assuming the mean values per board and when the tests were made perpendicularly to the lateral face.

The stiffness values in different load solicitation scenarios and experimental phases were also correlated. For E_m and $E_{c,0}$ a r^2 between 0.21 to 0.43 was found, whereas for E_m and $E_{t,0}$ better correlations were found with a r^2 between 0.39 to 0.67. With respect to the correlation between stiffness and strength, low to very low correlations were found between $E_{c,0}$ and $f_{c,0}$ in both mean/L-C-R and mean/total scales ($r^2 = 0.38$ and 0.22), whereas low to medium correlations were found between $E_{t,0}$ and $f_{t,0}$ for the same scales ($r^2 = 0.30$ and 0.54).

Considering the fitting of data to probability distributions, in the case of the sawn beams, $E_{m,g}$ is better defined in the lower tail by a Lognormal distribution, whereas for the upper tail a 2-p Weibull distribution tends to evidence a better approximation. The tails of $E_{m,l}$ distribution are better defined by a 2-p Weibull distribution for the lower tail and a Lognormal distribution for the upper tail, whereas a Gumbel distribution presents better approximation for the range of frequencies between 15% up to 50%. Although for different tails of the distributions, it is found that for sawn beams, Lognormal and 2-p Weibull distributions present better approximations to the analysed experimental results. With respect to the sawn boards, $E_{m,g}$ is rather well defined by a Gumbel distribution even for the lower tail, where also it is approximated to the Weibull distribution. Whereas, the tails of $E_{m,l}$ distribution are better defined by a Normal or a Weibull distribution while from 15% to 85% in frequency the experimental CDF is limited by the extreme distribution CDF (Weibull and Gumbel).

The division of bending MOE results in subsamples attending to different visual classes was considered, and it was found that Normal, Lognormal and Weibull distributions could be used for the representation of these results in different classes. However, regarding the nature of the measured parameter and simplicity of use, Lognormal distributions are considered a better choice.

The analysis of the probability papers together with the χ^2 goodness-of-fit significance test results produced similar conclusions about the suitability and fitting of the experimental data to the assumed probability distributions. Nevertheless, it was found that the experimental data may be better defined by the junction of different distributions aiming to more accurately attain information about the tails of the distribution. Therefore, the maximum likelihood estimates may be improved by performing a censored estimate with respect to the lower tails.

This page intentionally left blank

Chapter 5

Prediction of global bending stiffness by visual grading and random sampling of local bending stiffness

ABSTRACT: In the assessment of timber elements from existing structures, usually, only limited inspection of members (visual stress-grading) and mechanical characterization of small size specimens are possible (SDT), either due to onsite constraints or time and cost reasons. The present chapter, therefore, proposes and describes a consistent and feasible procedure for MOE prediction of chestnut timber elements by using localized MOE results obtained from smaller size samples, complemented with visual grading.

The predicting models take into account the visual strength classes and the influence of defects in the determination of the MOE. Moreover, random sampling selection is considered in order to demonstrate the possibility of using smaller representative samples, thus avoiding excessive need of removal of onsite samples and allowing for a lower number of mechanical tests. For this purpose, the database provided by the experimental campaign, described in chapter 3, will be considered. The local data obtained in the smaller size specimens is used to predict the global MOE of the full structural size members and is compared to the results of the experimental campaign.

5.1 Combining visual grading with bending properties

Bending is the most common loading type in the structural use of sawn timber and, consequently, bending strength is usually the critical strength property (Piazza and Riggio, 2008). Nevertheless, it is not feasible to assess directly the bending strength of a timber member, as this would only be possible by the destruction of the member itself. Therefore, bending strength is often assessed indirectly from other reference properties, such as the bending modulus of elasticity (MOE) in machine stress-grading.

Nocetti *et al.* (2010) found that the best predictor of strength properties of chestnut timber elements was the bending MOE, followed by a knot parameter. While in Cavalli and Togni (2011), the knot incidence (minimum knot diameter to depth/width ratio) and slope of grain, were considered as the most important influencing parameters and those that lead to more significant MOE reduction. Also in Piazza and Riggio (2008) it is stated that knots are by far the most important defects in the reduction of visual grading, being quite significant in the case of thick elements, like beams. The reduction in strength and stiffness is most likely caused by the combination of local grain deviation and reduction of the clear wood area in the cross section, even if the first factor is the most significant (Kollmann and Côte, 1984).

García *et al.* (2007) obtained coefficients of determination, r^2, for pine species up to 0.71 for predictive models of global MOE, including visual grading parameters, density and non-destructive variables (longitudinal wave transmission velocity) as independent variables. In Nocetti *et al.* (2010), lower linear regression correlations were found for hardwoods, compared to softwoods. In the case of chestnut timber, a r^2 of 0.54 was found between the MOE obtained in the laboratory and by machine stress-grading.

Lee *et al.* (2005) established a prediction model for bending properties of glued laminated timber using knot parameters and MOE distributions of lumber laminate as main input variables, obtaining strong correlations between predicted and measured MOE values. Lee and Kim (2000) also found better results in predicting glued laminated timber MOE with the use of localized MOE of lamella, when compared to the long span MOE of lamella. The relationship between local and global modulus of elasticity in bending has been investigated in several previous studies (Boström, 1999; Denzler *et al.*, 2008; Ravenshorst and Kuilen, 2009; Ridley-Ellis *et al.*, 2009), together with its consequences in structural timber grading (Nocetti *et al.*, 2013).

For the estimation of the mechanical properties of existing structural timber elements, it is common practice to attend to results of mechanical tests made to small clear wood specimens extracted from the element. However, this mechanical characterization often provides higher results compared to the mechanical behaviour of the structural element, as it is affected by the influence of defects. As mentioned by Kasal and Anthony (2004), the timber member mechanical properties will always be lower than those of small clear specimens because of the inevitable presence of defects in structural size pieces. When the specimen size increases also the stressed volume increases and for brittle materials or systems organized in series, a higher probability that a weak link occurs in the

volume exists (Weibull, 1939). On the other hand, visual inspection often leads to conservative estimates of the element's mechanical behaviour. Therefore, these two approaches provide an upper and lower bound for the mechanical characterization of existing timber elements.

The results from Wang *et al*. (2008b) indicated that the visual grades could identify different strength classes for timber samples, with higher visual grading corresponding to higher MOE in bending. However, Vega *et al*. (2012) concluded that, for chestnut timber elements, visual grading parameters of the elements did not play a significant role in the prediction of MOE. This is corroborated by Piazza and Riggio (2008), which pointed out that the adopted visual grading methods and NDT tests for chestnut elements showed lower correlations than other two tested softwood species, namely spruce (*Picea abies* Krast.) and larch (*Larix decidua* Mill.) from north of Italy.

5.2 Experimental data analysis

As previously presented, the results of the experimental campaign to the chestnut timber elements evidenced the relationship between the $E_{m,g}$, and $E_{m,l}$ within and between phases (different sizes). Strong correlations (r^2 between 0.82 and 0.89) were found within the same phase, whereas less strong correlations (r^2 between 0.68 and 0.71) were found between different phases. Although the strong correlations, a significant difference between results from different scales is still visible, and especially noticeable, for $E_{m,l}$ where the gauge length increase between scales induces higher differences. A slight better comparison is found when considering only the segments of boards included in the gauge length of the sawn beams (l_1), however still with significant difference between scales. Figure 5.1 provides the comparison of the cumulative distribution functions (CDF) for the different results of bending MOE in Phase 2 (sawn beams) and Phase 3 (sawn boards). The results were modelled by lognormal distributions regarding the probabilistic fitting considered previously. The found differences may be explained by the size effect in the mechanical properties of timber due to the probability of presence and influence of defects in different scales.

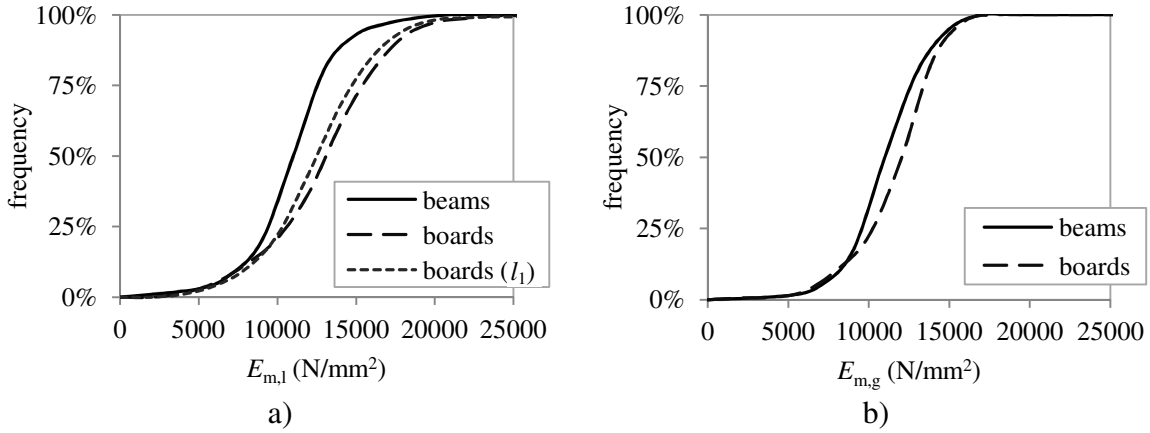

Figure 5.1: Correlation between bending tests in Phase 2 and 3: a) cumulative distribution functions for $E_{m,l}$; b) cumulative distribution functions for $E_{m,g}$.

Even at the same scale, the reduction of bending MOE is significant as proved by an ANOVA regarding the values of MOE for the segments of boards divided by visual grading. In this case, it is expectable that elements with higher percentage of segments with defects (lower visual grading) have lower values of bending MOE, whereas elements with higher percentages of clear wood segments (higher visual grading) will have higher values of bending MOE. To confirm this premise, the results of the visual grading made to the sawn boards were analysed and the percentage of segments of class I and class NC for each set of three boards were compared to the bending MOE (both local and global) of the sawn beams (Figure 5.2). Weak correlations with bending MOE of beams are found with the percentage of class I segments, although slightly increasing when considering the percentage of class NC segments. This evidences a higher importance in the consideration of segments with defects in the analysis, rather than the percentage of clear wood, even at a linear elastic range. However, Piazza and Riggio (2008) mention that clear wood has a stronger effect on stiffness than local weak spots, although stiffness is to a greater extent determined by average properties along the member. Therefore, in the case of the present study, it should be noted that the location of segments within the elements is an important factor, which was not considered in this initial analysis.

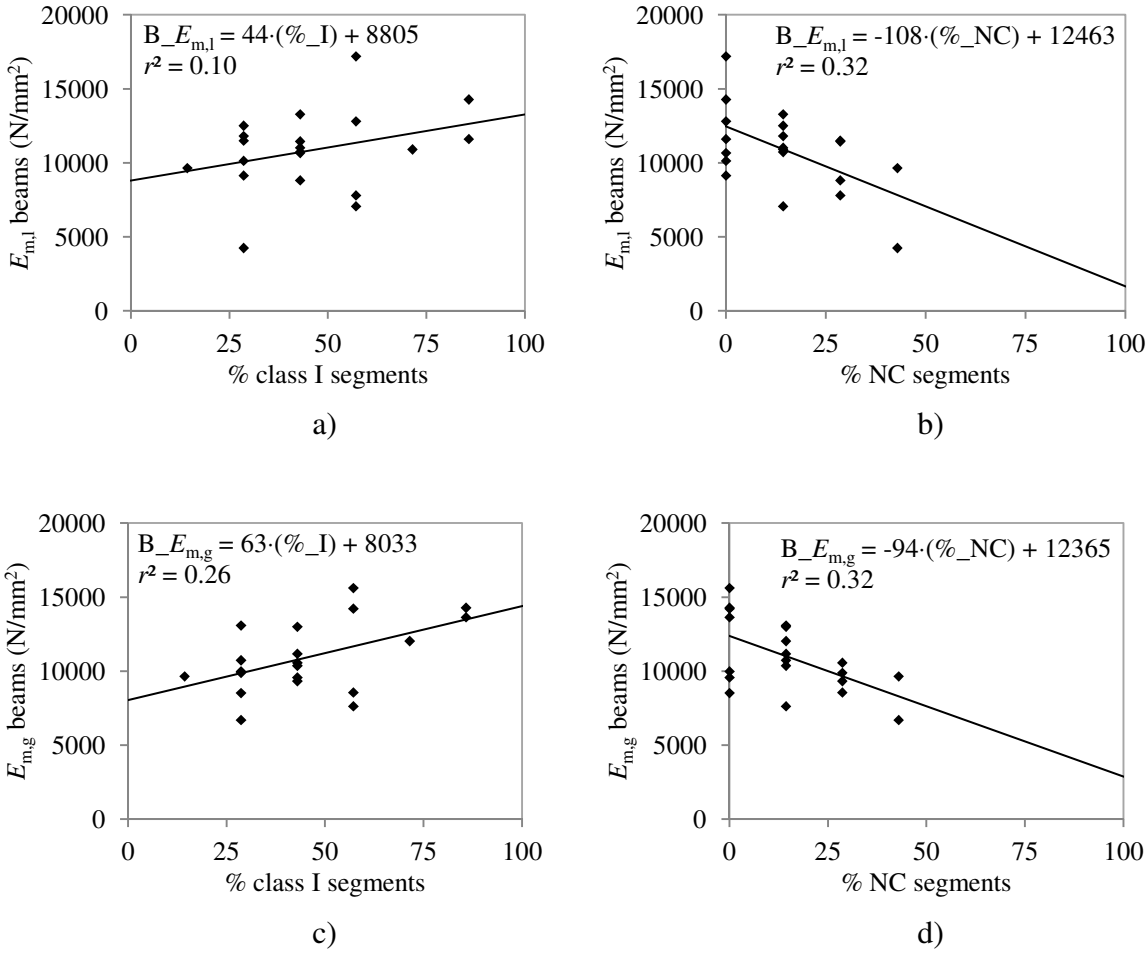

Figure 5.2: Correlation between bending MOE with percentage of segments in different visual grading: a) $E_{m,l}$ with class I segments; b) $E_{m,l}$ with class NC segments; c) $E_{m,g}$ with class I segments; d) $E_{m,g}$ with class NC segments.

Nevertheless, it is visible that there is an increase for bending MOE for beams with higher percentage of class I segments, as well as, that a decrease for bending MOE for beams is related with higher percentage of class NC segments. The influence of defects in the analysis will be further discussed in topic 5.3.

At this point, is clear that a strong correlation between MOE in different phases (scales: sawn beams and boards) is present, and that the consideration of visual grading could provide a better approximation and definition of the mechanical properties. This is an important consideration for the assessment of the mechanical properties of timber members onsite, since often only visual grading of the elements is possible with the combination of NDT or removal of small specimens for testing. In this pursuit, hereafter, the results in the experimental campaign from local measurements (board's segment scale) will be used to determine the possibility of prediction of the global mechanical properties (beam scale). To that aim $E_{m,l}$ of sawn boards' segments are combined with visual grading to determine the $E_{m,g}$ of sawn beams.

The results of $E_{m,g}$ of beams and the $E_{m,l}$ of boards' segments were fitted to lognormal probability distribution functions considering the prior use of probability papers and χ^2 goodness of fit tests (with 2.5% significance level). The frequency of the associated probability distributions for these results is presented in Figure 5.3. The results of $E_{m,l}$ of boards' segments are differentiated by visual classes, evidencing a higher variation for lower grade classes, as well as a lower mean value.

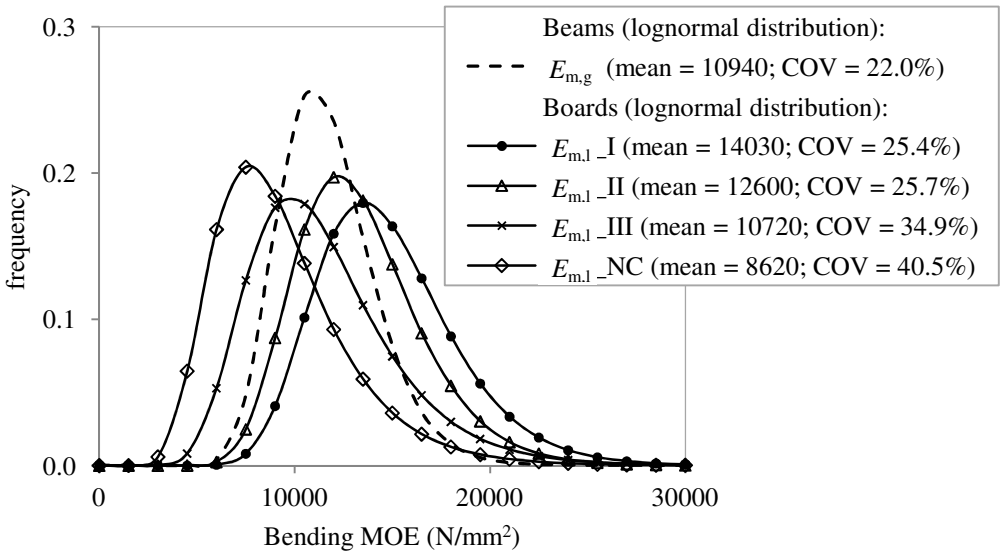

Figure 5.3: Frequency distribution and statistical parameters for $E_{m,g}$ of beams and $E_{m,l}$ of boards' segments differentiated by visual inspection classes.

Prior to consider any model regarding the prediction of the global properties of the sawn beams, a benchmark r^2 was defined attending to the values of the local measurements within each beam. This benchmark r^2 was obtained by means of multiple regression regarding the influence of each set of boards (top, lower and bottom) for the $E_{m,g}$ of the structural size sawn beam. This benchmark r^2 corresponds to the best possible correlation

regarding the optimization between the results found in the two different phases of bending tests.

When performing a multiple regression, the predicted value, $y^{\text{predicted}}$, is given by the sum of the weighted contribution, C_i, of the independent variables, x_i, and a constant, c, as:

$$y^{\text{predicted}} = C_1 \cdot x_1 + C_2 \cdot x_2 + ... + C_n \cdot x_n + c = \sum_{i=1}^{n} C_i \cdot x_i + c \tag{5.1}$$

In this case, the results of each board are assumed as independent variables and the beam's experimental result as a dependent variable, resulting in the relation given in Equation 5.2 for the predicted value of $E_{m,g}$, where $C_{top} = 0.224$, $C_{middle} = 0.193$, $C_{bottom} = 0.661$ and c = -1820 N/mm^2. These parameters indicate a larger contribution of the values of the lower boards for the prediction $E_{m,g}$.

$$E_{m,g}^{\text{predicted}} = C_{top} \cdot E_{m,l}^{top} + C_{middle} \cdot E_{m,l}^{middle} + C_{bottom} \cdot E_{m,l}^{bottom} + c \tag{5.2}$$

With this relation, the best linear fit with the experimental results ($r^2 = 0.84$) is attained, with the lowest residual between predicted and experimental (Figure 5.4). Here, B_$E_{m,g}$ indicates the MOE results of sawn beams in mechanical tests in Phase 2. The analysis of the correlation between each board and the corresponding beam leads to the conclusion that the lower board has a better linear fit to the experimental results with $r^2 = 0.74$, whereas the middle and top boards present lower correlations with, respectively, $r^2 = 0.59$ and 0.40.

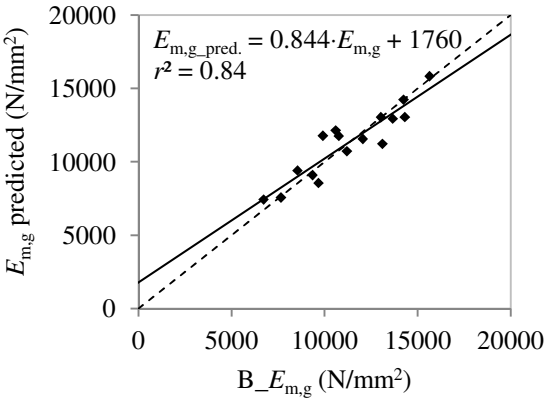

$$E_{m,g}^{\text{predicted}} = 0.224 \cdot E_{m,l}^{top} + 0.193 \cdot E_{m,l}^{middle} + 0.661 \cdot E_{m,l}^{bottom} - 1820 \text{ (N/mm}^2\text{)}$$

Figure 5.4: Correlation between experimental $E_{m,g}$ of beams with the predicted value taken from a multiple regression of sawn boards' $E_{m,l}$.

The larger contribution of the bottom board is mostly because that board was originally in the tension region of the structural beam (Figure 5.5), and timber is more sensible to tension effects, mainly due to the presence of defects. This is also evident in the timber beams that were taken to failure in bending, where the failure mechanism began always in the tensioned region of the beams.

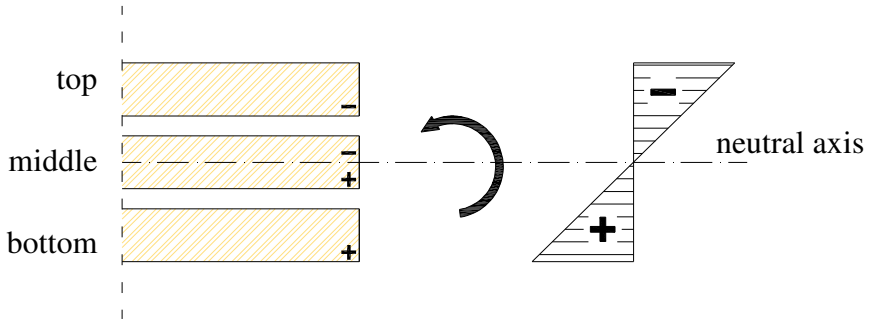

Figure 5.5: Location of the sawn boards in a moment induced stress diagram in a sawn beam section.

Generally, as mentioned by Biblis *et al.* (2004), any type and size of knot located in the lower part of the lumber can have a greater reducing effect on the mechanical properties since it interferes with the highest tensile stress.

5.3 Influence of defects in mechanical characterization

In order to verify the influence of visual inspected defects, and if the assumed visual inspection classes could distinguish segments with different stiffness values, the results of $E_{m,l}$ of the bottom sawn board were analysed.

In a first analysis, the mean values of $E_{m,l}$ of the bottom board segments visually graded as class I were compared to the B_$E_{m,g}$ for each beam. This analysis led to a moderate correlation ($r^2 = 0.66$), however, stiffness values higher than B_$E_{m,g}$ were predicted for each beam, since only clear wood samples (or with minor defects) were considered (Figure 5.6). Therefore, it is necessary to consider the influence of lower visual class segments and quantify the decrease in the mechanical properties for those classes.

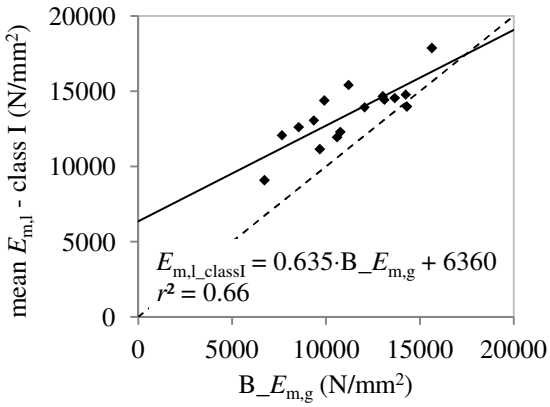

Figure 5.6: Correlation between experimental $E_{m,g}$ of structural beams (B_$E_{m,g}$) and mean $E_{m,l}$ of the segments in the bottom sawn boards graded as class I.

So as to include the influence of lower visual class segments, in a second analysis, the segments of each lower board were divided according to their visual inspection and the

$E_{m,l}$ of each group was statistically analysed. After, the mean reduction factor for $E_{m,l}$ to downgrade from class I to the remaining classes, was calculated. According to the obtained reduction factors and accounting for the number of segments in a given visual class, a weighted MOE can be calculated for each beam, as:

$$E_{weighted} = \frac{n_I \cdot E_I + n_{II} \cdot (E_I - \alpha_{II} \cdot E_I) + n_{III} \cdot (E_I - \alpha_{III} \cdot E_I) + n_{NC} \cdot (E_I - \alpha_{NC} \cdot E_I)}{n_I + n_{II} + n_{III} + n_{NC}} \quad (5.3)$$

where $E_{weighted}$ is the weighted $E_{m,l}$ considered for each beam, n_{class} is the number of segments, α_{class} is the reduction factor of a given visual class (I, II, III or NC) and E_I is the mean value of the $E_{m,l}$ for segments classified as class I.

In the case of indicative values given in UNI 11119 (UNI, 2004) for allowable stress values, the difference on the MOE between strength classes corresponds to a reduction of the value given for class I of 10% or 20%, respectively, when downgrading to class II or III, and no value is given when not classifiable (NC). In the present study, a mean reduction in $E_{m,l}$ of the class I sample of 6%, 21% and 27% was found, respectively, for downgrading to class II, III or NC.

According to the obtained reduction factors and accounting for the number of segments in a given visual class, a weighted MOE was calculated for each beam, as given in Equation 5.3. The results are presented in Figure 5.7, where it is visible that in comparison with the results from the analysis with only class I values, a stronger correlation is obtained ($r^2 = 0.82$), evidencing the improvement in the model when considering information from a visual inspection grading. However, the predicted values still overestimate the B_$E_{m,g}$ results.

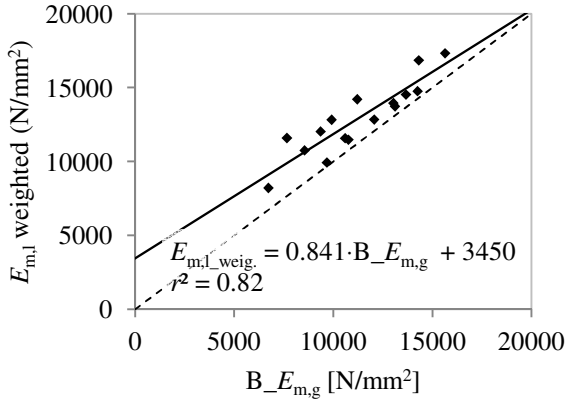

Figure 5.7: Correlation between experimental $E_{m,g}$ of structural beams (B_$E_{m,g}$) and weighted $E_{m,l}$ by visual inspection grading of the segments in the bottom sawn boards.

These results permit to conclude that it is possible to predict the global behaviour of an existing timber element with data from smaller clear wood specimens when complemented with a visual class grading made to critical sections and segments of the entire element.

5.4 Prediction models

With consideration to the experimental data analysis, it is plausible to assume that one may predict, within a confidence interval, the $E_{m,g}$ value of structural size timber elements by considering the $E_{m,l}$ of smaller size samples and the visually inspected distribution of defects along the length and height of the element.

To validate this hypothesis, structural models are proposed where the computation of MOE results in sawn boards was considered and compared with the measurements of structural size beams under bending tests. The information of visual inspection is also taken into account for model calibration and improvement.

After defining the benchmark r^2 and verifying the importance of considering segments with defects in the global behaviour of a timber member, two different models are proposed regarding the computation of measurements of boards' MOE. These measurements are inputted on the models either by modelling the sawn boards as separate elements or by modelling a reconstructed full sawn beam (see Figure 5.8).

For both models, the elements were defined by the combination of the results of $E_{m,l}$ in the sawn boards bending tests. To each segment of a board the $E_{m,l}$ corresponding to the nearest bending test result made to the sawn boards is attributed and, after, each segment is modelled as a beam element. Displacements of each node were obtained by use of the direct stiffness method, with the calculation of the $E_{m,g}$ of beams being based on the EN 408 (CEN, 2010a) formulation.

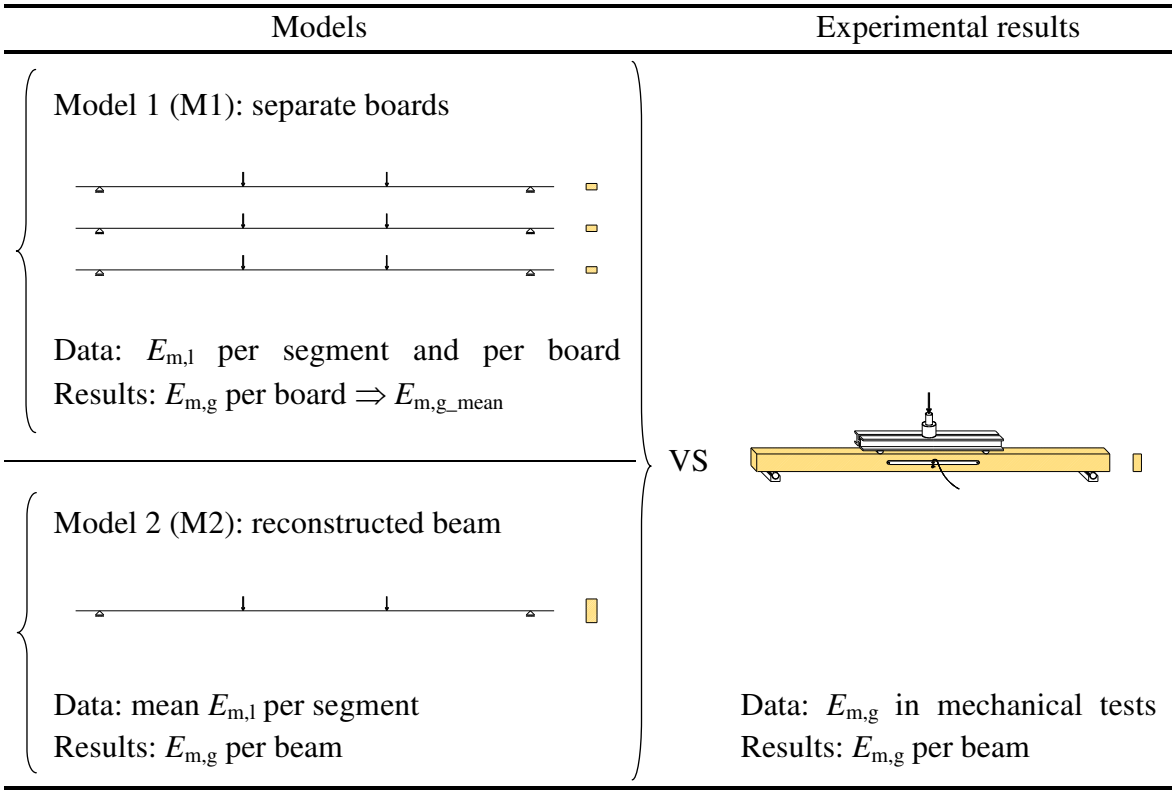

Figure 5.8: Models used for assembling the $E_{m,l}$ of sawn boards segments for comparison with $E_{m,g}$ in the beams' bending tests.

The first model (Model 1 - M1) considered the values taken to each segment of a sawn board and then, as result, the MOE would be calculated for the total span length between supports. Although modelling each board separately, the span between supports is equal to the span of a full size beam. The average of the three results for each group of sawn boards that previously composed a beam was taken and compared to the bending tests results obtained from the beams. Therefore, for each beam, three boards were modelled and a mean result was calculated.

The second model (Model 2 - M2) assumed the mean value for the measurements made to the same segment of each set of boards (*e.g.* measurements in A1 (top), A2 (middle) and A3 (bottom) for segments 1 (from 10-50 cm)), thus the mean MOE in height per segment. This mean MOE is afterwards considered for the modelling of a full cross section size reconstructed beam and then the results are compared to the beams' bending tests results.

For notation purposes, M1_$E_{m,g}$ and M2_$E_{m,g}$ correspond to the global modulus of elasticity ($E_{m,g}$) predicted respectively from Model 1 and Model 2.

The results of the models are compared to the B_$E_{m,g}$ (Figure 5.9), and strong correlations are found (r^2 = 0.76 to 0.78). When assuming the values of $E_{m,l}$ from modelling, it is found that the predicted values are in general higher than the experimental values (non-conservative approach). Still, one may conclude that the combination of the different properties of the singular segments may satisfactorily predict the behaviour of the global element. This seems also a reasonable assumption because the tests were conducted in linear elastic regime.

A similar conclusion is found in Aicher *et al.* (2002) where the results permitted to state that the measured local MOE and the experimental global MOE are consistent, since the global MOE may be predicted by beam theory or FEM analysis on the basis of the local MOE of segments. It is worthwhile mentioning that in this study, the measurements taken from smaller size specimens were able to adequately predict the higher scale element, despite the fact that both smaller and larger samples presented localized defects.

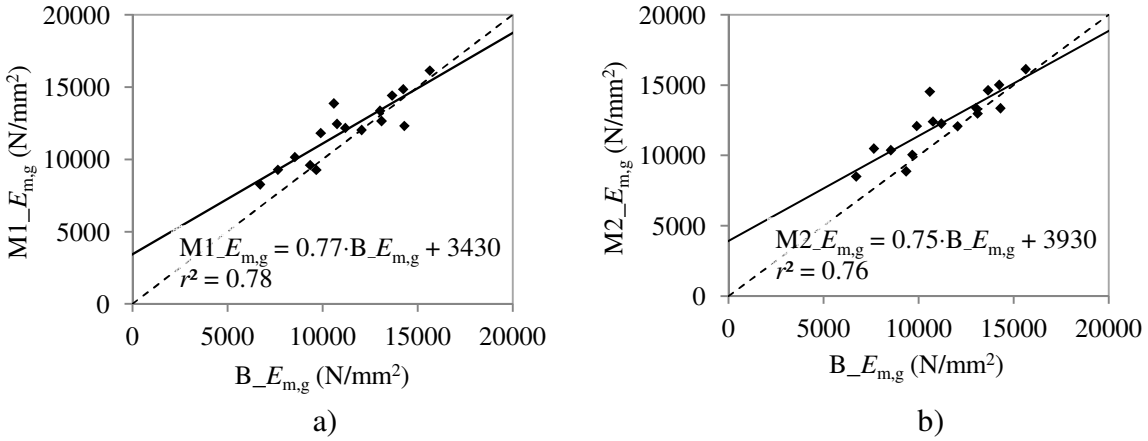

Figure 5.9: Correlation between experimental $E_{m,g}$ of structural beams (B_ $E_{m,g}$) and $E_{m,g}$, with use of boards' $E_{m,l}$, given by: a) M1; b) M2.

Besides the comparison to the benchmark r^2 (r^2 = 0.84, see Figure 5.4) it is also of interest to compare the results of the same procedure but considering the $E_{m,g}$ of sawn boards as an input datum. As the same parameter is used between the two size scales, a slight better correlation is obtained for both models (Figure 5.10) and a lower difference between predicted and experimental values is obtained. Nevertheless, the use of $E_{m,l}$ is still a good choice taking into account the intention of preferably using local measurements within the element.

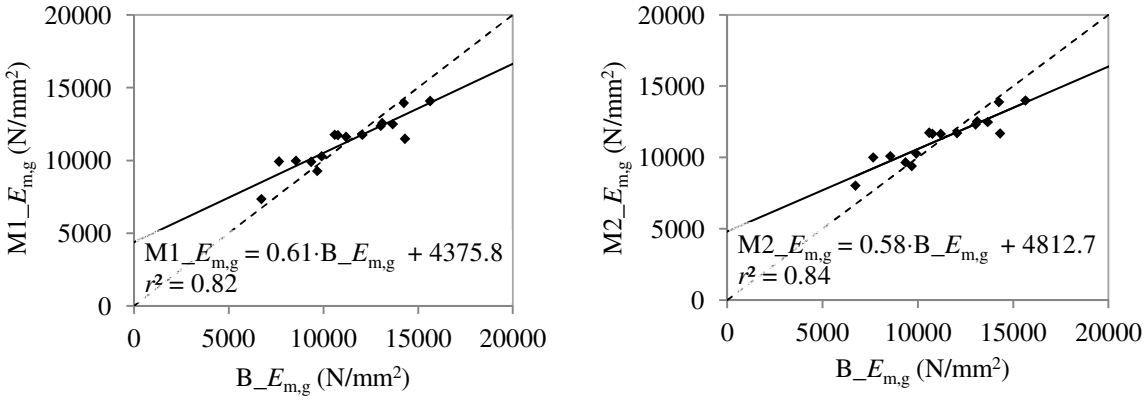

a) b)

Figure 5.10: Correlation between experimental $E_{m,g}$ of structural beams (B_ $E_{m,g}$) and $E_{m,g}$, with use of boards' $E_{m,g}$, given by: a) M1; b) M2.

5.5 Random sampling selection

When assessing the safety of an existing timber structure, it is not possible to obtain the different $E_{m,l}$ along the timber elements as in the experimental campaign carried out and presented in the previous chapters. Moreover, it is important to minimize the destructive component of the mechanical characterization related to the extraction of specimens from the timber members. Therefore, it is important to analyse if the use of a representative sample of the different segments in each visual inspection class would permit to obtain a reliable assessment of the global element.

For that purpose, after each segment being visually classified, one segment representative of each visual class is chosen randomly and its $E_{m,l}$ is considered for all the other segments with the same visual class. Then, the models will consider such information as input data and compute the $E_{m,g}$ of the reconstructed beam. The random selection of segments is repeated until a significant sample is obtained and then, the mean value is correlated to the experimental campaign results. The applied methodology is described in Figure 5.11.

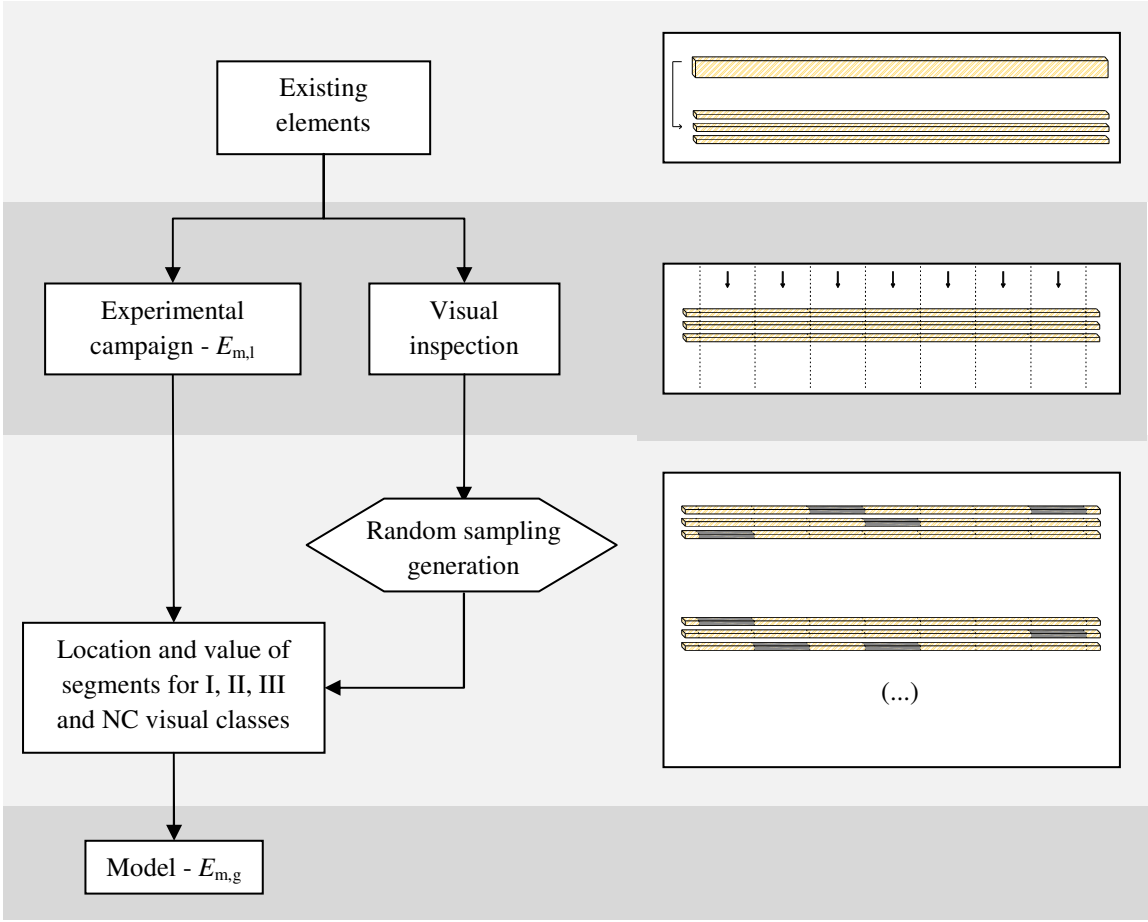

Figure 5.11: Implemented procedure for obtaining sets of random variable samples of segments in different visual classes for $E_{m,g}$ prediction by models M1 and M2.

The variation in the results of each beam regarding the randomly generated sample is determined with mean COV of 16.0% and 15.8% for M1 and M2, respectively. The results are presented in Figure 5.12 where, considering the previous benchmark correlation, again strong correlations were found (r^2 = 0.70 to 0.75).

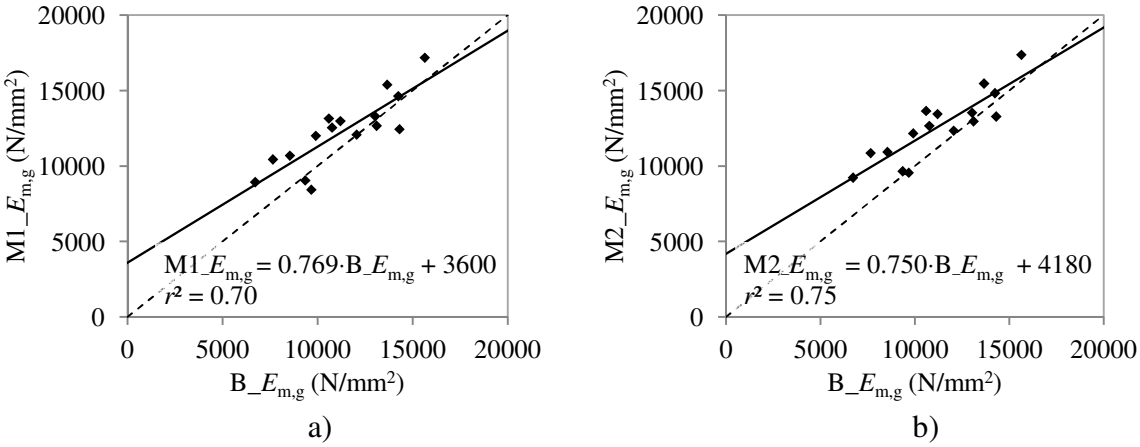

Figure 5.12: Correlation between experimental $E_{m,g}$ of beams with random generated sets of $E_{m,l}$ in segments according to the visual inspection: a) M1; b) M2.

In addition, an analysis is considered by selecting only a sample of class I and then assuming the remaining classes as a reduction of that value. Thus, only the information of

clear wood samples and the reduction factors according to the visual inspection are considered to attribute each value to the different segments in the model. As mentioned before, a mean reduction in $E_{m,l}$ for class I of 6%, 21% and 27% was found, respectively, for downgrading to class II, III or NC. Considering these reduction factors and a procedure analogous to the methodology presented in Figure 5.11, but only by randomly selecting the values of segments in class I, the MOE are calculated by models M1 and M2.

The results are presented in Figure 5.13 and the variation in the results of each beam regarding the randomly generated sample is also determined with mean COV of 15.2% and 15.4% for M1 and M2, respectively. The correlations between experimental results and the ones obtained by random selection of segments with a given visual class, evidenced strong correlations with r^2 between 0.76 and 0.79, with better results in M1 considering only a random selected value of class I and the reduction factors.

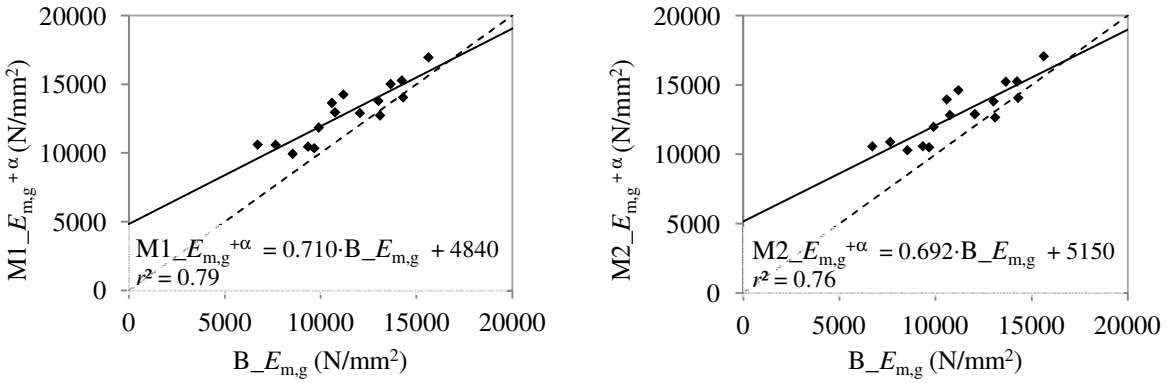

Figure 5.13: Correlation between experimental $E_{m,g}$ of beams with random generated sets of $E_{m,l}$ in segments with visual class I and reduction factors for the other classes: a) M1; b) M2.

Although strong correlations were found in the prediction of B_$E_{m,g}$ by use of the $E_{m,l}$ and visual inspection information in a random sampling selection, it is also important to evaluate if the error involved in this prediction is admissible regarding the inherent uncertainty in the assessment of timber structures. For that purpose, the percentage error was calculated by comparing the predicted value with the experimental quantity. In this case, the percentage error is the absolute value of the difference divided by the experimental value times 100.

Table 5.1 indicates the calculated percentage error and r^2 for the results of MOE in different test phases and for the different models. It evidences that the percentage error of the prediction models have a similar range to those obtained from the experimental campaign between different phases and do not exceed an average percentage error of 20%. The exception is the model that only considered the class I samples as representative visual class, with a percentage error of 23.4%, further demonstrating that the influence of lower visual grade segments must be considered.

Comparison to the indicative values given by UNI 11119 (UNI, 2004) is also considered accounting to the visual grading of the sawn beams. As no indicative value is suggested for the non classifiable (NC) segments, the initial calculation of the percentage

error was made for sawn beams classified only as I, II or III classes, obtaining a mean percentage error of 32.7%. As comparison, in Piazza and Riggio (2008), an absolute value of 28% was found for the error of the visual grading by UNI 11119 (UNI, 2004) in predicting stiffness of elements in structural size. In order to account the stiffness values of sawn beams graded as NC, the reduction factor found in the experimental results for downgrading from class I to class NC (27%) was considered and the percentage error was recalculated. By consideration of the sawn beams with class NC, a lower mean percentage error was obtained (29.7%).

Table 5.1: Percentage error, *% error*, and coefficient of determination, r^2, for the results of MOE in different test phases and for the diverse prediction models considered.

	x	y	x/y			*% error* =|1-x/y|·100 [%]			r^2
			min	max	mean	min	max	mean	
*	B_$E_{m,l}$	B_$E_{m,g}$	0.63	1.19	0.99	0.03	36.6	9.36	0.82
	b_$E_{m,l}$	b_$E_{m,g}$	1.00	1.24	1.10	0.48	24.3	10.4	0.89
	B_$E_{m,l}$	b_$E_{m,l}$	0.49	1.06	0.87	1.29	51.3	14.2	0.68
	b_$E_{m,g}$	B_$E_{m,g}$	0.84	1.46	1.07	1.72	46.2	12.6	0.71
	VI $^{\text{classes I, II, III}}$	B_$E_{m,g}$	0.56	0.94	0.67	6.28	43.8	32.7	0.39
	VI $^{\text{all classes}}$	B_$E_{m,g}$	0.56	1.09	0.71	4.49	44.3	29.7	0.40
**	B_$E_{m,g}^{\text{mult.regr.}}$	B_$E_{m,g}$	0.86	1.19	1.01	0.03	18.9	7.32	0.84
	M1_$E_{m,g}$	B_$E_{m,g}$	0.86	1.31	1.09	0.02	31.2	11.3	0.78
	M2_$E_{m,g}$	B_$E_{m,g}$	0.94	1.37	1.11	0.37	37.5	12.9	0.76
	$E_{m,g}^{\text{class I}}$	B_$E_{m,g}$	0.98	1.58	1.23	2.19	58.0	23.4	0.66
	$E_{m,g}^{\text{class I + α}}$	B_$E_{m,g}$	1.03	1.52	1.17	2.94	51.9	16.5	0.82
***	M1_$E_{m,g}^{\text{all classes}}$	B_$E_{m,g}$	0.87	1.37	1.11	0.44	36.8	14.7	0.70
	M2_$E_{m,g}^{\text{class I}}$	B_$E_{m,g}$	0.93	1.42	1.14	0.89	42.3	15.4	0.75
	M1_$E_{m,g}^{\text{class I + α}}$	B_$E_{m,g}$	0.97	1.58	1.16	1.71	58.1	17.0	0.79
	M2_$E_{m,g}^{\text{class I + α}}$	B_$E_{m,g}$	0.97	1.58	1.18	1.65	57.5	18.2	0.76

B = sawn beams; b = sawn boards; VI = visual inspection; M1 = model 1; M2 = model 2

* Experimental results in Phases 2 and 3;

** Models for analysis of defect influence;

*** Models using random sampling selection

By comparison to the experimental results, a mean underestimation of 29% is obtained when the UNI 11119 (UNI, 2004) indicative values are considered, while a maximum mean overestimation of 18% is obtained when models using random sampling were considered.

Table 5.1 also evidences that stronger correlations were obtained for the prediction of $E_{m,g}$ of sawn beams by $E_{m,l}$ of sawn boards when information of visual inspection classes was added.

5.6 Final remarks

This chapter addresses the correlation between different size scale experimental phases with the intention of obtaining a suitable source of information for predicting the global modulus of elasticity of structural size elements. Attention is given to the modulus of elasticity in bending regarding its correlation with other representative properties of timber. Different models for assembling the distribution of local moduli of elasticity, $E_{m,l}$, are combined with visual strength grading for use in predicting the global modulus of elasticity, $E_{m,g}$, of structural beams.

For $E_{m,g,}$ prediction, two different models were developed with correlation to the experimental values of r^2 between 0.76 to 0.78, and a multiple regression analysis indicated a larger contribution of the segments in tension for the determination of the $E_{m,g}$ of beams. Combination of the values for segments classified as class I (samples without significant macro defects) and of the percentage of the other classes in a given element led to higher correlations between predicted and experimental values when compared with the model that disregarded the influence of defects (r^2 increased from 0.66 to 0.82).

The main contribution of this work, evidenced by random sampling selection, is the demonstration that it is feasible to predict the behaviour of a full size scale element by definition of the mechanical properties of selected segments with visual inspection information with strong correlations (r^2 ranging between 0.70 to 0.79), thus minimizing the destructive component of the mechanical characterization related to the extraction of specimens from the timber members.

The mean percentage error found for all models are lower than 20%, with exception of the model that considered only the mean value of segments with class I. In random sampling selection, although higher correlations are found for the models that consider only a sample of class I and reduction factors between visual inspection classes, also higher mean percentage errors are found, compared with the models that assume random sampling for all classes.

This page intentionally left blank

Chapter 6

Updating of mechanical properties by Bayesian methods

ABSTRACT: This chapter addresses the possibilities of using NDT data for updating information and obtaining adequate characterization of the reliability level of existing timber structures and, also, for assessing the evolution in time of performance of these structures when exposed to deterioration. By improving the knowledge upon the mechanical properties of timber, better and more substantiated decisions after a reliability safety assessment are aimed at.

Bayesian methods are used to update the mechanical properties of timber and reliability assessment is performed using First Order Reliability Methods (FORM).

The updating data resulted from a literature database of NDT results and correlations obtained with ultrasound, resistance drilling and pin penetration equipments. The tests were conducted on chestnut wood (*Castanea sativa* Mill.) specimens, and were combined with tests to determine the compressive strength parallel to the grain. The uncertainty of the different NDT results is modelled by Maximum Likelihood estimates. Resistance distributions functions are considered to analyse the difference before and after updating by NDT. The proposed approach is then used for reliability assessment of different examples of structural timber elements and systems.

6.1 Updating mechanical properties

The accuracy on estimation of the mechanical properties of timber may be improved by carrying out a cross-validation of the information gathered by use of different NDT and SDT (Drdáký *et al*., 2005; Hanhijärvi *et al*., 2005), and also its correlation with destructive tests (Calderoni *et al*., 2010).

In addition to the difficulties in assessing existing timber elements, high variability in the mechanical and physical properties of wood occur due to the influence of natural growth defects, such as knots and fiber misalignment. This variability combined with the uncertainty of NDT results makes structural assessment based on full probabilistic methods (reliability methods) desirable. Probabilistic models for timber have been proposed by several authors (Faber *et al*., 2004; Köhler *et al*., 2007) and are implicitly defined in various codes and guidelines. The resistance models found on those codes may be considered as initial information when new and more complete data are available, as instance from mechanical tests results. In that case, it is stated that is possible to update the mechanical properties of timber (CEN, 2002; JCSS, 2006).

In an existing building, estimates from the design models can be replaced by information gathered in the actual structure allowing for better maintenance, repair and strengthening (Dietsch and Kreuzinger, 2011). The assessment of existing timber structures performance is dependent on the capacity to evaluate the physical and mechanical properties of structural timber elements, thus the interest in updating the material properties by use of visual inspection and NDT.

A grading methodology based on visual inspections associated with NDT results is a suitable source of information for updating stochastic models and, thereby, the probability of failure. For that purpose, Bayesian methods are often applied to include new information into the probabilistic assessment due to their simplicity of use and possibility of expressing different degrees of belief to a given information in form of probability distributions (Beck and Katafygiotis, 1998; Katafygiotis and Beck, 1998; Vanick *et al.*, 2000). Bayesian methods allow quantifying the uncertainty related to the estimated parameters, regarding the physical uncertainty of the variables, as well as the statistical uncertainty of the model parameters and the model uncertainty of the applied mathematical model.

6.2 Methodology

The present chapter aims at discussing the influence of NDT data in the reliability assessment of existing timber structures when using initial information together with new information. By improving the knowledge upon the mechanical properties of timber elements, it is aimed to allow for better and more substantiated decisions after a reliability safety assessment (Figure 6.1). It is noted that in most cases, the application of more data will result in a higher updated reliability (due to conservative designs), but in some cases,

where the prior information was too optimistic, a lower reliability may be the result. However, in both cases decisions on further inspections / repairs can be made on a better and more informed basis.

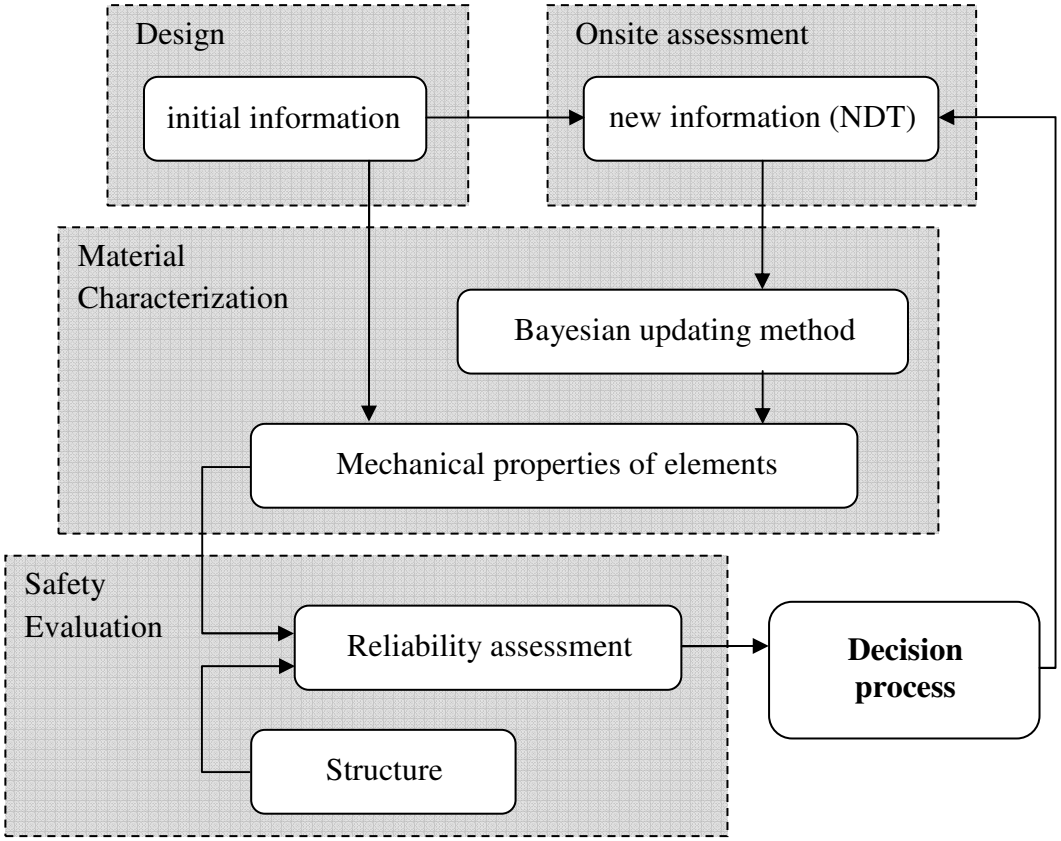

Figure 6.1: Flowchart of decision process accounting new information.

Regarding the proposed methodology in Figure 6.1, the prior information should consider the existing structure design at its initial condition. For that assessment, information about the structure may be given directly from the designer's structural plans, calculations and/or material specifications. However, not always this information is available and therefore, indicative values may be found for material properties in standards, often based on semi-empirical information, and from a geometrical survey. This first analysis is important in order to establish initial information on the structural behaviour and level of reliability. Here, it is proposed to assess first the design phase using the ultimate limit state equations in standards, such as Eurocode 5 (CEN, 2004). Indicative material properties are obtained from the PMC (JCSS, 2006) and EN 338 (CEN, 2009) for probabilistic and semi-deterministic reliability analysis.

In this chapter, the data selected for new information correspond to the database collected in Feio *et al.* (2007). This database was considered due to the moderate and strong correlations that were found between NDT and compression parallel to grain stiffness and strength. In addition, that study only considered the analysis of clear wood, which therefore corresponds to the material wood level. The combination with visual inspection results (detection and characterization of defects), was determined in the

previous chapter for prior prediction of a reference property, whereas the updating of the mechanical properties by Bayesian methods accounting visual stress-grading will be considered in the next chapter.

In the updating process, the procedure described in Chapter 2[6] and exemplified in Annex A is considered, and uncertainties of NDT methods are modelled through Maximum Likelihood where the estimates are included in the reliability assessment.

In the reliability assessment, FORM are used accounting different structural systems. The reliability analysis using FORM was performed with PRADSS software (Sørensen, 1987).

When evaluating the reliability level of an existing structure, it is important to assess which are the most likely failure modes and to identify which are the key elements. A key element is such that, if failing, would result in extensive failure or progressive collapse of the structure. Therefore, data regarding these elements will prove more important in an updating scheme, since the information will directly change the reliability level of the structural system. After determining the key elements of a structure, the failure sequences must be defined. In this case, a failure sequence corresponds to the succession of individual element failures that will produce a system failure. The probability of failure of a structure is determined by the difference between the resistance distribution (capacity) and the load effect distribution (demand). If the structure can be modelled by a series system, then the failure of one (key) element implies the failure of the system. Using a FORM approximation to assess the structural reliability, the safety margin concept of Equation 2.11 (see Chapter 2) is extended to the consideration of a safety margin, M_i, which is assumed to be formulated for each of the m failure modes (Madsen *et al*., 1985), as:

$$M_i = g_i(X) \quad , \quad i = 1, 2, ..., m \tag{6.1}$$

where $g_i(X)$ is the failure function related to failure mode i. The uncertain parameters are modelled by the stochastic variables X.

The probability of failure of the series system, p_f^S, is defined by:

$$p_f^S = P\left(\bigcup_{i=1}^{m}\{M_i \le 0\}\right) = P\left(\bigcup_{i=1}^{m}\{g_i(X) \le 0\}\right) \tag{6.2}$$

If the structure or a part of it can be modelled by a parallel system (*e.g.* a sequence of elements whose failure implies failure of the structure), then all n elements have to fail before the failure of the system. In this case the probability of failure, p_f^P can be estimated by:

$$p_f^P = P\left(\bigcap_{i=1}^{n}\{M_i \le 0\}\right) = P\left(\bigcap_{i=1}^{n}\{g_i(X) \le 0\}\right) \tag{6.3}$$

[6] Chapter 2, topic 2.3.3: Data updating methods

6.3 Updating data source

The results from NDT, namely, ultrasound, resistance drilling and pin penetration testing, conducted upon chestnut wood (*Castanea sativa* Mill.) specimens are used as new information in a Bayesian updating process. In Feio *et al.*, (2007), these results were correlated with compression parallel to the grain, $f_{c,0}$ (Figure 6.2).

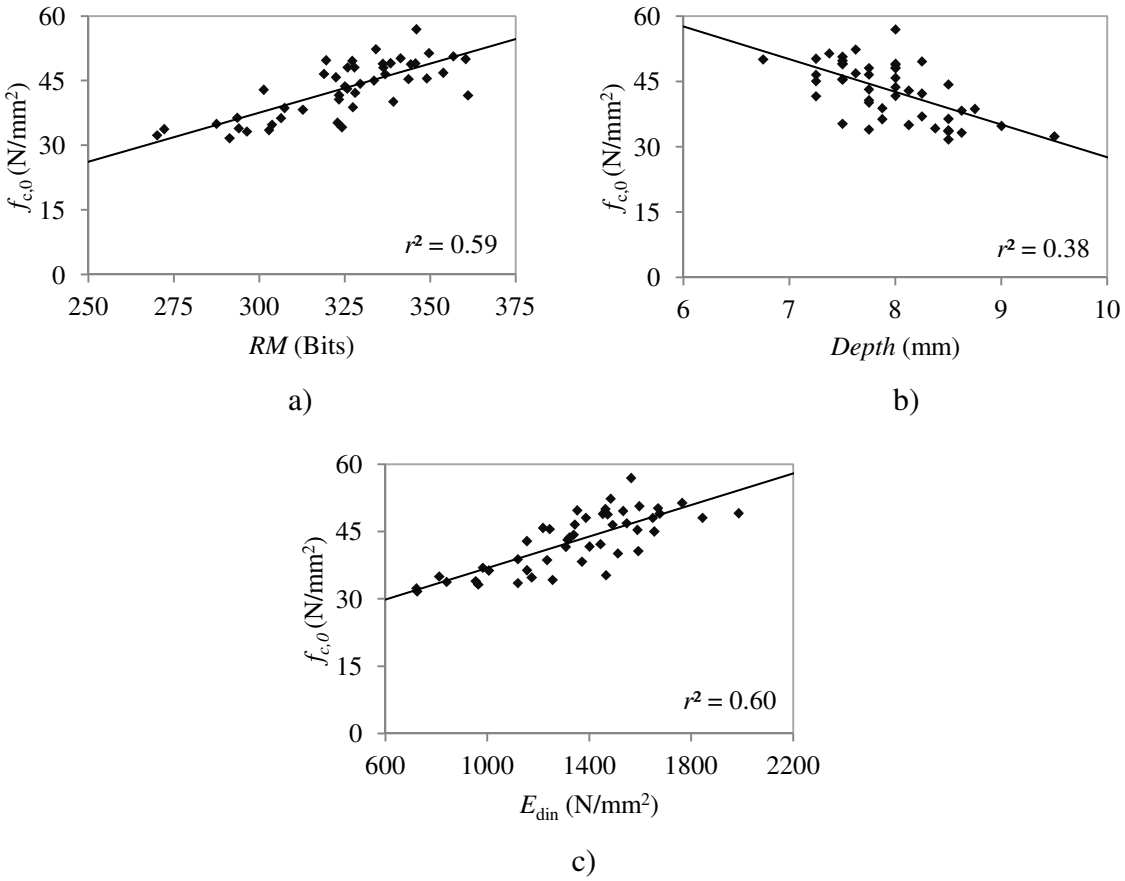

Figure 6.2: Correlation information between $f_{c,0}$ and NDT results for chestnut wood (adapted from Feio *et al.*, 2007): a) resistance drilling; b) pin penetration; c) ultrasound.

The uncertainties associated to the NDT methods are modelled and included in the reliability assessment through a Maximum Likelihood fit of the parameters using a linear regression model (Faber *et al.*, 2004) (method described in Annex D) of the dependency between $f_{c,0}$ and the considered indicator. In this case, α_0 and α_1 are the regression parameters and the model uncertainty is modelled by ε assuming that it follows a normal distribution with expected value zero and unknown standard deviation σ_ε. The regression parameters for the dependency between $f_{c,0}$ and the NDT indicators are provided in Table 6.1.

Table 6.1: Regression parameters and lack-of-fit standard deviation for the NDT results as a dependency of the compression strength $f_{c,0}$.

Test	units	α_0	α_1	σ_ε
Resistance drilling (*RM*)	(Bits)	-30.695	0.228	4.122
Pin penetration (*depth*)	(mm)	102.592	-7.507	5.124
Ultrasound (E_{din})	(N/mm^2)	19.247	0.018	4.061

6.4 Analysis of single element structures

The use of Bayesian data updating is now exemplified to define a reliability based assessment of existing timber structures considering the information given by NDT. Two examples are considered accounting individual members of a given timber structure, studied as single elements.

The first example consists of a simply supported beam, of solid timber, with rectangular cross section, with height h and width b. The loads are assumed uniformly distributed along the beam length, l (Figure 6.3).

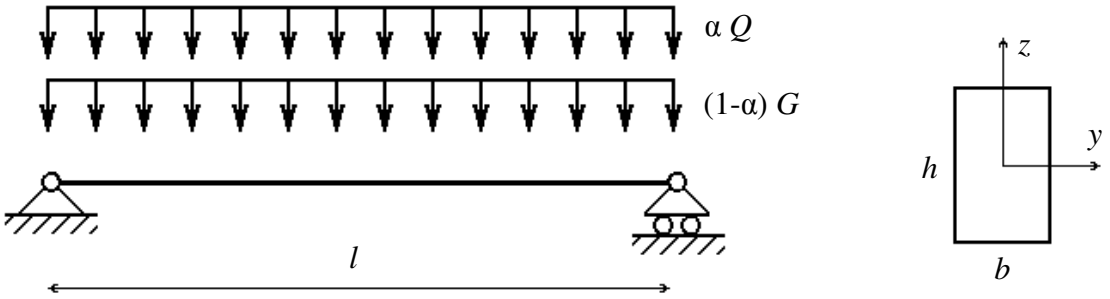

a) b)

Figure 6.3: Single supported beam: a) structural model; b) cross section.

The second example consists of a bottom clamped column with a square cross section (size b) and length l_s. The loads are modelled as concentrated loads applied at the top of the column (see Figure 6.4).

The load combination, in both examples, is defined by:

$$S = (1-\alpha)\cdot G + \alpha \cdot Q \tag{6.4}$$

where G is the permanent load and Q is the variable load (live load in this case), α is a factor between 0 and 1 modelling the fraction of variable and permanent load. Aiming to investigate the effect of the variable actions, a similar procedure for load combination is adopted by Honfi *et al*. (2012).

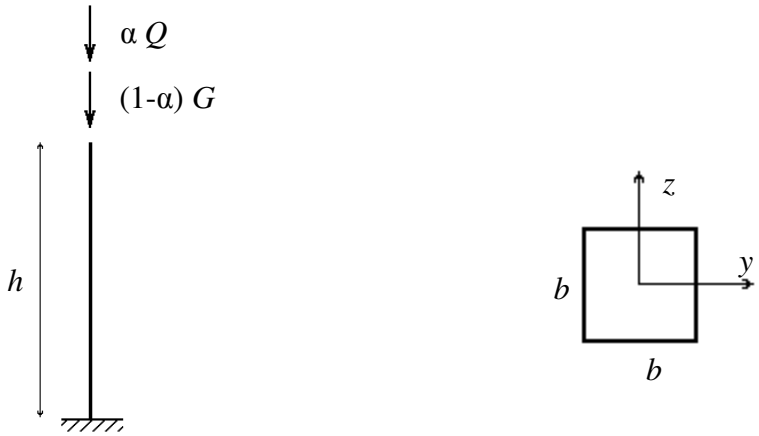

Figure 6.4: Bottom clamped column: a) structural model; b) cross section.

For the reliability verification of structures, limit state equations are required, which in this study were defined with reference to EN 1995-1-1 (CEN, 2004) with the necessary changes for a probabilistic analysis. The modification parameter regarding the effect of load duration and moisture content of timber, k_{mod}, is considered for the load with smaller duration. After the reliability assessment in design phase, the definition and influence of different climatic zones on decay models and the reliability throughout time are studied. Finally, reliability updating using the resistance drilling test data with different levels of belief and reliability updating using the correlations between NDT and mechanical tests are carried out.

6.4.1 Simply supported beam

In a simply supported beam with uniform loading the limit state equation, as formulated in Melchers (1999), can be written:

$$g = \frac{1}{6} \cdot b \cdot h^2 \cdot k_{\text{mod}} \cdot f_{\text{m}} - \frac{1}{8} \cdot l^2 \left((1-\alpha) \cdot G + \alpha . Q \right) \tag{6.5}$$

where f_m is the bending strength, G is the permanent load and Q is the variable load, α is the load fraction factor and b and h are the cross section width and height, respectively. The corresponding deterministic design equation, according to the combination of loads given by EN 1990 (CEN, 2002), considering the height, h, of the cross section as the design parameter, can be written as:

$$\frac{1}{6} \cdot b \cdot h^2 \cdot k_{\text{mod}} \cdot \frac{f_{\text{m,k}}}{\gamma_{\text{m}}} - \frac{1}{8} \cdot l^2 \left((1-\alpha) \cdot G_{\text{k}} \cdot \gamma_{\text{G}} + \alpha . Q_{\text{k}} \cdot \gamma_{\text{Q}} \right) \geq 0 \tag{6.6}$$

where $f_{m,k}$ is the characteristic bending strength (corresponding to a 5% percentile), γ_m is the partial safety factor for material properties, G_k and Q_k are the characteristic values for permanent and variable loads, corresponding to 95% and 98% percentiles, respectively,

and γ_G and γ_Q are the partial safety factors for permanent and variable loads, respectively. Both the material and the load partial safety factors also account for model uncertainties and dimensional variations.

The used partial factors are values that provide an acceptable level of reliability (target reliability) and have been selected assuming that an appropriate level of workmanship and of quality management applies (CEN, 2002). The target reliability values are the result of a calibration process that should lead to a reliability index according to the PMC (JCSS, 2000). The reliability targets are also compatible with observed failure rates and with outcomes of cost-benefit analyses (Rackwitz, 2000).

The reliability obtained using the design requirements for timber elements subjected to bending from Eurocode 5 (CEN, 2004) is shown in Figure 6.5. The design parameter h is determined for each value of α according to Equation 6.6. The obtained reliability level (or index), β, (with reference period equal to one year corresponding to an annual probability of failure) is always above $\beta = 4$, reaching values higher than $\beta = 4.7$ for $\alpha = 0.3$.

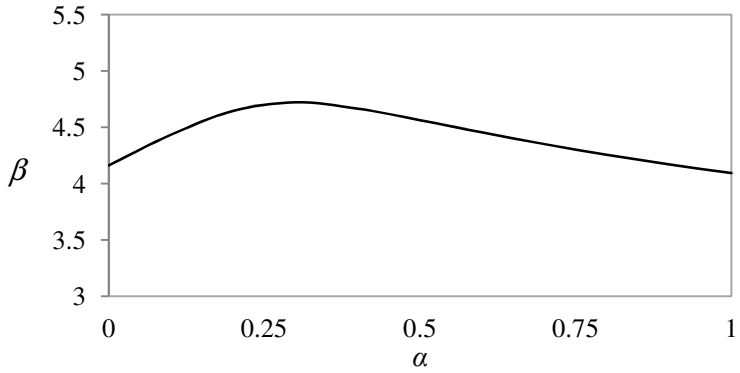

Figure 6.5: Reliability index with reference time one year for the simply supported beam with respect to design assessment with Eurocode 5 (CEN, 2004).

The presented results consider the design of any possible element with this configuration. However, when assessing existing structures, it is necessary to use the actual geometry of the structure and loading conditions. Considering a possible example, Table 6.2 shows the different variables involved in the reliability evaluation for this case.

The reliability index for different load combinations and with a fixed design parameter ($h = 400$ mm) is shown in Figure 6.6, where comparing to the initial design assessment, it is noticed that different relative fractions of load types led to lower or higher values of reliability index. In this case, it can be observed that the reliability index for lower values of α ($0 < \alpha \leq 0.60$) is higher for the existing structure, but for higher values of α, the reliability index of the existing structure is lower, which demonstrates the relevance of using a stochastic model for adequate reliability assessment.

Table 6.2: Variables used in the stochastic model for a simply supported beam (JCSS, 2006).

Variable [X]	Distribution	E [X]	COV [X]	Description	Characteristic values
f_m	Lognormal	25 N/mm^2	0.25	Bending strength	5%
G	Normal	6 N/mm	0.10	Permanent load	95%
Q	Gumbel	4 N/mm	0.40	Annual maximum live load	98%
h	Deterministic	400 mm	-	Height of the cross section	-
b	Deterministic	200 mm	-	Width of the cross section	-
l	Deterministic	6600 mm	-	Length of the beam	-

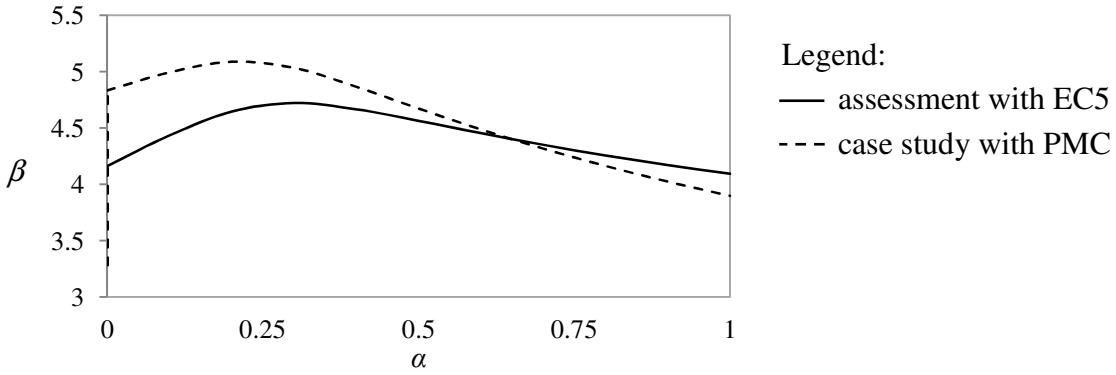

Figure 6.6: Reliability index with reference time one year for the simply supported beam with respect to design assessment with Eurocode 5 (CEN, 2004) (continuous line) and assessment of a case study using the PMC (JCSS, 2006) (dashed line).

For the case of $\alpha = 0.5$, the resistance and demand distributions curves are presented in Figure 6.7, where high reliability is denoted by the distance between curves and by the significantly small region where the demand is higher than the resistance.

At this point, with consideration to the methodology proposed in Figure 6.1, the first reliability analysis was made after definition of the mechanical properties by information of solely initial (or design) data. In order to evidence the significance of updating the mechanical properties of an existing timber member by new information, it is considered that the structure was exposed to a decay process and that NDT were made to infer about its present condition. With that aim, initially it is described the evolution of reliability in time regarding decay models with different hypothesis for climatic conditions. The definition of the different decay models that were considered, is described in Annex F.

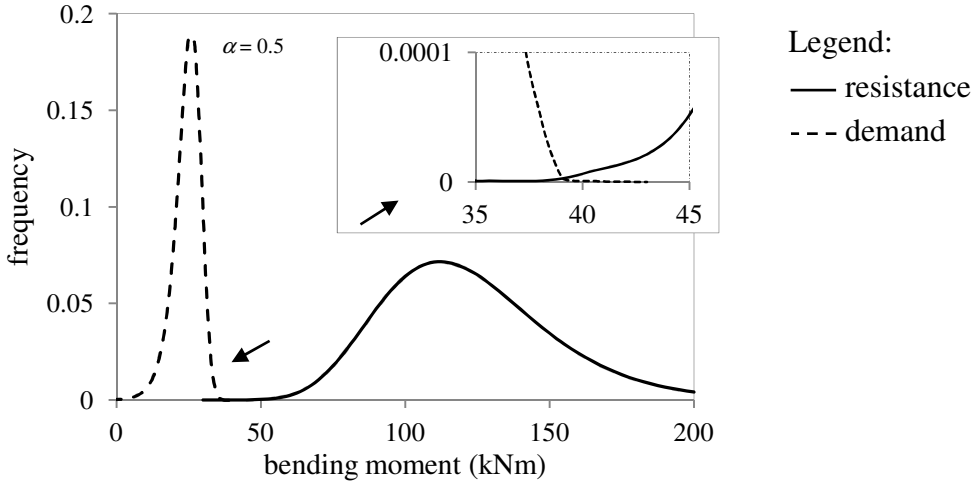

Figure 6.7: Resistance and demand distribution for the simply supported beam for the case study using the PMC (JCSS, 2006).

In order to evaluate the differences that climatic factors may have on the reliability level of a structure, an analysis is conducted varying the climatic zones, assuming the models proposed in Wang *et al.* (2008a) (climatic zones A to D, being A the less hazardous zone). The decay penetration of each model is dependent on the climatic zone and the durability class of the timber element. For the purpose of this example, durability class 1 was considered. The annual reliability indices for the different deterioration curves regarding different climatic zones are presented in Figure 6.8. A stochastic degradation model presented in Lourenço *et al.* (2013) is also used, with a lognormal distributed r with mean equal to 0.075 mm/year and COV of 0.70, which was chosen as representative of the decay agents found in South-western Europe (climate E) and local wood species. For illustrative purposes, a load coefficient $\alpha = 0.5$ is considered in all models.

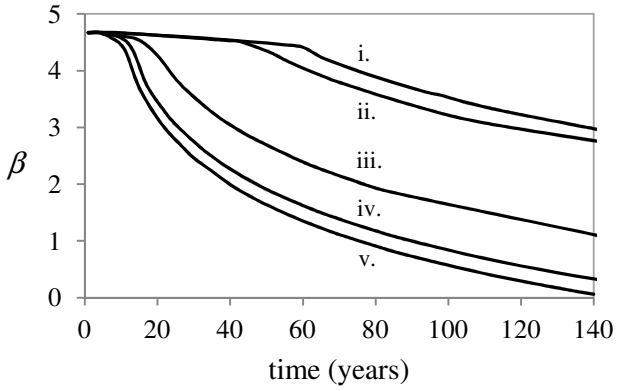

Legend (from top to bottom):

i. climatic zone E (r = 0.075 mm/year)
ii. climatic zone A (r = 0.08 mm/year)
iii. climatic zone B (r = 0.25 mm/year)
iv. climatic zone C (r = 0.41 mm/year)
v. climatic zone D (r = 0.50 mm/year)

Figure 6.8: Reliability indices evolution through time using deterioration models (Lourenço *et al.*, 2013; Leicester *et al.*, 2009) for different climatic zones.

The results evidence that the annual reliability index decreases faster when the climatic conditions are more hazardous, as the propagation of deterioration in the timber element is also faster. When comparing the different models, it is seen that the higher reliability curve is given by the stochastic model presented in Lourenço *et al.* (2013) with r = 0.075 mm/year, since it presents the lower penetration rate. The results of choosing

different deterioration models, in terms of resistance cumulative distributions, are presented in Figure 6.9, for time equal to 50 years. These distributions evidence lower values of resistance for the models which led to lower reliability levels, as the deterioration process is considered more severe for these models.

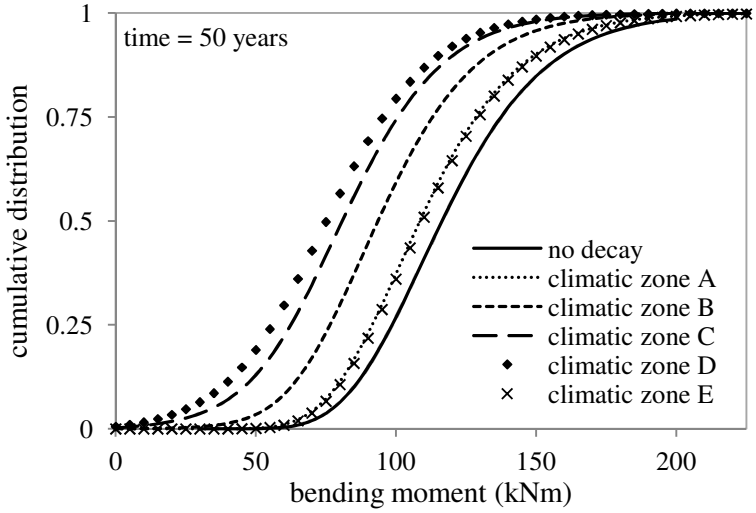

Figure 6.9: Example of the resistance distribution functions for the decay models in the simply supported beam, after 50 years.

To illustrate the advantages of using the updating scheme, an example of resistance drilling tests is used. These tests allow determining areas with different resistance to drilling, thus enabling the detection of decayed areas and the residual cross section. By assuming the loss of resistance as a consequence of decay and defining the time of exposure, it is possible to obtain the penetration rate of decay, r, with respect to the resistant area detected by resistance drilling measurements. Therefore, for each measurement of the NDT indicator it is possible to derive the residual cross section and to update the deterioration model with respect to the r parameter.

The resistance drilling tests performed on the structure are assumed to be performed in year 20. For illustrative purposes, the model that led to lower reliability in Figure 6.8, is considered and eight tests were performed obtaining different values of residual cross section (n = number of tests; m = sample mean; s = sample standard deviation) (Table 6.3).

Table 6.3: Sample of penetration rates derived from resistance drilling tests (eight cross section measurements are assumed).

	r (mm/year)								m	s
r_i	0.45	0.52	0.65	0.47	0.40	0.42	0.55	0.54	0.50	0.082
$Y_i = \ln(r_i)$	-0.799	-0.654	-0.431	-0.755	-0.916	-0.868	-0.598	-0.616	-0.70	0.160

With respect to the degree of belief in the updating data, two possibilities for prior information are considered: *i*) vague prior information on the mean value and standard

deviation equal to 0.35 and, *ii*) vague prior information on mean value and standard deviation. For vague information on mean value and standard deviation, the prior information parameters are such that:

- hypothetical sample average, m', and sample standard deviation, s', are not relevant;
- hypothetical number of observations for m', $n' = 0$;
- hypothetical number of degrees of freedom for s', $v' = 0$.

Thus, the posterior parameters become: $n'' = n = 8$; $v'' = n - 1 = 7$; $m'' = m = -0.70$ and $(s'')^2 = s^2 = 0.0256$. The predictive value of r is given by (JCSS, 1996):

$$r_d = \exp\left(m(Y)\right) \cdot \left(- t_{vd} \cdot s(Y) \cdot \sqrt{1 + \frac{1}{n}} \right) \tag{6.7}$$

where Y is the lognormal value of the sample of measurements with size n, and t_{vd} has a central t-distribution.

For the 95% quantile, $t_{vd} = -1.895$ and the predictive value for $r_d = 0.68$ mm/year is obtained with a standard deviation of 0.16 mm/year.

In a second approach, it is assumed that the information from the standard deviation of r is known to be equal to 0.35 mm/year. The prior information parameters become: m' is not relevant; $s' = 0.35$; $n' = 0$; $v' = \infty$ and the posterior parameters become: $n'' = n = 8$; $v'' = \infty$; $m'' = m = -0.70$ and $(s'')^2 = s^2 = 0.12$.

With respect to Equation 6.7, and assuming $t_{vd} = t_\infty = -1.645$ for the 95% quantile, a predictive value for $r = 0.91$ mm/year is obtained with associated standard deviation of 0.35 mm/year.

The influence of the updating process in the resistance distribution is presented in Figure 6.10, for a time of 20 years (date of inspection) and at time equal to 50 years (30 years after the inspection). In this case, the model updated with prior information presents closer reliability levels compared to the model with no updating, as the lower tail of the distributions are similar. The difference between resistance distributions for different time periods is therefore evidenced. In the case of time equal to 50 years, the lower variation for the model after updating compared to the model with no update is clear.

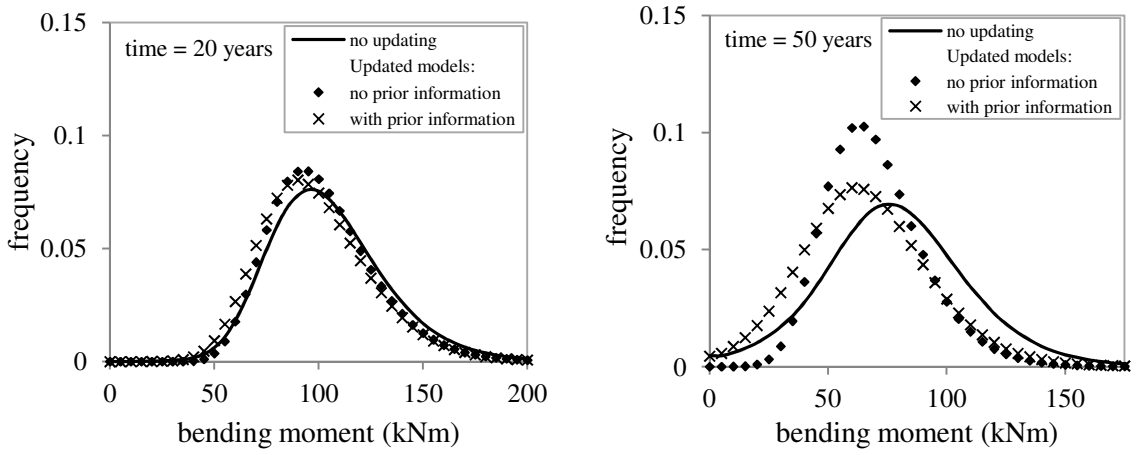

a) b)

Figure 6.10: Resistance distributions for the simply supported beam before and after updating, according to decay evolution: a) at 20 years (year of inspection); b) at 50 years.

The values for the updated stochastic model using the new information are implemented in the deterioration model, and the updated reliability is estimated again. Figure 6.11 shows the updated annual reliability indices. By calculating the probability of failure, p_f, and the corresponding reliability index, β, decisions on inspections and repairs can be initiated when the reliability index reaches a given critical threshold. Once a temporal record of β has been established, it is also possible to calculate the time when a particular value of β is reached (Moore *et al.*, 2012).

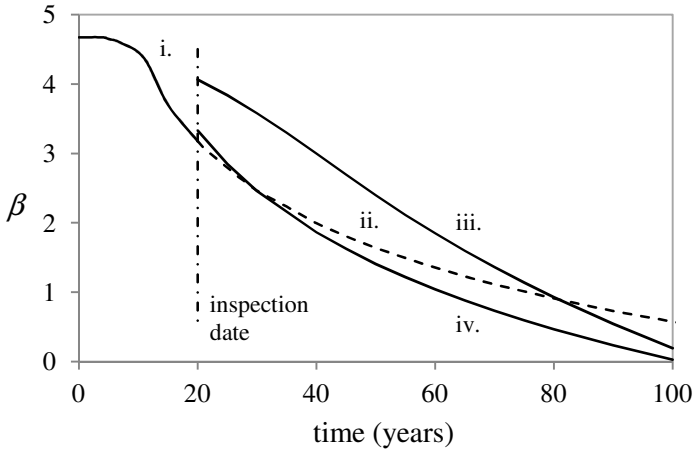

Legend: Decay models:

i. assumed before NDT information
ii. after NDT information, without updating
iii. updated model with NDT data, with no prior information
iv. updated model with NDT data with σ known

Figure 6.11: Reliability indices evolution through time with updating, using deterioration model in Leicester *et al*. (2009).

By updating the model with NDT data with uncertain information about the mean and standard deviation, an increase in the structural safety reliability values is visible compared to the expected by the decay model prediction. The differences, although significant, may be explained by different reasons in real practice, as the element may have not been exposed to extreme conditions of humidity or temperature or it might be from a higher durability class than originally assumed in the decay model. However, since an important difference between reliability values was found, and in this case may provide

unsafe reliability assessments, it is necessary to confirm the accuracy of the data with more information. From Figure 6.11, and between the two updated models, it is seen that with the model updated with σ known, it is possible to find lower values of the reliability index. The reason is that the COV in the prior information is higher than the one observed using the NDT results. From these results, two alternative conclusions can be made: *i*) in the case with vague information on the mean and standard deviation, either the information is not adequate to this specific structure and climate and thus, should be disregarded; *ii*), the number of tests is insufficient and therefore the observation sample is not adequate and should be improved with information about the standard deviation.

It is noted that results given by NDT may provide either an increase or decrease in structural safety reliability compared to the predictive models. Therefore, it is erroneous to conclude that updating a model leads to a better or worse level of safety reliability. In reality, it can only be stated that updating a model will only provide a more accurate and precise definition of the structural behaviour of a specific element or system of elements in terms of reliability.

6.4.2 Column

In a perfect column, the limit state equation is related to the maximum compressive stress along the height of the column, which by formulation of Melchers (1999), is given by:

$$g = k_{\text{mod}} \cdot f_{\text{c,0}} - \left((1-\alpha)\cdot G + \alpha.Q\right)/A \tag{6.8}$$

where $f_{\text{c,0}}$ is the compressive strength parallel to the grain, G is the permanent load and Q is the variable load, α is the load fraction factor and A is the cross section area.

Considering the area of the cross section, A, as the design parameter, the design equation, according to the combination of loads in Eurocode 0 (CEN, 2002), is:

$$k_{\text{mod}} \cdot \frac{f_{\text{c,0,k}}}{\gamma_{\text{m}}} - \left((1-\alpha)\cdot G_{\text{k}} \cdot \gamma_{\text{G}} + \alpha.Q_{\text{k}} \cdot \gamma_{\text{Q}}\right)/A \geq 0 \tag{6.9}$$

where $f_{\text{c,0,k}}$ is the characteristic compression parallel to grain strength (correspondent to a 5% percentile), γ_{m} is the partial safety factor for material properties, G_{k} and Q_{k} are the characteristic values for permanent and variable loads, corresponding to 95% and 98% percentiles, respectively, and γ_{G} and γ_{Q} are the partial safety factors for permanent and variable loads, respectively.

Based on a semi-deterministic approach using partial safety factors, the load variables are defined through their characteristic values, and the remaining parameters are deterministic. The reliability index obtained by the design of timber elements subjected to pure compression, as from Eurocode 5 (CEN, 2004), is presented in Figure 6.12 for each value of the fraction of variable load α. For this analysis the cross section area, A, of the

column should be such that buckling is disregarded (slenderness ratio $\lambda_{rel} \leq 0.3$ (CEN, 2004)).

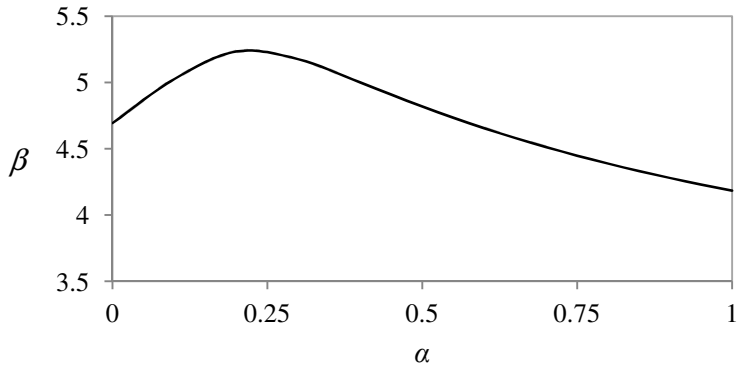

Figure 6.12: Annual reliability index with reference time one year for the column element with respect to Equation 6.9.

The obtained mean reliability index is approximately $\beta = 4.7$ ($p_f = 1.30 \times 10^{-6}$) which is higher than the suggested by JCSS (2000) for 1 year reference period and reliability class 1 ($\beta = 4.2$) but equal to the required in Eurocode 0 annex B (CEN, 2002) for reliability class RC2. Moreover, it is noticeable that this limit state equation for pure compression produces reliabilities with dependence of α similar to the simple bending limit state equation (see Figures 6.5 and 6.12). However, the reliability values obtained using the limit state equations suggested by Eurocode 5 (CEN, 2004) for design in pure compression are higher than for simple bending. Another difference is that, in this case, β for $\alpha = 1$ is much smaller than β for $\alpha = 0$.

In order to have a practical updating example, a cross section of 60×60 mm^2 is considered for analysis. The objective of this updating analysis is to have a suitable method to update the value of compressive strength parallel to the grain ($f_{c,0}$) of timber elements when NDT results are available and, also, to consider the uncertainty involved in this process. Then, a reliability analysis is conducted for evaluation of the validity of the considered correlations. This procedure aims also at analysing the influence of the uncertainty introduced by each separate NDT. Firstly, the resistance parameters of the column are implemented in the reference stochastic models considering the values for $f_{c,0}$ given by the mechanical characterization. Then, for an updating scheme, $f_{c,0}$ is determined with respect to the linear regression model obtained by the Maximum Likelihood method for each NDT.

The parameters of the models are given in Table 6.4. The two reference models for $f_{c,0}$ pretend to establish a benchmark for comparison. In the first model, the average value of $f_{c,0}$ is chosen equal to the sample average of DT with COV as proposed by JCSS (2006). In the second model, $f_{c,0}$ is modelled by the sample average and COV as obtained in the DT. For both models, lognormal distributions are assumed.

Table 6.4: Variables used in the stochastic model for a column example.

Variable [X]	Distribution	E [X]	COV [X]	Description
$f_{c,o}$	Lognormal	μ_{DT}	0.2	$f_{c,0}$ – average value of destructive tests (reference model)
$f_{c,o}$	Lognormal	μ_{DT}	$\sigma_{DT} = 0.15$	$f_{c,0}$ – average value and COV of destructive tests (reference model)
$f_{c,o}$	-	$\alpha_0 + \alpha_1 \cdot \mu_{RM} + \varepsilon$	-	$f_{c,0}$ – average value of resistance drilling tests
$f_{c,o}$	-	$\alpha_0 + \alpha_1 \cdot \mu_{depth} + \varepsilon$	-	$f_{c,0}$ – average value of pin penetration tests
$f_{c,o}$	-	$\alpha_0 + \alpha_1 \cdot \mu_{Edin} + \varepsilon$	-	$f_{c,0}$ – average value of ultrasound tests
ε	Normal	0	σ_ε	Uncertainty parameter of each NDT
G	Normal	60000 N	0.10	Permanent load
Q	Gumbel	40000 N	0.40	Annual maximum live load
A	Deterministic	3600 mm^2	-	Area of the cross section

According to the considered NDT data, three models are used with respect to each type of test. The results for the reference models and for the models updated by the correlations between $f_{c,0}$ and results from NDT are given in Figure 6.13. The results show higher values of reliability index for the models updated with NDT data. This is mainly due to the consideration of the correlation between DT and NDT used to update $f_{c,0}$. Although uncertainty is implemented through consideration of parameter ε, the variation of $f_{c,0}$ is lower than when the coefficient of variation of the reference models is used.

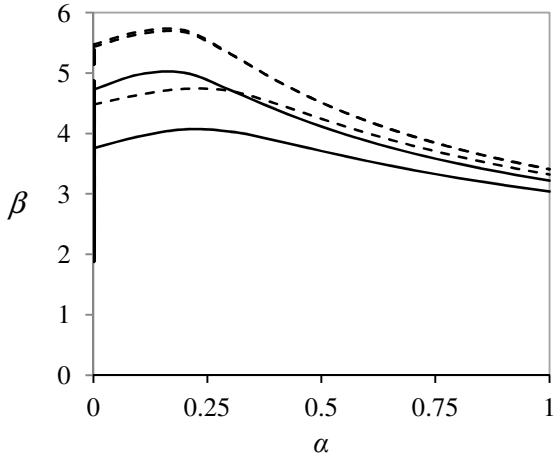

Legend (from top to bottom, in $\alpha = 0$):

Continuous line: *reference models*
$f_{c,0} = \mu_{DT}$; $COV_{DT} = 0.15$ ($\beta_{\alpha=0} = 2.39$)
$f_{c,0} = \mu_{DT}$; $COV = 0.20$ ($\beta_{\alpha=0} = 1.89$)

Dashed line: *models with NDT information*
$f_{c,0} = \alpha_0 - \alpha_1 \cdot \mu_{Edin} + \varepsilon$ ($\beta_{\alpha=0} = 3.08$)
$f_{c,0} = \alpha_0 - \alpha_1 \cdot \mu_{RM} + \varepsilon$ ($\beta_{\alpha=0} = 3.08$)
$f_{c,0} = \alpha_0 - \alpha_1 \cdot \mu_{depth} + \varepsilon$ ($\beta_{\alpha=0} = 2.60$)

Figure 6.13: Annual reliability index of reference models and updated models obtained by NDT data.

The resistance drilling and ultrasound updating schemes, which presented similar results, must be used with caution since they led to higher values of reliability than the references values. The updating scheme regarding the data from the pin penetration tests gave lower values of reliability. The main differences are found for the maximum value of the reliability curves around from $\alpha = 0$ to $\alpha = 0.25$. However, the data with respect to the pin penetration tests presented more approximated values to one of the reference models.

Figure 6.14 presents the demand distribution and the resistance distributions for the reference models and for the models after updating by NDT data, for $\alpha = 0.5$. A lower variation in the models after updating is visible with also higher expected values. As also indicated in the previously analysis, the pin penetration test data led to values closer to the reference models.

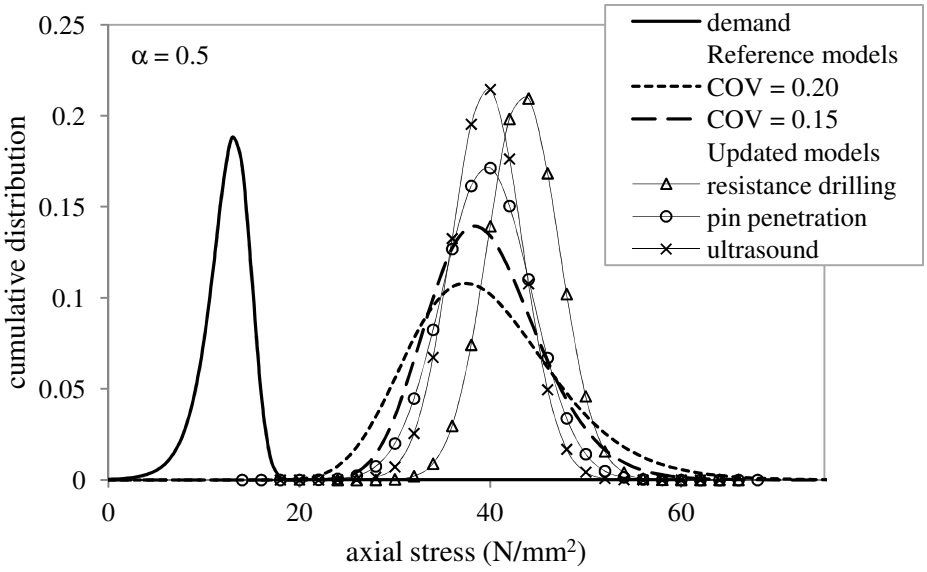

Figure 6.14: Resistance and demand distributions for the column for reference models (no updating) and models updated by NDT.

6.5 Analysis of structural system

An illustrative example of a structural system is considered for demonstration of the influence of updating an element's mechanical properties within the proposed methodology. For that purpose, a planar timber truss is considered (Figure 6.15), submitted to permanent, G, and live load, Q. Considering that the elements of this kind of structures are mainly subjected to axial stresses, three different limit state conditions are initially assumed. The limit state equations are related to tension and compression parallel to grain, and to instability due to buckling of compressed elements.

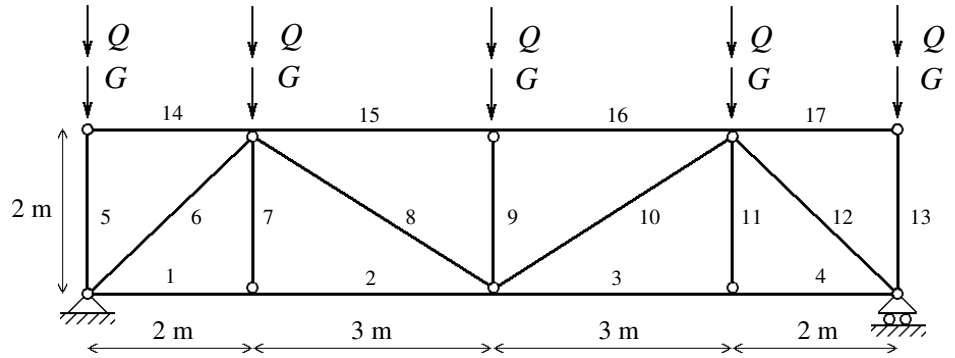

Figure 6.15: Structural model of a planar timber truss with elements' numeration and applied loading.

6.5.1 Design

Before conducting any reliability assessment, the different elements must be designed in terms of cross section dimensions. The structure is assumed to be constructed with chestnut wood, however with consideration, in the design procedure, of two different strength classes. The classes considered are D30 and D50 as given in EN 338 (2009). For both cases, the structural design respected the following hypotheses:

- tensile elements (1, 2, 3, 4, 8, 10) have 75% of the cross section used;
- compressive elements (5, 6, 9, 12, 13, 15, 16) have 95% of the cross section used, with respect to buckling verification;
- the cross sections are uniform in order to allow an easier construction process;
- the vertical elements (5, 7, 9, 11, 13) all have the same dimension, determined by the most stressed element (9);
- the chords are composed by single 10 m long elements.

These hypotheses provide that the most critical limit states are related to compression parallel to the grain, allowing the use of the previous NDT correlations as updating data. Taking into account that two different strength classes of timber were considered, for each design, different cross sections were obtained for the truss members. In the following description, each structure will be defined by D30 or D50 design, according to the used timber strength class.

In this example, failure of the lower or upper chords would correspond to the structural failure of the system, which is a series type behaviour in reliability analysis. Therefore, the chords represent key elements of the structure.

6.5.2 Reliability analysis

For the D30 design, the reliability index of the structure (reference period time of one year) for a series system is found to be $\beta = 5.18$ ($p_f = 1.11 \times 10^{-7}$) (failure of the upper chord by

instability), whereas for the D50 design the annual reliability index of the structural system is found to be $\beta = 4.64$ ($p_f = 1.74\times10^{-6}$) (failure of the upper chord by instability).

Although the reliability indices in D30 design for elements 6, 8, 10 and 12 are lower than the reliability indices of element 15 and 16, the failure of these elements does not correspond to a structural failure, whereas failure of one element of the upper chord leads to a global failure. As referred by Vrouwenvelder (2002), although the reliability targets refer to the structural system as a whole, in most cases, probabilistic design is performed at the element level. Therefore, the system failure is ruled by that particular element.

The design using D50 strength class produces lower values of reliability indices due to the assumed design considerations that defined different cross sections for each design. The reliability indices for each element regarding both designs are shown in Table 6.5.

Table 6.5: Reliability indices for each element of the truss structure with probability of failure in brackets (period reference one year).

Elements	Design	
	D30	D50
1, 4	5.22 (8.95×10^{-8})	4.95 (3.71×10^{-7})
2, 3	5.22 (8.95×10^{-8})	4.95 (3.71×10^{-7})
5, 13	10.39 ($<1\times10^{-15}$)	9.40 ($<1\times10^{-15}$)
6, 12	5.08 (1.89×10^{-7})	4.55 (2.68×10^{-6})
7, 11	*	*
8, 10	5.01 (2.72×10^{-7})	5.10 (1.70×10^{-7})
9	5.44 (2.66×10^{-8})	4.88 (5.30×10^{-7})
14, 17	*	*
15, 16	5.18 (1.11×10^{-7})	4.64 (1.74×10^{-6})

* for zero members $\beta \Rightarrow \infty$

As mentioned by Moore *et al.* (2012), in presence of degradation processes, the lifetime of components can be severely reduced. Therefore, after the evaluation of the safety level in an initial condition (design stage or present stage), also the deterioration of elements was taken into account in the evolution of reliability along time. However, when considering deterioration in a reliability analysis of a structure composed by a system of different elements, the key elements must first be found. In order to identify the key elements and the most critical limit state regarding deterioration of the timber elements, a reliability assessment was performed considering a perimetral loss of cross section, τ, for each element separately. The elements considered as key elements are those for which the influence of perimetral loss of cross section would be more pronounced corresponding to

lower reliability indices. A similar procedure is presented by Moore *et al*. (2012) in assessing the probability that a structural timber element will exceed a specific limit state as the effective cross section diameter decreases.

The key elements for each limit state are shown in Figure 6.16. The initial values ($\tau = 0$) for the most critical limit states are in accordance to usual design values. For D30, the reliability index of the key elements is $\beta = 5.01$ ($p_f = 2.72 \times 10^{-7}$), whereas for D50 the reliability index is $\beta = 4.88$ ($p_f = 5.30 \times 10^{-7}$). For the structure with D30 timber, tension parallel to grain is the most critical limit state at the beginning of loss of cross section in elements 8 and 10. However, when the reliability index values start to be smaller than 4.5 ($p_f = 3.40 \times 10^{-6}$), the most critical limit state condition is given by buckling in element 9. For D50 design, the buckling limit state is always the most critical, with element 9 as the key element. Since timber tensile behaviour is more influenced by the presence of defects than compression, tension strength parallel to grain is more sensitive to the strength class than compression strength parallel to grain. Element 9 is also considered as a key element because when weakened, or in case of failure, the stresses are redistributed to the other elements of the truss producing shear and bending stresses in the upper chord. Since the upper chord was not initially designed for that kind of stress, its reliability highly decreases and structural failure is a likely scenario. The increase of shear and bending stresses in the upper chord is mainly noticeable when elements 8, 9 or 10 are weakened.

Regarding the influence of a decay process in element 9, the structural reliability index (corresponding to the failure of a parallel system with first failure in the decayed element) would be $\beta = 6.28$ ($p_f = 1.69 \times 10^{-10}$) and $\beta = 5.90$ ($p_f = 1.82 \times 10^{-9}$) for D30 and D50 design, respectively. In D30 design, failure of element 9 by instability would be followed by the failure of the upper chord by shear. In D50 design, the failure of element 9 by instability would be followed by failure of the upper chord by lateral torsional instability.

For illustration of the applicability of an updating process regarding NDT information and its use in the assessment of evolution in time of performance regarding the key elements of an existing timber structure, the data obtained by the Maximum Likelihood estimates given in Table 6.1 are considered as example data to update the reliability of the truss system. In this case, the NDT data does not intend to replace the strength grading provided by EN 338 (CEN, 2009), but to be considered as possible new information given by an onsite evaluation. Therefore, the cross section geometry is taken from the design procedures, however $f_{c,0}$ is updated by the NDT information.

For illustration purposes, the truss designed with D50 strength class was analysed considering the information given by the pin penetration tests. D50 design was considered because the data from the NDT in Feio *et al*. (2007) correspond to results obtained from small clear specimens that are better compared to higher strength grading classes, where lower percentages of defects are admissible. The data from the pin penetration tests was considered due to its better fit found in the assessment of the single column element (see

Figure 6.13) when compared to one of the reference models that considered the data from the DT.

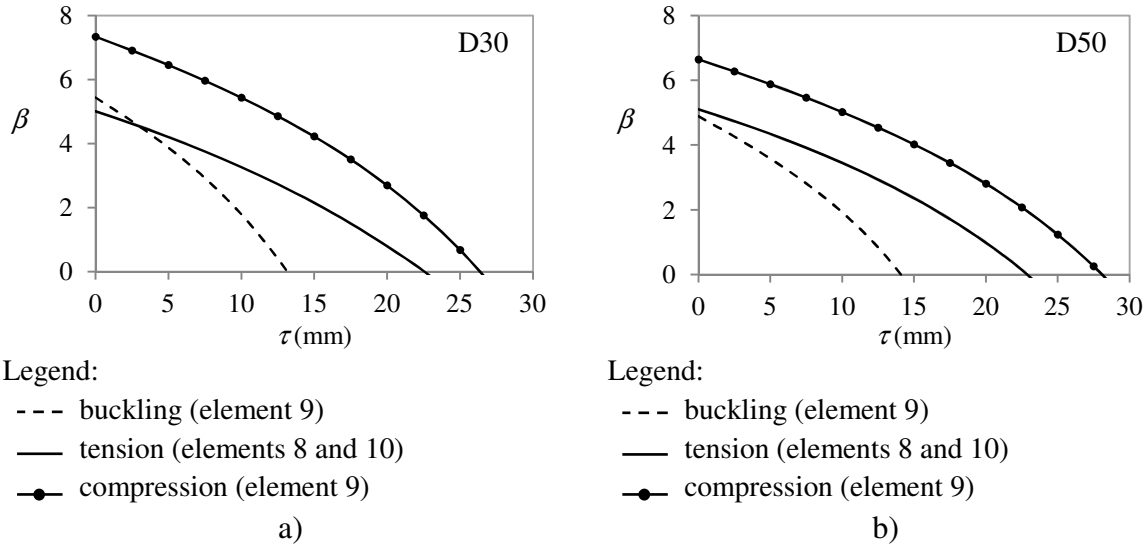

Figure 6.16: Annual reliability index with respect to perimetral loss of cross section for the limit state conditions of buckling (element 9) – dashed line, tension (elements 8 and 10) – continuous line, compression (element 9) – dotted line, in: a) D30 design; b) D50 design.

In order to analyse the safety reliability assessment and updating process, the demand and resistance distributions curves are exemplified for element 9 according to the most conditioning limit state in this case (instability by buckling) (Figure 6.17). To that aim, resistance curves for D50 design without updating and the results of the updating process with the pin penetration tests, are considered. In this case, the updating process led to higher values of resistance with lower variation, and therefore an increase in the safety reliability level was obtained.

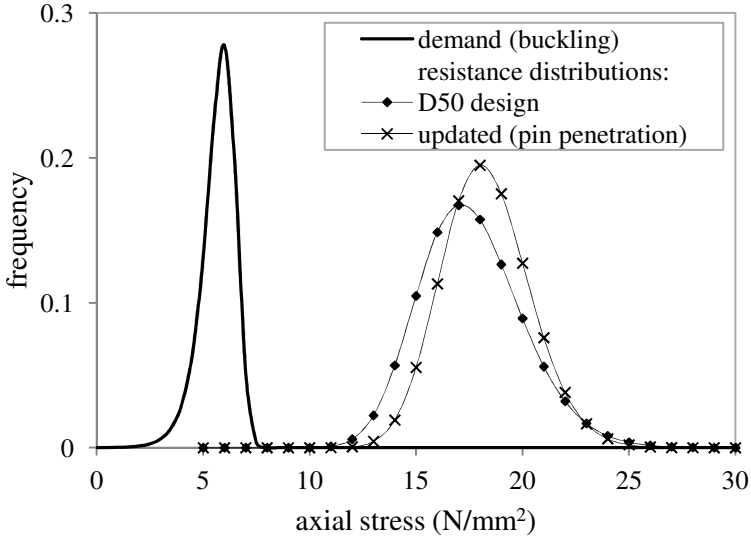

Figure 6.17: Resistance and demand distributions (buckling limit state) for element 9 of the truss for D50 design and model updated by pin penetration test data.

6.6 Final remarks

When discussing the behaviour of single element structures, it was shown how it is possible to update decay model parameters by use of NDT data through Bayesian methods. In this approach, different degrees of belief in the updating data resulted in significant differences in the evolution of the reliability analysis. Moreover, regarding existing correlations from a database of NDT and laboratorial tests, the compressive strength parallel to grain of chestnut elements was determined using linear regression models obtained by Maximum Likelihood estimates, allowing the modelling of the uncertainty of each NDT.

Uncertainty related to physical parameters, as strength and geometric parameters, were considered in the reliability assessment. For compressive strength parallel to the grain, a Bayesian stochastic model is applied, where at a design stage the prior model is used for reliability assessment. In this chapter, additional indicators are used to obtain the measured values for the physical variables. This introduces an additional model uncertainty which was estimated through the Maximum Likelihood method. For the reassessment stage, where data from NDT is available, the posterior model is used conditional to the measured values. Therefore, the reliability level could be both larger and smaller depending on the considered data, concluding that the objective of NDT data updating is to allow a better understanding of the characteristics of the structural elements, particularly with respect to the key elements of the structure, and to allow a more precise safety assessment. Epistemic uncertainty regarding statistical and measurement uncertainties, can also be implemented to the applied Bayesian model, however were not considered in the presented analysis.

Using NDT information as updating data in a probabilistic analysis, the results given by the pin penetration tests were similar to the reference experimental model with mean value and COV given by the results of the laboratorial tests. The resistance drilling and ultrasound updating schemes led to higher level of reliability than the reference model values, therefore these updating data should be considered with caution, as they can result in unsafe results for the reliability in comparison to the reference models.

In the truss structure example, the same design hypotheses led to different reliability levels regarding different timber strength classes. Identification of the key elements according to the type of load / action was demonstrated to be a fundamental step in order to understand the level of reliability of an existing structure. The compressive strength parallel to the grain was updated by use of NDT data and a revaluation of the reliability assessment was made.

Chapter 7

Hierarchical modelling: Use of Bayesian Probabilistic Networks

ABSTRACT: The information gathered in the experimental campaign is hierarchically modelled by use of Bayesian Probabilistic Networks, accounting for different sources of information (visual and mechanical grading) and different size scales. The objective is to infer on chestnut timber mechanical properties, namely bending stiffness and strength, by a framework that allows to incorporate the influence of visual grading, on both scales (micro and meso), and mechanical grading of smaller size scale specimens on the probabilistic models of structural size timber beams' mechanical properties, and to update these models with new information. Thereafter, this framework is formalized in a safety assessment example contemplating different prior information and the updated results retrieved from the Bayesian Probabilistic Networks.

7.1 Data for the networks

Taking into account distinct sources of information and the variability of the reference properties that influence the correlation to other mechanical properties of timber, it is useful to hierarchically model the problem at hand by defining the different situations or characteristics that allow to obtain information about the target result. Such a hierarchical approach, proves to be beneficial as means to provide information about a complex structural system by knowledge solely from information of the material and element scales and their relation to the system. To that aim, the use of visual inspection combined with information of local MOE in bending in small scale samples has been considered to predict the stiffness and strength properties of full size scale members, in this chapter, by use of Bayesian Probabilistic Networks (BPNs).

The variability of stiffness properties within an individual board was studied by several approaches as in Kline *et al*. (1986), Taylor and Bender (1991) and Aicher *et al*. (2002), while in Fink and Köhler (2011) and Sousa *et al*. (2012), special attention was given to the influence of defects in stiffness. Also, through the analysis of results found in the experimental campaign previously described in Chapter 3, it was noticed that the partition of results of bending MOE with consideration to visual strength grading allowed to obtain samples with significant statistic variation values between them.

The within element variability of strength was studied in the works of Czomch *et al.* (1991), Isaksson (1999) and Köhler (2007) regarding the subdivision of the timber elements in sections with or without major knots and knot clusters. Regarding the analysis of bending strength, f_m, it is patent that timber failures are more prone to take place in weak sections corresponding to sections with significant defects (or neighbouring sections), as previously evidenced in Chapter 3 and Chapter 4.

The results presented in Chapter 3 are considered as initial data for the construction of the hierarchical levels and its interrelationships within the BPN. The considered BPNs are defined by discrete nodes and the inference engine of Hugin (2008) was applied to build the network and to calculate the marginal probability values, for both BPNs for quantification of bending stiffness and strength. The probabilities within each BPN are updated through Bayes' theorem regarding the belief propagation within the arrangements of nodes of the different considered BPNs.

The results were modelled by posterior probabilistic distribution parameters, accounting the results of MLE and χ^2 tests initially performed to the global sample (see Chapter 4). Attending to the obtained results and according to PMC (JCSS, 2000 and JCSS, 2006) recommendations, lognormal distributions are assumed to represent the underlying results obtained from the BPN, for both MOE and f_m, accounting to different levels of evidence. The results of the data inference of the BPNs were then used in the verification of ultimate and serviceability limit state functions for the example of a simply supported beam.

7.2 Bayesian Probabilistic Networks

7.2.1 Bending stiffness networks

Firstly, BPNs are used to infer on MOE in bending by information regarding the structural size, *S*, and visual grading, *VI*. The states of *S* consider results in beams, S_B, and in boards, S_b, while the states in *VI* correspond to the different visual grades (I, II, III and NC). In other words, subscripts *B* and *b* correspond to the beams tested in Phase 2 and to the boards tested in Phase 3, respectively.

Visual grading was considered as parent node in the following analysis, as it provides a link between scales and, also is commonly an available parameter in the assessment of existing timber structures. The relationship between visual grading in different size scales (Phases 2 and 3) is confirmed in Figure 7.1, especially for extreme classes (class I and NC). In this case, a higher percentage of boards with VI_b = I is found for beams with VI_B = II, decreasing progressively as the visual grading in beams also decreases. The higher percentage of segments with VI_b = NC is found for beams with VI_B = NC.

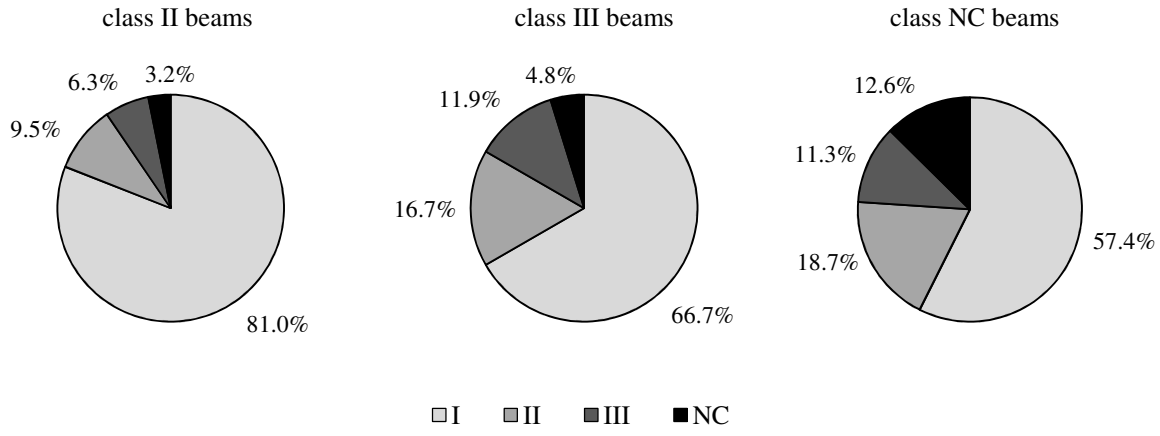

a) b) c)

Figure 7.1: Percentage distribution of boards visual grading given the visual grade in beams with: a) class II; b) class III; c) class NC.

Simple converging BPN

The first BPN serves as a direct representation of the experimental results obtained in the 4-point bending tests, having *S* and *VI* as parent nodes, in a simplified converging model (Figure 7.2), and therefore, aims at validating the possibility of use of these parent nodes as prior information on the inference of MOE in bending. The results of MOE in bending, regarding each state of the parent nodes, are defined in discrete intervals in the child node through the calculation of the conditional probability tables. Intervals of 2000 N/mm^2, starting from 0 and up to 32000 N/mm^2 are considered for the discrete representation of the child node MOE. This first BPN is repeated so as to consider for results either from local, $E_{m,l}$, or global, $E_{m,g}$, MOE.

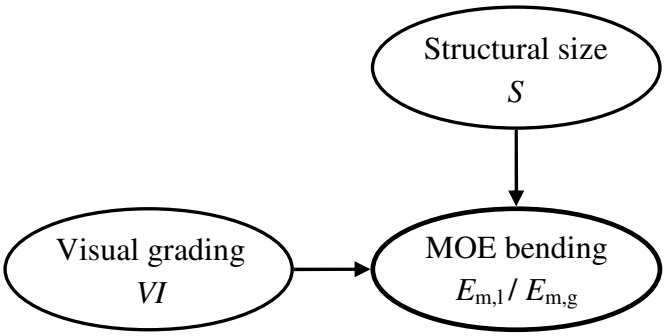

Figure 7.2: Simplified converging BPN model, for experimental data validation in the inference of MOE in bending.

Firstly, the results of the simple converging model with parent nodes *S* and *VI* are considered, with different levels of evidence, in Figure 7.3. The results regarding the inference of local and global MOE are considered in terms of cumulative frequency of the posterior updated probability tables of the respective discrete functions. Moreover, information about the histograms of the relative frequency are provided for each level of prior evidence. It should be noted that, as no beam was graded with class I, information about the probability distribution is not reliable when updating with prior evidence such as $VI = \text{I} \cap S = \text{beam}$ and, thus in the present case, should not be considered for reliability assessment.

A well defined differentiation of results regarding different visual grades is noticeable, when inferring on the posterior stiffness distributions for either board or beam. Evidence entered as *VI* = III or *VI* = NC, when *S* = board, propagates to a posterior distribution for either E_{m,l_b} or E_{m,g_b} with higher frequency values for lower levels of stiffness comparing to the case without evidence in *VI*. On the other hand, for the same conditions but considering *VI* = I, higher frequency values are found for higher levels of stiffness. In this case, evidence entered as *VI* = II provides similar cumulative frequency distributions compared to the prior distribution without evidence in *VI*. For the beam scale, which means *S* = beam, also a clear separation between frequency distributions of different *VI* is found for the case of $E_{m,l\_B,}$ however less defined in the case of E_{m,g_B}. In either case, lower values of stiffness are present comparing to the prior distribution without evidence in *VI*, mainly after cumulative frequency of approximately 12.5%. The shift of all posterior distributions to one side of the cumulative frequency distribution of the prior distribution, in the case of the beam scale, especially noted in the tails of the distributions (frequency values below 10% or above 90%) is found due to need of considering a constant residual frequency for *VI* = I for enabling the evidence propagation algorithm.

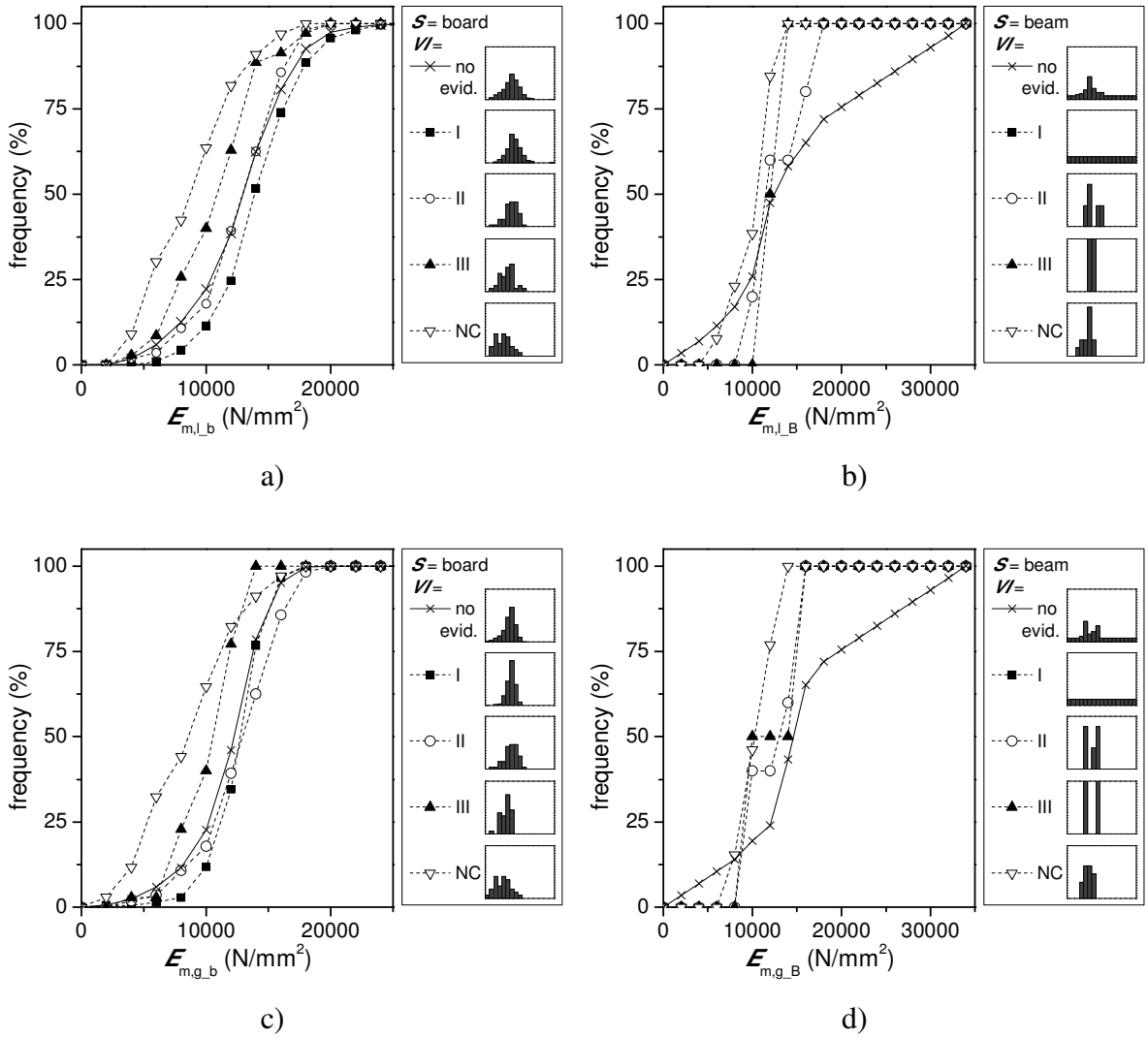

Figure 7.3: Cumulative frequency results for local and global MOE in bending obtained from the converging BPN with evidence in scale and visual inspection: a) $E_{m,l}$ in boards; b) $E_{m,l}$ in beams; c) $E_{m,g}$ in boards; d) $E_{m,g}$ in beams.

Double visual grading node converging BPN

As the complexity of the BPNs are increased, by introduction of new nodes or by rearrangement of the existing ones, graphical indication is given regarding the size scale of the elements and of the different tests, so as to define the hierarchical interrelationships between nodes. In this light, the BPN is modified to differentiate between visual inspections made to the timber element at different scales. It is important to highlight the visual grading made to different scales as it is commonly found that, due to the high variability in timber, a knot or cluster of knots (or any other relevant defect) may be confined to a section or segment, leaving the neighbouring sections unaffected, and thus the visual grading of the element as a whole may be conservative regarding the clear wood segments that may be found along its length.

Initially, the division of visual grading by scales is considered in a converging BPN, thus considering an independent relationship between visual grading at different size scales (Figure 7.4). For this BPN, prior information on a visual inspection scale will not change the marginal probabilities of the visual grading states in the other scale.

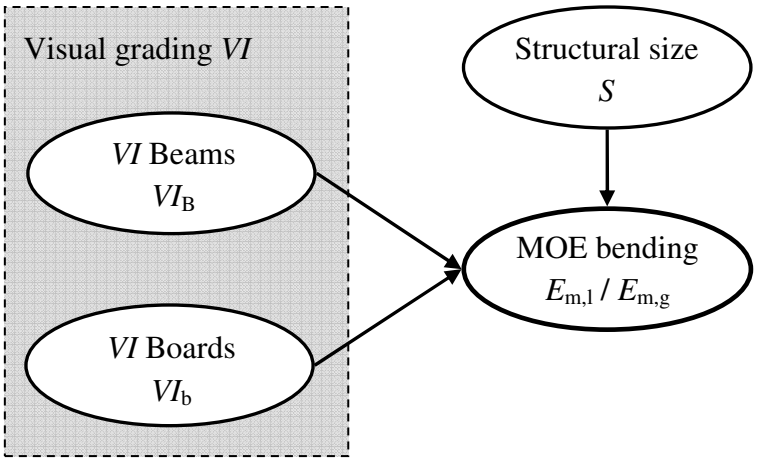

Figure 7.4: Converging BPN model with two nodes for different size scales in visual grading, for inferring the MOE in bending.

The division of visual grading by different size scales allowed a better definition of states within parent nodes VI_b and VI_B, which, in the present case, was of special interest as no beam was graded as class I. Therefore, by this division it was possible to assume the states I, II, III and NC for VI_b, whereas only the states II, III and NC were assumed for VI_B. The results from the division of the parent node *VI* in two nodes with consideration to the visual grading in different size scales, VI_B and VI_b, in a converging BPN are presented in Figure 7.5 for evidence of *S* = beam and in Figure 7.6 for evidence of *S* = board.

The results regard every possible combination when evidence is given simultaneous to both visual inspection scales (evidence in VI_B and VI_b). In each graph, for a given size scale and visual grading of the same scale, comparison is made between cumulative frequencies corresponding to different evidences in visual grade in the other scale. For all cases, indication of the posterior probabilities are also provided by graphical representation in the form of histograms, allowing an easy understanding of the decrease in value of the mechanical property in study, when either or both visual gradings in different size scales, tend to lower grades.

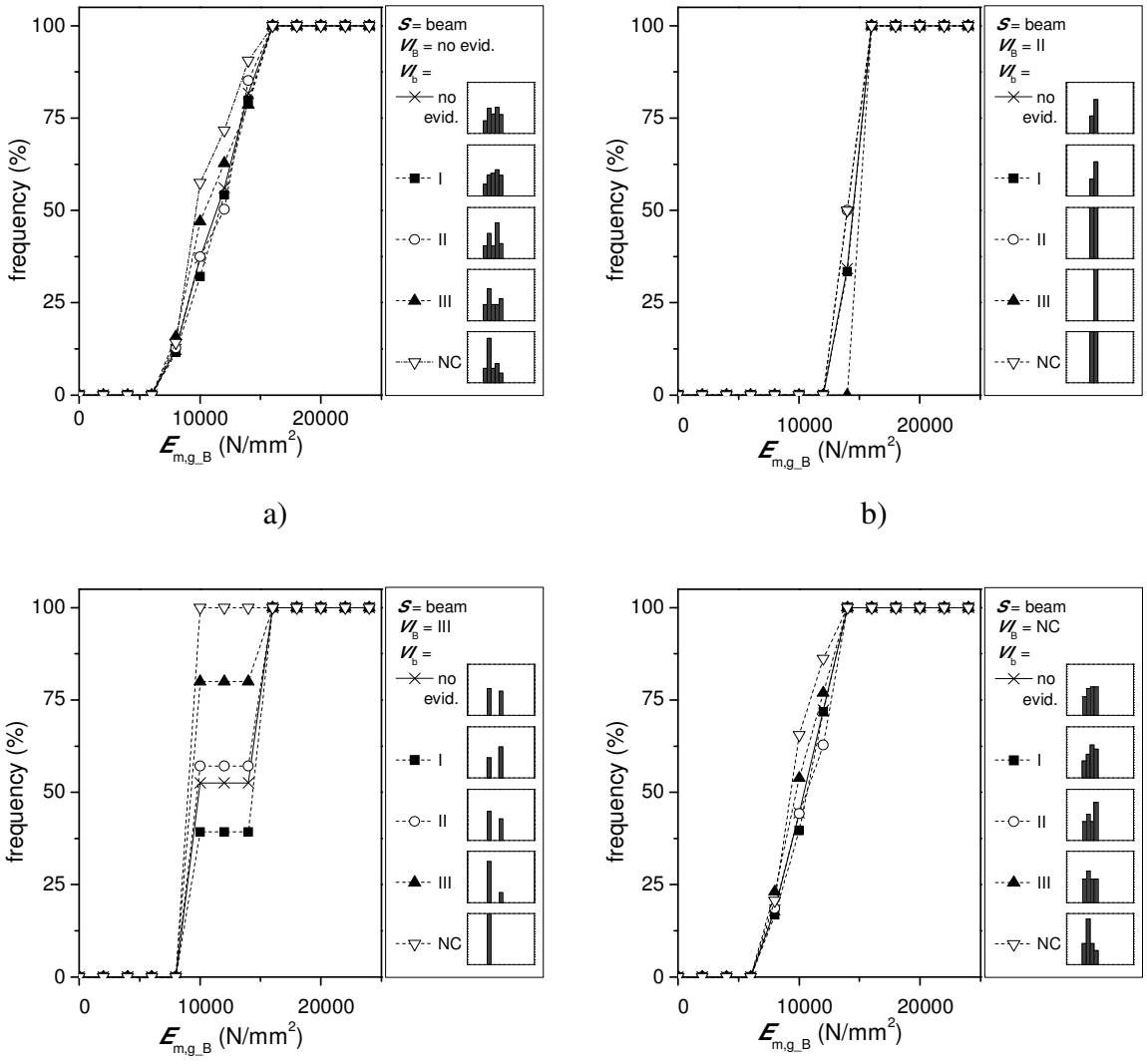

Figure 7.5: Cumulative frequency results for $E_{m,g}$ in beams with different evidence in visual inspection of boards and information about visual inspection of beams as: a) no evidence; b) class II; c) class III; d) class NC.

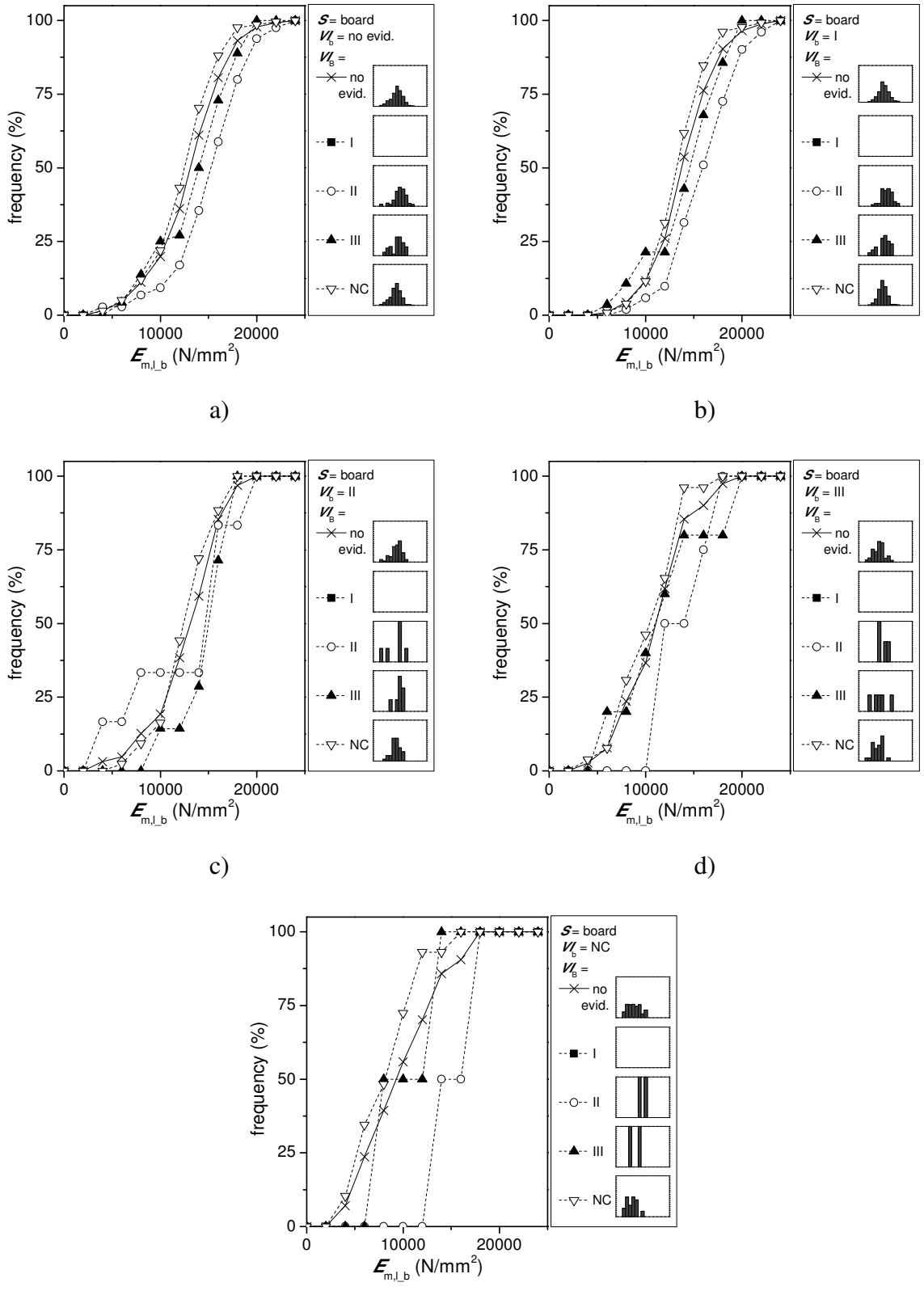

Figure 7.6: Cumulative frequency results for $E_{m,l}$ in boards with different evidence in visual inspection of beams and information about visual inspection of boards as: a) no evidence; b) class I; c) class II; d) class III; e) class NC.

Double visual grading node series BPN

In the BPN represented in Figure 7.4 it is assumed that visual inspection made to different scales are independent events however, since the sawn boards were retrieved from the beams, a logical relation should be assumed. With regard to this premise, a series connection is considered between visual grading in different scales, before converging to the child node which infers the MOE in bending (Figure 7.7).

The order, in which the visual grading nodes are arranged, depends on the aim of the study and available data. If only a visual grading was made to the structural size beams, for instance as in a visual inspection made to an existing timber element on a construction site, and the study aims at analysing the possibility to use segments or regions with good mechanical properties, even if the overall inspection made to the timber members indicated lower mechanical properties, the first parent node should correspond to the visual grading in the sawn beam scale and after directed to the smaller scale visual grading. On the other hand, if visual inspection was made to small segments or performed continuously along the length of an element, such as in machine strength grading, thus obtaining a localized visual grading, and the study aims at quantifying the global mechanical properties of structural sized members, then the first parent node should correspond to the visual grading made to the smaller elements.

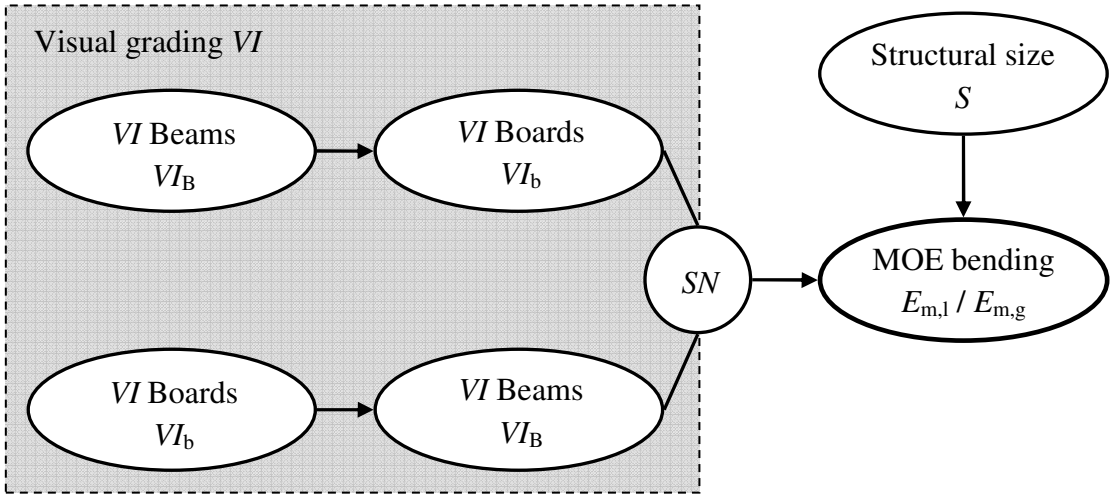

Figure 7.7: BPN model with series connection in visual grading of different size scales, for inferring the MOE in bending (considering two different possible node arrangements with the introduction of a switch node).

The representation of the BPN in Figure 7.7 contemplates a switch node, *SN*, which allows to consider both the above possibilities for visual grading. The *SN* has two states, corresponding to each of the visual grading arrangements converging to it. By choosing one of the states, the information regarding the other visual grading arrangement will not be considered. This *SN* does not incorporate any conditional probability, and therefore, does not conjecture about any node descending from it. Also, it should be noted that the converging links connected to this node do not present any arrow, as this is only a path connection from the visual grading nodes to the MOE child node. The different

arrangements of nodes found within the *VI* level, as presented in Figure 7.7, will have equal joint probabilities before reaching the *SN*, independently of the position of nodes. Therefore, evidence in a *VI* grade of one node will provide the same updated probabilities to the other *VI* node, regardless of the chosen arrangements of nodes. However, the results of MOE in bending will greatly depend on the node located immediately before the *SN*, as the conditional probability table for the child node will depend upon the evidence given in the predecessor parent node, therefore, the different combinations will tend to render different results on the MOE in bending.

The results for the BPNs that combine visual grades in different size scales in a series arrangement are given in Figure 7.8 when VI_B is the first parent node and, otherwise in Figure 7.9 when VI_b is the first parent node. As it is common practice to have visual grading made only to a size scale of the member, the results of updated cumulative frequencies are presented when evidence is entered solely to one scale size of *VI* (either VI_B or VI_b). This also allows to determine in which level of the BPN, information should be entered in order to produce higher differentiation in the results. Moreover, inference results are only presented for $E_{m,g}$ when information is given in the beam scale, and for $E_{m,l}$ when information is given in the board scale, with aim at inferring about the global behaviour of structural size elements and at a local material level. By these premises, it is intended to explore the potential of these BPNs to produce information about the stiffness of an existing timber element, both in terms of material and structural characterization, regarding information of visual inspection made only in one scale.

The analysis of the possible sequences for the arrangement of the visual grading in different scales, evidences that information entered in the second parent node (the nearest to the child node) will provide a more significant differentiation between posterior probabilities. For the case in study, if information is provided to the first parent node (a root node), the posterior probabilities of MOE in bending will only present minor differences compared to the prior probability distribution. This situation occurs due to similar conditional probability found between cases in different visual grading (*e.g.* $P(VI_b = \text{III} \mid VI_B = \text{II}) \approx P(VI_b = \text{III} \mid VI_B = \text{III}) \approx P(VI_b = \text{III} \mid VI_B = \text{NC})$), meaning that similar percentages of grading of smaller segments were found for beams with different visual grading (Figure 7.1). Slight differences are only found for the cases where both visual gradings indicate either higher classes (*e.g.* $VI_B = \text{II} \cap VI_b = \text{I}$) or lower classes (*e.g.* $VI_B = \text{NC} \cap VI_b = \text{NC}$), as they presented higher conditional probabilities than those given by evidence on other visual grading classes.

Comparing these results with the first simplified converging BPN, it is found that the posterior distributions for E_{m,l_b} in Figure 7.8a and for E_{m,g_B} in Figure 7.9b, are similar to those previously obtained in Figure 7.3, therefore evidencing the validity of the division of node *VI* into two different nodes with respect to the scale of the element. As only the 16 beams that were graded in both scales were considered for the conditional probabilities in the BPN with double *VI* nodes in series, Figure 7.9b shows, in the posterior distribution of E_{m,g_B}, a difference to the first BPN when $VI_B = \text{II}$. This is consequence of the different number of beams considered with class II, because within the beams that were not

considered two were graded as class II and the other two as class NC. The difference is more noticeable in class II than in class NC, because on the overall sample, fewer beams were classified as class II and, therefore the disregard of two beams in that class was more significant than in class NC.

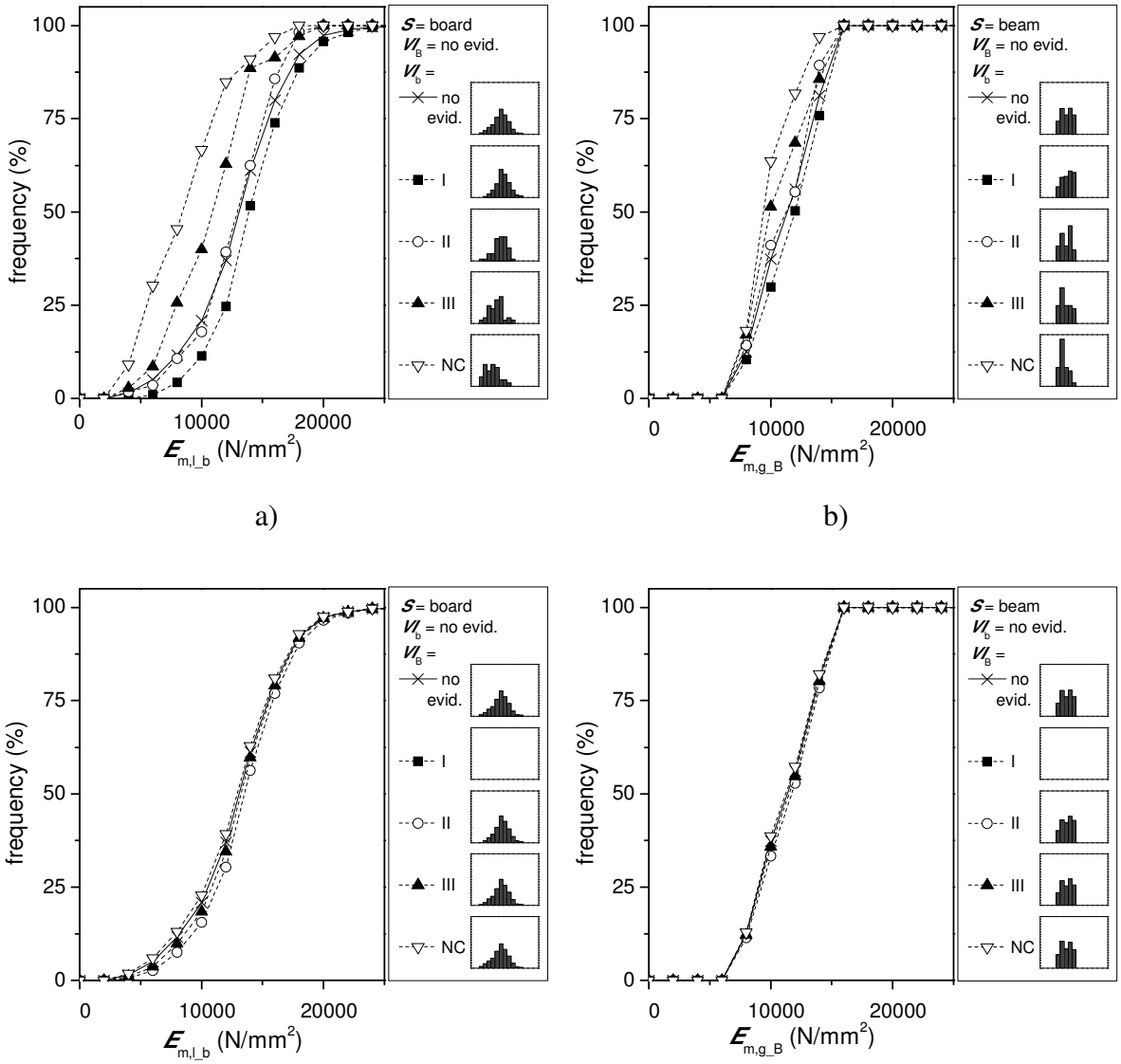

Figure 7.8: Cumulative frequency results for $E_{m,l}$ in boards and $E_{m,g}$ in beams with evidence in: a), b) visual inspection of boards; c), d) visual inspection of beams.

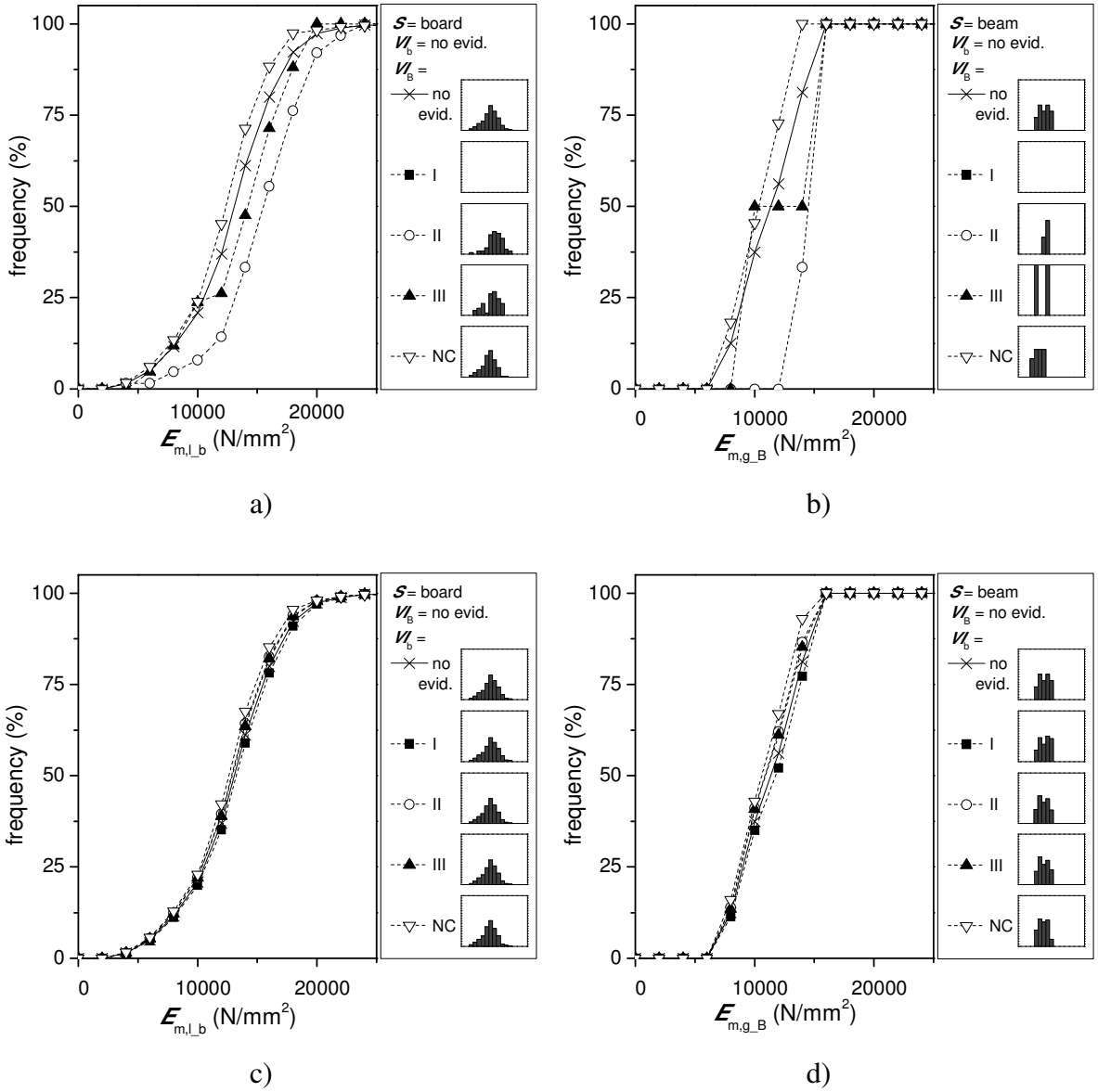

Figure 7.9: Cumulative frequency results for $E_{m,l}$ in boards and $E_{m,g}$ in beams with evidence in: a), b) visual inspection of beams; c), d) visual inspection of boards.

Hierarchical BPN

The last of the proposed BPN for inferring MOE in bending considers a hierarchical arrangement of the information given by different experimental tests in the different size scales (Figure 7.10). The purpose of this BPN is to obtain information about the global stiffness in bending of structural size beams, E_{m,g_B}, by prior localized information of smaller size scale elements. To that aim, both boards' visual inspection, VI_b, and local MOE in bending, E_{m,l_b}, are considered as parent nodes. The proposed network is an extension of the network given in Figure 7.7. In order to obtain a suitable definition of information within nodes, only the sixteen beams that are used also in the board assessment are considered (the 4 beams led to failure are not considered).

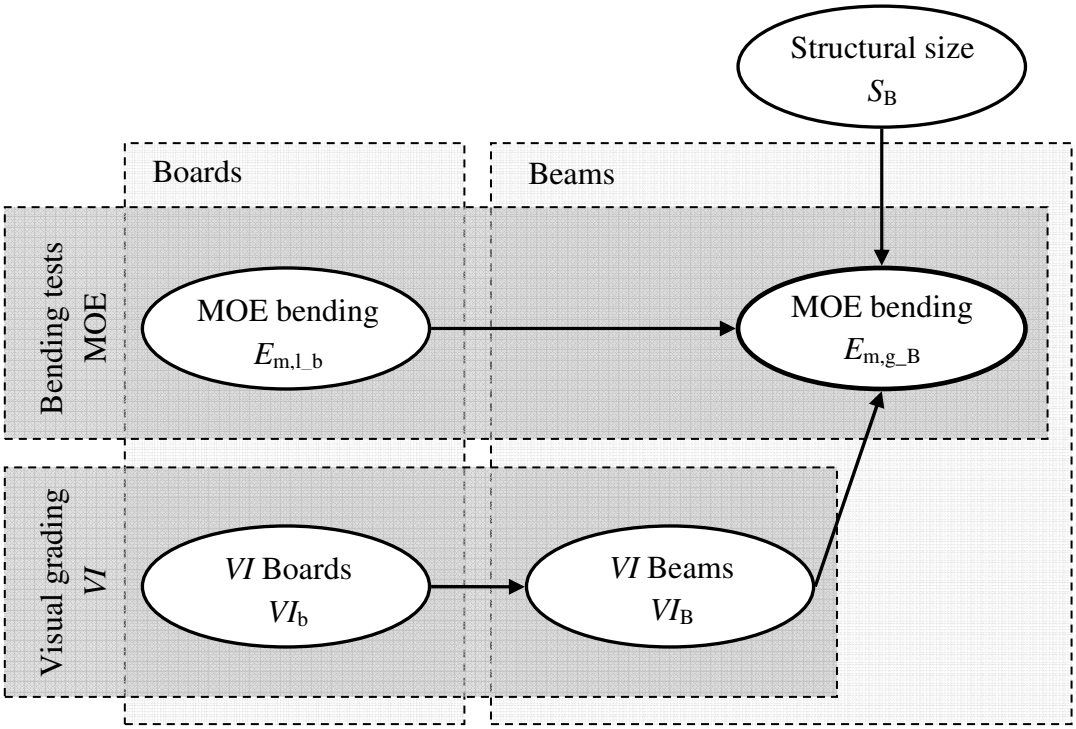

Figure 7.10: Hierarchical BPN to infer about global MOE in bending of structural size elements by prior localized information in smaller size elements.

The results from the hierarchical BPN that infers about E_{m,g_B} by prior localized information of smaller size scale elements are presented in Figure 7.11, regarding variation of evidence in E_{m,l_b} with a given VI_B, and in Figure 7.12, regarding variation of evidence in VI_b with a given E_{m,l_b}. Figure 7.11 allows for a sensitivity analysis of the importance of entering information regarding smaller size specimens in the definition of structural size elements mechanical properties, not only when a given VI_B is considered but also between different VI_B. On the other hand, Figure 7.12 considers the combination of information regarding only the smaller scale specimens by evidence in VI_b and E_{m,l_b}, allowing for the assessment of the evolution of E_{m,g_B} based in the variation of that evidence.

Distinct ranges for E_{m,g_B} are clearly defined for different evidences in VI_B, as shown in Figure 7.11. Class II beams present posterior distributions with higher values of E_{m,g_B} than the prior distribution. For those beams, cumulative frequency above 10% are only found for values of E_{m,g_B} higher than 13000 N/mm^2, independent of the evidence in E_{m,l_b}. Lowering the VI_B to class III produces posterior frequency distributions around the range of the prior distribution without evidence in E_{m,l_b}, whereas lowering the VI_B to class NC produces posterior distributions with lower values of E_{m,g_B} than the prior distribution without evidence in E_{m,l_b}. Exception to these defined ranges are found when VI_B = NC and $E_{m,l\_b} > 17000$ N/mm^2, where the posterior distributions still present higher values of E_{m,g_B} than the prior distribution, at the lower tail of the distributions and almost until 50% of cumulative frequency, evidencing that information about E_{m,l_b} is relevant in the resulting distribution of E_{m,g_B} in this hierarchical BPN.

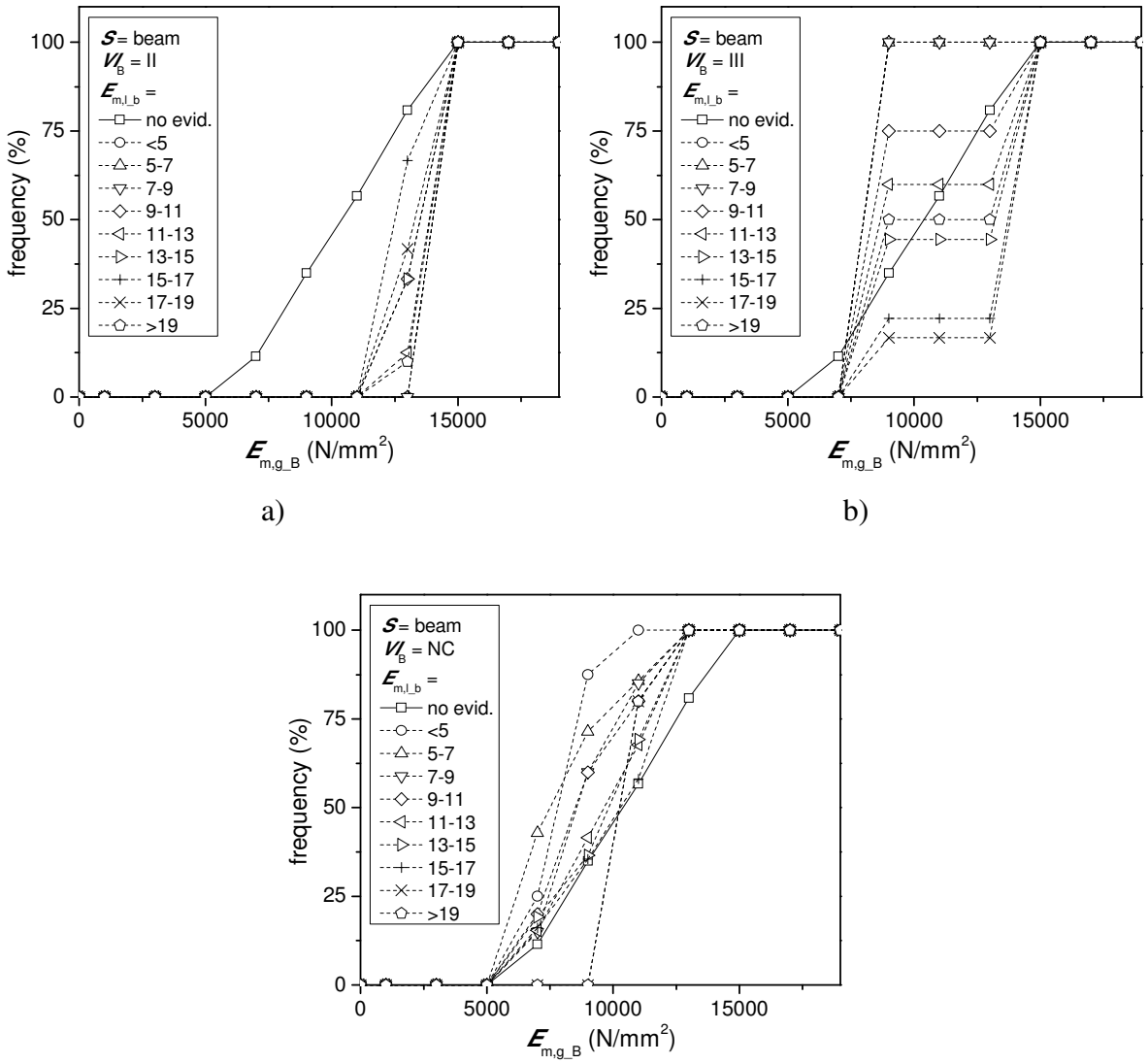

Figure 7.11: Cumulative frequency results for global MOE in bending for beams obtained with evidence in E_{m,l_b} results and beams' visual grade: a) VI_B = II; b) VI_B = III; c) VI_B = NC.

The relevance of E_{m,l_b} is further highlighted in Figure 7.12, where is shown that values of E_{m,l_b} lower than 11000 N/mm^2 produces lower values of E_{m,g_B} than the prior distribution, whereas, only above 15000 N/mm^2 for E_{m,l_b}, higher values of E_{m,g_B} are found in the lower tail for any possible evidence in VI_b. For evidences in E_{m,l_b} ranging from 11000 to 15000 N/mm^2 the posterior distribution are similar to the prior distribution without evidence in E_{m,l_b}.

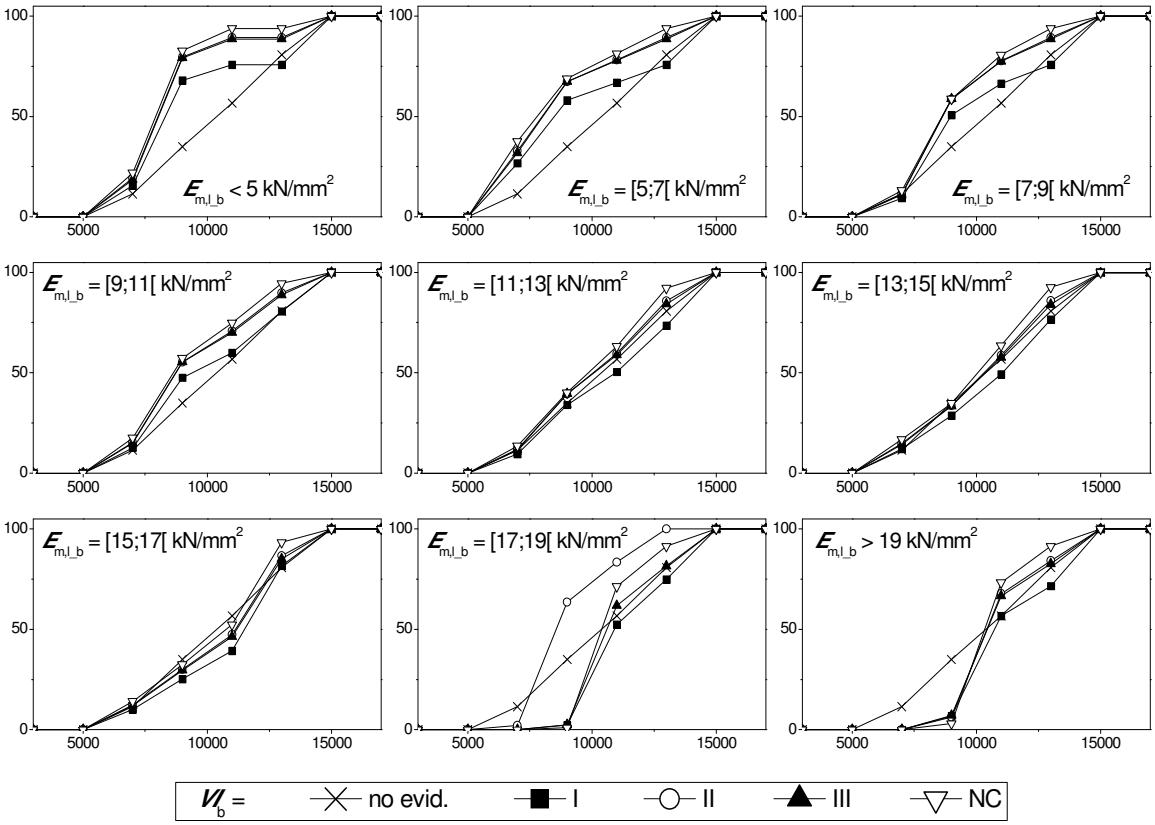

Figure 7.12: Evolution of cumulative frequency results with evidence in VI_b, throughout increasing of prior E_{m,l_b} (horizontal axes are E_{m,g_B} in N/mm^2 and vertical axes are frequency in %).

When extracting small specimens from a structural element intending at its mechanical characterization, often clear wood samples are taken for reference values as they present less variability than specimens with defects. Moreover, clear wood specimens also present advantages regarding an easier cutting process and preparation of specimens for testing. In this study, clear wood specimens are visually graded as class I, therefore, accounting for the application of this BPN into the assessment of an existing timber element, the results of the posterior probabilities of E_{m,g_B} are presented with consideration of evidences provided by a small element graded as class I (VI_b = I) combined with the different possible evidences in E_{m,l_b}, in Figure 7.13. For the case of VI_b = I, a clear trend for higher values of E_{m,g_B} is found when increasing the values in the evidence of E_{m,l_b}. When comparing with the prior distribution, no evidence in E_{m,l_b}, posterior distributions with lower values of E_{m,g_B} are found when evidence in E_{m,l_b} indicates values lower than 11000 N/mm^2, while evidence indicating E_{m,l_b} higher than 11000 N/mm^2 infers in posterior distributions with higher E_{m,g_B} values than the prior distribution.

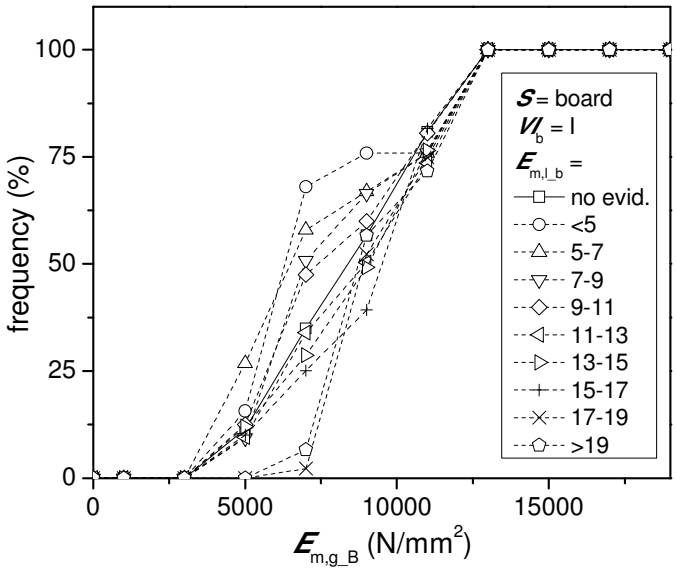

Figure 7.13: Cumulative frequency results for global MOE in bending for beams obtained with evidence in E_{m,l_b} results and for boards' visual grade I.

The statistical parameters regarding the results obtained in the posterior distributions, with evidence in VI_b and E_{m,l_b} or in VI_B and E_{m,l_b}, are presented in Table 7.1. Mean and COV were determined based on the posterior probability histograms, while the characteristic value (corresponding to the 5th percentile) was derived considering lognormal distributions adjusted to each case. In general, a decrease of the mean and characteristic values is found when lowering the visual grading class, whereas increasing for higher values of E_{m,l_b}.

Accounting the difference between mean values of E_{m,g_B} among consecutive visual grades within a same E_{m,l_b} class, an average decrease on mean of 2.5% or 15.1% are found, respectively for visual grade evidence given on VI_B or VI_b. Concurrently, an average increase on mean of 2.9% and 2.5% are found, respectively for visual grade evidence given on VI_B or VI_b, between consecutive E_{m,l_b} classes within a same visual grade. Comparing to the case where no evidence is given either to VI or E_{m,l_b}, an average decrease on mean of 4.2% is found considering all cases with evidence in VI_b, whereas an average increase on mean of 6.0% is found considering all cases with evidence in VI_B.

Table 7.1: Mean and characteristic values for different evidences in the hierarchical BPN for infer in E_{m,g_B}.

E_{m,l_b} (kN/mm^2)	VI_b					VI_B			
	no evid.	I	II	III	NC	no evid	II	III	NC
no evid.	11323 (22.9) 7768	11550 (22.9) 7924	10995 (22.8) 7558	11047 (23.1) 7560	10723 (22.0) 7462	11323 (22.9) 7768	14443 (6.3) 13030	11701 (25.8) 7652	10400 (20.1) 7466
< 5	9957 (27.8) 6305	10294 (ND) ND	9451 (ND) ND	9500 (28.8) 5919	9143 (22.8) 6283	9957 (27.8) 6305	15000 (ND) ND	9000 (ND) ND	8750 (14.6) 6876
[5;7[	10129 (29.9) 6193	10450 (34) 5975	9643 (33.5) 5558	9686 (33.6) 5577	9363 (28.4) 5867	10129 (29.9) 6193	15000 (ND) ND	9000 (ND) ND	9001 (24.7) 6000
[7;9[	10678 (24.8) 7107	10950 (26.3) 7099	10257 (26.0) 6684	10279 (26.2) 6678	10067 (22.7) 6933	10678 (24.8) 7107	15000 (ND) ND	9000 (ND) ND	9800 (19.2) 7147
[9;11[	10725 (24.8) 7130	10989 (25.3) 7253	10374 (26.5) 6703	10418 (25.8) 6815	10118 (26.3) 6569	10725 (24.8) 7130	14334 (8.1) 12555	10500 (28.6) 6563	9800 (21.2) 6918
[11;13[	11416 (23.2) 7788	11651 (23.4) 7932	11074 (23.4) 7538	11118 (24.1) 7478	10818 (24.5) 7235	11416 (23.2) 7788	14750 (4.8) 13631	11400 (28.8) 7095	10506 (20.5) 7502
[13;15[	11452 (23.0) 7850	11672 (22.8) 8015	11142 (24.0) 7508	11150 (26.5) 7209	10844 (27.1) 6949	11452 (23.0) 7850	14334 (6.8) 12816	12336 (25.6) 8092	10502 (21.0) 7440
[15;17[	11703 (21.4) 8235	11876 (21.0) 8401	11469 (22.6) 7907	11542 (26.6) 7457	11152 (ND) ND	11703 (21.4) 8235	13666 (7.2) 12139	13668 (19.4) 9942	10806 (21.0) 7648
[17;19[	12246 (14.0) 9724	12415 (14.4) 9799	10022 (19.3) 7293	12087 (ND) ND	11724 (ND) ND	12246 (14.0) 9724	14166 (7.3) 12569	13998 (17.5) 10494	11400 (7.8) 10020
> 19	12114 (15.6) 9379	12303 (16.2) 9429	11839 (ND) ND	11874 (ND) ND	11641 (ND) ND	12114 (15.6) 9379	14800 (4.3) 13795	12000 (35.4) 6708	11400 (7.8) 10020

Mean and coefficient of variation according to posterior probabilities in the updated discrete histograms for E_{m,g_B}.

Coefficient of variation in brackets, in percentage.

Characteristic values corresponding to the 5th percentile based on a lognormal distribution.

ND: not defined (due to low number of events for the combination of evidences).

7.2.2 Bending strength network

Following, the proposed BPN, as shown in Figure 7.14, takes into account prior information concerning the visual inspection grading, VI_b, and global MOE, E_{m,g_b}, in

boards for quantification of the bending strength, f_{m_b}, at the same size scale. The states in VI_b correspond to the different visual grades (I, II, III and NC), whereas the states of E_{m,g_b} are considered by intervals of 2500 N/mm^2 up to 17500 N/mm^2, with an initial interval of [0,5000[N/mm^2 so as to prevent an interval without any event. Intervals of 10 N/mm^2, starting from 0 and up to 90 N/mm^2 are considered for the discrete representation of the child node f_{m_b}.

In this BPN the E_{m,g_b} was chosen as prior information for f_{m_b}, instead of E_{m,l_b}, as it provided a better correlation ($r^2 = 0.69 > 0.38$), regarding the experimental data in Chapter 3. The arrangement of the parent nodes was conditioned by the available data results and expert decision. As insufficient data regarding the bending strength of beams was available for the validation of a BPN, only the size scale of boards was here considered. Also in this experimental campaign, segments that were given higher visual grading (I and II classes) and evidenced high values of E_{m,g_b}, did not produce any event with low value of f_{m_b}. On the other hand, segments that were given lower visual grading (III and NC classes) and evidenced low values of E_{m,g_b}, did not produce any event with high value of f_{m_b}. Therefore in a discrete BPN, this prior information cannot be described by two converging nodes, as the conditional probability tables for the child node would evidence non-existing events. To prevent this situation, a series BPN was considered having as first parent node the VI_b followed by the E_{m,g_b}.

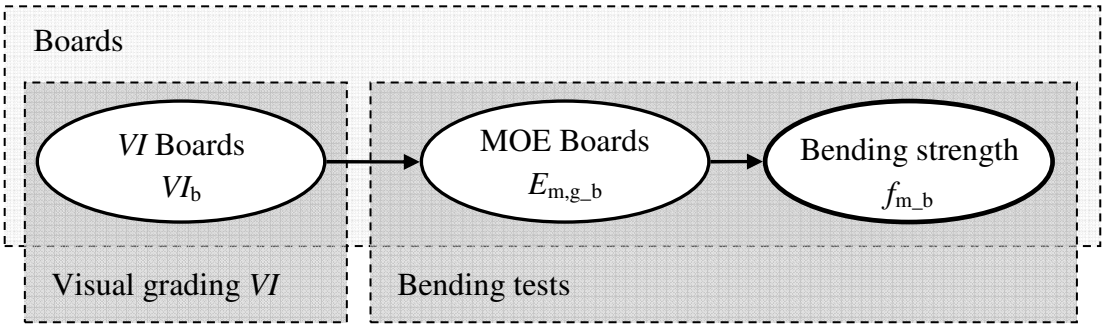

Figure 7.14: Simplified converging BPN model to infer about bending strength in local segments.

The value of this network resides in the possibility to gather information about the localized bending strength of a section regarding its visual inspection and bending stiffness, which can be very useful for the assessment of the structural size element since, as mentioned before, the failure of the global element is often associated to a specific weak section.

The results of the proposed series BPN, to infer on f_{m_b}, regarding the posterior probabilities expressed by distribution frequency curves, are presented in Figure 7.15 with evidence entered at the parent node VI_b. Lognormal distributions were adjusted regarding the statistical parameters of the posterior probabilities histogram.

The propagation of evidence through the BPN allows the analysis to both E_{m,g_b} and f_{m_b}. In both cases, a clear distinction is found between PDF of different VI_b evidence,

indicating higher values for the mechanical properties as the visual grade also increases. Also, higher variation is found for the PDF with lower visual grade classes. By comparison with the prior PDF (VI_b = no evidence), in the case of infer on E_{m,g_b} similar values are found in the posterior PDF with VI_b = III, meanwhile in the case of inferring on f_{m_b} similar values are found in the posterior PDF with VI_b = II. Therefore, it is sufficient to consider class III in VI_b, to observe a decrease in the value of f_{m_b} comparing to the prior PDF, whereas it is necessary to consider class NC to find a substantial decrease when considering E_{m,g_b}. This situation supports that the BPN correctly models the behaviour of timber, as the bending strength is usually more influenced by defects (and thus firstly related to visual grading) than MOE in bending.

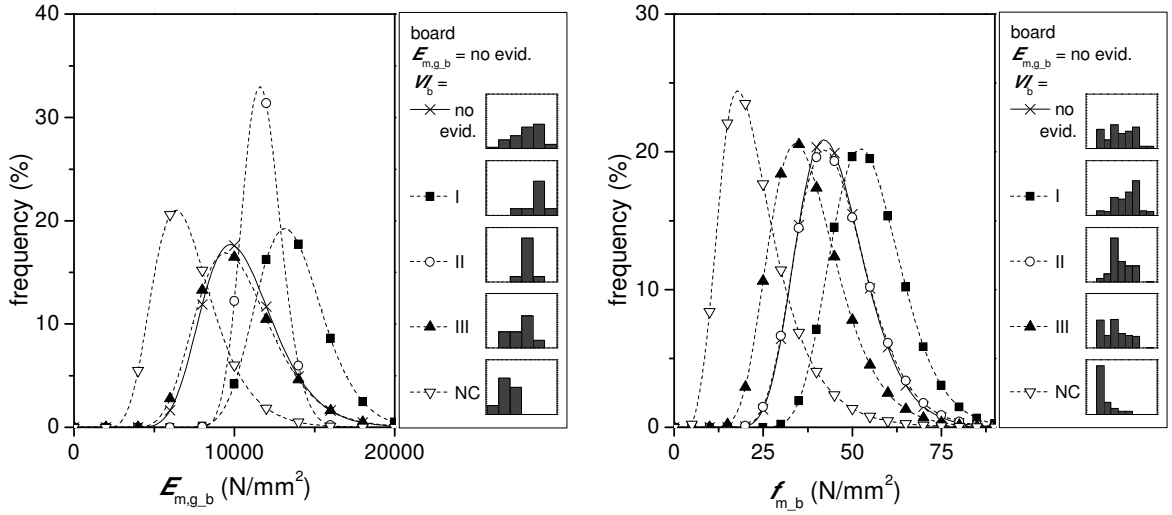

Figure 7.15: Cumulative frequency results in board scale, obtained with different evidences in VI_b, for a): E_{m,g_b}; b) f_{m_b}.

The statistical parameters regarding the results obtained in the posterior distributions, with evidence in VI_b, are presented in Table 7.2. Mean and COV were determined based on the posterior probability histograms, while the characteristic value (corresponding to the 5th percentile) was derived considering the CDF provided in Figure 7.15.

To all cases, a decrease of the mean and characteristic values is found when lowering the visual grade. The average difference between mean values of consecutive grading classes points a decrease of 25.2% and of 19.5%, respectively when analysing E_{m,g_b} and f_{m_b}. Higher decrease in the mechanical properties is found when lowering from class III to class NC (40.6% and 31.9%, respectively for E_{m,g_b} and f_{m_b}).

Table 7.2: Mean and characteristic values for different evidences in the BPN for infer in f_{m_B}.

Mechanical property	VI_b no evid.	I	II	III	NC
E_{m,g_b} (N/mm^2)	10053	13125	11250	9860	6719
	(23.8)	(16.1)	(10.5)	(25.7)	(31.3)
	6795	10066	9469	6460	4012
$f_{m,b}$ (N/mm^2)	42.8	52.6	43.1	35.8	21.3
	(23.6)	(19.4)	(24.4)	(29.6)	(49.9)
	29.1	38.2	28.9	22.0	9.4

Mean and coefficient of variation according to posterior probabilities in the updated discrete histograms for E_{m,g_b} and f_{m_b}.
Coefficient of variation in brackets, in percentage.
Characteristic values corresponding to the 5th percentile based on a lognormal distribution.

7.3 Analysis of a single element structure

The example considered in Chapter 6, regarding the assessment of a simply supported beam is hereby taken into account to demonstrate the use of the proposed BPNs and to investigate the influence of different prior information in the reliability analysis.

7.3.1 Ultimate limit state verification

Initially, the mechanical properties are provided given the mean and coefficient of variation of the posterior probability distribution resulting from the inference within the BPN without any prior evidence. In a first step, the results deriving from the BPN that infers on bending strength, f_m (see Table 7.2), are applied.

The same loading scenario is considered and also the span between supports is equal to the previous example. However, in order to obtain reliability indices of comparable order with the obtained previously, the cross section dimensions were reconsidered in the design parameter, which in this case was considered to be the height, h, of the cross section (see Equation 6.6). With a load fraction factor of $\alpha = 0.5$, a height of 300 mm was found to provide a similar reliability index as the previous example in Chapter 6, for reference period of one year. In this case, the resistance of the global element (beam scale) was considered to be equal to the resistance of the critical section (board scale), thus information is considered to be retrieved and representative of that critical section. With these premises an initial reliability index of $\beta = 4.70$ is attained (≈ 4.67, obtained in Chapter 6 with $h = 400$ mm) when no prior evidence is considered.

Following the same structural conditions and loading scenario, different levels of information were introduced to the parent node regarding visual inspection in the lower size scale (Figure 7.16). When information is given as $VI_b = \text{I}$, the reliability index is

higher than the one obtained with no prior evidence, whereas for VI_b = III or VI_b = NC the reliability index is lower. The consideration of VI_b = II led to similar reliability index compared with the case of no prior evidence.

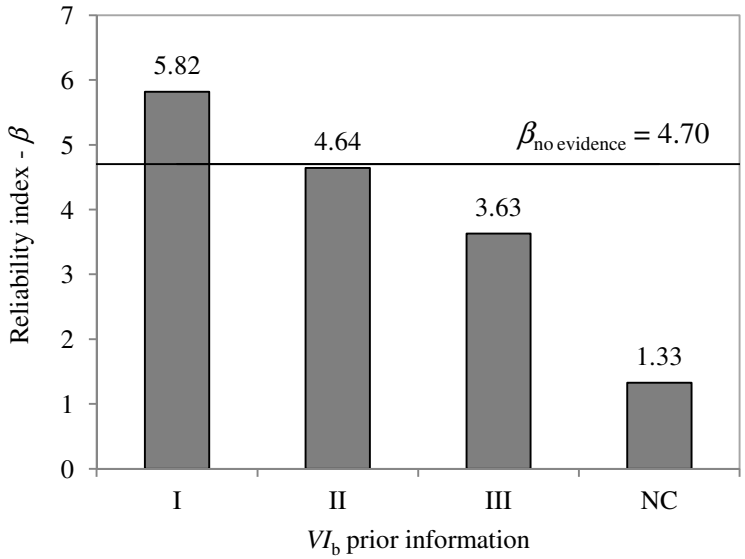

Figure 7.16: Reliability indices for different levels of prior information.

With exception of the case VI_b = NC, the introduction of new information still resulted in the indication of an acceptable level of structural safety. Moreover, in the case of VI_b = I, the cross section could even be redesigned to optimize the use of material (consideration of a smaller height).

The case of VI_b = NC results in a high decrease compared to the visual grade immediately before (class III), and even indicates an unsafe structural level. This is mainly due to the large variation found in that class combined with a lower mean value of bending strength.

The influence of different levels of information is also assessed in terms of design value by determining the cross section height, for each case with evidence, which would provide the same reliability level of the case with no evidence. In this example, when having VI_b = I, a 15.7% smaller height would provide a β = 4.70, whereas the other cases would need an increase of height to provide the same reliability index. These increases would be of 1.0%, 21.7% and 132.7% for VI_b = II, VI_b = III and VI_b = NC, respectively.

7.3.2 Serviceability limit state verification

After assessing the safety level regarding the ultimate limit state, the results deriving from the hierarchical BPN that infers on bending stiffness (see Table 7.1), are applied. In this case, the deflection in service limit state will be assessed. For structures consisting of elements, components and connections with the same creep behaviour and under the assumption of a linear relationship between the actions and the corresponding

deformations, the final deformation may be taken as the sum of the effect of each action considered separately (CEN, 2004). Each component of deflection is then affected by the stiffness modification factor, k_{def}, according to the service class, and by the factor for quasi-permanent value for variable loads, ψ_2.

The component of deflection for permanent load, u_G, was obtained through Equation 7.1 and the component for variable load, u_Q, was obtained through Equation 7.2:

$$u_G = \left(\frac{5}{384} \cdot \frac{(1-\alpha) \cdot G \cdot l^4}{\text{MOE} \cdot b \cdot h^3/12} \right) \cdot (1 + k_{def}) \tag{7.1}$$

$$u_Q = \left(\frac{5}{384} \cdot \frac{\alpha \cdot Q \cdot l^4}{\text{MOE} \cdot b \cdot h^3/12} \right) \cdot (1 + \Psi_2 \cdot k_{def}) \tag{7.2}$$

where MOE is the bending modulus of elasticity, G is the permanent load and Q is the variable load, α is the load fraction factor and b and h are the cross section width and height, respectively, k_{def} is the stiffness modification factor and ψ_2 is the factor for quasi-permanent value for the live load. Considering that the structure is in a residential area, and is made of solid timber in a service class 1 environment, the values of $k_{def} = 0.6$ and $\psi_2 = 0.3$ are attained (CEN, 2002 and 2004).

The deflection of the beam is assessed for the centre section by considering the service limit state equation as:

$$g = \delta_L - (u_G + u_Q) \tag{7.3}$$

where δ_L is the allowable deflection limit dependent of the span length (in this case $\delta_L = l/350$ was adopted).

The same loading scenario is considered and also the span between supports is equal to the previous example. However, the height h (design parameter) was dimensioned in order to provide a $\beta = 2.90$ when no evidence is given in the BPN. This reliability level is considered from the indication of Annex C of CEN (2002) C for reliability class 2. With a load fraction factor of $\alpha = 0.5$, a height of 435 mm was found to provide a $\beta = 2.92$, for reference period of one year. Comparing to the ultimate state verification, it is found that the serviceability limit state is the most conditioning in terms of cross section height.

Following the same structural conditions and loading scenario, different levels of information were introduced to the parent nodes regarding visual inspection in different size scales and information of $E_{m,l}$ in the board scale. The results are presented in Table 7.3 considering the reliability index and the percentage difference on the height of the cross section necessary to obtain the same reliability level when no evidence is provided to the BPN. Combination of evidences that had low number of events in the experimental campaign were not considered.

Table 7.3: Reliability indices for different levels of prior information and percentage difference of the design value.

E_{m,l_b} (kN/mm^2)	VI_b					VI_B			
	no evid.	I	II	III	NC	no evid	II	III	NC
no evid.	2.92	3.02 (-0.69)	2.78 (0.92)	2.80 (0.92)	2.66 (1.84)	2.92	4.18 (-8.51)	3.05 (-0.92)	2.53 (2.76)
< 5	2.22 (4.83)	ND	ND	1.95 (6.67)	1.82 (7.36)	2.22 (4.83)	ND	ND	1.66 (8.51)
[5;7[	2.28 (4.37)	2.38 (3.68)	1.96 (6.44)	1.98 (6.44)	1.88 (7.13)	2.28 (4.37)	ND	ND	1.71 (8.05)
[7;9[	2.61 (2.07)	2.72 (1.38)	2.39 (3.68)	2.40 (3.45)	2.34 (4.14)	2.61 (2.07)	ND	ND	2.23 (4.60)
[9;11[	2.63 (2.07)	2.75 (1.15)	2.45 (3.22)	2.48 (2.99)	2.32 (4.14)	2.63 (2.07)	4.14 (-8.28)	2.48 (2.99)	2.21 (4.83)
[11;13[	2.96 (-0.23)	3.02 (-0.92)	2.81 (0.92)	2.82 (0.69)	2.68 (1.61)	2.96 (-0.23)	4.29 (-9.20)	2.89 (0.23)	2.58 (2.30)
[13;15[	2.98 (-0.23)	3.07 (-0.92)	2.83 (0.69)	2.81 (0.92)	2.66 (1.84)	2.98 (-0.23)	4.15 (-8.28)	3.31 (-2.53)	2.57 (2.53)
[15;17[	3.10 (-1.15)	3.17 (-1.61)	2.99 (-0.46)	2.97 (-0.46)	ND	3.10 (-1.15)	3.92 (-6.67)	3.85 (-6.21)	2.71 (1.38)
[17;19[	3.37 (-2.99)	3.44 (-3.45)	2.35 (3.91)	ND	ND	3.37 (-2.99)	4.09 (-7.82)	3.98 (-7.13)	3.06 (-0.92)
> 19	3.31 (-2.53)	3.38 (-2.99)	ND	ND	ND	3.31 (-2.53)	4.30 (-9.20)	3.04 (-0.69)	3.06 (-0.92)

Percentage difference of the design value to obtain the same reliability level when no evidence is provided in the BPN presented within brackets, in percentage.

A positive value in the percentage difference means a need to increase the height of the cross section, whereas a negative value means a need to decrease the height of the cross section in order to obtain a $\beta = 2.92$ (case without any evidence).

ND: not defined (due to low number of events for the combination of evidences).

The results in Table 7.3 evidence that lower reliability indices are found when evidence indicates lower visual grading and lower values of E_{m,l_b} and, on the opposite case, that higher reliability indices are found when evidence indicates higher visual grading (VI_b = I, II or VI_B = II) and higher values of E_{m,l_b}. Significant differences are found on the reliability indices between cases with different evidences in E_{m,l_b}.

Overall, according to the different combinations of evidence, the cross section height could be reduced up to 9.20% ($VI_B = II \cap E_{m,l\_b} > 19$ kN/mm^2) or have to be increased 8.51% ($VI_B = NC \cap E_{m,l\_b} < 5$ kN/mm^2), as to obtain the same reliability index of the case when no evidence is provided.

Although the relative differences in height are rather small for some cases, it is important to notice that these values may be comparable to the loss of cross section in existing timber structures exposed to decay. In that case, the combination of results of visual grading and local mechanical tests, combined through the proposed method, proves to be effective in the verification of serviceability limit states for a decayed structure.

7.4 Final remarks

The implementation of grading procedures, which allow for an explicit consideration of information during the grading process itself and also for use in reliability assessment, is further challenging when it concerns grading existing timber elements already in use. Various approaches for grading have been addressed, however, many reside within the same basic concept that the main properties of interest may be assessed indirectly by means of other properties.

The use of visual inspection and information from small size specimens are common available data for the mechanical assessment of timber elements. In that light, the previous described BPNs allowed to infer about bending stiffness and strength of timber elements influenced by visual grading and mechanical tests made in different size scales. Given these influencing factors, the proposed BPNs were capable of updating the conditional probability distributions and showed that the marginal probability distributions of timber mechanical properties were significantly altered when provided different evidences. Clearly, more refined predictions of the mechanical properties can be obtained by increase of the states in either or both parent and child nodes. Nevertheless, an increase of the refinement of states must be accompanied with a larger number of events (number of visual grading and mechanical test measurements) for a consistent and trustworthy assessment.

The different proposed BPNs, with increasing level of complexity and hierarchy, demonstrated that more detailed information may be obtained by adding new parent nodes or by dividing pre-existing ones. Therefore, extension of the BPNs may be accomplished by adding nodes representing variables to which information is known or may become available, and after updating the interrelationships and probability distribution functions of those variables. These premises were implemented throughout the BPNs inferring on bending MOE, making possible to validate a BPN where the $E_{m,g}$ of structural size timber elements could be derived by information of mechanical test results made to small specimens combined with visual grading of the elements at different size scales.

Moreover, the predicted marginal probability functions were used to determine the mean and characteristic values of the timber elements' mechanical properties, consisting in an important step regarding the possible allocation of each sub-sample into a specific structural class. As example, the strength class system provided by EN 338 (CEN, 2009) considers for grade assignment the characteristic values (5th percentile) for strength properties and density, and the mean values for MOE and shear modulus. Within the scope of this strength class system, the importance of the BPN inferring on both E_{m,g_b} and f_{m_b} is noticeable when evidence is given on VI_b. In this case and assuming the statistical results of the underlying probability distribution for the bending stiffness and strength, a D24 class is attributed when no evidence is given to visual grading. An increase in strength class to D30 or D40 is present, respectively when VI_b = II or VI_b = I. On the other hand, a decrease to strength class D18 is present when VI_b = III and no strength class is admitted for VI_b = NC since the required values are not fulfilled. In all cases of evidence in VI_b, the limiting strength grading parameter was the mean MOE in bending. These results evidenced that the use of BPN combined with multi-scale information on visual grading and mechanical testing provides a consistent basis for strength grading of existing timber elements. Furthermore, this methodology may be applied to reliability assessment, as the uncertainty of each variable is passed throughout the propagation of different evidences and reflected on the BPN results, as posterior marginal probability distributions.

The results of the data inference of the BPNs were used in the verification of ultimate limit state in bending for a simply supported beam, and also for the deflection serviceability limit state. A comparison of the reliability indices and of the design values are considered between different cases of inputted evidence, evidencing that the cross section may be optimized regarding the results from localized information and visual grading in different size scales.

This page intentionally left blank

Chapter 8

Conclusions and future developments

ABSTRACT: The conclusions of this work are presented in this last chapter. The main findings are evidenced and its value to the research community is highlighted.

As for all research activities, every answer opens a door to a new question, and therefore, the limitations of this work and indications for future research topics are addressed.

8.1 Retrospect and motivation

The safety evaluation of existing timber structures is currently made by use of deterministic or semi-probabilistic codes, even though these methods are oriented for the assessment of new construction and do not allow for a complete evaluation of the uncertainty related to the mechanical properties of timber. Attending to the inherit variability of the mechanical properties of timber, both within and between elements, it is recommended their characterization and definition by probabilistic methods. Several efforts have been made in that direction and is now possible to use probabilistic methods in the assessment of existing timber structures. Nevertheless, the reliability of these methods greatly depends on the capability to obtain data, both qualitatively and quantitatively, necessary for the inference of timber's reference properties and prediction of the remaining ones by correlation.

At the present state of knowledge, due to several research projects, rational design rules, based on a detailed material description validated by comparison with significant number of empirical results, are made available to a timber construction designer. However, safety assessment of existing structures and characterization of traditional wooden building techniques remain a true challenge.

The distribution of stiffness and strength along a timber element is dependent of several factors namely, among others, the distribution of clear wood and sections with defects and the size effect. Despite the significant efforts in the development of models for the consideration of these factors, methods that allow for their onsite application to the assessment of existing timber structures are still missing. Within this scope, the objective of this work was to provide an insight of different methods for the assessment and prediction of the mechanical properties of elements in existing timber structures. These methods were conceived based on different sources of information, in particular, by the analysis of small scale specimens aided by the information of visual grading and non-destructive testing, combined with different size scales. To that purpose, a hierarchical modelling was adopted for inference on bending stiffness and strength reference properties with the possibility of being updated with new information.

8.2 Summary of results

The main premises and findings of this work are provided through Chapters 2 to 7. In Chapter 2, the main issues regarding methodologies for safety assessment of existing timber structures are reviewed and discussed. Focus was given to the topics which were considered relevant for this work. Testing of the mechanical properties of timber through different procedures regarding its level of damage to the timber member are presented and discussed. Moreover, distinct methods of timber grading are outlined and compared. Assessment of structural safety was presented regarding semi-deterministic and probabilistic approaches. Different hierarchical models were discussed and the framework

for updating probabilistic models by Bayesian methods was addressed and further mentioned in the framework of inference by probabilistic network.

Chapters 3 and 4 represent the description and analysis of an experimental campaign made to chestnut timber beams, which allowed for the material characterization and the definition of correlations within and between different size scales. In Chapter 3, the experimental campaign evidenced the results of visual grading and of non and semi-destructive tests made in different scales of timber, regarding the size of specimens, with respect to a visual stress-grading. A combination of bending tests made to structural size elements and tests made in the parallel to the grain direction for clear wood specimens was considered for the mechanical grading of timber.

The variation and relationship between scales was discussed in more detail in Chapter 4, where moderate and high correlations were obtained within the same scale, with a trend to lower correlations between different scales, due to the size effect. In some cases, the correlations with non-destructive tests were moderately low and therefore, for quantitative analysis, these methods can only be used in combination with mechanical characterization. The variation of results was also found to be lower within the same element but in different proportions regarding the direction of measurement (along the height of the cross section or length of the timber member). The fit to probabilistic parameters regarding different possible probability distributions was dealt accounting Maximum Likelihood methods and goodness-of-fit tests. These analyses evidenced that the mechanical properties of timber could be better represented by combination of different distributions mainly the extreme values found at the tails of the distributions.

Chapters 5 to 7 represent the application and exemplification of methods to predict different mechanical properties of timber and also possible procedures for updating these models. Within Chapters 5 and 7, structural timber was considered attending to the identification and classification of defects made in Chapter 2, whereas Chapter 6 provided an insight on data updating through clear wood information gathered in literature.

In Chapter 5, the prediction of bending stiffness in structural size elements using information of visual grading and bending tests in smaller size scales was considered. High correlations between models and experimental campaign were found with acceptable percentage error, even when considering random sampling of the measurements and using reduction factors regarding the visual grades. Regarding this sample, it was concluded that visual inspection combined with information of clear wood's bending stiffness could provide a suitable prior information

In Chapter 6, exemplification of a Bayesian updating procedure was given regarding prior information by non-destructive evaluation and by clear wood mechanical properties characterization in the parallel to the grain direction. Both single element structures and a truss system, were discussed. The introduction of new information revealed to provide a significant difference in the assessment of structures both regarding short and long evaluation of safety. More substantiated maintenance plans and also its calibration are made possible by these procedures.

The last chapter of development of this work, comprised the evaluation of bending stiffness and strength by use of Probabilistic Bayesian Networks using the information gathered in the analysed experimental campaign. Chapter 7 provided an evolution in the definition of a hierarchical model for bending stiffness taking into account visual grading and bending tests made at different size scales. The results are comparable to the empirical evidence and proved to identify different posterior information accounting different initial conditions. The networks were also designed in order to consider different combinations of available information in an onsite assessment. Furthermore, a model regarding failure of weak sections within a structural timber member is proposed and exemplified in a case study. The results evidence the gains obtained in the safety evaluation of the timber element when different levels of information were considered.

8.3 Originality of the work

The present work had the main objective of proposing different models for safety evaluation of timber structures by prediction and inference of the mechanical properties of timber at the element level. The models were based on empirical data obtained through an experimental campaign and literature data, and updating was provided by use of probabilistic methods.

The originality of this work resides in the prediction of the mechanical properties of timber in different size scales, with information that may be available in an onsite assessment combined with small specimens mechanical characterization. The correlations found between and within scales are fundamental to this analysis and also pose as an original point of this work regarding its use for visual stress-grading in different scales. The results of these research points have been pointed in several publications (Sousa *et al.*, 2012, in press_b and in press_c).

Furthermore, the updating through non-destructive data is considered new and original accounting the use of different quantitative and qualitative data (Sousa *et al*., 2013b), as well as accounting the differentiation of samples by visual stress-grading (Sousa *et al.*, 2013a) and bending mechanical properties. The resulting hierarchical model using probabilistic networks and its fundamental methodology, are a meaningful contribution for the safety evaluation of existing timber structures. By the proposed methodologies it is intended to have a more reliable and informed decision making process, regarding possible interventions or maintenance in timber elements.

The exemplification of different case studies in the structural element size, with the illustration of how timber material properties can be updated in regard to different types of information and decay models, also allowed for the further development of the understanding of timber as a structural material (Brites *et al*., 2013; Lourenço *et al*., 2013; Sousa *et al*., in press_a).

8.4 Limitations and future work

This work mainly considers the inference and assessment of the mechanical properties at the element scale. However, the safety assessment and reliability of a timber structure is not only dependent of the properties of the individual elements, but also to a large extent should consider its joints and interaction between elements. As evidenced in several events, failure of timber structures often occur not only due to low mechanical properties of the elements but, specially, due to the combination of several errors and unfavourable conditions. To that aim, it is proposed that this work can be combined in a global assessment framework which also considers the assessment of structural joints.

The assessment of existing timber elements also comprises the evaluation of decay which in the present work was assessed only by bi-parametric models that consider the progress of decay. In this case, the models were not fully calibrated as only insufficient data from monitoring and case studies was available. Within this scope, future work should be considered regarding the retrieval of data from long term monitoring and onsite evaluation of elements with decay. Moreover, the influence of decay in joints is an important issue to further analyse and discuss.

Due to the availability of material, the proposed methodologies and models were calibrated with consideration to the results of an experimental campaign made to a relatively small sample. Although the principles of the models can be extended to other species, it is necessary to calibrate the grading procedures and confirm its validity of use. Even for the same species, it is suggested that different origins should be assessed.

Finally, density was not considered as a defining parameter in the prediction and in the hierarchical models, as it did not provide strong correlations with other properties. Nevertheless, density might be relevant in the distinction and assessment between different wood species.

This page intentionally left blank

References

ABNT (1997) Nbr7190/1997. Projeto de Estruturas de Madeira. Brasil. Associação Brasileira de Normas Técnicas (in Portuguese).

AENOR (2011) UNE 56546:2011 - Visual grading for structural sawn timber. Hardwood timber. Asociacíon Española de Normalización y Certificación.

Aguilera, P. A., Fernández, A., Fernández, R., Rumí, R., & Salmerón, A. (2011). Bayesian networks in environmental modelling. *Environmental Modelling & Software*, 26(12), 1376-1388.

Aicher, S., Höfflin, L., & Behrens, W. (2002). Determination of local and global modulus of elasticity in wooden boards. *Otto-Graf Journal*, 13, 183-198.

Allen, J. F. (1981). An interval-based representation of temporal knowledge. In Proceedings of 7th International Joint Conference on Artificial Intelligence, Vancouver, Canada (pp. 221-226).

Almazán, F. J. A., Prieto, E. H., Martitegui, F.A., & Richter, C. (2008). Comparison of the Spanish visual strength grading standard for structural sawn timber (UNE 56544) with the German one (DIN 4074) for Scots pine (*Pinus sylvestris* L.) from Germany, *Holz als Roh-und Werkstoff* 66(4): 253–258.

Anthony, R. W., Dugan, K. D., & Anthony, D. J. (2009). A Grading Protocol for Structural Lumber and Timber in Historic Structures. *APT Bulletin*, 40(2), 3-9.

ASTM (1989). ASTM 494-89 Standard practice measuring velocity in materials. American Society for Testing Materials, EUA, 34 p.

ASTM (2000a). ASTM D143-94e1 - Standard test methods for small clear specimens of timber, American Society for Testing Materials, EUA.

ASTM (2000b). ASTM D245-00 - Standard practice for establishing structural grades and related allowable properties for visually graded lumber, American Society for Testing Materials, EUA.

ASTM (2008). ASTM E178 - Standard practice for dealing with outlying observations. American Society for Testing Materials, EUA.

Attoh-Okine, N. O., & Bowers, S. (2006). A Bayesian belief network model of bridge deterioration. In Proceedings of the ICE-Bridge Engineering, 159(2), 69-76.

Badel, E., & Perré, P. (2007). The shrinkage of oak predicted from its anatomical pattern: validation of a cognitive model. *Trees*, 21(1), 111-120.

Baldassino, N., Piazza, M., & Zanon, P. (1996). In situ evaluation of the mechanical properties of timber structural elements. In Proceedings of International symposium on nondestructive testing of wood (pp. 369-377).

Baltrušaitis, A. (1999). Estimation of strength of glulam beams depending on defect of layers, *Statyba* 5(4): 245–249 (in Lithuanian).

Bartlett, N. R., & Lwin, T. (1984). Estimating a relationship between different destructive tests on timber. *Applied statistics*, 65-72.

Bayraktarli, Y. Y., Ulfkjaer, J., Yazgan, U., & Faber, M. H. (2005). On the application of Bayesian probabilistic networks for earthquake risk management. In Proceedings of 9th international conference on structural safety and reliability, Rome, Italy.

Beall, F. C. (2002). Overview of the use of ultrasonic technologies in research on wood properties. *Wood Science and Technology*, 36(3), 197-212.

Beck, J. L., & Katafygiotis, L. S. (1998). Updating models and their uncertainties. I: Bayesian statistical framework. *Journal of Engineering Mechanics*, 124(4), 455-461.

Biblis, E., Meldahl, R., Pitt, D., & Carino, H. F. (2004). Predicting flexural properties of dimension lumber from 40-year-old loblolly pine plantation stands. *Forest products journal*, 54(12), 109-113.

Biernacki, J. M., & Beall, F. C. (1993). Development of an acousto-ultrasonic scanning system for nondestructive evaluation of wood and wood laminates. *Wood and fiber science*, 25(3), 289-297.

Bodig J., & Jayne B. A. (1993). Mechanics of Wood and Wood Composites. Krieger Publishing.

Bonamini, G. (1995). Restoring timber structures—inspection and evaluation. Timber Engineering, STEP, 2.

Bonamini, G., Noferi, M., Togni, M., Uzielli, L. (2001). Il Manuale del Legno Strutturale - Vol.I: Ispezione e diagnosi in opera. Mancosu Editore, Roma.

Bonamini, G., Togni, M., & Pascucci, R. (1998). Classification rules for chestnut beams (in Italian). Edizioni C.L.U.T, Torino

Boström, L. (1999). Determination of the modulus of elasticity in bending of structural timber–comparison of two methods. *European Journal of Wood and Wood Products*, 57(2), 145-149.

Brancheriau, L., Bailleres, H., & Guitard, D. (2002). Comparison between modulus of elasticity values calculated using 3 and 4 point bending tests on wooden samples. *Wood Science and Technology*, 36(5), 367-383.

Branco, J. M., Peixoto, T., Lourenço, P. B., & Medeiros, P. (2011). Mechanical characterization of old chestnut beams. In Proceedings of SHATIS'11. Lisbon, Portugal.

Branco, J. M., Piazza, M., & Cruz, P. J. (2010). Structural analysis of two King-post timber trusses: Non-destructive evaluation and load-carrying tests. *Construction and Building Materials*, 24(3), 371-383.

Brites, R. D., Lourenço, P. B., & Machado, J. S. (2012). A semi-destructive tension method for evaluating the strength and stiffness of clear wood zones of structural timber elements in-service. *Construction and Building Materials*, 34, 136-144.

Brites, R. D., Neves, L. C., Saporiti Machado, J., Lourenço, P. B., & Sousa, H. S. (2013). Reliability analysis of a timber truss system subjected to decay. *Engineering Structures*, 46, 184-192.

Brown, H. P., Panshin, A. J., & Forsaith, C. C. (1952). Textbook of Wood Technology. Volume II. The physical, mechanical, and chemical properties of the commercial wood of the United States. New York: McGraw-Hill.

Brunetti, M., Cremonini, C., Crivellaro, A., Togni, M, & Zanuttini, R. (2009). Chestnut timber for structural use (in Italian). Castanea 2009, 58 Convegno Nazionale Castagno and 1st European Congress on Chestnut. Cuneo, Italy

Bucur, V., & Böhnke, I. (1994). Factors affecting ultrasonic measurements in solid wood. *Ultrasonics*, 32(5), 385-390.

Bucur, V., & Feeney, F. (1992). Attenuation of ultrasound in solid wood. *Ultrasonics*, 30(2), 76-81.

Burgert, I. (2006). Exploring the micromechanical design of plant cell walls. *American Journal of Botany*, 93(10), 1391-1401.

Burley, J, Evans J, and Younquist J (Editors) (2004). Mechanical properties of wood. Encyclopedia of Forest Science. Elsevier Publishing Co., Oxford, England. 2000 p.

Calderoni, C., De Matteis, G., Giubileo, C., & Mazzolani, F. M. (2010). Experimental correlations between destructive and non-destructive tests on ancient timber elements. *Engineering Structures*, 32(2), 442-448.

Cavalli, A. & Togni, M. (2011). Combining NDT and visual strength grading to assess ancient timber beams stiffness to evaluate strengthening interventions suitability. In Proceedings of 17th International Nondestructive testing and evaluation of wood symposium, Hungary, 2:593-601

Ceccotti, A., & Uzielli, L. (1989). Sul grado di affidabilità strutturale sulle strutture in legno antiche. In Proceedings of 2 Congresso Nacionale sul Restauro del Legno. Nardini, Florence, Italy. 14 pp.

CEN (1994a) EN 350-1: Durability of wood and wood-based products. Part 1: Guide to the principles of testing and classification of the natural durability of wood". Office for Official Publications of the European Communities. Brussels, Belgium.

CEN (1994b) EN 350-2: Durability of wood and wood-based products. Natural durability of solid wood. Part 2: Guide to natural durability and treatability of selected wood species of importance in Europe". Office for Official Publications of the European Communities. Brussels, Belgium.

CEN (1997) EN 518:1997 Structural Timber - Grading - Requirements for Visual Strength Grading Standards, European Committee for Standardization, Brussels.

CEN (1999) EN 1194:1999 Timber structures. Glued laminated timber. Strength classes and determination of characteristic values, European Committee for Standardization, Brussels.

CEN (2002) EN 1990:2002, Eurocode 0: Basis of Structural Design, European Committee for Standardization, Brussels.

CEN (2004) EN 1995-1-1:2004, Eurocode 5: design of timber structures. Part 1-1: General common rules and rules for buildings, CEN European Committee for Standardization, Brussels..

CEN (2009) EN 338:2009. Structural timber – strength classes. CEN European Committee for Standardization, Brussels.

CEN (2010a). EN 408:2010 - Timber structures - Structural timber and glued laminated timber - Determination of some physical and mechanical properties, European Committee for Standardization, Brussels.

CEN (2010b). EN 384:2010 - Structural timber. Determination of characteristic values of mechanical properties and density, European Committee for Standardization, Brussels.

CEN (2012) EN 1912:2012. Structural timber – strength classes. Assignment of visual grades and species. CEN European Committee for Standardization, Brussels.

Ceraldi, C., Mormone, V., & Ermolli, E. R. (2001). Resistographic inspection of ancient timber structures for the evaluation of mechanical characteristics. *Materials and structures*, 34(1), 59-64.

Conedera, M., & Krebs, P. (2007). History, present situation and perspective of chestnut cultivation in Europe. In Proceedings of II Iberian Congress on Chestnut 784 (pp. 23-28).

Cornell, C. A. (1969). A probability-based structural code. *Journal of the American Concrete Institute*. ACI Journal Proceedings, 66(12). ACI.

Cown, D. J. (1978). Comparison of the pilodyn and torsiometer methods for the rapid assessment of wood density in living trees. *New Zealand Journal of Forestry Science*, 8(3), 384-391.

Cruz, H., Yeomans, D., Tsakanika, E., Macchioni, N., Jorissen, A., Touza, M., Mannucci, M., & Lourenço, P. B. (2013). Guidelines for the on-site assessment of historic timber structures. *International Journal of Architectural Heritage*, DOI: 10.1080/15583058.2013.774070

Czomch, I. (1991). Lengthwise variability of bending stiffness of timber beams. In Proceedings of the International Timber Engineering Conference, London, United Kingdom, 2158-2165.

Czomch, I., Thelandersson, S., & Larsen, H. (1991). Effect of within member variability on bending strength of structural timber. In Proceedings of the CIB-W18 Meeting 24, Paper 24-6-3, Oxford, United Kingdom.

Denzler, J.K., Stapel, P., & Glos, P. (2008). Relationship between global and local MOE. CIB W18 Meeting 41, St. Andrews, Canada. Paper 41-10-3.

Deublein, M., Schlosser, M., & Faber, M. H. (2011). Hierarchical modelling of structural timber material properties by means of Bayesian Probabilistic Networks. Applications of Statistics

and Probability in Civil Engineering. Faber, Köhler & Nishijima (eds) Taylor & Francis Group, London. 1377-1385.

Diamantidis, D. (2001). Report 32: Probabilistic Assessment of Existing Structures-A publication for the Joint Committee on Structural Safety (JCSS) (Vol. 32). Rilem Publications.

Dietsch, P., & Kreuzinger, H. (2011). Guideline on the assessment of timber structures: Summary. *Engineering Structures*, 33, 2983-2986.

Dinwoodie J.M. (1989). Nature's Cellular, Polymeric Fibre-composite. The Institute of Metals, London.

Ditlevsen, O. D., & Källsner, B. (1998). System effects influencing the bending strength of timber beams. In Reliability and Optimization of Structural Systems, Proceedings of 8th IFIP WG 7.5 Working Conference, Krakow, Poland (pp. 129-136).

Divos, F., & Tanaka, T. (2005). Relation between static and dynamic modulus of elasticity of wood. *Acta Silvatica et Lignaria Hungarica*, 1(1), 105-110.

Drdáký, M., Jirovský, I., & Slizková, Z. (2005). On structural health and technological survey of historical timber structures. In: Tampone G (ed) Proceedings of the international conference Conservation of the historic wooden structures, Florence, 1, 278-84.

Ehlbeck, J.I., & Görlacher, R. (1990). Zur Problematik bei der Beurteilung der Tragfähigkeit von altem Konstruktionsholz. *Bauen mit Holz*, 2(90), 117–120.

Emerson, R. N., Pollock, D. G., McLean, D. I., Fridley, K. J., Ross, R. J., & Pellerin, R. E. (1999). Nondestructive testing of large bridge timbers. In Proceedings of 11th International Symposium on Nondestructive Testing of Wood, Madison, WI (pp. 175-184).

Emerson, R., Pollock, D., Kainz, J., Fridley, K., McLean, D., & Ross, R. (1998). Non-destructive evaluation techniques for timber bridges. In Proceedings of 5th World Conference on Timber Engineering, Montreux, 670-677.

Faber, M. H. (2012). Statistics and Probability Theory: In Pursuit of Engineering Decision Support. Springer. ISBN: 9400740557. 190p.

Faber, M. H., Köhler, J., & Sørensen, J. D. (2004). Probabilistic modelling of graded timber material properties. *Structural Safety*, 26(3), 295-309.

Faggiano, B., Grippa, M. R., Marzo, A., & Mazzolani, F. M. (2011). Experimental study for non-destructive mechanical evaluation of ancient chestnut timber. *Journal of Civil Structural Health Monitoring*, 1(3-4), 103-112.

Faria, J. A. (2002). European Timber Buildings as an Expression of Technological and Technical Cultures. (ed) Bertolini, C., Faria, J. A., & Soikkeli, A. Elsevier.

Feio A. (2005) Inspection and diagnosis of historical timber structures: NDT correlations and structural behaviour. PhD thesis, University of Minho, Portugal.

Feio, A. O., Lourenço, P. B., & Machado, J. S. (2007). Non-destructive evaluation of the mechanical behaviour of chestnut wood in tension and compression parallel to grain. *International Journal of Architectural Heritage*,1(3), 272-292.

Fink, G., & Köhler, J. (2011). Multiscale variability of stiffness properties of timber boards. Applications of Statistics and Probability in Civil Engineering. Faber, Köhler & Nishijima (eds) Taylor & Francis Group, 1369-1376.

Fioravanti, M., & Galotta, G. (1998). Valutazione degli effetti del trattamento selvicolturale sulla qualità del legno di castagno (*Castanea sativa* Mill.) proveniente da bosco ceduo. Convegno nazionale sul castagno, Cison di Valmarino, Treviso, pp. 367-376.

Foley, C. (2001). A three-dimensional paradigm of fiber orientation in timber. *Wood Science and Technology*, 35(5), 453-465.

Frattari, A., & Pignatelli, O. (2005) Dendrochronology and non-destructive testing: synergies for dating ancient wooden structures of historic and cultural interest. In Proceedings of 8th International Conference on Non Destructive Investigations and Microanalysis for the Diagnostics and Conservation of the Cultural and Environmental Heritage. Lecce , Italy.

Friis-Hansen, A. (2000). Bayesian networks as a decision support tool in marine applications. Department of Naval Architecture and Offshore Engineering, Technical University of Denmark.

Galligan, W. L., Snodgrass, D. V., & Crow, G. W. (1977). Machine Stress Rating: Practical Concerns for Lumber Producers (No. FSGTR-FPL-7). Forest Products Lab Madison Wisconsin.

Garcia, M. C., Seco, J. I. F., & Prieto, E. H. (2007). Improving the prediction of strength and rigidity of structural timber by combining ultrasound techniques with visual grading parameters. *Materiales de Construcción*, 57(288), 49.

Gehri, E. (1997). Timber as a natural composite: explanation of some peculiarities in the mechanical behaviour – Case: Assessment of the modulus of elasticity of timber parallel to grain. CIB-W18A/30-6-3.

Ghahramani, Z. (1998). Learning dynamic Bayesian networks. In Adaptive processing of sequences and data structures (pp. 168-197). Springer Berlin Heidelberg.

Gloss, P. (1986). Ermittlung der nationalen und internationalen Standes des maschinellen Holzsortierung. München: Deutsche Gesellschaft fur Holzforschung e.V.-Schlussbericht. Forschungsprojekt BOS021D(B).

Golfín, J. F., Díez, R., Hermoso, E., Baso, C., & Casas, J. M. (2007). Caracterización de la madera de E. globulus para uso estructural. *Boletín Informativo CIDEU*, (4), 91-100.

Görlacher, R. (1987). Non destructive testing of wood: an in-situ method for determination of density, *Holz as Roh-und Werkstoff*, 45, pp. 273-278.

Görlacher, R. (1991) Untersuchung von altem Konstruktionsholz: Bestimmung des Elastizitätsmodulus. *Bauen mit Holz*. 8(91), 582-586.

Greaves, B. L., Borralho, N. M., Raymond, C. A., & Farrington, A. (1996). Use of a Pilodyn for the indirect selection of basic density in Eucalyptus nitens. *Canadian Journal of Forest Research*, 26(9), 1643-1650.

Grönlund, U. (1995). Quality improvements in forest products industry: classification of biological materials with inherent variations. Doctoral thesis. Luleå University of Technology, Sweden.

Gyftodimos, E., & Flach, P. A. (2002). Hierarchical Bayesian networks: A probabilistic reasoning model for structured domains. In Proceedings of the ICML-2002 Workshop on Development of Representations. University of New South Wales (pp. 23-30).

Gyftodimos, E., & Flach, P. A. (2004). Hierarchical Bayesian networks: an approach to classification and learning for structured data. In Methods and Applications of Artificial Intelligence (pp. 291-300). Springer Berlin Heidelberg.

Hanhijärvi, A., Ranta-Maunus, A., & Turk, G. (2005). Potential of strength grading of timber with combined measurement techniques. Report of the Combigrade project - phase 1. Espoo. VTT publication no 568.

Hansen C. P. 2000. Application of the Pilodyn in forest tree improvement. DFSC Series of Technical Notes. TN55. Danida Forest Seed Centre, Humlebaek, Denmark

Heckerman, D., & Breese, J. S. (1996). Causal independence for probability assessment and inference using Bayesian networks. IEEE Transactions on Systems, Man and Cybernetics, Part A: Systems and Humans, 26, 826-831.

Heckerman, D., Mamdani, A., & Wellman, M. P. (1995). Real-world applications of Bayesian networks. Communications of the ACM, 38(3), 24-26.

Hoffmeyer, P. (1978). The Pilodyn instrument as a non-destructive tester of the shock resistance of wood. In Proceedings of 4th symposium on the non-destructive testing of wood: proceedings, Washington State University, 1978 (pp. 47-66).

Hofstetter, K., & Gamstedt, E. K. (2009). Hierarchical modelling of microstructural effects on mechanical properties of wood. A review COST Action E35 2004–2008: Wood machining–micromechanics and fracture. Holzforschung, 63(2), 130-138.

Honfi, D., Mårtensson, A., & Thelandersson, S. (2012). Reliability of beams according to Eurocodes in serviceability limit state. *Engineering Structures*, 35, 48-54.

HouJiang, Z., Lei, Z., YanLiang, S., & XiPing, W. (2011). Determining main mechanical properties of ancient architectural timber. *Journal of Beijing Forestry University*, 33(5), 126-129.

Huber, H. A., McMillin, C. W., & McKinney, J. P. (1985). Lumber defect detection abilities of furniture rough mill employees. *Forest Production Journal*, 35(11/12).

Hugin (2008). Hugin Researcher, Aalborg, Hugin Experts A/S.

Imposa, S., Mele, G., Corrao, M., Coco, G., & Battaglia, G. (2012). Characterization of Decay in the Wooden Roof of the S. Agata Church of Ragusa Ibla (Southeastern Sicily) by Means of Sonic Tomography and Resistograph® Penetration Tests. *International Journal of Architectural Heritage*, DOI: 10.1080/15583058.2012.685924.

IPQ (1995) NP 4305, Madeira Serrada de Pinheiro Bravo para Estruturas. Classificação Visual. Instituto Português da Qualidade (in Portuguese).

Isaksson, T. (1999). Modelling the variability of bending strength in structural timber. Report TVBK-1015, Dept. of Structural Engineering, Lund University, Sweden.

Isik, F., & Li, B. (2004) Rapid assessment of wood density of live trees using IML Resi for selection in tree improvement programs. *Canadian Journal of Forest Research*, 33, 1-10.

ISO (1975a). ISO 3030:1975 - Wood - Determination of moisture content for physical and mechanical tests. International Organization for Standardization, Geneva.

ISO (1975b). ISO 3031:1975 - Wood - Determination of density for physical and mechanical tests. International Organization for Standardization, Geneva.

ISO (2010). ISO 16269-4:2010. Statistical interpretation of data - Part 4: Detection and treatment of outliers. International Organization for Standardization, Geneva.

Jayne, B.A. (1955). A nondestructive test of glue bond quality. *Forest Products Journal*. 5(5): 294–301.

JCSS (1996). Project Team Eurocode 1.1: Background documentation Eurocode 1 (ENV 1991) Part 1: Basis of Design, Working Document, European Convention for Constructional Steelwork, First Edition.

JCSS (2000). JCSS Probabilistic Model Code, Part 1: Basis of Design. Probabilistic Model Code, Joint Committee on Structural Safety, Internet Publication: www.jcss.ethz.ch.

JCSS (2006). JCSS Probabilistic Model Code, Part 3: Resistance Models – 3.5 Properties of Timber. Probabilistic Model Code, Joint Committee on Structural Safety, Internet Publication: www.jcss.ethz.ch.

Jensen, F. V., & Nielsen, T. D. (2007). Bayesian networks and decision graphs. Springer.

Kahl, T., Wirth, C., Mund, M., Böhnisch, G., & Schulze, E. D. (2009). Using drill resistance to quantify the density in coarse woody debris of Norway spruce. *European Journal of Forest Research*, 128(5), 467-473.

Kasal, B. (2003). Semi-destructive method for in-situ evaluation of compressive strength of wood structural members. *Forest products journal*, 53(11-12), 55-58.

Kasal, B. (2010). In Situ Assessment of Structural Timber: State-of-the-Art, Challenges and Future Directions. *Advanced Materials Research*, 133, 43-52.

Kasal, B., & Anthony, R. W. (2004). Advances in in situ evaluation of timber structures. *Progress in Structural Engineering and Materials*, 6(2), 94-103.

Kasal, B., & Tannert, T. (2010). In situ assessment of structural timber. RILEM state of the art reports.

Kasal, B., Drdacky, M., & Jirovsky, I. (2003). Semi-destructive methods for evaluation of timber structures. *Advances in architectures series*, 835-842.

Katafygiotis, L. S., & Beck, J. L. (1998). Updating models and their uncertainties. II: Model identifiability. *Journal of Engineering Mechanics*, 124(4), 463-467.

Kliger, I. R., Perstorper, M., & Johansson, G. (1998). Bending properties of Norway spruce timber. Comparison between fast- and slow-grown stands and influence of radial position of sawn timber. *Annales des Sciences Forestières*, 55, 349-358.

Kline, D. E., Woeste, F. E., & Bendtsen, B. A. (1986). Stochastic model for modulus of elasticity of lumber. *Wood and fiber science*, 18(2), 228-238.

Köhler, J. (2007) Reliability of timber structures. PhD thesis, Institute of Structural Engineering Swiss Federal Institute of Technology, Zurich, Switzerland.

Köhler, J., Sørensen, J. D., & Faber, M. H. (2007). Probabilistic modelling of timber structures. *Structural Safety*, 29(4), 255-267.

Kollmann F. F. P., & Côté W. A. (1984). Principle of Wood Science and Technology. Vol. I: Solid Wood. Springer-Verlag Berlin.

Lakes, R. (1993). Materials with structural hierarchy. *Nature*, 361(6412), 511-515.

Langseth, H., & Portinale, L. (2007). Bayesian networks in reliability. Reliability Engineering & System Safety, 92(1), 92-108.

Langseth, H., Nielsen, T. D., Rumí, R., & Salmerón, A. (2009). Inference in hybrid Bayesian networks. *Reliability Engineering & System Safety*, 94(10), 1499-1509.

Lauritzen, S. L. (1992). Propagation of probabilities, means, and variances in mixed graphical association models. *Journal of the American Statistical Association*, 87(420), 1098-1108.

Lear, G. C. (2005). Improving the assessment of in situ timber members with the use of nondestructive and semi-destructive testing techniques. Master Thesis, North Carolina State University, United States of America.

Lee, J. J., & Bae, M. S. (2004). Determination of ratio of wood deterioration using NDT technique. *Mokchae Konghak*, 32(3), 33-41.

Lee, J. J., & Kim, G. C. (2000). Study on the estimation of the strength properties of structural glued laminated timber I: determination of optimum MOE as input variable. *Journal of wood science*, 46(2), 115-121.

Lee, J. J., Park, J. S., Kim, K. M., & Oh, J. K. (2005). Prediction of bending properties for structural glulam using optimized distributions of knot characteristics and laminar MOE. *Journal of wood science*, 51(6), 640-647.

Leicester, R. H. (2001). Engineered durability for timber construction. *Progress in Structural Engineering and Materials*, 3(3), 216-227.

Leicester, R. H., Wang, C. H., Nguyen, M. N., & MacKenzie, C. E. (2009). Design of exposed timber structures. *Australian Journal of Structural Engineering*, 9(3), 217.

Lourenço, P. B., Feio, A. O., & Machado, J. S. (2007). Chestnut wood in compression perpendicular to the grain: non-destructive correlations for test results in new and old wood. *Construction and Building Materials*, 21(8), 1617-1627.

Lourenço, P. B., Sousa, H. S., Brites, R. D., & Neves, L. C. (2013). In situ measured cross section geometry of old timber structures and its influence on structural safety. *Materials and Structures*, 46, 1193-1208.

Lycken, A. (2006). Comparison between automatic and manual quality grading of sawn softwood. *Forest Products Journal*, 56(4), 13-18.

Machado, J. S. (2000). Avaliação da variação das propriedades mecânicas de pinho bravo (*Pinus pinaster* Ait.) por meio de ultra-sons. PhD thesis in Forestall Engineering, Universidade Técnica de Lisboa, Instituto Superior de Agronomia, Lisboa, Portugal.

Machado, J. S., & Cruz, H. P. (2005). Within stem variation of Maritime Pine timber mechanical properties. *Holz as Roh- und Werkstoff*, 63, 154-159.

Machado, J. S., & Palma, P. (2011). Non-destructive evaluation of the bending behaviour of in-service pine timber structural elements. *Materials and structures*,44(5), 901-910.

Machado, J. S., Costa, D., & Cruz, H. (2003a). Evaluation of pine timber strength by drilling and ultrasonic testing. In Proceedings of 13th International Symposium for Non-Destructive Testing in Civil Engineering.

Machado, J. S., Cruz, H., & Nunes, L. (2003b). Mitos e factos relacionados com o desempenho de elementos de madeira em edifícios. 3ºENCORE–Encontro sobre a conservação e reabilitação de edifícios, 1281-1290.

Machado, J. S., Lourenço, P. B., & Palma, P. (2011). Assessment of the structural properties of timber members in situ: a probabilistic approach. In Proceedings of SHATIS 11. Lisbon, Portugal.

Machado, J., & Cruz, H. (1997). Avaliação do estado de conservação de estruturas de madeira. Determinação do perfil densidade por métodos não destrutivos. *Revista Portuguesa de Engenharia de Estruturas*, 42, 15-18.

Machado, J., Palma, P., & Simões, S. (2009). Ultrasonic indirect method for evaluating clear wood strength and stiffness. In Proceedings of the 7th international symposium on non destructive testing in civil engineering - NDTCE(Vol. 9, pp. 969-974).

Madsen, H.O., Krenk, S., & Lind, N.C. (1986). Methods of Structural Safety. Prentice-Hall Inc., Englewood Cliffs, New Jersey, USA.

Marquez, D., Neil, M., & Fenton, N. (2010). Improved reliability modelling using Bayesian networks and dynamic discretization. *Reliability Engineering & System Safety*, 95(4), 412-425.

McDonald, K.A. (1978) Lumber quality evaluation using ultrasonics. In Proceedings of 4th International NDT Symposium of Wood, Vol. 4, 5-14.

Medeiros, P., Sousa, H.S., Lourenço, P.B., & Ferreira, F. (2010). Plano de reconhecimento e inspecção do futuro Centro Interpretativo do Tapete de Arraiolos - Arraiolos. Relatório 10-DEC/E-17, Universidade do Minho, 95 pp (in Portuguese).

Melchers, R.E. (1999). Structural Reliability Analysis and Prediction. Second Edition. John Wiley & Sons, INC., New York.

Montes-Iturrizaga, R., Heredia-Zavoni, E., Vargas-Rodríguez, F., Faber, M. H., & Straub, D. (2009). Risk Based Structural Integrity Management of Marine Platforms Using Bayesian Probabilistic Nets. *Journal of Offshore Mechanics and Arctic Engineering*, 131, 011602.

Moore, J. C., Glenncross-Grant, R., Mahini, S. S., & Patterson, R. (2012). Regional Timber Bridge Girder Reliability: Structural Health Monitoring and Reliability Strategies. *Advances in Structural Engineering*, 15(5), 793-806.

Moral, S., Rumí, R., & Salmerón, A. (2001). Mixtures of truncated exponentials in hybrid Bayesian networks. In Symbolic and Quantitative Approaches to Reasoning with Uncertainty (pp. 156-167). Springer Berlin Heidelberg.

Muñoz, G.R., Gete, A.R., & Saavedra, F.P. (2011). Implications in the design of a method for visual grading and mechanical testing of hardwood structural timber for assignation within the European strength classes. *Forest Systems INIA* 20 (2), pp 235-244.

Neil, M., Tailor, M., Marquez, D., Fenton, N., & Hearty, P. (2008). Modelling dependable systems using hybrid Bayesian networks. *Reliability Engineering & System Safety*, 93(7), 933-939.

Neves, L. A., & Cruz, P. J. (2001). Introdução à análise probabilística simplificada da segurança estrutural. Engenharia Civil - UM, 12, 65–80.

Nguyen, M., Leicester, R. H., Wang, C., Foliente, G. C. (2008) A draft proposal for as1720.5: Timber service life design code. Forest & Wood Products Australia. CSIRO, 2008.

Nishijima, K., Maes, M. A., Goyet, J., & Faber, M. H. (2009). Constrained optimization of component reliabilities in complex systems. *Structural Safety*, 31(2), 168-178.

Nocetti, M., Bacher, M., Brunetti, M., Crivellaro, A., & van de Kuilen, J. W. G. (2010). Machine grading of Italian structural timber: preliminary results on different wood species. In Proceedings of World Conference on Timber Engineering, Trentino, Italy.

Nocetti, M., Brancheriau, L., Bacher, M., Brunetti, M., & Crivellaro, A. (2013). Relationship between local and global modulus of elasticity in bending and its consequence on structural timber grading. *European Journal of Wood and Wood Products*, DOI 10.1007/s00107-013-0682-7.

Oliveira, F., Candian, M., Lucchette, F. F., Calil Jr., C., & Sales, A. (2003). Avaliação de propriedades mecânicas de madeira por meio de ultra-som. In Proceedings of III Pan-American Conference for Nondestructive Testing, Vol. 3, Brazil.

Ormarsson, S., Dahlblom, O., & Persson, K. (1998). Influence of varying growth characteristics on stiffness grading of structural timber. In Proceedings of Meeting 31 of CIB-W18, Document CIB-W18/31–5-1. Savonlinna.

Palanti, S., Macchioni, N., Paoli, R., Feci, E., & Scarpino, F. (2013). A case study: The evaluation of biological decay of a historical hayloft in Rendena Valley, Trento, Italy. *International Biodeterioration & Biodegradation*. DOI 10.1016/j.ibiod.2013.06.026.

Pearl, J. (1988). Probabilistic Reasoning in Intelligent Systems: Networks of Plausible Inference. Morgan Kaufmann Pub. 552pp.

Piazza, M., & Riggio, M. (2008). Visual strength-grading and NDT of timber in traditional structures. *Journal of Building Appraisal*, 3(4), 267-296.

Piazza, M., & Turrini, G. (1983). Il recupero dei solai in legno, Esperienze e realizzazioni. Recuperare, Vol. 7.

Plackett, R. L. (1983). Karl Pearson and the Chi-Squared Test. International Statistical Review (International Statistical Institute (ISI)) Vol. 51 (1). pp. 59–72.

Rackwitz, R. (2000). Optimization: the basis of code-making and reliability verification. *Structural Safety*, 22(1), 27-60.

Ramos, L. (2010). SAHC SA4 lectures, Advanced Masters in Structural Analysis of Monuments and Historical Constructions, Erasmus Mundus Programme, University of Minho, Guimarães, Portugal.

Ramundo, F., Migliore, M. R., & Spina, G. (2011). Analysis of ancient timber structures performance capacity. In Proceedings of SHATIS 11. Lisbon, Portugal.

Ravenshorst, G,J., & van de Kuilen, J.W. (2009). Relationship between local, global and dynamic modulus of elasticity for soft- and hardwoods. CIB W18 Meeting 42, Dübendorf, Switzerland. Paper 42-10-1.

Riberholt, H., & Madsen, P. H. (1979). Strength of timber structures, measured variation of the cross sectional strength of structural lumber. Report R 114, Struct. Research Lab., Technical University of Denmark.

Ridley-Ellis, D., Moore, J., & Khokhar, A. M. (2009). Random acts of elasticity: MoE, G and EN408. In Proceedings of Wood EDG Conference, 23rd April 2009, Bled, Slovenia.

Rinn, F., Schweingruber, F. H., & Schär, E. (1996). Resistograph and X-ray density charts of wood. Comparative evaluation of drill resistance profiles and X-ray density charts of different wood species. *Holzforschung-International Journal of the Biology, Chemistry, Physics and Technology of Wood*, 50(4), 303-311.

Ronca, P., & Gubana, A. (1998). Mechanical characterisation of wooden structures by means of an in situ penetration test. *Construction and Building Materials*, 12(4), 233-243.

Ross, R. J., & Pellerin, R. F. (1994). Nondestructive testing for assessing wood members in structures. USDA. FPL-GTR-70, 1-40.

Ross, R., Brashaw, B., & Pellerin, R. (1998). Non-destructive evaluation of wood. *Forest Products Journal*. 48 (1), 101-105.

Rug, W., & Seemann, A. (1991). Strength of old timber. *Building Research and Information*, 19, 31–37.

Salmén, L., & Burgert, I. (2009). Cell wall features with regard to mechanical performance. A review COST Action E35 2004–2008: Wood machining–micromechanics and fracture. *Holzforschung*, 63(2), 121-129.

Sánchez, F. P., Martitegui, F. A., Casasús, A. G., Esteban, L. G., Camacho, C. K., Gallego, G. M., Palacios, P. P., & Vásquez, M. T. (2004). Especies de maderas: para carpintería, construcción y mobiliario. Aitim.

Sandoz, J. L. (1989). Grading of construction timber by ultrasound. *Wood Science and Technology*, 23(1), 95-108.

Schneider, J. (1997). Introduction to safety and reliability of structures. Structural Engineering documents 5. IABSE, Zurich, Switzerland.

Silvén, O., Niskanen, M., & Kauppinen, H. (2003). Wood inspection with non-supervised clustering. *Machine Vision and Applications*, 13(5-6), 275-285.

Solli, K. H. (2000). Modulus of elasticity—local or global values. In: Proceedings of the 6th World Conference on Timber Engineering, 31st July–3rd August, Whistler, Canada.

Sørensen, J. D. (1987). PRADSS: Program for Reliability Analysis and Design of Structural Systems. Structural Reliability Theory, Paper No. 36, The University of Aalborg, Denmark.

Sørensen, J. D. (2003). Statistical analysis using the Maximum-Likelihood Method, Aalborg University, Aalborg, Denmark.

Sousa, H. S., Branco, J. M., & Lourenço, P. B. (2012). Assessment of strength and stiffness variation within old timber beams. In Proceedings of 8th International Conference on Structural Analysis of Historical Constructions, SAHC, Wroclaw, Poland.

Sousa, H. S., Branco, J. M., & Lourenço, P. B. (2013a). Effectiveness and subjectivity of visual inspection as a method to assess bending stiffness and strength of chestnut elements. Trans Tech Publications: *Advanced Materials Research*, Vol. 778. pp 175-182.

Sousa, H. S., Sørensen, J. D., Kirkegaard, P. H., Branco, J. M., & Lourenço, P. B. (2013b). On the use of NDT data for reliability-based assessment of existing timber structures. *Engineering Structures*, 56, 298-311.

Sousa, H. S., Branco, J. M., & Lourenço, P. B. (in press_a) Characterization of cross sections from old chestnut beams weakened by decay. *International Journal of Architectural Heritage*.

Sousa, H. S., Branco, J. M., & Lourenço, P. B. (in press_b) Prediction of global bending stiffness of timber beams by local sampling data and visual inspection, *European Journal of Wood and Wood Products*.

Sousa, H. S., Branco, J. M., & Lourenço, P. B. (in press_c) Use of bending tests and visual inspection for multi-scale experimental evaluation of chestnut timber beams stiffness, *Journal of Civil Engineering and Management*.

Stapel, P., & van de Kuilen, J. W. G. (2013). Effects of grading procedures on the scatter of characteristic values of European grown sawn timber. *Materials and Structures*, 46, 1587-1598.

Straub, D. (2009). Stochastic modelling of deterioration processes through dynamic Bayesian networks. *Journal of Engineering Mechanics*, 135(10), 1089-1099.

Tampone, G. (1996a). Il restauro delle strutture di legno. Collana BTH. Hoepli, Milan, Italy.

Tampone, G. (1996b). Timber structure rehabilitation. 1st Edn. Hoepli, Milan. Italy.

Tampone, G., Mannucci, M., Macchioni, N., & Gambetta, A. (2002). Strutture di legno: cultura, conservazione, restauro. De Lettera. Milan, Italy.

Tanasoiu, V., Miclea, C., & Tanasoiu, C. (2002). Non-destructive testing techniques and piezoelectric ultrasounds transducers for wood and built in wooden structures. *Journal of Optoelectronics and Advanced Materials*, 4, 949-957.

Tannert, T., Anthony, R. W., Kasal, B., Kloiber, M., Piazza, M., Riggio, M., Rinn, F.; Widmann, R., & Yamaguchi, N. (2013). In situ assessment of structural timber using semi-destructive techniques. *Materials and Structures*. DOI 10.1617/s11527-013-0094-5

Taylor, S. E., & Bender, D. A. (1991). Stochastic model for localized tensile strength and modulus of elasticity in lumber. *Wood and fiber science*, 23(4), 501-519.

Toratti, T., Schnabl, S., & Turk, G. (2007). Reliability analysis of a glulam beam. *Structural Safety*, 29(4), 279-293.

U. S. Forest Products Laboratory (1999). Wood Handbook – Wood as an Engineering Material. U. S. Department of Agriculture, Forest Service, Forest Products Laboratory. Madison, Wisconsin, United States of America.

Ukrainetz, N. K., & O'Neill, G. A. (2010). An analysis of sensitivities contributing measurement error to Resistograph values. *Canadian journal of forest research*, 40(4), 806-811.

UNI (2003a). UNI 11035-1 Structural timber. Visual strength grading for Italian structural timbers: terminology and measurement of features. UNI Milano.

UNI (2003b). UNI 11035-2 Structural timber. Visual strength grading rules and characteristic values for Italian structural timber population. UNI Milano.

UNI (2003c). UNI 13183-1 Umiditá di un pezzo di legno segato - Determinazione tramite il metodo per pesata. UNI Milano.

UNI (2003d) UNI 13183-2 Umiditá di un pezzo di legno segato - Stima tramite il metodo elettrico. UNI Milano.

UNI (2004) UNI 11119:2004 Cultural Heritage - Wooden artifacts - Load-bearing structures - On site inspections for the diagnosis of timber members. UNI Milano.

UNI (2010). UNI 11035-2:2010 Structural timber. Visual strength grading for structural timbers. Part 2: Visual strength grading rules and characteristic values for structural timber population. UNI Milano.

Uzielli, L. (1992). Valutazione della capacità portante degli elementi strutturali lignei. L'Edilizia, Vol. 12: pp. 753-762.

Vanik, M. W., Beck, J. L., & Au, S. (2000). Bayesian probabilistic approach to structural health monitoring. *Journal of Engineering Mechanics*, 126(7), 738-745.

Vega, A., Arriaga, F., Guaita, M., & Baño, V. (2013). Proposal for visual grading criteria of structural timber of sweet chestnut from Spain. *European Journal of Wood and Wood Products*, 71, 529-532.

Vega, A., Dieste, A., Guaita, M., Majada, J., & Baño, V. (2012). Modelling of the mechanical properties of Castanea sativa Mill. structural timber by a combination of non-destructive variables and visual grading parameters. *European Journal of Wood and Wood Products*, 70(6), 839-844.

Vrouwenvelder, A. C. W. M. (2002). Developments towards full probabilistic design codes. *Structural Safety*, 24(2), 417-432.

Vrouwenvelder, T. (1997). The JCSS probabilistic model code. *Structural Safety*, 19(3), 245-251.

Wang, C. H., Leicester, R. H., & Nguyen, M. (2008a). Probabilistic procedure for design of untreated timber poles in-ground under attack of decay fungi. *Reliability Engineering & System Safety*, 93(3), 476-481.

Wang, S. Y., Chen, J. H., Tsai, M. J., Lin, C. J., & Yang, T. H. (2008b). Grading of softwood lumber using non-destructive techniques. *Journal of materials processing technology*, 208(1), 149-158.

Wang, S. Y., Chiu, C. M., & Lin, C. J. (2003). Application of the drilling resistance method for annual ring characteristics: evaluation of Taiwania (Taiwania cryptomerioides) trees grown with different thinning and pruning treatments. *Journal of Wood Science*, 49(2), 116-124.

Weber, P., Medina-Oliva, G., Simon, C., & Iung, B. (2012). Overview on Bayesian networks applications for dependability, risk analysis and maintenance areas. *Engineering Applications of Artificial Intelligence*, 25(4), 671-682.

Wei, X., & Borralho, N. M. G. (1997). Genetic control of wood basic density and bark thickness and their relationships with growth traits of Eucalyptus urophylla in south east China. *Silvae Genetica*, 46(4), 245-249.

Weibull, W. (1939). A statistical theory of the strength of materials. In Proceedings of the Royal Swedish Institute of Engineering Research, N.151, Stockholm.

Wilson, A. G., & Huzurbazar, A. V. (2007). Bayesian networks for multilevel system reliability. *Reliability Engineering & System Safety*, 92(10), 1413-1420.

Wu, S. J., Xu, J. M., Li, G. Y., Risto, V., Lu, Z. H., Li, B. Q., & Wang, W. (2010). Use of the pilodyn for assessing wood properties in standing trees of Eucalyptus clones. *Journal of Forestry Research*, 21(1), 68-72.

Yin, Y. F., Wang, L. J., & Jiang, X. (2008). Use of Pilodyn tester for estimating basic density in standing trees of hardwood plantation. *Journal of Beijing Forestry University*, 30(4), 7-11.

Zombori, B. (2001). In situ non-destructive testing of built in wooden members. NDT.net – Vol. 6, No. 03.

This page intentionally left blank

Annex A

A. Example of updating by Bayesian methods

Consider a resistance model R with a normal distribution characterized by mean value μ and standard deviation σ. The *prior* distribution is now denoted $f_{R'}(\mu,\sigma)$ and is considered to be defined as:

$$f_{\mathrm{R}}^{'}(\mu \mid \sigma) = k\sigma^{-(\nu'+\delta(n')+1)} \exp\left(-\frac{1}{2\sigma^2}\left(\nu'(s')^2 + n'(\mu - m')^2\right)\right) \tag{A.1}$$

with:

$$\delta(n') = 0 \quad \text{for } n' = 0 \tag{A.2}$$

$$\delta(n') = 1 \quad \text{for } n' > 0 \tag{A.3}$$

The *prior* information about the standard deviation σ is given by parameters s' and ν'. The expected value and coefficient of variation of σ can asymptotically (for large ν') be expressed as:

$$E(\sigma) = s' \tag{A.4}$$

$$\mathrm{COV}(\sigma) = \frac{1}{\sqrt{2\nu'}} \tag{A.5}$$

The *prior* information about the mean μ is given by parameters m', n' and s'. The expectation and coefficient of variation of μ can asymptotically (for large ν') be expressed as:

$$E(\mu) = m' \tag{A.6}$$

$$\mathrm{COV}(\mu) = \frac{s'}{m'\sqrt{n'}} \tag{A.7}$$

Another possible way to interpret the *prior* information is to consider the results of hypothetical prior test series, for mean and standard deviation analysis. For that case the standard deviation is characterized by:

- s' is the hypothetical sample value;
- ν' is the hypothetical number of degrees of freedom for s'.

The information about the mean is given by:

- m' is the hypothetical sample average;
- n' is the hypothetical number of observations for m'.

Usually for a test it is considered that $\nu = n - 1$, but the *prior* parameters n' and ν' are independent from each other.

The consideration of these parameters allows defining the expected values of mean and standard deviation of the *prior* information, and also permits to consider the degree of uncertainty related to those values. For low or lack of information, n' and ν' are to be considered equal to zero, whereas when almost deterministic knowledge of the mean and standard deviation is available this will lead to higher values of n' and ν' (*i.e.* 20 or 40).

When new information is available, the resistant model given by the *prior* distribution $f_R'(\mu,\sigma)$ may be updated according to Equation 2.28, with the parameters:

$$n'' = n' + n \tag{A.8}$$

$$\nu'' = \nu' + \nu + \delta(n') \tag{A.9}$$

$$m''n'' = n'm' + nm \tag{A.10}$$

$$\nu''(s'')^2 + n''(m'')^2 = \nu'(s')^2 + n'(m')^2 + \nu s^2 + nm^2 \tag{A.11}$$

Assuming, as previously mentioned, that $\nu = n - 1$ and that $\delta(n')$ is given by Equations A.2 and A.3.

With this procedure and taking into account Equation 2.29 the predictive value of the resistance R is given by:

$$f_R = m'' - t_{\nu''} s'' \sqrt{\left(1 + \frac{1}{n''}\right)} \tag{A.12}$$

where $t_{\nu''}$ has a central t-distribution. The appropriate choice of value for $t_{\nu''}$ makes possible the calculation of characteristic values, each are often in Eurocodes given as the fifth percentile for resistance and 95th or 98th for loads.

For this case, a parametric analysis upon the influence of the number of sampling test pieces of new information in the resultant characteristic value was considered. For this the following premises were taken:

- new information was gathered from a trial of tests. The number of test pieces n is the focus of this study. The sample mean m is equal to 75 kN and the sample standard deviation s is equal to 15 kN. On a first step, both m and s are constant regardless of the number of test pieces n, although physically not coherent;
- from *prior* information the sample mean was equal to 80 kN, but with high variation. The standard deviation s' is equal to 17 kN with a coefficient of variation of 25%.

By varying the number of test pieces n the characteristic value for resistance R_k is influenced as shown in Figure A.1. From the analysis of the evolution of R_k, it is concluded

that, in a first stage an increase of the number of test pieces is highly advantageous as, even a small increase in n, produces a large increase in R_k. However, this curve tends to stabilize in a horizontal asymptote and, thus, even high increments of n lead to small increments of R_k. Although, as previously mentioned, the assumption of constant mean and standard deviation for different values of n may be found questionable, the value of this preliminary study is found when dealing with cost assessment when defining the number of necessary tests.

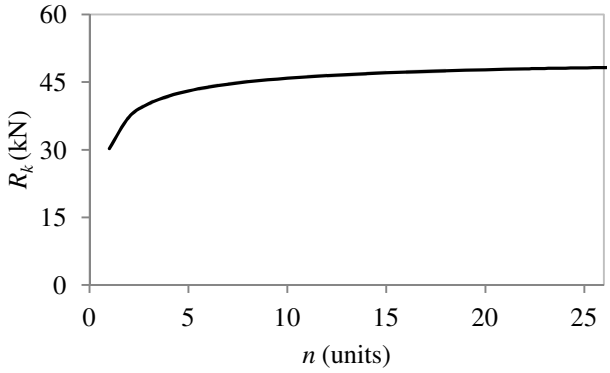

Figure A.1: Variation of the characteristic value for resistance with number of test pieces.

For the same example, a parametric analysis was conducted to assess the importance of different parameters regarding the characteristic resistance versus number of test samples. The results are presented in Figure A.2. From the results, the following conclusions were taken for this example:

- by varying the standard deviation of the new information s (Figure A.2a) it is observed that the values of R_k are very influenced. For lower values of s the values of R_k increase towards the value of m. The values of R_k tend to stabilize for minor values of n in a faster way when the values of s increases, concluding that for smaller s the gain in R_k is further available with more test samples;
- by varying the hypothetical number of samples for m' and therefore the uncertainty related to this parameter (Figure A.2b) it is observed that, for even small increases of this parameter n' the gain in R_k is high for small numbers of n. Nevertheless, for higher numbers of n the importance of n' is less significant because $n'' = n' + n$;
- when varying the value of the coefficient of variation for the standard deviation of the *prior* information (Figure A.2c) it is noticed, that no significant changes were caused to the R_k versus n graph;
- for different levels of n' the importance of m' (Figures A.2d, e, f) was observed to be higher for lower levels of n, but as seen before the relation $n'' = n' + n$ leads to smaller influence of n' as n increases. This also results in a smaller influence of m' as the influence of n' decreases.

The main conclusion is that an increase on the number of test samples or a decrease on the uncertainty related to either or both *prior* and new information will eventually lead

to similar results. Therefore, both ways must be compared in terms of effectiveness and cost optimization in order to obtain a more adequate procedure for data updating.

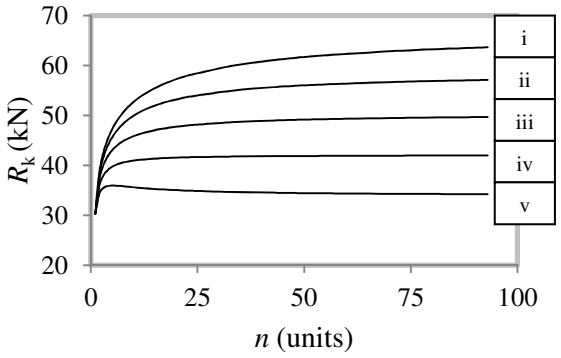

s = i:5; ii:10; iii:15; iv:20; v:25 (kN)

a)

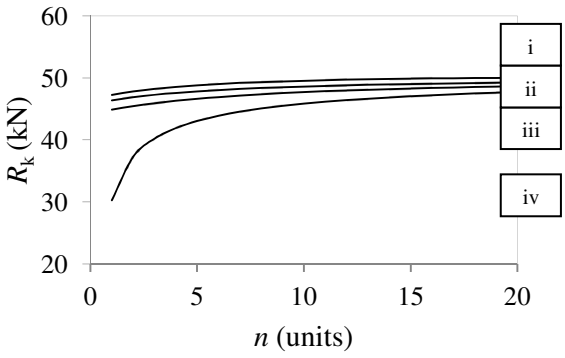

n' = i:20; ii:10; iii:5; iv:0 (observations)

b)

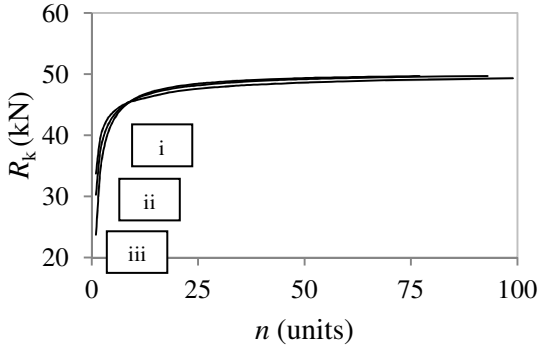

COV(σ) = i:15; ii:25; iii:35 (%)

c)

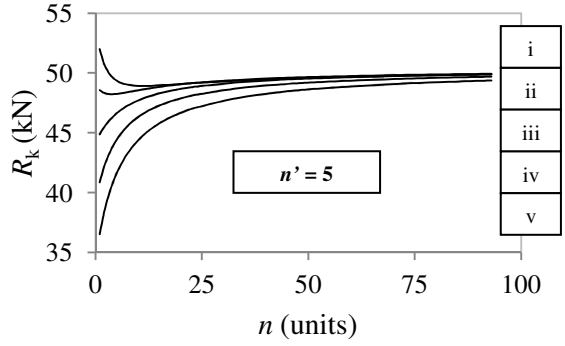

m' = i:90; ii:85; iii:80; iv:75; v:70 (kN)

d)

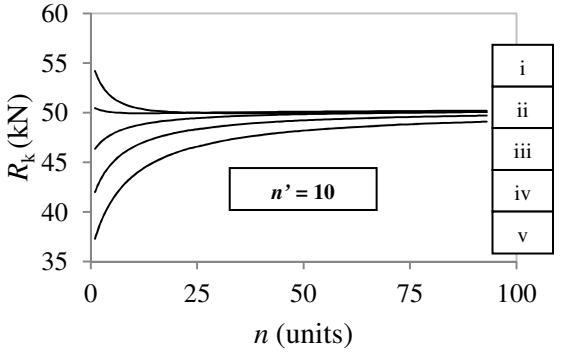

m' = i:90; ii:85; iii:80; iv:75; v:70 (kN)

e)

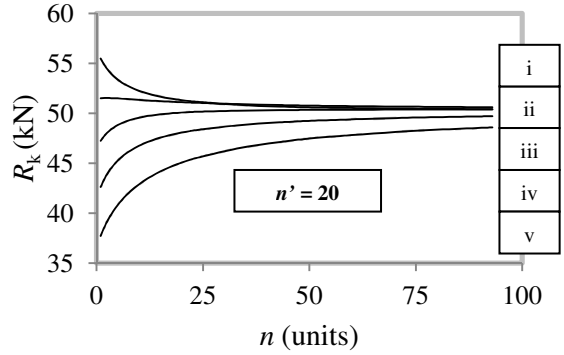

m' = i:90; ii:85; iii:80; iv:75; v:70 (kN)

f)

Figure A.2: Results for multi-parameter analysis regarding characteristic resistance R_k versus number of test samples n.

Also the observation of this example might prove its importance when considering a quality control scheme. As stated in JCSS (1996), the Eurocode 0, Annex D (CEN, 2002) provides an estimation of the characteristic value of a batch, given that the batch passes a certain quality control procedure, which may be in most cases too conservative. The reason for this statement is found when considering that, due to continuous quality controls, *prior* information is well defined and also the producer aims at a very small fraction of rejected batches. So, as previously mentioned, a better definition of the *prior* knowledge of the production characteristic allows increasing the characteristic resistance value.

The above updating procedure is straightforward when *prior* information is fully or well known. Nevertheless, this is not always the most common situation and many times only vague or scarce information is available. When standard deviation σ is known but vague *prior* information is offered, the parameters are given as:

- $n' = 0$;
- $\nu' = \infty$;
- m' = not relevant;
- $s' = \sigma$.

Considering n observations with mean value m the updating parameters become:

- $n'' = n$;
- $\nu'' = \infty$;
- $m'' = m$;
- $s''^2 = \sigma^2$.

With this procedure, and taking into account Equation 2.29, the predictive value of the resistance R is now given by:

$$f_R = m - t_\infty \sigma \sqrt{\left(1 + \frac{1}{n}\right)} \tag{A.13}$$

where t_∞ has a central t-distribution with corresponding value of $\nu'' = \infty$.

When standard deviation σ is also unknown and vague *prior* information is offered, the parameters are given as:

- $n' = 0$;
- $\nu' = 0$;
- m' = not relevant;
- s' = not relevant.

Considering n observations with mean value m and standard deviation s, the updating parameters become:

- $n'' = n$;
- $\nu'' = n - 1$;

- $m'' = m$;
- $s''^2 = s^2$.

With this procedure, and taking into account Equation 2.29, the predictive value of the resistance R is now given by:

$$f_R = m - t_{n-1} s \sqrt{\left(1 + \frac{1}{n}\right)} \tag{A.14}$$

where t_{n-1} has a central t-distribution with corresponding value of $\nu'' = n - 1$.

Although normal distributions are relatively easier to implement than other more complicated probability distributions, sometimes restraints or restrictions may make necessary the use of other distributions. Lognormal distributions are often associated to resistance models because no negative values are possible. The evaluation based on a lognormal distribution is in some occasions also simple. Considering the above example and a number of observations X with lognormal distribution, so that $Y = \ln(X)$ has a normal distribution. Then, for the case of vague *prior* information on the mean or, on both mean and standard deviation the updating scheme goes as follows, regarding that Y is defined by:

$$m(Y) = \frac{1}{n} \sum_{i=1}^{n} Y_i \tag{A.15}$$

$$s(Y)^2 = \frac{1}{n-1} \sum_{i=1}^{n} (Y_i - m(Y))^2 \tag{A.16}$$

with $Y_i = \ln(X_i)$.

Then the predictive function for a design value is stated as:

$$X_d = \exp(m(Y)) \exp\left(t_{\nu d} s(Y) \sqrt{\left(1 + \frac{1}{n}\right)} \right) \tag{A.17}$$

where $t_{\nu d}$ has a central t-distribution with corresponding value of $\nu'' = \nu d$.

Although there is a useful number of distribution types of great importance for several reliability based structural reassessment, not all practical situations allow for an analytical solution. In this case, FORM techniques to integrate over the possible outcomes of the uncertain distribution parameters are possible, and by this, permitting to assess the predictive distribution (Madsen *et al.*, 1986).

Annex B

B. Definition of scales for correlation analysis

Table B.1: Definition of scales for correlation analysis.

beam	board	sections (cm)		left - middle - right		total/board		l_1 region		mean/section		mean/L-C-R		mean/Total		mean/ l_1 region	
X	1	10-50	$x_{1,1}$	10-130	$\bar{x}_{1,(1,2,3)}$	10-290	$\bar{x}_{1,j}$			10-50	$\bar{x}_{i,1}$	10-130	$\frac{\bar{x}_{i,1}+\bar{x}_{i,2}+\bar{x}_{i,3}}{3}$	10-290	$\bar{x}_{(1,2,3),i}$		
		50-90	$x_{1,2}$														
		90-130	$x_{1,3}$	90-210	$\bar{x}_{1,(3,4,5)}$			90-210	$\bar{x}_{1,(3,4,5)}$	50-90	$\bar{x}_{i,2}$						
		130-170	$x_{1,4}$														
		170-210	$x_{1,5}$														
		210-250	$x_{1,6}$	170-290	$\bar{x}_{1,(5,6,7)}$					90-130	$\bar{x}_{i,3}$	90-210	$\frac{\bar{x}_{i,3}+\bar{x}_{i,4}+\bar{x}_{i,5}}{3}$			90-210	$\frac{\bar{x}_{i,3}+\bar{x}_{i,4}+\bar{x}_{i,5}}{3}$
		250-290	$x_{1,7}$														
	2	10-50	$x_{2,1}$	10-130	$\bar{x}_{2,(1,2,3)}$	10-290	$\bar{x}_{2,j}$			130-170	$\bar{x}_{i,4}$						
		50-90	$x_{2,2}$														
		90-130	$x_{2,3}$	90-210	$\bar{x}_{2,(3,4,5)}$			90-210	$\bar{x}_{2,(3,4,5)}$	170-210	$\bar{x}_{i,5}$						
		130-170	$x_{2,4}$														
		170-210	$x_{2,5}$														
		210-250	$x_{2,6}$	170-290	$\bar{x}_{2,(5,6,7)}$					210-250	$\bar{x}_{i,6}$	170-290	$\frac{\bar{x}_{i,5}+\bar{x}_{i,6}+\bar{x}_{i,7}}{3}$				
		250-290	$x_{2,7}$														
	3	10-50	$x_{3,1}$	10-130	$\bar{x}_{3,(1,2,3)}$	10-290	$\bar{x}_{3,j}$			250-290	$\bar{x}_{i,7}$						
		50-90	$x_{3,2}$														
		90-130	$x_{3,3}$	90-210	$\bar{x}_{3,(3,4,5)}$			90-210	$\bar{x}_{3(3,4,5)}$								
		130-170	$x_{3,4}$														
		170-210	$x_{3,5}$														
		210-250	$x_{3,6}$	170-290	$\bar{x}_{3,(5,6,7)}$												
		250-290	$x_{3,7}$														

$\bar{x}_{i,j}$ = mean value, with i = 1,2,3 and j = 1,2,...,6,7

Annex C

C. Probability distributions for engineering problems

One of the most commonly used distribution in the engineering scope is the normal or Gaussian distribution. The PDF of the distribution can be expressed as:

$$f_{\mathrm{X}}(x) = \frac{1}{\sigma_{\mathrm{X}}\sqrt{2\pi}} \exp\left[-\frac{1}{2}\left(\frac{x-\mu_{\mathrm{X}}}{\sigma_{\mathrm{X}}}\right)^2\right], -\infty < x < +\infty \quad \text{(C.1)}$$

where the mean μ_{X} and the standard deviation σ_{X} are the two parameters of the distribution, usually estimated from the available data. The corresponding CDF can be expressed as:

$$F_{\mathrm{X}}(x) = \int_{-\infty}^{x} \frac{1}{\sigma_{\mathrm{X}}\sqrt{2\pi}} \exp\left[-\frac{1}{2}\left(\frac{x-\mu_{\mathrm{X}}}{\sigma_{\mathrm{X}}}\right)^2\right] dx \quad \text{(C.2)}$$

This distribution is applicable for any value of a random variable from -∞ to +∞. It presents symmetry about the mean, and the mean, median and modal values are identical and can be estimated directly from the data. In order to estimate a given probability, instead of integrating CDF, it is often used a transformation of the original random variable to a standard normal variable with zero mean and unit standard deviation.

In many engineering problems, a random variable cannot have negative values due to the physical aspects of the problem, such as when considering resistance properties. In order to eliminate the possibility of negative values the variable may be modelled by considering the natural logarithm of the variable *X*. When the natural logarithm of a random variable has a normal distribution, the underlying distribution is denominated lognormal. The PDF of a lognormal distribution is given by:

$$f_{\mathrm{X}}(x) = \frac{1}{\sqrt{2\pi}\zeta_{\mathrm{X}}x} \exp\left[-\frac{1}{2}\left(\frac{\ln x-\lambda_{\mathrm{X}}}{\zeta_{\mathrm{X}}}\right)^2\right], 0 \le x < +\infty \quad \text{(C.3)}$$

where λ_{X} and ζ_{X} are the two parameters of the lognormal distribution, which can be derived from the parameters of a normal distribution as:

$$\lambda_{\mathrm{X}} = \ln \mu_{\mathrm{X}} - \frac{1}{2}\zeta_{\mathrm{X}}^2 \quad \text{(C.4)}$$

and:

$$\zeta_{\mathrm{X}}^2 = \ln\left[1 + \left(\frac{\sigma_{\mathrm{X}}}{\mu_{\mathrm{X}}}\right)^2\right] \quad \text{(C.5)}$$

This distribution is applicable for values between 0 and +∞. Its PDF is unsymmetrical, and thus its mean, median and modal values are expected to be different.

Often, in engineering applications, the extreme values of random variables are of particular interest and importance since in these cases the largest or smallest values of random variables may dictate a particular design. In constructing an extreme value

distribution, an underlying random variable with a particular distribution is necessary. Therefore the underlying distribution of a variable governs the form of the corresponding extreme value distribution.

Considering a random variable X with known distribution function, and n as a given number of samples from population X, then the extreme values of the sample, either the minimum value Y_1 or the maximum value Y_n are defined respectively as:

$$Y_1 = \min(X_1, X_2, \dots, X_n) \tag{C.6}$$

$$Y_n = \max(X_1, X_2, \dots, X_n) \tag{C.7}$$

where, different minimum and maximum values exist if different sets of samples of size n are considered for X. Then, a distribution function for these extreme values may be constructed if considering all these sets. The CDF of the smallest and largest values then become, respectively:

$$P(Y_1 > y) = P(X_1 > y,\ X_2 > y, \dots,\ X_n > y) = 1 - F_{Y_1}(y) \tag{C.8}$$

$$P(Y_n \leq y) = P(X_1 \leq y,\ X_2 \leq y, \dots,\ X_n \leq y) = F_{Y_n}(y) \tag{C.9}$$

which, for identically distributed and statistically independent variables of X_i may be given by:

$$F_{Y_1}(y) = 1 - [1 - F_X(y)]^n \tag{C.10}$$

$$F_{Y_n}(y) = [F_X(y)]^n \tag{C.11}$$

However, often the tails of the distribution present an unsymmetrical behaviour, evidencing an asymptotic distribution, where some approach a known mathematical distribution function. From these distributions the most well known and commonly used in engineering were classified by Gumbel as Type I, Type II and Type III extreme value distributions. Type I or also known as extreme value distribution is a distribution of maxima in sample sets converging from a population with an exponential tail (e.g. normal distribution). Type II is also a distribution of maxima in sample sets but converging from a population with a polynomial tail (e.g. lognormal distribution). Type III or also referred as Weibull distribution may be obtained by the convergence of most of the commonly known distributions that have a lower bound, thus used commonly for describing materials with fragile strength behaviour. Extreme distributions do not need to be treated any differently from other distributions and in the majority of cases, its parameters can be estimated with information about the mean and coefficient of variation. Attending to its applicability in engineering, Type I (Gumbel) and Type III (Weibull) extreme value distributions are further discussed, with especial attention for the right tail of the Gumbel distribution (maxima values) and left tail of the Weibull distribution (minima value).

When considering the largest value of an initial variable X, the CDF for a Gumbel distribution is:

$$F_{Y_n}(y_n) = \exp\left[-e^{-\alpha_n(y_n - u_n)}\right] \tag{C.12}$$

The corresponding PDF is:

$$f_{Y_n}(y_n) = \alpha_n e^{-\alpha_n(y_n-u_n)}\exp\left[-e^{-\alpha_n(y_n-u_n)}\right], -\infty < y_n < +\infty \quad \text{(C.13)}$$

For both equations the parameters of the distribution are defined as u_n, which is the characteristic largest value of the initial variable X and α_n, which is an inverse measure of dispersion of the largest value of X. These parameters are related to the mean, μ_{Y_n}, and standard deviation, σ_{Y_n}, of Y_n as:

$$\alpha_n = \frac{1}{\sqrt{6}}\left(\frac{\pi}{\sigma_{Y_n}}\right) \quad \text{(C.14)}$$

$$u_n = \mu_{Y_n} - \frac{\gamma}{\alpha_n} \quad \text{(C.15)}$$

where γ is the Euler-Mascheroni constant ≈ 0.5772.

When considering the smaller value of an initial variable X, the CDF for a two-parameter Weibull distribution is:

$$F_{Y_1}(y_1) = 1 - \exp\left[-\left(\frac{y_1}{w_1}\right)^k\right] \quad \text{(C.16)}$$

The corresponding PDF is:

$$f_{Y_1}(y_1) = \frac{k}{w_1}\left(\frac{y_1}{w_1}\right)^{k-1}\exp\left[-\left(\frac{y_1}{w_1}\right)^k\right], y_1 \geq 0 \quad \text{(C.17)}$$

For both equations the parameters of the distribution are defined as w_1, which is the characteristic smallest (also known as scale parameter) and k, which is the shape parameter. These parameters are related to the mean, μ_{Y_1}, and coefficient of variation, COV_{Y_1}, of Y_1 as:

$$\mu_{Y_1} = w_1\Gamma\left(1+\frac{1}{k}\right) \quad \text{(C.18)}$$

$$COV_{Y_1} = \left[\frac{\Gamma\left(1+\frac{2}{k}\right)}{\Gamma^2\left(1+\frac{1}{k}\right)} - 1\right]^{1/2} \quad \text{(C.19)}$$

where $\Gamma(\ )$ is the gamma function, such that $\Gamma(n) = (n\text{-}1)!$ for all positive integers n. However, for practical applications when μ_{Y_1} and COV_{Y_1} are known, the distribution parameters may be approximated by:

$$k = {COV_{Y_1}}^{-1.08} \quad \text{(C.20)}$$

and:

$$w_1 = \frac{\mu_{Y_1}}{\Gamma\left(1+\frac{1}{k}\right)} \quad \text{(C.21)}$$

Annex D

D. Maximum Likelihood Method

Description of method

A possible way of defining the Maximum Likelihood method may be taken by the following premises (Köhler, 2007). Considering that the parameters $\theta = (\theta_{1,...,} \theta_n)^T$ of the distribution of X are known, the joint probability of a random sample X_1, X_2, ..., X_n can be written as:

$$f_X(x \mid \theta) = f_{X1}, f_{X2},..., f_{Xn}(x_1, x_2,..., x_n \mid \theta) = f_{X1}(x_1) f_{X2}(x_2)...f_{Xn}(x_n) = \\ = \prod_{i=1} f_X(x_i \mid \theta) \quad \text{(D.1)}$$

However, it is often the contrary situation that is present in engineering applications, such that a sample $\hat{x}_1, \hat{x}_2,..., \hat{x}_n$ is observed and the distribution parameters are unknown. In that sense, Equation D.1 can be understood as a relative measure for the likelihood that the distribution determined by the parameters θ is appropriate in the statistical definition of the sample $\hat{x}$. Along the full domain of all possible parameters θ the likelihood L(.) that the parameters belong to the sample is:

$$L(\theta \mid \hat{x}_1, \hat{x}_2,..., \hat{x}_n) = \prod_{i=1}^{n} f_X(\hat{x}_i \mid \theta) \quad \text{(D.2)}$$

The maximum likelihood estimates can be defined by the parameters $\hat{\theta}$ which maximize the likelihood function L(.) over the domain of θ, thus being assumed as the most likely to represent the data sample, as:

$$\theta = \max_{\theta} L(\theta \mid \hat{x}_1, \hat{x}_2,..., \hat{x}_n) \quad \text{(D.3)}$$

The Maximum Likelihood Method besides being used to fit the statistical parameters in distribution functions can also be used to fit the parameters in linear and non-linear regression analysis (Sørensen, 2003). Also when considering a sample of results taken from tests a linear regression may be estimated including an uncertainty parameter or also called lack-of-fit parameter.

For parameter estimation for linear regression lines, the following linear regression model in x_1, ..., x_m –space is considered:

$$y = \alpha_0 + \alpha_1 x_1 + ... + \alpha_m x_m + \varepsilon \quad \text{(D.4)}$$

where α_0, α_1, ..., α_m are the regression parameters and ε models the lack-of-fit. ε is assumed to be Normal distributed with expected value 0 and standard deviation σ_ε.

It is assumed that n sets of observations or test results of (x,y) are available and denoted as: (x_1, y_1), ..., (x_n, y_n). The regression parameters are determined using a Maximum Likelihood method. The Likelihood function is written with x_{ij} being the j th coordinate of the i th observation:

$$\mathrm{L}(\alpha_0, \alpha_1, ..., \alpha_m) = \prod_{i=1}^{m} P(y_i = \alpha_0 + \alpha_1 x_{i1} + ... + \alpha_m x_{im} + \varepsilon) \tag{D.5}$$

or, as in this case if it is used that ε is Normal distributed and σ_ε is included as a parameter to be estimated, then it follows:

$$\mathrm{L}(\alpha_0, \alpha_1, ..., \alpha_m, \sigma_\varepsilon) = \prod_{i=1}^{m} \frac{1}{\sqrt{2\pi\sigma_\varepsilon}} \exp\left(-\frac{1}{2}\left(\frac{y_i - (\alpha_0 + \alpha_1 x_{i1} + ... + \alpha_m x_{im})}{\sigma_\varepsilon} \right)^2 \right) \tag{D.6}$$

The Log-Likelihood function becomes:

$$\ln \mathrm{L}(\alpha_0, \alpha_1, ..., \alpha_m, \sigma_\varepsilon) = -n \ln\left(\sqrt{2\pi\sigma_\varepsilon}\right) - \sum_{i=1}^{m} \frac{1}{2}\left(\frac{y_i - (\alpha_0 + \alpha_1 x_{i1} + ... + \alpha_m x_{im})}{\sigma_\varepsilon} \right)^2 \tag{D.7}$$

The optimal parameters are determined from the optimization problem:

$$\max_{\alpha_0, \alpha_1, ..., \alpha_m, \sigma_\varepsilon} \ln \mathrm{L}(\alpha_0, \alpha_1, ..., \alpha_m, \sigma_\varepsilon) \tag{D.8}$$

Results

The results of Phases 2 and 3, regarding bending MOE in sawn beams and boards, were fitted to different probability distributions by the Maximum Likelihood method. The estimates are presented from Table D.1 and D.2 for sawn beams, and from Table D.3 to D.4 for sawn boards. The 95% confidence intervals of each estimated parameter are also presented. The estimated maximum likelihood distributions for each case are also defined in terms of mean and coefficient of variation.

Table D.1: Maximum likelihood estimates for $E_{m,l}$ of sawn beams.

Distribution	Parameter	Maximum Likelihood Estimate	95% confidence interval		Estimated distribution	
			lower bound	upper bound	mean (N/mm^2)	COV (%)
Normal	μ: mean	10841	9557	12125	10841	24.7
	σ: standard deviation	2674	2086	4007		
Lognormal	μ: normal mean	9.255	9.118	9.392	10890	29.1
	σ: normal st. deviation	0.285	0.222	0.427		
Gumbel	*u*: location parameter	12172	10901	13444	10595	33.1
	α: scale parameter	2733	2015	3705		
Weibull	*w*: scale parameter	11851	10682	13147	10807	25.5
	k: shape parameter	4.448	3.208	6.167		

Table D.2: Maximum likelihood estimates for $E_{m,g}$ of sawn beams.

Distribution	Parameter	Maximum Likelihood Estimate	95% confidence interval		Estimated distribution	
			lower bound	upper bound	mean (N/mm^2)	COV (%)
Normal	μ: mean	10940	9812	1832	10940	21.5
	σ: standard deviation	2348	12067	3519		
Lognormal	μ: normal mean	9.277	9.172	9.381	10943	22.0
	σ: normal st. deviation	0.218	0.170	0.326		
Gumbel	*u*: location parameter	12140	11067	13213	10809	27.4
	α: scale parameter	2306	1665	3195		
Weibull	*w*: scale parameter	11897	10859	13035	10934	22.6
	k: shape parameter	5.082	3.633	7.108		

Table D.3: Maximum likelihood estimates for $E_{m,l}$ of sawn boards.

Distribution	Parameter	Maximum Likelihood Estimate	95% confidence interval		Estimated distribution	
			lower bound	upper bound	mean (N/mm^2)	COV (%)
Normal	μ: mean	12910	12487	13332	12910	30.4
	σ: standard deviation	3923	3653	4252		
Lognormal	μ: normal mean	9.410	9.372	9.449	13019	36.9
	σ: normal st. deviation	0.358	0.333	0.388		
Gumbel	*u*: location parameter	14878	14340	15417	12139	50.1
	α: scale parameter	4745	4450	5060		
Weibull	*w*: scale parameter	14289	13838	14754	12860	31.5
	k: shape parameter	3.517	3.252	3.804		

Table D.4: Maximum likelihood estimates for $E_{m,g}$ of sawn boards.

Distribution	Parameter	Maximum Likelihood Estimate	95% confidence interval		Estimated distribution	
			lower bound	upper bound	mean (N/mm^2)	COV (%)
Normal	μ: mean	11661	11375	11946	11661	22.8
	σ: standard deviation	2654	2471	2877		
Lognormal	μ: normal mean	9.329	9.297	9.361	11765	30.4
	σ: normal st. deviation	0.298	0.277	0.323		
Gumbel	*u*: location parameter	12893	12640	13146	11603	24.7
	α: scale parameter	2235	2062	2422		
Weibull	*w*: scale parameter	12651	12386	12922	11654	21.7
	k: shape parameter	5.290	4.854	5.765		

Annex E

E. χ^2 goodness-of-fit tests

Description of method

The χ^2 goodness-of-fit test is performed by grouping the data into bins, calculating the observed and expected frequency for those bins, and computing the χ^2 test statistic, as follows:

$$\chi^2 = \sum_{i=1}^{k} (O_i - E_i)^2 / E_i \tag{E.1}$$

where O is the observed frequency and E is the expected frequency. The expected frequency is calculated by:

$$E_i = N\left(F(Y_u) - F(Y_l)\right) \tag{E.2}$$

where $F(\ )$ is the CDF for the distribution being tested, Y_u is the upper limit for class i, Y_l is the lower limit for class i, and N is the sample size. This test statistic has an approximate χ^2 distribution when the frequencies are sufficiently large, with (k - c) degrees of freedom where k is the number of non-empty cells (number of bins) and c is the number of estimated parameters (including location, scale and shape parameters) for the distribution plus 1. Therefore, the hypothesis that the data are from a population with the specified distribution is rejected if:

$$\chi^2 > \chi^2_{1-\alpha,k-c} \tag{E.3}$$

where $\chi^2_{1-\alpha,k-c}$ is the χ^2 critical value with $(k-c)$ degrees of freedom and significance level α.

Choice of number of groups (therefore, the bins width) for goodness-of-fit tests is important, but only rules based on experience are often given (since the optimal bin width depends on the distribution). For this analysis, bins in either tail with an expected count less than 5 are pooled with neighbouring bins until the count in each extreme bin is at least 5. When bins in the interior have less than 5 data points, fewer bins were used. By default 10 bins were considered and a significance level of 2.5% was chosen for this study. Due to the limited sample size of the sample for MOE in sawn beams, the χ^2 goodness-of-fit tests were made exclusively for the data derived from the bending tests in sawn boards.

Results

The χ^2 goodness-of-fit tests for the MOE of sawn boards with respect to different probabilistic functions with parameters obtained by method of moments (MM) and maximum likelihood estimates (MLE) is presented in Table E.1.

Table E.1: χ^2 goodness-of-fit tests for the experimental MOE of sawn boards sample data with respect to different probabilistic functions ($\alpha = 2.5\%$).

Data	Distribution parameters	Distribution (*)			
		Normal	Lognormal	Gumbel	Weibull
$E_{m,l}$ (sawn boards)	MM	H_0 (0.0302)	H_1 (2.104×10^{-6})	H_1 (0.0141)	H_1 (0.0089)
	MLE	H_0 (0.0310)	H_1 (4.663×10^{-10})	H_1 (2.200×10^{-14})	H_1 (0.0039)
$E_{m,g}$ (sawn boards)	MM	H_1 (8.588×10^{-5})	H_1 (3.083×10^{-14})	H_0 (0.3917)	H_1 (0.0084)
	MLE	H_1 (8.665×10^{-5})	H_1 (5.734×10^{-20})	H_0 (0.2860)	H_0 (0.0477)

MM: method of moments corresponding to the statistical parameters of the experimental data;
MLE: maximum likelihood estimates;
H_0: null hypothesis;
H_1: alternative hypothesis;
(*) value in brackets is the *p-value*: probability of observing the given result, or one more extreme, by chance if the null hypothesis is true. If *p-value* < α the H_0 is rejected.

The χ^2 goodness-of-fit tests for the MOE of sawn boards in each separate visual class with respect to different probabilistic functions with parameters obtained by method of moments and maximum likelihood estimates are presented in Table E.2 for $E_{m,l}$ and in Table E.3 for $E_{m,g}$.

Table E.2: χ^2 goodness-of-fit tests for the experimental $E_{m,l}$ of sawn boards sample data divided into different visual inspection classes, with respect to different probabilistic functions ($\alpha = 2.5\%$).

Data	Distribution parameters	Distribution (*)			
		Normal	Lognormal	Gumbel	Weibull
$E_{m,l}$ (sawn boards): class I	MM	H_0 (0.4575)	H_0 (0.1324)	H_1 (0.0012)	H_0 (0.1834)
	MLE	H_0 (0.4713)	H_0 (0.0340)	H_1 (1.899×10^{-12})	H_1 (0.0211)
$E_{m,l}$ (sawn boards): class II	MM	H_0 (0.3592)	H_0 (0.0931)	H_0 (0.5065)	H_0 (0.4285)
	MLE	H_0 (0.3635)	H_1 (0.0224)	H_0 (0.5672)	H_0 (0.4683)
$E_{m,l}$ (sawn boards): class III	MM	H_0 (0.2069)	H_0 (0.0561)	H_0 (0.1650)	H_0 (0.1987)
	MLE	H_0 (0.2042)	H_0 (0.1043)	H_0 (0.1026)	H_0 (0.2045)
$E_{m,l}$ (sawn boards): class NC (**)	MM	H_0 (0.9702)	H_0 (0.6059)	H_0 (0.5431)	H_0 (0.9889)
	MLE	H_0 (0.9673)	H_0 (0.7022)	H_0 (0.5726)	H_0 (0.9885)

MM: method of moments corresponding to the statistical parameters of the experimental data;
MLE: maximum likelihood estimates;
H_0: null hypothesis;
H_1: alternative hypothesis;
(*) value in brackets is the *p-value*: probability of observing the given result, or one more extreme, by chance if the null hypothesis is true. If *p-value* < α the H_0 is rejected.
(**) Minimum value of the expected count in the tails bin was considered to be 3 regarding the large variation of values.

Table E.3: χ^2 goodness-of-fit tests for the experimental $E_{m,g}$ of sawn boards sample data divided into different visual inspection classes, with respect to different probabilistic functions ($\alpha = 2.5\%$).

Data	Distribution parameters	Distribution (*)			
		Normal	Lognormal	Gumbel	Weibull
$E_{m,g}$ (sawn boards): class I	MM	H_1 (0.0191)	H_1 (3.999×10^{-5})	H_0 (0.5038)	H_0 (0.1735)
	MLE	H_1 (0.0201)	H_0 (2.011×10^{-10})	H_0 (0.1426)	H_0 (0.4623)
$E_{m,g}$ (sawn boards): class II	MM	H_0 (0.1616)	H_0 (0.0549)	H_0 (0.3700)	H_0 (0.2355)
	MLE	H_0 (0.1676)	H_1 (0.0167)	H_0 (0.3286)	H_0 (0.3222)
$E_{m,g}$ (sawn boards): class III	MM	H_0 (0.7170)	H_0 (0.2983)	H_0 (0.8696)	H_0 (0.8299)
	MLE	H_0 (0.7060)	H_0 (0.2521)	H_0 (0.8875)	H_0 (0.7902)
$E_{m,g}$ (sawn boards): class NC (**)	MM	H_0 (0.4126)	H_0 (0.7834)	H_0 (0.0614)	H_0 (0.3554)
	MLE	H_0 (0.4222)	H_0 (0.1652)	H_0 (0.0626)	H_0 (0.3659)

MM: method of moments corresponding to the statistical parameters of the experimental data;
MLE: maximum likelihood estimates;
H_0: null hypothesis;
H_1: alternative hypothesis;
(*) value in brackets is the *p-value*: probability of observing the given result, or one more extreme, by chance if the null hypothesis is true. If *p-value* < α the H_0 is rejected.
(**) Minimum value of the expected count in the tails bin was considered to be 3 regarding the large variation of values.

Annex F

F. Decay modelling

The evolution of decay along time has been studied regarding the possibility of using models that may predict timber performance in a quantitative and probabilistic format (Leicester, 2001; Wang *et al.*, 2008a; Leicester *et al.*, 2009). The decay models are assumed as bi-parametrical idealized models given by a bilinear function (Figure F.1a). The two parameters are t_{lag} (year) corresponding to the time before noticeable decay commences and r (mm/year) corresponding to an annual decay penetration rate depending on climate, durability and structural conditions of the timber element. On those models, it is assumed that non-decayed wood suffers no strength loss and that the transition zone is a narrow band, which can be lumped on a decay front along the longitudinal axis of the structural members and within the cross section (Figure F.1b).

As example of decay models, Wang *et al.* (2008a) researched about timber poles in-ground in Australian soil and subjected to fungi attack, where first order probability theories were used, and gave the following relations to define the decay parameters:

$$t_{lag} = 3 \cdot r_{ingr}^{-0.4} \tag{F.1}$$

$$r_{ingr} = k_{climate\_ingr} \cdot k_{wood\_ingr} \tag{F.2}$$

where $k_{climate\_ingr}$ is a climate parameter, k_{wood_ingr} is a wood durability parameter and r_{ingr} (mm/year) corresponds to the annual decay penetration rate for in-ground timber elements. Considering a probabilistic analysis, the decay penetration rate parameter is modelled by a lognormal distributed stochastic variable with a COV between 0.85 and 1.2 depending on the timber durability class and climatic conditions (Wang *et al.*, 2008a). The t_{lag} parameter is defined as function of the penetration rate (Wang *et al*., 2008a; Nguyen *et al.*, 2008).

Other decay models based on observation could also be used, with due care regarding the reliability of information and amount of data. In Leicester *et al.* (2009), the previous model was extended and calibrated for the design of exposed timber members of common wood species and exposed to the Australia climate. The extended model permitted to consider the size and orientation of the cross section, the presence of

connectors and existence of painting. Moreover, it also permitted to obtain different penetration rates for each side of the element. To that aim, the following relations for the decay parameters were proposed:

$$t_{\text{lag}} = 8.5 \cdot r^{-0.85} \tag{F.3}$$

$$r = k_{\text{climate}} \cdot k_{\text{wood}} \cdot k_{\text{t}} \cdot k_{\text{w}} \cdot k_{\text{n}} \cdot k_{\text{g}} \cdot k_{\text{p}} \tag{F.4}$$

where k_{climate} is a climate parameter, k_{wood} is a wood durability parameter, k_{t} is a thickness parameter, k_{w} is a width parameter, k_{n} is a connector parameter, k_{g} is a geometry parameter and k_{p} is a paint parameter.

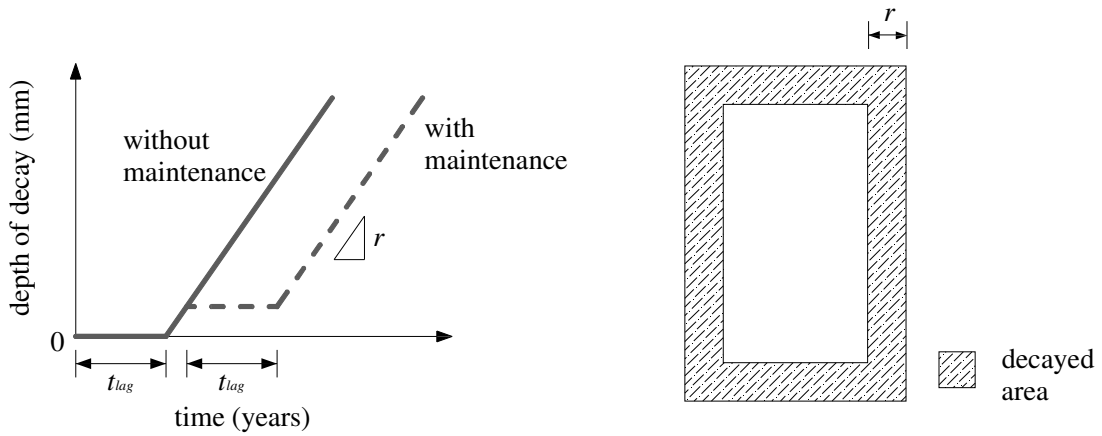

a) b)

Figure F.1: Progress of decay: a) idealized model (adapted from Leicester (2001)); b) damage penetration on a decayed cross section.

Annual decay penetration rates calibrated with existing timber members above ground, using onsite inspection and NDT, are proposed in Lourenço *et al*. (2013) and Brites *et al.* (2013) for roof elements made of pine timber, and in Sousa *et al*. (in press_a) for chestnut floor beams in Northern Portugal. Here, to assess the decay evolution in the timber members, it was assumed that decay was regularly spread along the perimeter of the cross section progressing to the core of the element.